Novel lysine-based reducible copolymers for intracellular gene delivery

---

A dissertation Presentation to

The Department of Pharmacological and Pharmaceutical Sciences

University of Houston

In Partial Fulfillment of

The Requirement for the Degree

Doctor of Philosophy

By

Mohamed Ismail Nounou

December 2011

"Out of life's school of war: What does not destroy me, makes me stronger."

Friedrich Nietzsche, The Twilight of the Idols (1899)

German philosopher (1844–1900)

"Your time is limited, so don't waste it living someone else's life. Don't be trapped by dogma. Don't let the noise of others' opinions drown out your own inner voice, and most important, have the courage to follow your heart and intuition. They somehow already know what you truly want to become. Everything else is secondary"

"Stay Hungry. Stay Foolish."

Steve Jobs (1955-2011)

To

The four beautiful and great girls in my life,

Malak *(my daughter),*
Laila *(my mother),*
Kamilia *(my wife)*
and ***Wahiba*** *(my grandmother)*

I hope God can always help me to make you happy.

and

My Great Father,

Mahmoud Ismail Nounou, Ph.D.

Please rest in peace; I will always remember you.

Table of contents

Abstract

The development of biodegradable gene delivery systems, which have the ability to effectively deliver therapeutic DNA to a target tissue, is paramount to the success of nonviral gene delivery. One approach to developing biodegradable polymers is to introduce disulfide bonds along the backbone of the polymers to ensure release of the DNA in the reductive environment of the cytoplasm, whilst simultaneously reducing the molecular weight of the polymers. There is a crucial need to develop biocompatible and biodegradable polymers, which have low cytotoxicities so as to maintain cell viability and hence increase transfection efficiencies. Therefore, to produce a biocompatible gene delivery system, we have designed and synthesized novel reducible copolymers of the type $(AB)_n$, which consist of repeating units of the natural amino acid, L-lysine and cystamine bisacrylamide (CBA). These novel reducible linear L-lysine copolymers (LLCs) were then modified with ethylenediamine so as to introduce primary amines for efficient DNA condensation. The molecular weight (MW) of the copolymers was found to be ~3.2 kDa with a polydispersity index of ~1.2. Gel retardation assays showed complete condensation of DNA at N/P ratios greater than 20/1 and exceptional LLC/pDNA polyplex stability during incubation with DNase I. To investigate the mechanism of DNA release from the polymer/pDNA complexes,

fluorescence spectroscopy studies were performed with 1,4-dithio-DL-threitol (DTT). These data showed a significant reduction in fluorescence intensity following the addition of LLCs to DNA. After the addition of DTT, there was a 95 % increase in fluorescence intensity, which indicated the reduction of the disulfide bonds and the release of the DNA from the complexes. The particle sizes of LLC/pDNA polyplexes were found to be between 100-231 nm with surface charges of 0.8-17 mV respectively. The transfection efficiencies of the polyplexes as determined with a luciferase assay showed that LLC polyplexes produced five times higher transfection efficiencies in HDF cells, three times higher transfection efficiencies in MCF-7 cells, and four times higher transfection efficiencies in MA cells as compared to the optimal PLL control. The LLC/pDNA polyplexes showed significantly lower cytotoxicities as compared to the PLL/pDNA control in HDF, MCF-7, and MA cells at certain N/P ratios.

Finally, in an *exvivo* study, LLCs were used as a nonviral gene carrier system to generate genetically modified stem cells to produce sufficient amounts of the angiogenic cytokine, vascular endothelial growth factor ($VEGF_{165}$). These genetically modified stem cells were used to promote revascularization of an infarcted region of the heart, which can reduce myocardial damage and scar formation. A myocardial infarction model was generated in SCID mice deficient in T and B cells by permanent ligation of the left anterior descending coronary

(LAD) artery. Cardiac hemodynamics, H&E staining and immunohistostaining results from this *ex vivo* study presented improved cardiac contractility, potential differentiation of hMSCs, new blood vessel formation, and a reduction in infarct size after treatment with the LLC genetically modified stem cells compared to the control animals.

In conclusion, these results suggest that these novel LLCs are efficient, reducible and biocompatible polymers for nonviral gene delivery. Moreover, LLCs, as a nonviral gene carrier vector, hold great potential for the treatment of myocardial infarction in conjunction with stem cell therapy. Finally, adoption of novel nano-therapeutics strategies and techniques combining gene and cell therapies together could open the gate towards endless possibilities in the future of therapeutics and medicine.

List of Figures

List of Tables

List of Abbreviations

^{1}H-NMR	Proton nuclear magnetic resonance
4T1	Mouse breast cancer cells
APCs	Antigen presenting cells
ATCC	American type culture collection
BCA	Bicinchoninic acid
BPEI	Branched polyethylenimine
BRCs	Biocompatible reducible copolymers
CAT	Chloramphenicol acetyl transferase expression assay
CBA	Cystamine bisacrylamide
CD-31	Cluster of differentiation 31
CMV	Cytomegalovirus
D_a	Dalton
DAPI	4',6-Diamidino-2-phenylindole
DC-Chol	3ß-[N-(N',N'-dimethylaminoethane)-carbamoyl]cholesterol
DCM	Dichloromethane
DIPEA	N,N-Diisopropylethylamine
DMAEMA	2-(Dimethylamino)ethyl methacrylate
DMEM	Dulbecco's modified eagle medium
DMF	Dimethylformamide
DMRIE	(1,2-Dimyristyloxypropyl-3-dimethyl-hydroxy ethyl ammonium bromide)
DMSO	Dimethyl sulfoxide
BOC	Di-*tert*-butyl dicarbonate
DOGS	Dioctadecylamidoglycyl carboxyspermine
DOPE	1,2-Dioleoyl-sn-glycero-3-phosphoethanolamine
DOSPA	N-(1-(2,3-dioleyloxy)propyl)-N-(2-(sperminecarboxamido) ethyl)-N,N-dimethy- lammonium trifluoroacetate
DOTAP	N-[1-(2,3-dioleoyloxy)propyl]-N,N,N-trimethylammonium chloride
DOTMA	N-[1-(2,3-dioleyloxy)propyl]-N,N,N-trimethylammonium chloride
DTT	1,4-Dithio-D-threitol
EDC	1-Ethyl-3-(3-dimethylaminopropyl)carbodiimide
EDPVR	End-diastolic pressure-volume relation
EDTA	Ethylenediaminetetraacetic acid
EDV	End-diastolic volume

EGFP	Enhanced green fluorescent protein
ELSD	Evaporative light scattering detector
EMA	Ethidium monoazide
EMEM	Eagle's minimum essential medium
ESPVR	End-systolic pressure-volume relation
ESV	End-systolic volume
Etbr	Ethidium bromide
Factor VIII	Von Willebrand factor
FBS	Fetal bovine serum
GPC	Gel permeation chromatography
GSH	Glutathione
GSSG	Oxidized Glutathione
H&E	Hematoxylin and eosin stain
HDF	Human dermal fibroblasts
HEK-293s	Human embryonic kidney cells
HGF	Human growth factor
hMSCs	Human meschenchymal stem cells
HPLC	High performance/pressure liquid chromatography
IACAC	The Institutional Animal Care and Use Committee
IR	Infra-red spectroscopy
LAD	Left anterior descending coronary artery
Lc	Lipid tail critical length
LDH or LD	Lactate dehydrogenase
LLCs	Linear L-lysine copolymers
LPEI	Linear polyethylenimine
Luc	Luciferase
LVP	Left ventricular pressure
MA	Adipose stromal cells
MALDI-TOF	Matrix-assisted laser desorption/ionization time of flight
MCF-7	Human breast cell carcinoma
MEF	Mouse embryonic fibroblasts
MeOH	Methanol
MI	Myocardial infarction
Mn	Number average molecular weight
MTT	(3-(4,5-Dimethylthiazol-2-yl)-2,5-diphenyltetrazolium bromide
Mw	Weight average molecular weight
MW or MWT	Molecular weight
MWCO	Molecular weight cut-off
N-boc EDA	N-boc ethylene diamine

N/P	Ratio of nitrogen residues to phosphate residues
NADP	Nicotinamide adenine dinucleotide phosphate
NCS	Newborn calf serum
NLS	Nuclear localization signal/sequence
NMP	N-Methylpyrrolidone
NOS	Nitric oxide synthase
PAA	Polyacrylic acid
PBS	Phosphate buffer saline
PDI	Polydispersity index
PDMAEMA	Poly(2-(dimethylamino)ethyl methacrylate)
pDNA	Plasmid DNA
PECAM-1	Platelet endothelial cell adhesion molecule
PEG-FA	Pegylated folic acid
PLL	Poly(L-lysine)
PU	Polyurethanes
PV loops	Pressure-Volume loops
rCPP	Reducible polycopeptide
RES	Reticuloendothelial system
RHB	Reducible hyperbranched poly(amidoamine)
RLU	Relative luminescence/light units
SCID	Severe combined immunodeficiency
SD	Standard deviation
SDS or SLS	Sodium docecyl/lauryl sulfate
SEC-HPLC	Size exclusion high performance liquid chromatography
SS-PAED	Disulfide poly(amido ethylenediamine)
SS-PAEI	Reducible poly(amido ethylenimine)s
SU	Sulfonylurea
SV	Simian virus
SW	Stroke volume
TCEP	Tris-(2-carboxyethyl)phosphine, hydrochloride
TEA	Triethyl amine
TFA	Trifluoroacetic acid
TnT	Cardiac troponin T
TRITC	Rhodamine-labeled Antibodies
VEGF	Vascular endothelial growth factor
X-SCID	X-linked severe combined immunodeficiency
α-SMA	Alpha smooth muscle actin

Acknowledgments

First and foremost, I thank God for helping me through with this work. I would like to express my sincere gratitude to my committee members for their valuable suggestions and constant support. In particular, I would like to acknowledge Dr. Ananth Annapragada and Dr. Brad McConnell for their guidance and support in the research, which have added value to our findings. I would also like to thank Dr. KeHe Ruan for his valuable suggestions and support in research. I am grateful to Dr. Brian Knoll, Dr. Douglas Eikenburg, and Dr. Junghae Suh for her help and guidance during this project. I would like to acknowledge Dr. Malavosklish Bikram, my former academic advisor, for her scientific contribution and ideas. I would also like to thank Dr. Jason Eriksen for teaching basic and advanced concepts of confocal microscopy.

I would also like to sincerely acknowledge the entire PPS faculty for mentoring and teaching so passionately. I also thank Dr. Michael Rea and Dr. Michael Johnson for helping in the project. I am grateful to all my lab mates and friends who have helped me in the project and provided immense support. My special thanks to Kamilia Abdelraouf, Dr. Vicky Mody, Dr. Song Gao, Lili Cui, Tao Nui, Adarshi Ghandi, Pranav Shah, Yong Ma, Summit Basu, Renu Singh, Jie He,

Kirk Braggs, Wen Jiang, Tanay Samant, and Zhen Yang for their full-hearted support throughout this period.

In the end, I would like to acknowledge my mother, grandmother, my wife and my daughter for their constant encouragement; this dissertation would not have been possible without their support. I dedicate this thesis to my beloved mother (Ms. Laila Morsy Ahmed) and grandmother (Ms. Wahiba Mohamed Ragab), who have been the source of lifelong inspiration and my true strength in life. My wife, Ms. Kamilia Abdelraouf has been my support system in difficult phases and her encouragement has been central to all my achievements in life. My daughter, Ms. Malak Mohamed Nounou, has been my main source of inspiration and my key driving force for success. She is the reason why I work as hard as possible to make a better tomorrow. I would also like to acknowledge my family member, Mr. Essam Morsy, Ms. Magda Morsy, Ms. Faten Morsy, Dr. Zeinab El_Ghoneimy, Dr. Khaled Rasheed and Dr. Mohamed Rasheed Abdelraouf for their invaluable support.

I extend my sincere gratitude to all those who have been associated directly and indirectly with this dissertation. Thank you.

1. Literature review on nonviral gene delivery carriers

1.1. Introduction

Proteins and/or drugs are typically administered for the treatment of various diseases and genetic disorders; however, gene therapy has the potential to surpass these common therapies and arise as a leader in molecular medicine. Gene therapy fundamentally delivers a genetic sequence encoding for therapeutic proteins that are created on a cellular level. Furthermore, the potential for the treatment of such a wide range of genetic abnormalities could possibly lead to correcting a genetic defect for the treatment of diseases such as Duchenne muscular dystrophy (Duan 2011), cystic fibrosis (Conese, Ascenzioni et al. 2011; Griesenbach and Alton 2011; Hida, Lai et al. 2011), and Smith-Magenis syndrome (Greenberg, Guzzetta et al. 1991; Moncla, Livet et al. 1991). The number of clinical gene therapy protocols and their target diseases show that cancer remains by far the most targeted disease (Gao, Kim et al. 2007).

The concept of gene therapy includes not only the addition of genes to genetically deficient cells, but also the use of transgenes encoding several peptides that function to enhance the capacity of cells or to regulate cell differentiation (Louise 2006; Ma and Diamond 2001; Park, Jeong et al. 2006; Wu and Wu 1991).

Although there are multiple methods for transgene expression, viral and nonviral gene carriers are the most common. The number of clinical trials with viral carriers dwarfs that of nonviral carriers due to the high degree of transfection and the high persistence of gene expression with viral carriers. During the past thirty years, rapid development of non-viral gene delivery systems based on cationic polymers has been witnessed.

1.2. Viral gene carriers and their disadvantages

Viral gene carriers provide effective gene transfection, but with a significant cost in immunogenicity as seen by the tragic death of Jesse Gelsinger in 1999 (Stolberg 1999; Wilson 2010). Viral gene carriers have domains to promote receptor-mediated endocytosis, protein transduction, fusogenicity, and nuclear translocation. These domains can also be attached to nonviral gene carriers to produce comparable degrees of targeting, endosomal escape, or karyophily. Viral vectors are also limited in the size of the therapeutic gene payload that they may hold, whereas nonviral gene carriers can complex much larger therapeutic plasmids. Finally, viral vectors are inherently immunogenic, whereas this feature does not hinder nonviral carriers. The numerous downsides of viral carriers have led to the development of a number of nonviral gene carriers and techniques including cationic polymers, cationic lipids, optimization of naked

pDNA constructs, chemical precipitation, and mechanical means of efficient transfection.

1.3. Nonviral gene carriers

There has been a fast progress in nonviral gene delivery systems based on cationic polymers and lipids for the treatment of both genetically inherited and acquired diseases. Nonviral gene carriers contain primarily of a cationic region to condense the anionic therapeutic plasmid, commonly referred to as a polyelectrolyte, thereby protecting the plasmid from degradative nucleases. The condensation of pDNA is primarily through ionic interactions (electrostatic) between cationic groups on the carrier and the anionic phosphate backbone of the pDNA. In addition, complex formation may also be a function of hydrogen bonds, solvent exclusion, and hydrophobic interactions, which also factors into cationic lipid/pDNA complex formation. Upon cellular internalization and nuclear transportation, the transgene is transcribed into messenger RNA (mRNA) encoding the protein of interest. After the introns are cleaved from the mRNA molecule, the mRNA is exported and translated in the cytosol producing the therapeutic protein. This protein may then be used for local and/or systemic treatment for disease. The cost in cytotoxicity for nonviral gene carriers is typically low; however, the transfection efficiency is lower compared to viral gene

carriers. The cytotoxicity of nonviral gene carriers, as seen with branched polyethylenimine (BPEI) MW 25k, is typically quite high due to the high cationic charge. This high cationic charge state allows for unfavorable interactions with anionic species in vivo such as erythrocytes and albumin.

1.3.1. Cationic lipids

Cationic lipids are some of the most studied and used nonviral gene vectors to date. The chemical composition of cationic lipids used in nonviral gene delivery is: (1) a polar cationic headgroup, (2) a lipid anchor, and (3) a linker between the headgroup and hydrophobic anchor (Wasungu and Hoekstra 2006; Zhang, Zhao et al. 2007). Cationic lipids, generally used in conjugation with neutral helper lipids, can be mixed with DNA to form a positively charged complex named a lipoplex (Wasungu and Hoekstra 2006). Geometry represents a crucial factor in the use of cationic lipids as a nonviral gene carrier system. Cationic lipids can take various structural phases in aqueous media, including the micellar, lamellar, cubic, inverted hexagonal phase and vesicular structure. This is governed by the packing parameter, P. This packing parameter, (P = v/alc), is defined as the ratio of the hydrocarbon volume, (v), and the product of the effective head group area, (a), and the lipid tail critical length, (lc) (Hsu, Chen et al. 2005). This parameter governs the ratio of the area occupied by the

hydrophobic region versus that of the hydrophilic region. Accordingly, when P exceeds the value of 1, i.e. the area occupied by the hydrocarbon chains is much larger than that of the head group; the cationic lipid tends to take the inverted hexagonal phase. Such an inverted hexagonal shape plays an important role in gene delivery mechanisms that cationic carrier systems use because it is a bilayer destabilizing structure, which facilitates the endosomal escape of DNA (Koltover, Salditt et al. 1999; Montier, Benvegnu et al. 2008; Tros de Ilarduya, Sun et al. 2010; Zhang, Xu et al. 2004). When P is more than half and less than one, this promotes the vesicular structure formation along with flexible bilayer structure. On the other hand, spherical micelles are formed when P is less than 0.33 (Hsu, Chen et al. 2005). Generally, dioleoylphosphatidylethanolamine (DOPE) or cholesterol are used with cationic lipids as helper lipids. These helper lipids potentially promote the transformation of the lamellar lipoplex phase into a non-lamellar structure, which improve cationic lipid mediated transfection efficiency.

First, a polar cationic headgroup is crucial for the efficacy of the lipid carrier system. The amount of positive charge on the headgroup will govern its ability to complex anionic genetic material. In addition, the cationic headgroup will enhance the cellular uptake of the lipoplexes as it interacts with the anionic lipids of the cellular membrane (Byk, Dubertret et al. 1998; Gao and Huang 1991).

Moreover, The cationic headgroup has also been modified chemically to enhance the ability of the carrier system to condense and complex DNA. Conjugation of polyethylenimine (PEI), either in its branched or linear form, to the polar cationic headgroup has been reported to be effective for gene delivery because of the increased positive charge which will aid strong complex formation and of PEI ability to escape endosomes due to the proton-sponge effect of PEI (Abdallah, Hassan et al. 1996; Li, Nie et al. 2008).

Second, a hydrophobic lipid anchor is necessary for enhanced DNA stability in the bloodstream and carrier system cellular uptake. The cholesterol, which is commonly used in anchor lipids, is a biocompatible naturally occurring lipid (Liu, Liggitt et al. 1995; Liu, Mounkes et al. 1997). Cellular uptake is enhanced by the favorable interaction between the hydrophobic groups of the gene carrier and the cellular membrane.

Finally, the linker between the hydrophobic anchor and the polar headgroup governs the biodegradability of carrier system. The linker group should have a biodegradable structure so as to diminish toxicity and boost carrier system efficiency (Byk, Dubertret et al. 1998). Cationic lipids can be subdivided into monovalent cationic lipids such as DOTMA, DC-Chol, and DMRIE or multivalent cationic lipids such as GL-67, DOGS, and DOSPA.

1.3.1.1 Monovalent cationic lipids

N-[1-(2,3-dioleyloxy)propyl]-N,N,N-trimethylammonium chloride, or DOTMA, was one of the first synthesized and commercially available cationic lipids used as a gene carrier system (Figure 1.1). DOTMA contains two unsaturated oleoyl chains ($C18:\Delta^9$), bound by an ether bond to a glycerol bakbone. DOTMA has a quaternary amine as the cationic head group. The oleoyl unsaturated fatty acid chains represent DOTMA hydrophobic domain resulting in a pseudo-linear orientation with a cationic, tertiary amine for pDNA condensation. DOTMA resembles N-[1-(2,3-Dioleoyloxy)]-N,N,N-trimethylammonium propane methylsulfate (DOTAP) in structure (Figure 1.1). In the late 80s, DOTMA was one of the most efficient gene carrier systems offering up to 100 fold more transfection efficiency than DEAE-detran or calcium phosphate (Felgner, Gadek et al. 1987). DOTMA was commercialized in a 1/1 ratio with neutral co-lipid dioleoylphosphatidylethanolamine (DOPE) as lipofectin (Felgner, Gadek et al. 1987). The inclusion of DOPE is crucial to enhance genetic material release from the late endosomal compartment following fusion with the lysosome and subsequent drop in pH. This is due to the pH buffering capacity of DOPE, which enhanced the transfection efficiency of DOTMA.

3β[N-(N',N'-dimethylaminoethane)-carbamoyl]cholesterol, (DC-Chol) is another monovalent cationic lipid, which was first synthesized by Gao and Huang in 1991

(Gao and Huang 1991). DC-Chol contains a primary amine as the cationic headgroup for electrostatic condensation and cholesterol as the hydrophobic domain (Figure 1.1). The biocompatibility of cholesterol and its ability to stabilize the lipid bilayer structure were the main reasons for using DC-Chol. DC-CHOL provided two- to four-fold greater chloramphenicol acetyltransferase expression and a four-fold reduction in cytotoxicity versus Lipofectin in transfections in various cell lines (Gao and Huang 1991).

1.3.1.2. Multivalent Cationic Lipids

Multivalent cationic lipids use multivalent headgroups primarily derived from spermine and spermidine. The use of the spermine functional group provides more efficient packing of DNA in terms of lipoplex size (Jain, Zon et al. 1989). Multivalent cationic lipids require the use of a fusogenic lipid, such as DOPE. This is due to DOPE pH buffering capacity, which enables the gene carrier system to escape the degradative endosomes.

The most notable multivalent cationic lipid is 2,3-dioleyloxy-N-[2(sperminecarboxamido)ethyl]-N,N-dimethyl-l-propanaminium trifluoroacetate, or DOSPA (Figure 1.1), a DOTMA derivative. DOSPA resembles DOTMA in chemical structure except for a spermine group, which is bound via an amide linkage to the hydrophobic chains. DOSPA is commercialized as the most used and trusted to date transfection agent, “Lipofectamine™”. Lipofectamine™ is

composed of DOSPA, used with the neutral helper lipid DOPE at a 3 : 1 ratio (Liu and Huang 2002; Luo and Saltzman 2000). The widespread use of Lipofectamine™ is mainly due to its good safety profile and transfection efficiency and its capacity to yield high expression level in a wide range of cell lines.

Di-octadecyl-amido-glycyl-spermine, or DOGS, has a structure similar to DOSPA (Figure 1.1). Dioctamido-decylamidoglycylspermine (DOGS) consists of two primary amines and two secondary amines bound to a single, alkyl chain. Both DOSPA and DOGS share a multivalent spermine head group and two 18-carbon alkyl chains. DOGS is commercially available under the name Transfectam™.

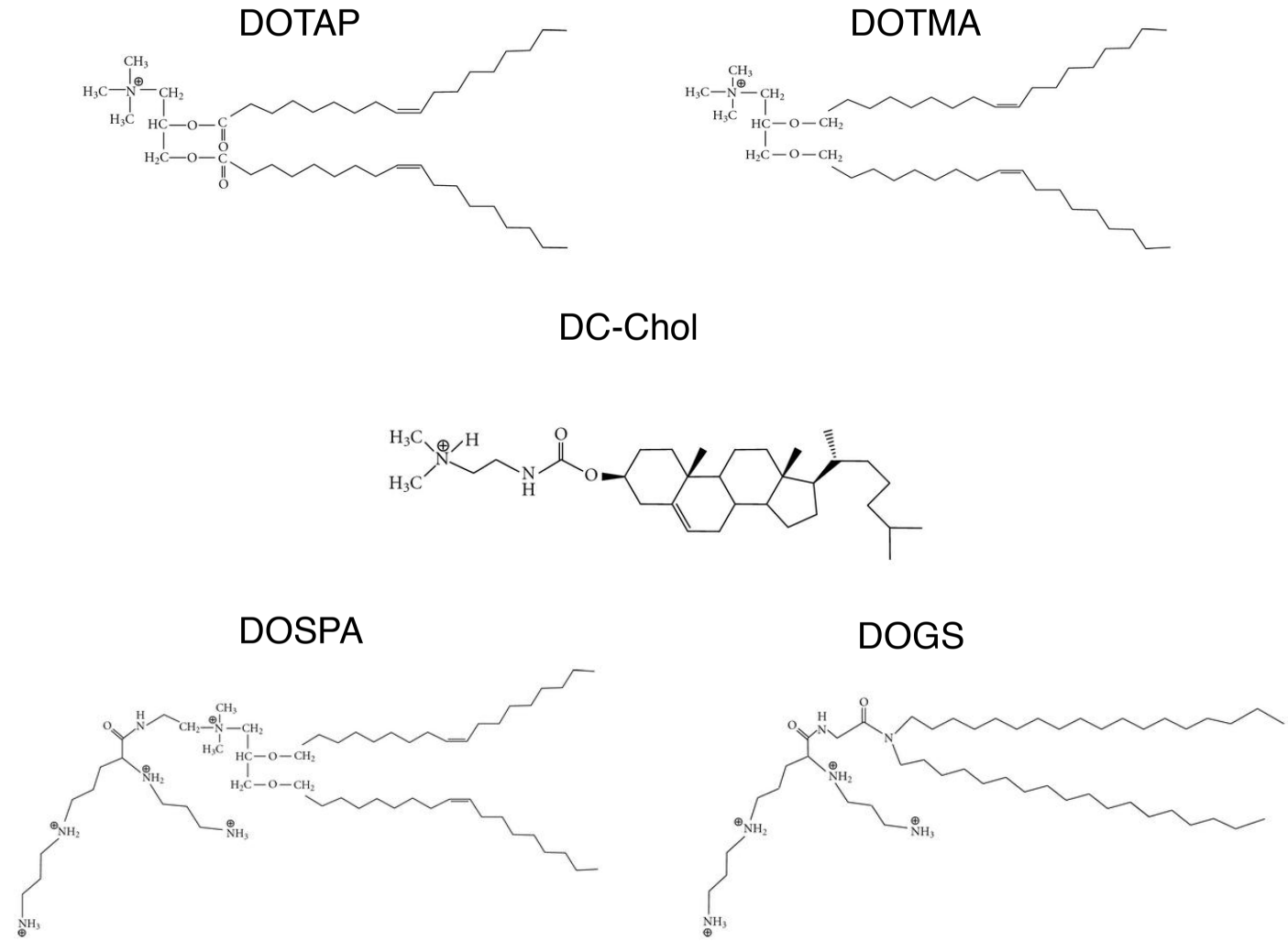

Figure 1.1: Chemical structures of common cationic lipids used as nonviral gene delivery carrier systems.

1.3.2. Cationic polymers

Cationic polymers are widely used in non-viral gene delivery systems (Gao, Kim et al. 2007; Kawakami, Higuchi et al. 2008; Ohlfest, Freese et al. 2005). Natural cationic polymers including chitosan(Mansouri, Lavigne et al. 2004) and atelocollagen (Sano, Maeda et al. 2003) or synthetic cationic polymers including poly(L-lysine) (PLL) (Oupický, Howard et al. 2000), polyethylenimine (PEI) (Eliyahu, Barenholz et al. 2005; Lungwitz, Breunig et al. 2005; Vasir and Labhasetwar 2006), and dendrimer (Eliyahu, Barenholz et al. 2005; Satija, Gupta et al. 2007) are used for pDNA delivery. The advantages of natural cationic polymers are their biocompatibility, biodegradability and lack of toxicity. On the other hand, synthetic polymers are flexible in gene delivery system design. Also, they can be tailored to fit the appropriate size and topology of the gene intended to be delivered. Also, hybrid systems of synthetic and natural cationic polymers are used synergistically to deliver DNA to target cells e.g. Chitosan-Polyetylenimine hybrid systems (Jiang, Kim et al. 2008). In gene delivery systems, degradation of the polymeric vector was also proposed to increase the transfection efficiency by facilitating the unpacking of the polymer/DNA complexes (polyplexes) after endocytosis (Ou, Wang et al. 2008). The unpacking of the polymer/DNA nanoplexes represents a major barrier for efficient transfection for many non-viral gene delivery systems.

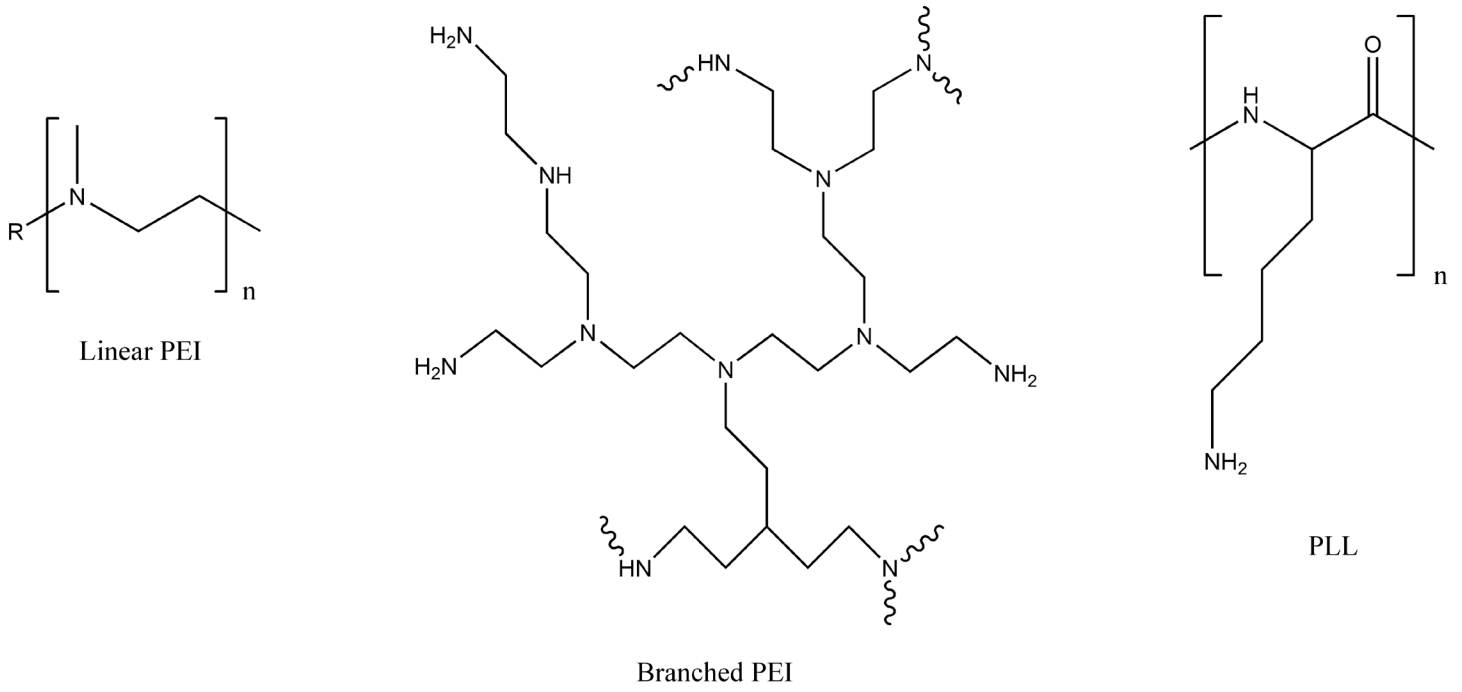

Figure 1.2: Chemical structures of linear and branched Polyethylenimine (LPEI and BPEI respectively) and poly(L-lysine) (PLL).

1.3.2.1. Chitosan

Chitosan is a natural highly biocompatible linear polysaccharide consisting of two randomly distributed subunits, D- glucosamine and N-acetyl-D-glucosamine linked by a β(1,4) glycosidic bond. Chitosan is a natural polymer produced commercially by deacetylation of chitin, which is the structural component in the exoskeleton of crustaceans. The cationic charge needed for pDNA condensation is generated from the primary amine in the monomer. Chitosan is available commercially in variable molecular weights, ~100 kD_a and ~ 22 kD_a. Low molecular weight chitosan (~ 22 kD_a) chitosan is generated through the addition of the high molecular weight chitosan to water followed by acetic acid (Kasaai 2009; Patel, Patel et al. 2010; Prabaharan 2008).

The transfection efficiency of chitosan is moderate compared to other polymeric carriers such polyethylenimine and is dependent on cell type (Erbacher, Zou et al. 1998). Moreover, the molecular weight of the used chitosan directly affects the transfection efficiency (Sato, Ishii et al. 2001). It was found that low molecular weight chitosans provides higher transfection efficiency and lower cytotoxicity than higher molecular weight chitosans (Lee, Nah et al. 2001). Chitosan has been modified to promote its efficacy, specificity and targetability with various chemical groups. These chemical groups include hydrophobic groups (Lee, Kwon et al. 1998), fusogenic peptides (MacLaughlin, Mumper et al.

1998), galactose for hepatocyte targeting (Cheng, Li et al. 2011; Gao, Chen et al. 2003; Jiang, Wu et al. 2011; Jiang, Kim et al. 2010; Jiang, Kwon et al. 2008; Jiang, Kwon et al. 2007; Lu, Wu et al. 2010) and other targeting moieties (Jiang, Kim et al. 2009).

1.3.2.2. Polyetylenimine (PEI)

No other polymer has been as widely studied in nonviral gene delivery than polyethylenimine (PEI) as it has the highest cationic density of any synthetic polymer currently available (Figure 1.2). PEIs were first synthesized and presented by Behr in 1995 (Boussif, Lezoualc'h et al. 1995), and have become one of the gold standards of nonviral gene delivery. Highly branched PEI and linear PEI are most commonly used, and were found to be capable of transfecting cells efficiently in-vitro as well as in vivo. PEIs offer a significantly more effective transfection and more effective shelter against nuclease degradation than other polycations such as PLL possibly due to their higher charge density, which results in more efficient complexation with negatively charged DNA. The high charge density resulting in more positive charge, however, presents some drawbacks. It results in a rather high toxicity of PEI polymers. The toxicity and the non-biodegradable of PEI are its main rate-limiting factors for its transition from bench to bedside.

The "proton sponge effect" is probably one of the most important factors contributing to the high transfection efficiency of PEI, which is mainly attributed to the high density of primary, secondary, and tertiary amino groups creating a significant buffering capacity to the polymers over a wide pH range.

1.3.2.3. Poly-l-lysine (PLL)

PLL was one of the first polymers used in nonviral gene delivery (Figure 1.2). PLL represents a large variety of polymers with different molecular weights (Wolfert, Dash et al. 1999). Poly(L-lysine) and its derivatives are effective gene delivery carriers with much less cytotoxicity compared with PEI (El-Aneed 2004; Hong, Leroueil et al. 2006; Jeon, Kim et al. 2003; Li, Zhu et al. 2009; Suh, Chung et al. 2001; Walsh, Tangney et al. 2006; Yamagata, Kawano et al. 2007). Transfection efficiency of PLL is significantly lower than PEI despite of the fact that both of them are comparably well taken up by the cells (Pouton, Lucas et al. 1998). This could be attributed to the lack of the PEI proton sponge effect (Merdan, Kunath et al. 2002). On the other hand, PLL also has a significant problem of prolonged cytotoxicity due to their high molecular weight. Thus, biodegradable forms of PLL have been developed to overcome these hurdles (Ahn, Chae et al. 2004; Jeong and Park 2002; Li, Y., L. C. Cui et al. 2007).

1.3.3. Biodegradable polymers

As discussed earlier, the main problems with the current strategies employed in non-viral gene carrier systems based on cationic polymers are their low transfection efficiency and their high cell cytotoxicity (Eliyahu, Barenholz et al. 2005). Previously, biodegradable polymers such as polyurethanes (PUs) that contain tertiary amines on the backbone and primary, secondary, and tertiary amines on the side chains have been synthesized as nonviral gene delivery vectors (Hung, Shau et al. 2009). To improve the solubility and biocompatibility of the polymers, the authors conjugated glycidol into the structure. These backbone modifications resulted in higher transfection efficiencies comparable to the well-known non-degradable gene carrier poly(2-(dimethylamino)ethyl methacrylate (PDMAEMA) and lower cytotoxicities. Similarly, Green and coworkers developed hydrolytically degradable poly(β-amino esters) as cationic polymers for gene transfer, which produced about four times higher gene expression in human embryonic stem cells with minimal toxicity (Green, Zhou et al. 2008). In addition, many other hydrolysable polymers such as poly(ester amines) (Arote, Hwang et al. 2008; Xu, Jere et al. 2008; Yamanouchi, Wu et al. 2008), poly(esters) (Bikram, Lee et al. 2005), ketalized PEI (Shim and Kwon 2009; Shim and Kwon 2009; Shim and Kwon 2008), chitosans (Jiang, Kim et al.), dendrimers (Eliyahu, Barenholz et al. ; Satija, Gupta et al.), and polyphosphazenes (Jun, Kim et al.

2007; Luten, van Steenis et al. 2003; Yang, Xu et al. 2008) have been developed to increase gene delivery whilst limiting cytotoxicities.

1.3.4. Bioreducible polymers

Recently, reducible disulfide-containing cationic polymers have also been extensively explored as an alternative to nondegradable gene delivery systems due to the difference in redox potential between the reducing cytoplasm and the oxidizing extracellular space (Saito, Swanson et al. 2003). As a way to enhance the biodegradability and reduce cytotoxicity, disulfide bonds are used as an efficient intra-polymer linkage to introduce biodegradability into polymer backbone. Inclusion of the disulfide bond is an innovative strategy using the normal biochemical mechanisms of the cell to delivery drugs and genes to target organs. A disulfide bond (–S–S–) is a covalent linkage, which is often found in secretory proteins and exoplasmic domains of membrane proteins. Two important characteristics that render this bond attractive in designing gene delivery systems are its reversibility and its relative stability in plasma. The high redox potential difference between the oxidizing extracellular space and the reducing intracellular space makes the disulfide bond a potential delivery tool. Thus, the covalent disulfide linkage is dependent on the location of the target tissue relative to the cellular compartments; a controlled cleavage and release of

reduced components can occur upon cell entry due to high redox potential difference. Thus, the inclusion of disulfide bonds within the polymeric carriers would render the polymers biodegradable as a result of the reduction of the bonds to free thiols in the cytosol followed by the concomitant release of the nucleic acid cargo.

Lots of trials and attempts have been proposed to overcome the drawbacks of non-viral gene delivery systems through the proper design of a reducible cationic polymeric backbone structure (Gao, Kim et al. 2007; Lungwitz, Breunig et al. 2005; Luten, van Nostrum et al. 2008; Martin and Rice 2007). The disulfide bond has been successfully applied in the preparation of bioresponsive and bioreducible polycations such as modified PEIs (Carlisle, Etrych et al. 2004; Gosselin, Guo et al. 2001; Lee, Mo et al. 2007; Wang, Chen et al. 2006), PLL (Miyata, Kakizawa et al. 2004), and fusogenic peptides (Kwok, McKenzie et al. 1999; McKenzie, Kwok et al. 2000; McKenzie, Smiley et al. 2000) for gene delivery carrier systems.

An important example of enhancing transfection efficiency through the inclusion of disulfide linkages in the polymer backbone is Poly(amidoamine)s or PAAs. The degradation of PAAs under physiological conditions is very slow, however, and it can be expected that amide hydrolysis does not contribute to the intracellular release of DNA from polyplexes of this polymer. Nevertheless, the

inclusion of disulfide bonds showed promise with respect to transfection efficiency and cytotoxicity (Lin, Blaauboer et al. ; Piest, Lin et al.). A novel family of linear poly(amidoamine)s was reported by Lin *et al.* that contains repetitive disulfide linkages in their main chain (SS-PAAs) as highly efficient intracellularly degradable gene delivery vectors (Lin, Blaauboer et al. ; Piest, Lin et al.). These SS-PAAs are relatively stable in the extracellular setting but are prone to fast degradation in a reductive environment analogous to that in the cytoplasm. Also it was reported that disulfide cross-linking of low molecular weight PEI results in largely improved transfection properties, attaining levels comparable to 25 kD_a branched PEI, while maintaining low degrees of cytotoxicity (Breunig, Hozsa et al. ; Peng, Zhong et al.). Peng *el al.*(Peng, Xiao et al. 2009; Peng, Zhong et al. 2008) synthesized a disulfide cross-linked polyethylenimine (PEI) via thiolation of low molecular weight PEI and it proved to be an efficient and less toxic gene carrier system. Jeong and coworkers showed triggered release of pDNA following reduction of disulfide-containing poly(amidoethylenimines) (SS-PAEIs) within the cytosol of several cell lines to increase transfection efficiency 20-fold compared with PEI (Hoon Jeong, Christensen et al. 2007).

Furthermore, Ou *et al.*(Ou, Wang et al.) demonstrated a poly(disulfide amine) for gene delivery with efficiency and low cytotoxicity. Another novel reducible disulfide poly(amido ethylenediamine) (SS-PAED) polymer carrier

represents another disulfide bond containing copolymer that was studied in vitro and in vivo by Kim *et al.* (Christensen, Chang et al. 2007). Mok *et al.*(Mok and Park 2008) developed a novel self-crosslinked and reducible fusogenic peptide (KALA, with two cysteine residues at the termini crosslinked via disulfide linkages) for stable formation of cationic complexes with an siRNA-PEG conjugate to enhance transfection efficiency and cell viability.

Reducible hyperbranched poly(amido amine) (RHB) polycation and plasmid DNA in the form of Layer-by-layer (LbL) films assembled on a flexible stainless steel substrate were tested in vivo and in vitro as a gene delivery carrier (Blacklock, You et al. 2009). Poly(DAH/CBA) synthesized through polyaddition of 1,6-diaminohexane and cystamine bisacrylamide represents another example of a reducible gene delivery carrier that was able to tightly condense PGE(2)-siRNA conjugate to form nanosize polyplexes having a diameter of 100-150 nm (Kim, Jeong et al. 2008). Histidine containing reducible polycations based on CH(6)K(3)H(6)C monomers (His6 RPCs) represent another highly effective DNA transfection agents. This polymer combines the pH buffering endosomal escape mechanisms from histidine along with fast release of its DNA content in reductive environment of the cytoplasm (Stevenson, Ramos-Perez et al. 2008). Another example of the use of histidine-based copolymers is a reducible copolypeptide (rCPP) carrier containing different molar ratios of a histidine-rich peptide (HRP)

and a nuclear localization sequence (NLS) peptide to control the intracellular trafficking of transfected siRNA and primary RNA transcripts (pri-miRNA) (Rahbek, Howard et al. 2008). Reducible polycations based on oligomers of 2-dimethylaminoethyl methacrylate (DMAEMA) containing terminal thiol groups represent promising carriers of therapeutic nucleic acids (You, Manickam et al. 2007; You, Manickam et al. 2007; You, Zhou et al. 2007).

Although all of the previously mentioned polymers, PEI, PLL and PAA, enclose disulfide bonds within their backbone structures resulting in good cell viability and transfection efficiency profiles, they are not fully biodegradable and safe. These findings highlight a critical need for developing biodegradable and biocompatible cationic polymers, which have low cytotoxicities so as to maintain cell viability and high transfection efficiencies.

1.4. Barriers for nonviral Gene Delivery

Although there is serious effort to design new effective and safe nonviral gene delivery systems and the use of various synthetic lipids and polymers gene therapy for the last 25 years, numerous hurdles hinder the proper design of a complete nonviral gene delivery formulation that can properly deliver the genetic material from a convenient route of administration to the desired site of action. There are five major steps that summarize the journey of the gene carrier system

from site of administration to the site of action. These steps illustrated in figure 1.3 are (1) efficiently reaching the target organ, (2) carrier system cell uptake, (3) escaping from the endosomes or avoiding its harm, (4) transport through the target cell cytoplasm, (5) unpacking of genetic material or (6) carrier system nuclear uptake (Kay 2011).

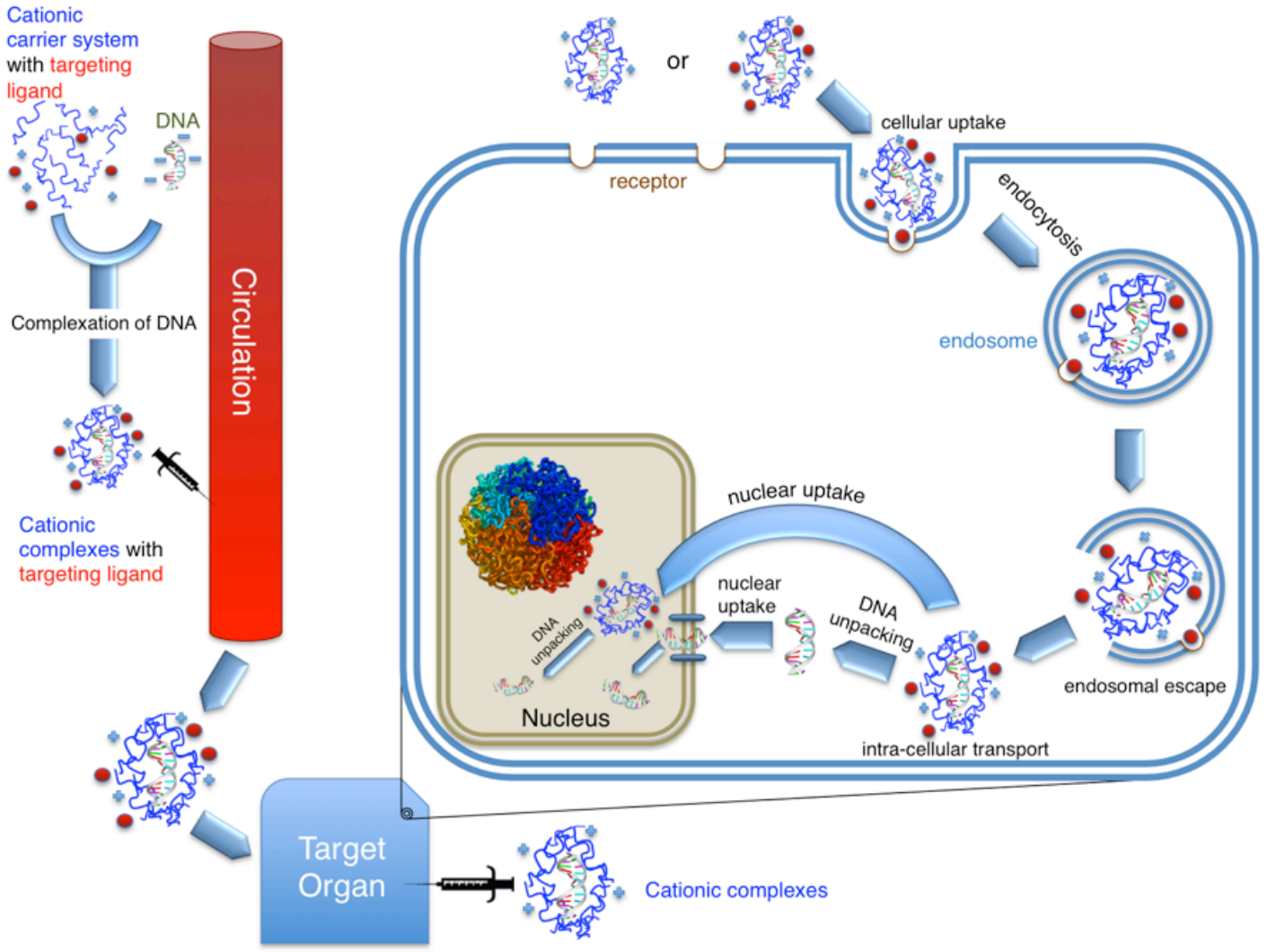

Figure 1.3: Pathway for nonviral gene delivery vehicles from site of administration to the site of action.

1.4.1. Gene delivery system administration and translocation to target organ

For the first step to be successful, a gene therapy carrier system should be administered into the body locally (local administration such as, tissue injection) or systemic administration (such as, intravenous injection or infusion) (Kay 2011). This system must reach the target tissue to allow for therapeutic levels of transgene expression. The general trend and strategy adopted by most researchers is the use of local administration to bypass the first barrier in gene delivery. This could be a successful strategy in the short term to concentrate on overcoming the other barriers but in order for gene therapy to succeed, a convenient route of administration should be used, especially because most transgene expression is transient and not permanent. Moreover, using a proper route of administration such as the IV route will require lots of effort, as it will be dealing with a double formulation. Such double formulation will include the DNA packages within its cationic carrier system and the second formulation will be packaging the cationic carrier system within a targeted stable delivery system to transport and release the cationic carrier system safely to the site of action. Moreover, extensive research is crucial for nonviral gene delivery systems to achieve biocompatibility, targeting, persistence of gene expression and sufficient cellular trafficking and nuclear trafficking.

1.4.2. Targeting of nonviral gene carrier system

Formulation of a fully targeted gene carrier system is the ultimate goal for gene therapy. Targeting of nonviral gene carrier system provides a remarkable benefit of reaching the target organ. For targeting strategy to be successful, it must be specific and circumvent uptake by the reticuloendothelial system (RES). One of the widely used techniques to evade the immune system defense through the RES is Pegylation. Pegylation involves conjugating the carrier system covalently to a PEG spacer (Abuchowski, McCoy et al. 1977). PEGylation provides the advantages of avoiding the RES uptake, scavenger macrophages, and Kupffer cells (Bhadra, Bhadra et al. 2002; Caliceti and Veronese 2003; Chaudhari, Ukawala et al. 2011; Roberts, Bentley et al. 2002). This is basically achieved through hiding the formulation within a large PEG layer creating a stealth carrier system (Bhadra, Bhadra et al. 2002; Guo and Huang 2011). Pegylation provides several advantages for gene and drug delivery including: (1) favorable protection of the gene or drug from the surrounding nucleases in vivo through an extensive shielding profile beyond the hydrodynamic radius of the PEG layer, (2) prevents damage to the drug or gene through the binding of the serum components in the circulation and (3) keeping a sufficient distance between the carrier system and the target receptor (Jain and Jain 2008; Milla, Dosio et al. 2011; Veronese and Pasut 2005; Yang, Lopina et al. 2008).

Targeting can be active or passive. Active targeting uses targeting ligands for specific receptors on the target cells. Various targeting ligands have been used in gene delivery systems. For example, sugar moieties, such as galactose, are used for targeting the asialoglycoprotein receptors on hepatic cells. (Fisher and Wilson 1994; Han, Lim et al. 1999; Hashida, Takemura et al. 1998; Kawakami, Fumoto et al. 2000; Nishikawa 2005; Wakebayashi, Nishiyama et al. 2004; Wu and Wu 1991). Jiang *et al*, have used galactose to target hepatocytes for gene therapy using PEI and chitosan/tripolyphosphate (Jiang, Wu et al. 2011; Jiang, Kim et al. 2010; Jiang, Kwon et al. 2008; Jiang, Kwon et al. 2007). Another sugar moiety used for active targeting is mannose. Mannose conjugated to PEI has been shown to target dendritic cells and antigen presenting cells (APCs) for non viral gene delivery (Diebold, Kursa et al. 1999; Diebold, Lehrmann et al. 1999; Jiang, Kim et al. 2009; Park, Kim et al. 2008; Sato, Kawakami et al. 2001). Other targeting groups include sulfonylurea (SU), which is used to target pancreatic islet cells (Kang, Kim et al. 2005).

Various ligands are used for targeting genes to cancer cells including folic acid and transferrin. Transferrin has been widely used as a tumor cell target due to its abundant expression on tumor cells (Crane, Arts et al. 2011; D'Angelica, Ammori et al. 2011; Dixon, Mulligan et al. 1992). Folate receptor mediated gene targeting provides the benefit of high concentration of gene delivery to specific

cancer sites including brain, lung, ovary, uterus and kidney where folate receptors are over expressed. Morris and Sharma used folic acid for tumor targeting using poly(ethylene glycol)-folic acid (PEG-FA) conjugate coupled with an arginine modified oligo (alkylaminosiloxane) graft poly(ethyleneimine) gene carrier system (Morris and Sharma 2011). This system showed enhanced transfection efficiency compared to poly(ethyleneimine) (Morris and Sharma 2011).

On the other hand, passive targeting uses the delivery system's physicochemical parameters such as charge and size to facilitate targeting to a tissue without using specific ligands. Most nonviral gene delivery carrier systems have a positive charge, which creates an electrostatic attraction to negatively charged cell membranes, due to the presence of anionic sialic acid groups on the cell surface, facilitating mammalian cell entry (Karmali and Chaudhuri 2007; Opanasopit, Nishikawa et al. 2002).

1.4.3 Cellular uptake and intracellular transport

The mechanism of cell entry and transport through the cytosol are two main factors hindering nonviral gene delivery carriers from surpassing viral carriers in transfection efficiency. The uptake of a cationic gene carrier system is primarily initiated via the electrostatic attraction forces between the

cationic complexes and the anionic sialic acid molecules on the cell membrane surface. Afterwards, cationic complexes may be internalized by nonspecific adsorptive endocytosis, pinocytosis, or phagocytosis (Leonetti, Degols et al. 1990; Mannisto, Reinisalo et al. 2007). Pinocytosis and phagocytosis are functions of particle size with pinocytosis mainly accounts for particles with particle size less than 200 nm. Targeting ligands such as folic acid, transferrin and sugar moieties linked to cationic polymers have been widely used to enhance cellular internalization simulating viruses, which typically use receptor-mediated pathway for cellular internalization.

1.4.4. Endosomal escape

Many of its limitations of nonviral gene delivery are related to compartmentalisation of the genetic material along with the carrier system within the endosomes (Dominska and Dykxhoorn 2010). Gene expression and transfection efficiency enhancers have become an essential part of manipulating endosomal escape and/or release, as well as protecting the genetic material from intracellular degradation. However, disruption of the endosomes can also release degradative proteases, which can initiate apoptotic pathways (Minchin and Yang 2010). Endosomal escape involves two general mechanisms: membrane disruption and proton sponge effect. Lately, the use of the membrane disrupting

fusogenic compounds has drawn much attention for the design of nonviral gene delivery carriers. Histidines with its fusogenic activity were shown to disrupt the membrane of acidic subcellular compartments such as endosomes and lysosomes. Histidines are uncharged at physiological pH and positively charged in acidic environment, which imparts selective membrane disruption in the acidic endosome. The imidazole group of histidine has a pKa of ~ 6.0, therefore allowing it to become protonated in the acidic environment of the endosome inducing a strong buffering capacity within the cells (Kichler, Leborgne et al. 2003; Midoux, Kichler et al. 1998; Midoux, LeCam et al. 2002; Midoux and Monsigny 1999; Pichon, Goncalves et al. 2001). In addition, histidine has been shown to fuse with lipid bilayers upon protonation of imidazole groups as a result of interaction with negatively charged membrane phospholipids (Wang and Huang 1984). Endosomal escape has been shown to increase with conjugation of other fusogenic membrane-active peptides to cationic vectors, such as melittin and its analogs (Boeckle, Fahrmeir et al. 2006), GALA (Li, Nicol et al. 2004), influenza virus A/WSN/33 hemagglutinin fusion peptide chain (HA2) (Plank, Oberhauser et al. 1994), influenza virus X-31 (H3N2) amino-terminal peptide sequence (Macosko, Kim et al. 1997).

Polyethylenimine, on the other hand, uses its buffering capacity to escape from the endosomal compartment. The main reason for the effectiveness of PEI

as a gene delivery carrier is due to its tremendous buffering capacity commonly refered to as the “proton sponge effect” ranging between pH 7.2 and 5.0. The average pKa’s of bPEI are reported to be 9.5, 6.9 and 3.9 for the protonable 1˚, 2˚, and 3˚ amines in a 1:2:1 ratio respectively. In the proton sponge effect, there is a lowering of pH due to the ATPase pumps activated by the maturation of the endosomes to lysosomes, which actively move protons into the vesicles accompanied by passive influx of chloride and water ions (Boussif, Lezoualc'h et al. 1995; De Smedt, Demeester et al. 2000; Kircheis, Wightman et al. 2001; Kircheis, Wightman et al. 2001; Zanta, Boussif et al. 1997). As a consequence, the endosomal vesicles swell and rupture and their contents are delivered into the cytosol. For this reason, PEI overcomes the limitations of the endosomal degradative pathway and provides high transfection efficiency. Cationic lipids require the use of a neutral colipid for endosomal release as compared to PEI (Hafez, Maurer et al. 2001).

1.4.5. Nuclear translocation and uptake

The nuclear translocation and uptake are key obstacles towards successful and efficient nonviral transfection and gene therapy. After delivery of the gene carrier system to the cytoplasm, the therapeutic plasmid must travel to the nucleus to impart its therapeutic effect. The carrier system/pDNA

decomplexation is crucial for transfection efficiency. The decomplexation of the carrier system/pDNA complexes should take place at or after the late endosomes to prevent the break down of the pDNA by the endosomal degradative system. There is a critical need for in-depth mechanistic studies of the polymer/pDNA decomplexation and development of smart polymeric carrier systems, which facilitate polymer/pDNA decomplexation in the cytoplasm while keeping the pDNA stable and intact. Usually, pDNA dissociates from the late endosomal complex. The microtubule network that mobilizes vesicles within the cellular compartment facilitates the transportation of the gene carrier system within the cytoplasm to the nucleus and aids increased nonviral gene expression. A rate limiting factor for efficient nonviral gene delivery is the cytosolic distance that must be travelled prior to nuclear import (Lam and Dean 2010). Unexpectedly, in some cases, the polymer/pDNA complexes may end up in the nucleus intact. In these cases, it is not necessary for pDNA/carrier system to decomplex for nuclear uptake. The mechanism of such pDNA/carrier nuclear uptake is unknown (Godbey, Wu et al. 1999). The nuclear pore complex (NPC) is another rate limiting barrier for efficient nonviral gene expression. In case of actively dividing cells, the passage through the nuclear pore complex is not essential as a thinning of the nuclear envelope takes place facilitating the entry of the therapeutic pDNA. On the other hand, in the case of nondividing cells, passage through the nuclear

pore complex is required. Furthermore, the size and the topology of the genetic material may affect the rate and the degree of nuclear uptake of the genetic material (Kamiya, Yamazaki et al. 2002). A main technique to enhance nuclear translocation and uptake is the use of nuclear localization signals (NLS) (Aronsohn and Hughes 1998; Jans, Chan et al. 1998; Zanta, Belguise-Valladier et al. 1999). A nuclear localization signal or sequence (NLS) is an amino acid sequence, which 'tags' a protein/carrier system for uptake into the cell nucleus. Nuclear localization signals are usually lysine and arginine rich peptide sequences (Ritter, Plank et al. 2003). NLS bound carrier systems will bind sturdily to importin forming a complex. The complex will have the ability to pass the nuclear pore. Upon nuclear entry, the carrier system/protein will be released with the aid of Ran-GTP. Ran-GTP will bind to the importin-protein complex. Afterwards, importin will lose affinity for the carrier system/protein. Finally, Ran-GTP/importin complex will traffic back out of the nucleus through the nuclear pore (Jans, Chan et al. 1998).

1.4.6. Biocompatibility and in vivo stability

In spite of the fact that viral vectors are capable of high degrees of transgene expression and integration into the host genome, these same benefits also prove disadvantageous to its transition from bench to bedside. Many

incidents during in vivo trials adversely affected the development of the viral gene carrier systems and prompted the use of alternative nonviral gene carrier systems, including the death of Jesse Gelsinger in 1999 from retroviral treatment for a metabolic disorder (2000; Somia and Verma 2000; Stolberg 1999; Teichler Zallen 2000) along with the emergence of leukemia as a side effect through treatment of children with X-SCID (Ashcroft 2004; Engel, Kohn et al. 2003; Kaiser 2005; Kaiser 2003; Thrasher, Gaspar et al. 2006; Woods, Bottero et al. 2006). Such disastrous consequences of the viral gene therapy clinical trials have grown into public criticism of gene therapy trials as a whole, further limiting the advancement of clinical gene therapy trials.

Stability in vivo is a key concern for efficient gene transfection. Proteases and nucleases present throughout the systemic circulation represent a main degradative threat to gene carrier systems. Furthermore, the cationic gene carrier systems may suffer from harmful electrostatic interactions with anionic serum components such as albumin. Such interaction creates a protein coating, which promotes the clearance rate of cationic complexes through the reticuloendothelial system (RES) pathway. Additionally, this protein buildup around the carrier system would diminish the transfection efficiency and transgene expression. Creating a stealth layer of PEG (PEGylation) on the gene carrier system has been used to overcome protein binding and uptake by the RES.

1.4.7. Toxicity and immunogenicity

Although the viral gene delivery systems received most of the attention in clinical trials for gene therapy, delivery of foreign DNA using viral vectors has not been without its problems. The main problems involving viral carrier system include limited gene size, low production yield, mutagenicity and immunogenicity (Debyser 2003; Giordano, Causa et al. 2006; Kay, Glorioso et al. 2001). The ability of viruses to elicit an immune response can lead to catastrophic consequences as seen with the adenoviral-mediated multisystem organ failure with Jesse Gelsinger and leukemia in children being treated for X-linked severe combined immunodeficiency (X-SCID) as a result of insertional mutagenesis by the retroviral vector (Ashcroft 2004; Kaiser 2005; Kaiser 2003; Science and AAAS 2000; Smith and Byers 2002; Thrasher, Gaspar et al. 2006; Woods, Bottero et al. 2006; Yi, Noh et al. 2011). Moreover, industrial scale-up of viral gene carriers is burdened with possible faults and the costs of production. Considering that a million viral particles used in gene therapy may be injected into a human, the probability that the entire batch is free of all harmful sequences is impossible. Nonviral gene carriers have been deployed as an alternative to viral gene delivery systems. Nonviral gene carriers are not typically prone to elicit immunogenic responses; however, high molecular weight polymers such as BPEI and LPEI may contribute to an increased immunogenic response due to some

cytotoxic effects. BPEI 25k has been shown to provide effective levels of transfection efficiency and transgene expression; however, it is limited in use due to cytotoxic effects (Chollet, Favrot et al. 2002). The high molecular weight of PEI is the main reason for its toxicity, which causes the disruption of the cell membrane. Moreover, the buffering capacity of PEI, which is the main reason for its high transfection efficiency, causes swelling and rupture of the endosomal vesicles and their contents are delivered into the cytosol, which initiates the apoptotic cell death mechanism. PLL and its derivatives have been shown to be very effective gene delivery carriers with much less cytotoxicity compared with PEI (El-Aneed 2004; Hong, Leroueil et al. 2006; Jeon, Kim et al. 2003; Li, Zhu et al. 2009; Suh, Chung et al. 2001; Walsh, Tangney et al. 2006; Yamagata, Kawano et al. 2007). However, PLL and its derivatives also pose a significant problem of prolonged cytotoxicity due to their high molecular weight. Thus, biodegradable forms of PLL and PEI have been developed to overcome these limitations (Ahn, Chae et al. 2004; Jeong and Park 2002; Li, Y., L. Cui et al. 2007).

As the scope and extent of nonviral gene delivery research grows, there is a critical need for a reliable *invivo invitro* correlation for cytotoxicity of nonviral gene carrier systems. Such correlation will decrease the possible risks in in-vivo clinical trials. Currently, various steps are being considered in in-vitro studies to

better optimize nonviral gene delivery systems for applications in-vivo and ex-vivo. First, transfection efficiency studies are commonly performed in cell culture without the presence of serum. Following the proper optimization of the transfection efficiency study, media containing serum, usually 5 - 10% v/v are being used in subsequent transfection efficiency studies. Zelphati and Szoka *et al.* suggested the use of higher serum concentrations for in vitro assays before moving to the in vivo model (Zelphati, Uyechi et al. 1998). Moreover, different cell viability assays should be adopted in-vitro in cell cultures before processing for in-vivo or ex-vivo studies. This could provide a more comprehensive overview of the cytotoxicity of the gene carrier system. For example, MTT and LDH cell viability assays are base on the cell mitochondrial activity and cell membrane integrity, respectively. Combining the results from both assays would provide a clear overview of the cytotoxicity of the gene carrier system.

2. Objective and specific aims

To address the current challenges of nonviral cationic polymers, our aim in this thesis is to develop nonviral linear lysine based peptidomimetic biocompatible reducible copolymers (LLCs) as an efficient and safe nonviral gene delivery system. Poly(L-lysine) and its derivatives have been shown to be very effective gene delivery carriers with much less cytotoxicity compared with PEI. However, these carriers also pose a significant problem of prolonged cytotoxicity in clinical applications due to their high molecular weight. Thus, biodegradable forms of PLL have been developed to overcome these hurdles. Therefore, to further develop PLL as an efficient biodegradable and bioreducible alternative to non-biodegradable gene delivery systems, we report the synthesis of novel disulfide-reducible linear L-lysine modified copolymers (LLCs). LLCs consist of repeating peptidomimetic blocks of lysine functionalized with ethylenediamine as a source of 1° amines joined together by reducible disulfide bonds as an alternative to non-biodegradable PLL and PEI. Incorporation of lysines will facilitate polymer/DNA compaction. We **hypothesize** that low molecular weight lycationic blocks linked together by disulfide bonds would produce a biocompatible nonviral gene delivery system with high transfection efficiency. Our **rationale** is that the combination of reducible backbone structure and cationic biocompatible lysine based blocks will facilitate efficient delivery of the nucleic

acid cargo into the cytoplasm to significantly increase the subcellular trafficking and hence the transfection efficiency with negligible cytotoxicity.

We propose the following specific aims:

Specific Aim 1: To synthesize and characterize novel biocompatible reducible linear L-lysine modified copolymers (LLCs). The working hypothesis is that lysine peptidomemetic backbone linked by disulfide bonds and functionalized with 1° amines would be a successful gene carrier system through providing high transfection efficiency and cell viability.

Specific Aim 2: To characterize the physicochemical properties of DNA/LLC polyplexes *in vitro*. Our working hypothesis is that LLCs with the design attributes discussed in specific aim 1 would provide strong DNA compaction and stable DNA/LLC polyplexes of higher transfection efficiency and lower cytotoxicity than the high molecular weight PLL.

Specific Aim 3: To investigate the *in vitro* efficacy of DNA/LLC polyplexes for transfecting human mesenchymal stem cells to express VEGF, creating a transplantable continuous source of angiogenic cytokines for *in vivo* treatment of myocardial infarction. The hypothesis is that these genetically modified stem cells would promote revascularization of an infarcted region of the heart, reducing myocardial damage and scar formation.

The development of nonviral biodegradable polymeric carrier systems that can overcome the extracellular and intracellular barriers and maintain high transfection efficiencies is a key milestone towards the transformation of gene therapy from bench to bedside. The current design of LLCs with the reducible disulfide backbone will significantly enhance the cytosolic delivery and intracellular localization of the therapeutic gene. These LLCs represent a promising reducible platform technology for nonviral gene therapy, which will potentially enhance gene expression and cell viability.

3. Design, synthesis and characterization of reducible linear lysine-based copolymers (LLC)

3.1. Introduction

Cationic polymers provided one of the first promising methods of nonviral gene delivery toward providing effective gene delivery without the immunogenicity and toxicity commonly seen with viral vectors. They have advantages such as non-immunogenicity, convenience of handling, and unlimited delivery capacity of genetic materials over viral vectors (Demeneix, Behr et al. 1998; Liu and Huang 2002; Luo and Saltzman 2000).

To address the current challenges of nonviral cationic polymers, our objective is to develop a nonviral linear lysine-based peptidomimetic biocompatible reducible copolymers (LLCs) as an efficient and safe nonviral gene delivery system. Poly-L-lysine and its derivatives have been shown to be very effective gene delivery carriers with much less cytotoxicity compared with PEI (Akinc, Thomas et al. 2005; Boussif, Lezoualc'h et al. 1995; Hunter 2006; Moghimi, Symonds et al. 2005). However, these carriers also pose a significant problem of prolonged cytotoxicity in clinical applications because of their high molecular weight (Ahn, Chae et al. 2004; Guping, Guping et al. 2005; Li, Y., L. Cui et al. 2007). Thus, biodegradable forms of PLL have been developed to

overcome these hurdles (Dekie, Toncheva et al. 2000; Dubruel, Dekie et al. 2003; Li, Y., L. C. Cui et al. 2007).

Therefore, to develop PLL further as an efficient biodegradable and bioreducible alternative to non-biodegradable gene delivery systems, we report the synthesis of novel disulfide-reducible linear L-lysine modified copolymers (LLCs) based on the natural amino acid, L-lysine, as cationic polymers for nonviral gene delivery via Michael addition (Figure 3.1). We hypothesize that the use of natural amino acids can yield polymers that have very low cytotoxicities but high transfection efficiencies because of the presence of reducible disulfide bonds in the polymer backbone structure. LLCs consist of repeating peptidomimetic blocks of lysine functionalized with ethylenediamine as a source of 1° amines joined by reducible disulfide bonds as an alternative to non-biodegradable PLL and PEI. Incorporation of lysines will facilitate polymer/DNA compaction. This section contains results from one completed study published in the Journal of Controlled Release (Nounou, Emmanouil et al. 2010) and presented at various pharmaceutical and bioengineering conferences.

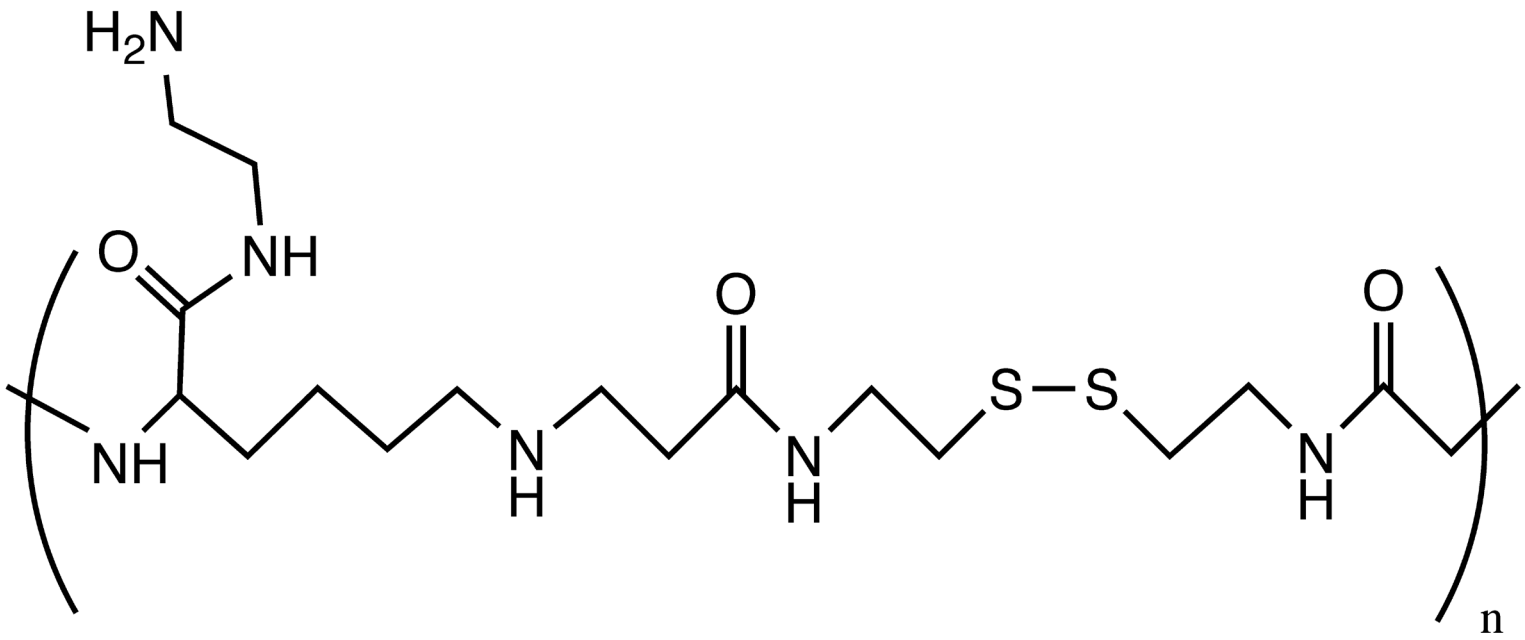

Figure 3.1: Chemical structure of the Linear L-lysine Modified Copolymers (LLCs).

3.2. Materials and methods

3.2.1. Materials

N-butyloxycarbonyl ethylenediamine, L-lysine HCl, hyperbranched polyethylenimine (bPEI, MW 25 kD_a), trifluoroacetic acid (TFA), poly-L-Lysine (PLL, MW 20900 D_a), dithiothreitol (DTT), ethidium bromide (EtBr), ninhydrin reagent, 3-(4,5-dimethyl-2-thiazolyl)-2,5-diphenyl-2H-tetrazolium bromide (MTT), and sodium dodecyl sulfate (SDS) were purchased from Sigma-Aldrich (St. Louis, MO). N,N´-cystaminebisacrylamide (CBA) was purchased from PolySciences, Inc. (Warrington, PA). The molecular weights of the various polymers were determined by size exclusion chromatography (SEC) on a Shimatzu Prominence HPLC system (Shimadzu Scientific Instruments, MD) equipped with a Shodex SB-803-HQ (Particle size = 6 nm) and Shodex SB-806-HQ (particle size = 13 nm) columns in series and detected using photodiode array (PDA) and low temperature evaporative light scattering detectors (ELSD-LTII) (Columbia, MD).

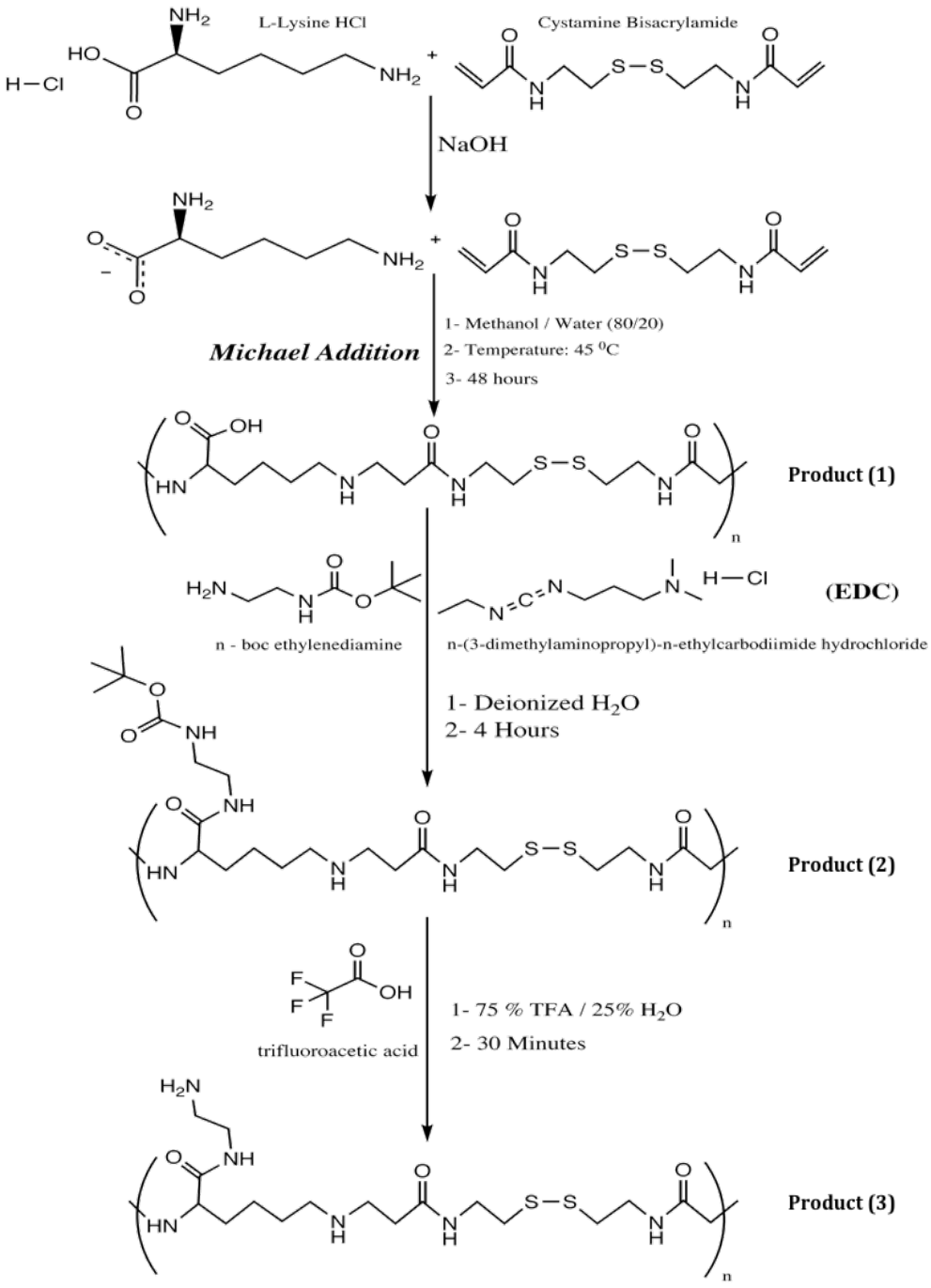

Figure 3.2: Synthesis scheme of the Linear L-lysine Modified Copolymers (LLCs).

3.2.2. LLC Synthesis

3.2.2.1. Synthesis of reducible linear L-lysine-modified copolymers (LLC) backbone (without ethylenediamine)

A novel reducible linear L-lysine-modified copolymers (LLC) was synthesized by Michael addition (Michael 1887) between N,N′ cystaminebisacrylamide (CBA) and L-Lysine HCl. The lysine monomers were activated by neutralization of the acid form of the amino acid with sodium hydroxide (NaOH) and the activated lysine then was reacted with CBA. Briefly, 730.6 mg L-lysine HCl (4 moles) and 1060 mg CBA (4 moles) were weighed and transferred to a 50 ml round-bottom flask. 160 mg of NaOH was used (4 moles) to neutralize the HCl present in the L-Lysine starting material. Then, 10 ml of a mixture (80/20 v/v) of methanol/water (MeOH/ H_2O) was added to the flask, which was stirred in an oil bath at 45° C to dissolve the reagents. The reaction then was stirred in the dark under a nitrogen atmosphere for 2 days. The resulting solution then was dissolved in ultrapure water and the reaction solution was purified via dialysis (MWCO 2000) against water for 2 days to remove low molecular weight polymeric products and any remaining traces of the starting materials. The dialyzed solution then was transferred to a sterile conical tube and lyophilized for 2 days. The reaction scheme is shown in Figure 3.2. The resulting

polymers were characterized with proton nuclear magnetic resonance (^{1}H NMR), gel permeation chromatography (GPC), and matrix-assisted laser desorption ionization-time of flight (MALDI-TOF).

3.2.2.2. Conjugation of N-boc ethylenediamine to the synthesized reducible LLC backbone

For the objective of increasing the efficacy of the condensation of the synthesized polymers to the therapeutic DNA, increasing the number of nitrogen atoms on the polymer backbone is advantageous. Conjugation of the synthesized polymer with N-boc ethylenediamine has been used for this purpose. To optimize the conjugation of N-boc ethylenediamine to the polymer backbone, 5 different copolymers were prepared by varying the amounts of EDC and N-boc. Briefly, 100 mg each of reducible LLC (0.033 moles) were weighed and transferred to 5 different round-bottom flasks to which 6 ml of deionized water was added to fully dissolve the polymers with stirring. To the dissolved polymers 5, 10, 15, 20, and 25 molar excess of EDC (192, 384, 576, 768 and 960 mg respectively) and N-boc ethylenediamine (60, 120, 180, 240 and 300 mg respectively) then were added to each of the respective reaction mixtures, which were stirred in an oil bath at 40° C in the dark under a nitrogen atmosphere for 4 hours. After this time, the reaction solutions were transferred to separate dialysis bags (MWCO 2000)

and dialyzed against deionized water for 2 days to purify the copolymers from the starting materials. The dialyzed polymers then were transferred to sterile conical tubes and dried on a lyophilizer for 2 days. The resulting polymers were characterized with ^{1}H NMR, GPC, and MALDI-TOF.

3.2.2.3. Deprotection of N-boc-conjugated reducible LLC

The acid-liable N-boc amine protection group present on the conjugated ethylenediamine was removed with a trifluoroacetic acid (TFA)/H_2O mixture (75/25 v/v). Briefly, 100 mg of reducible LLC was added to a round-bottom flask to which 10 ml of deionized H_2O were added. Afterward, 30 ml of TFA were added. The dissolved copolymers were stirred for 30 minutes at room temperature. The final polymers then were purified by dialysis (MWCO 2000) against deionized water for 2 days to remove the free N-boc groups and TFA. The dialyzed polymers then were transferred to a sterile conical tube and dried on a lyophilizer for 2 days. The resulting polymers were characterized with ^{1}H NMR, GPC, and MALDI-TOF. The reducible LLC that showed the maximum amount of ethylenediamine conjugation as determined with ^{1}H NMR then was designated the optimum reducible LLC and was selected for use in subsequent assays.

The bioreducible modified copolymers LLC were analyzed by ^{1}H NMR (300 MHz, D_2O) and the data are listed in the results section.

3.2.3. Characterization of LLC intermediates and final product

The bioreducible modified copolymers (LLC) intermediates and final product were analyzed by ^{1}H NMR (300 MHz, D_2O) at room temperature to determine and verify the chemical structure. The peptide concentration used in all ^{1}H NMR experiments was 4 mg/ml.

The content of the primary amine group in the primary, intermediate, and final polymer was quantified by a ninhydrin test at 570 nm. The assay was conducting at 100° C for 15 minutes. Glycine was used to construct standard curves.

The molecular weights of the various polymers were determined by size exclusion chromatography (SEC) on a Shimatzu Prominence HPLC system (Shimadzu Scientific Instruments, MD, USA) equipped with a Shodex SB-803-HQ (Particle size = 6 nm) and Shodex SB-806-HQ (particle size = 13 nm) in series, and PDA and low temperature evaporative light scattering detectors (ELSD-LTII), eluted with ammonium acetate buffer using (0.15 M) of pH 4.4 with methanol (80/20) at a rate of 1 ml/minute. The detector temperature was adjusted to 40 °C. Molecular weights were calibrated using a polyethylene glycol kit with different

molecular weights. The HPLC data of the polymers are given in the supporting information.

The molecular weights of the various polymers were also determined by DE-STR (PerSeptive Biosystems/ABI) mass spectrometer with MALDI ionization at the University of Utah, Mass Spectrometry and Proteomics Core Facility. The matrix used was saturated alpha-cyano-4-hydroxycinnamic acid dissolved in 50/50 acetonitrile/water with 0.1% TFA with polymer concentration 1mg/ml. 8ul of the polymer was spotted with an equal volume of matrix, and air-dried on the plate.

3.3. Results and discussion

The use of cellular and subcellular targeting moieties, delivery-enhancing molecules, or functional entities along with the backbone of a drug moiety and/or their delivery systems has become an essential and important approach in the field of novel drug delivery. For bioconjugates, the nature of the linker between the drug moiety and the delivery-augmenting moiety dictates the degree of successful delivery. Among various covalent linkages, is the readily reversible yet relatively stable linkage of disulfide bonds.

The LLC copolymers of the type $(AB)_n$ consisting of repeating units of the natural amino acid, L-lysine and cystamine bisacrylamide (CBA) were successfully synthesized via Michael addition reaction. These novel reducible linear L-lysine copolymers (LLCs) were then modified with ethylenediamine so as to introduce primary amines for efficient DNA condensation. The chemical synthesis was reproducible and of high yield (~ 78%). The only limitation in this chemical synthesis was that any deviation from the temperature (45° C) and reaction duration (2 days) variables yielded shorter molecular weight polymer.

The structures of starting, intermediate, and final polymers were confirmed by ^{1}H NMR (300 MHz, D_2O) (Figures 3.3-3.9). Also, using the ^{1}H-NMR spectra of the N-Boc peak (I) for the intermediate polymer using different molar ratios with

N-Boc ethylene diamine and EDC, the molar ratios of 5, 10, 15, 20 and 25 N-Boc Ethylene diamine with respect to the parent polymer yielded conjugation ratios of 1.957, 3.33, 3.84, 7.5 and 2.3 respectively (Figures 3.4-3.8, Table 3.1). The degree of EDA conjugation to the copolymer backbone as determined with ^{1}H NMR, was found to be 25%, 42%, 48%, 94% and 29% for the 5, 10, 15, 20, and 25 molar excess of N-boc EDA respectively. Thus, the data showed that only a maximum of 94% conjugation of EDA to the polymer chains was possible, which was probably because of steric hindrance of approaching nearby EDA molecules at higher molar concentrations that limit further conjugation to the polymers. These data show that a molar ratio of 20 (94% conjugation) for N-Boc ethylene diamine with respect to the parent polymer yielded the best conjugation efficiency, as from 7 to 8 carboxylic groups on the parent polymer backbone out of 8 to 10 carboxylic groups are readily reacted with N-Boc ethylenediamine to yield eight extra amino group on the polymer backbone. The ^{1}H-NMR results shown below confirmed that our polymers have defined structures as expected and no branches or crosslinking were observed.

The reducible LLCs with 94% conjugated EDA then were used in subsequent assays as the final LLCs.

The identified ^{1}H-NMR peaks were as follows:

Intermediate (1): δ 1.231 (a; 2H), δ 1.434 (b; 2H), δ 1.581 (c; 2H), δ 2.957 (d; 2H), δ 3.178 (e; 1H), δ 2.776 (f; 4H), δ 3.436 (g; 4H), δ 2.479 (x; 4H) and δ 2.379 (y; 4H). **(Figure 3.3)**

Intermediate (2): δ 1.114 (a; 2H), δ 1.518 (b; 2H), δ 1.719 (c; 2H), δ 2.957 (d and f; 6H), δ 1.331 (l; 9H), δ 3.183 (e, h and s; 5H), δ 3.431 (g, 4H), δ 2.508 (x and y; 8H). **(Figures 3.4-3.8)**

Final product: δ 1.103 (-NH-CH-CH_2-CH_2-CH_2-CH_2-NH-) (a; 2H), δ 1.565 (-NH-CH-CH_2-CH_2-CH_2-CH_2-NH-) (b; 2H), δ 1.814 (-NH-CH-CH_2-CH_2-CH_2-CH_2-NH-) (c; 2H), δ 2.811 (-NH-CH-CH_2-CH_2-CH_2-CH_2-NH-, -S-CH_2-CH_2-NH-, -NH-CH_2-CH_2-NH_2) (f, d and h; 8H), δ 3.178 (-NH-CH-CH_2-CH_2-CH_2-CH_2-NH-, -NH-CH_2-CH_2-NH_2) (e and s; 3H), δ 2.562 (-NH-CH_2-CH_2-CO-) (x and y; 8H), δ 3.456 (-S-CH_2-CH_2-NH-) (g; 4H). **(Figure 3.9)**

These ^{1}H-NMR results confirmed that our polymers have defined structures as expected and no branches or crosslinking were observed.

ChemNMR Pro 12.0 and ChemDraw Ultra 12.0 Suite (PerkinElmer Inc., Previously known as CambridgeSoft®) were used to Predict ^{1}H-NMR spectra with splitting patterns using the ChemNMR algorithm. Spectra and peaks were linked to the structure for clear interpretation. These ^{1}H-NMR spectra predictions and simulations were used to properly assign the various ^{1}H-NMR peaks.

Finally, the sharp, amplified and significant methyl ^{1}H-NMR peak of Boc at 1.4 ppm (Figure 3.4-3.8) disappeared completely in Figure 3.9, which demonstrated the successful elimination of the Boc group after the deprotection step using 75% TFA in water for 30 minutes.

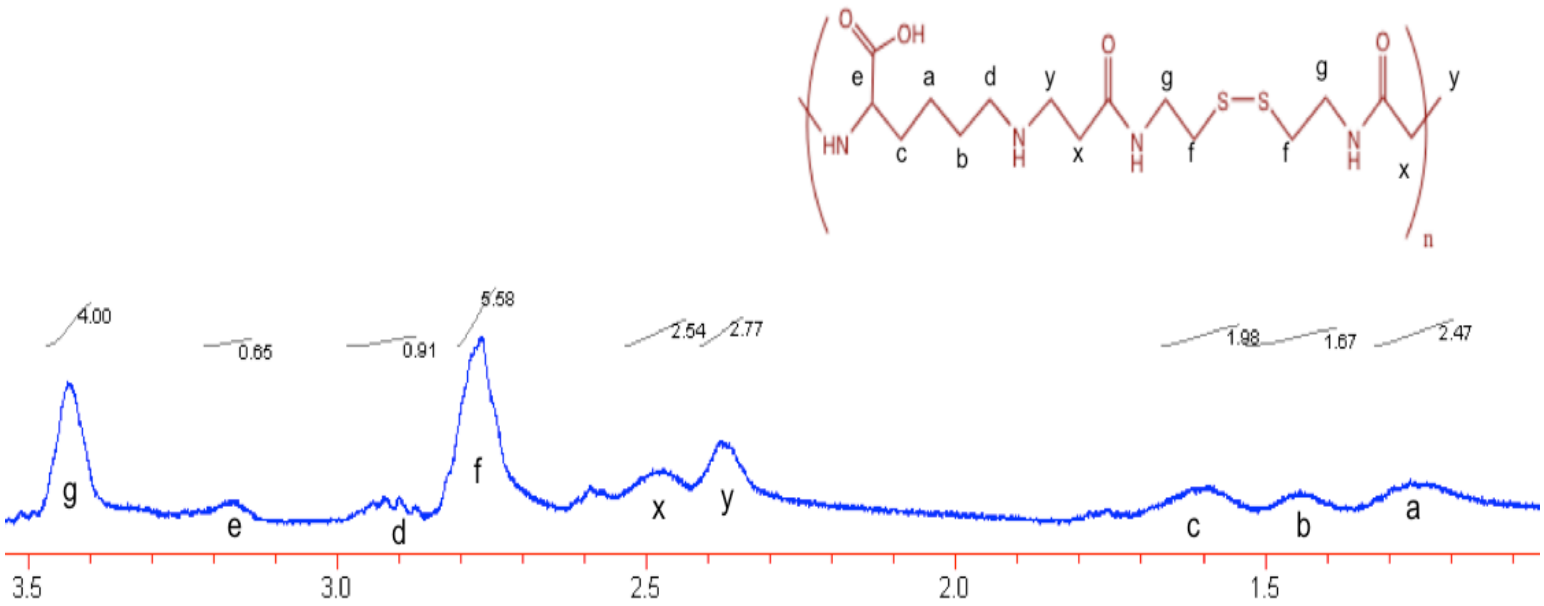

Figure 3.3: ^{1}H-NMR spectra of intermediate (1).

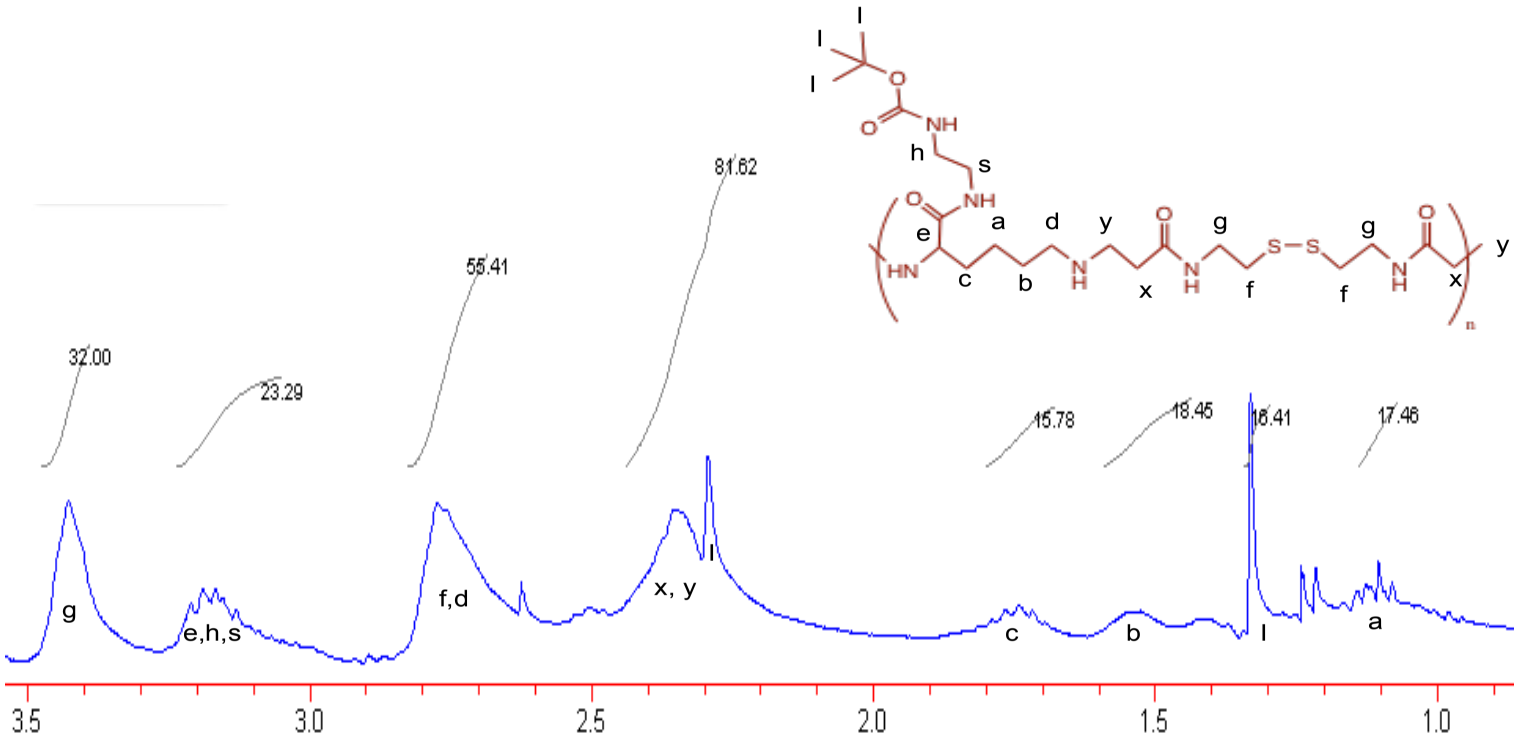

Figure 3.4: ^{1}H-NMR spectra of intermediate (2) with conjugation ratio of 5 with N-Boc ethylenediamine.

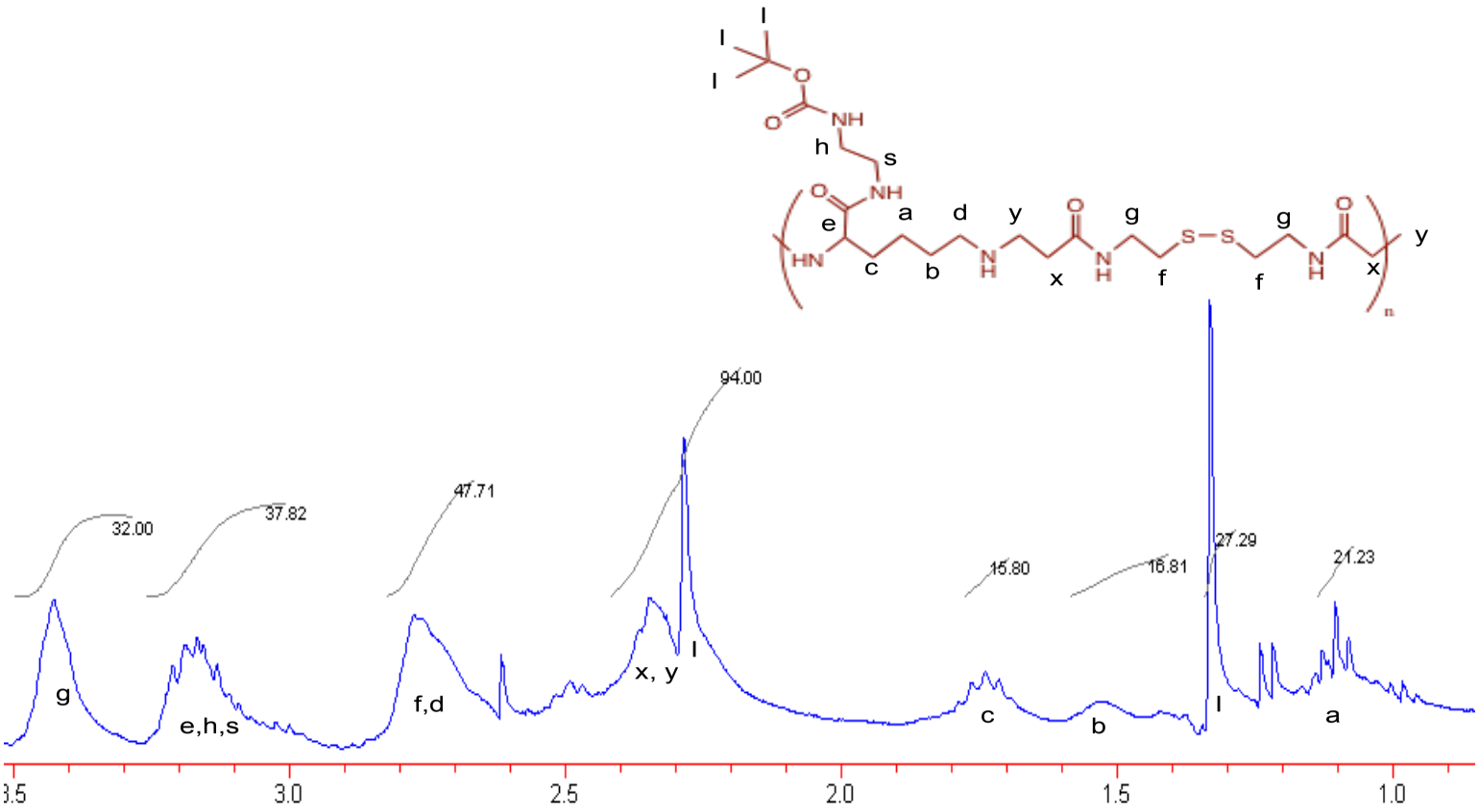

Figure 3.5: [1]H-NMR spectra of intermediate (2) with conjugation ratio of 10 with N-Boc ethylenediamine.

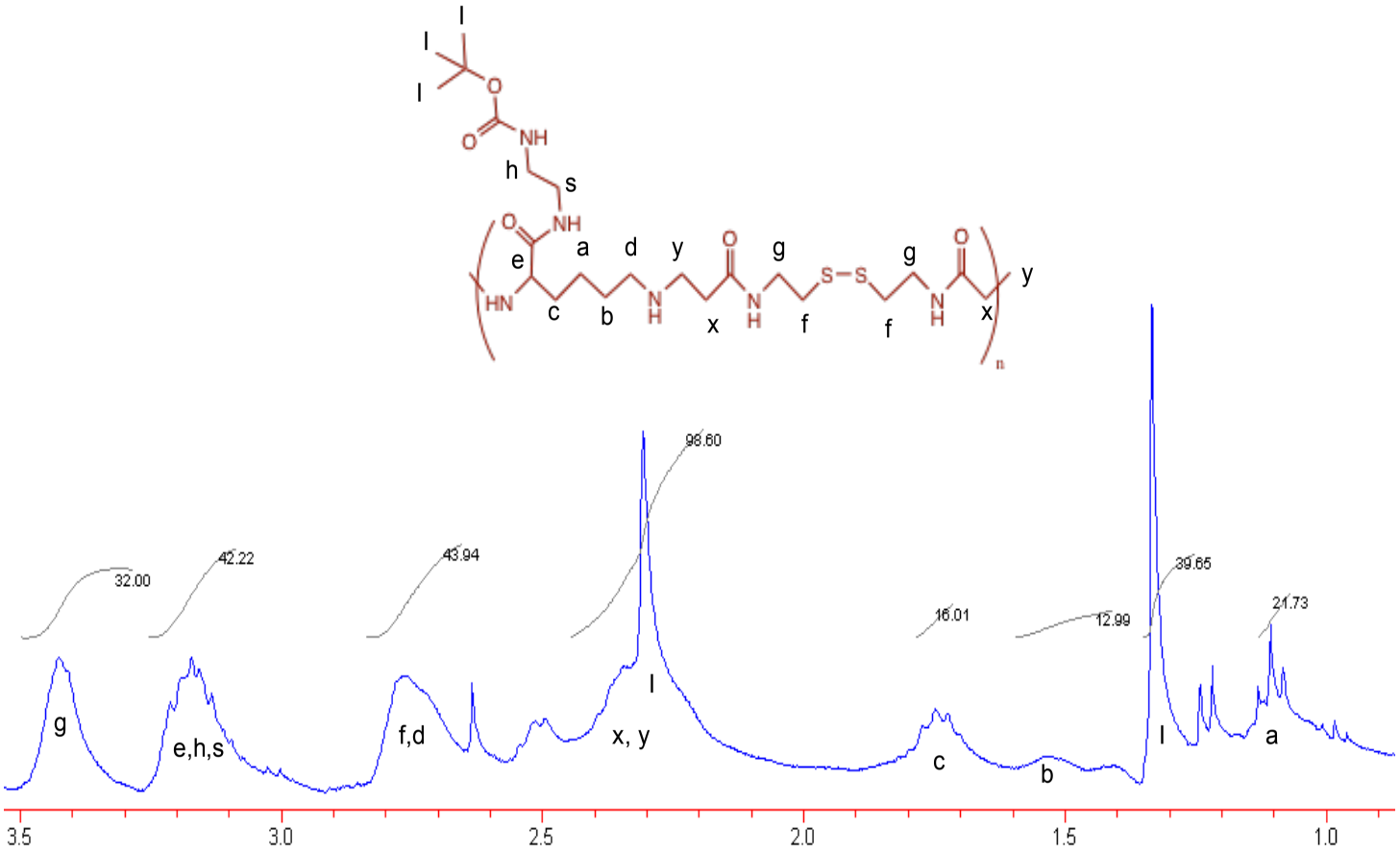

Figure 3.6: ^{1}H-NMR spectra of intermediate (2) with conjugation ratio of 15 with N-Boc ethylenediamine.

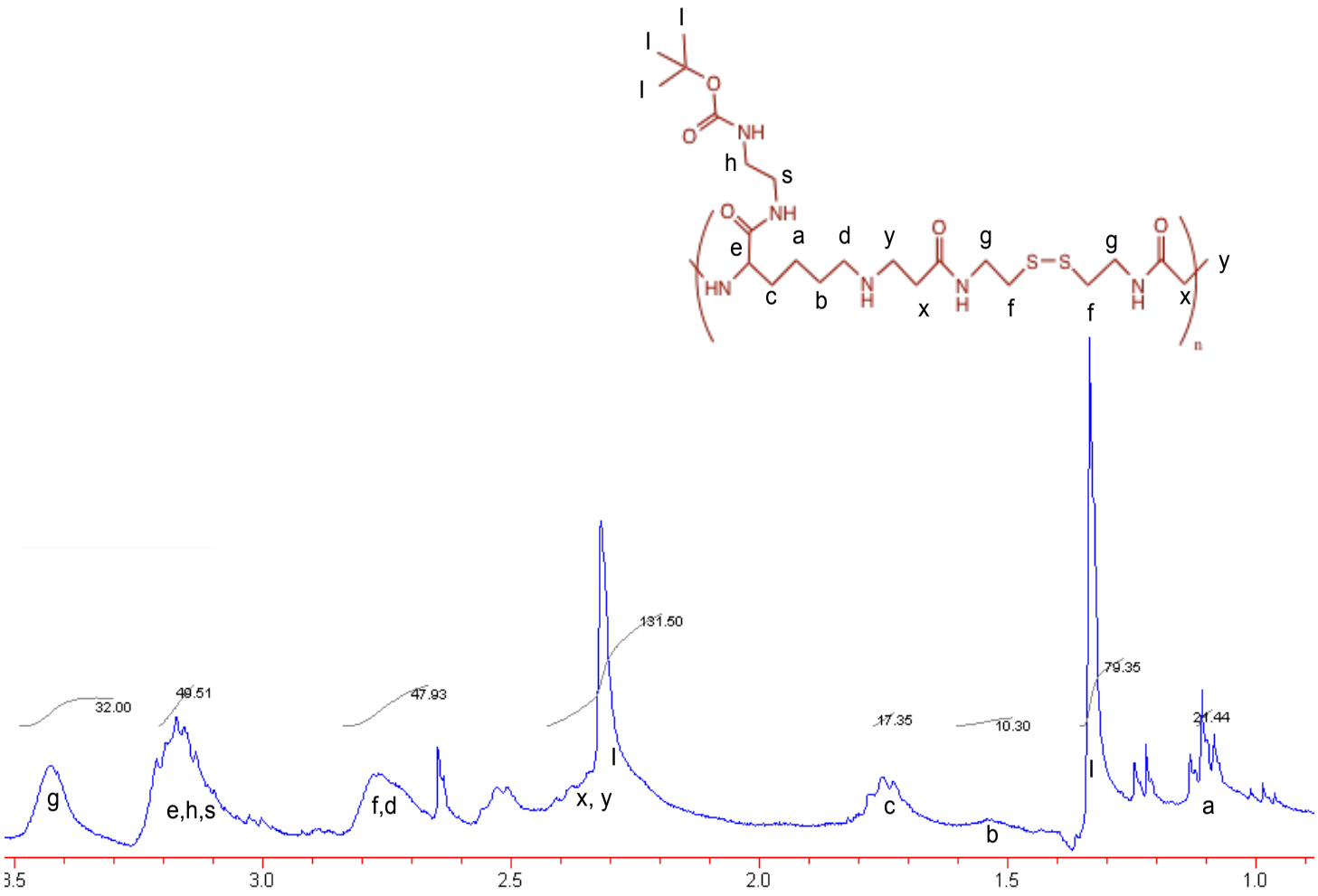

Figure 3.7: ^{1}H-NMR spectra of intermediate (2) with conjugation ratio of 20 with N-Boc ethylenediamine.

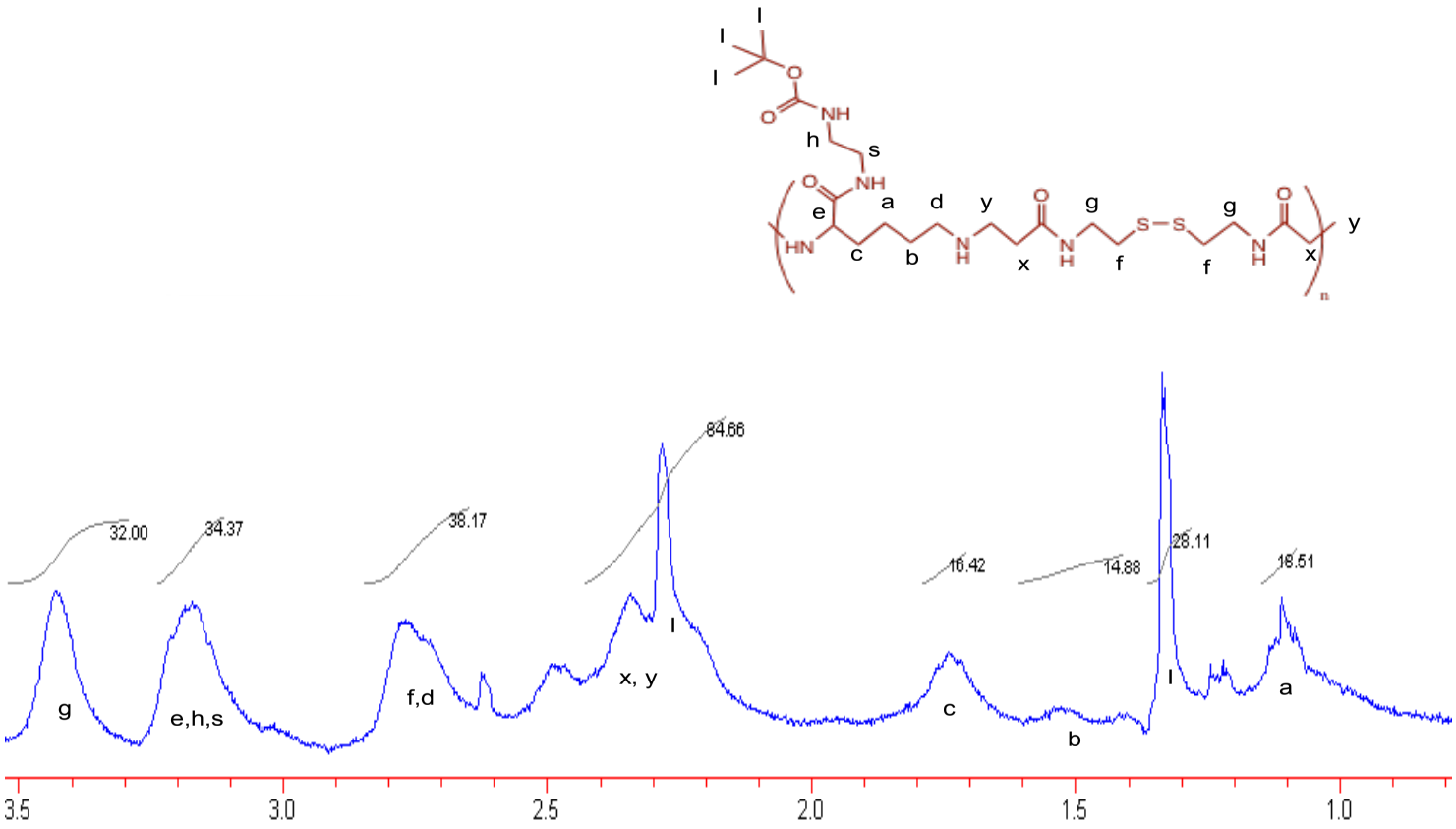

Figure 3.8: ^{1}H-NMR spectra of intermediate (2) with conjugation ratio of 25 with N-Boc ethylenediamine.

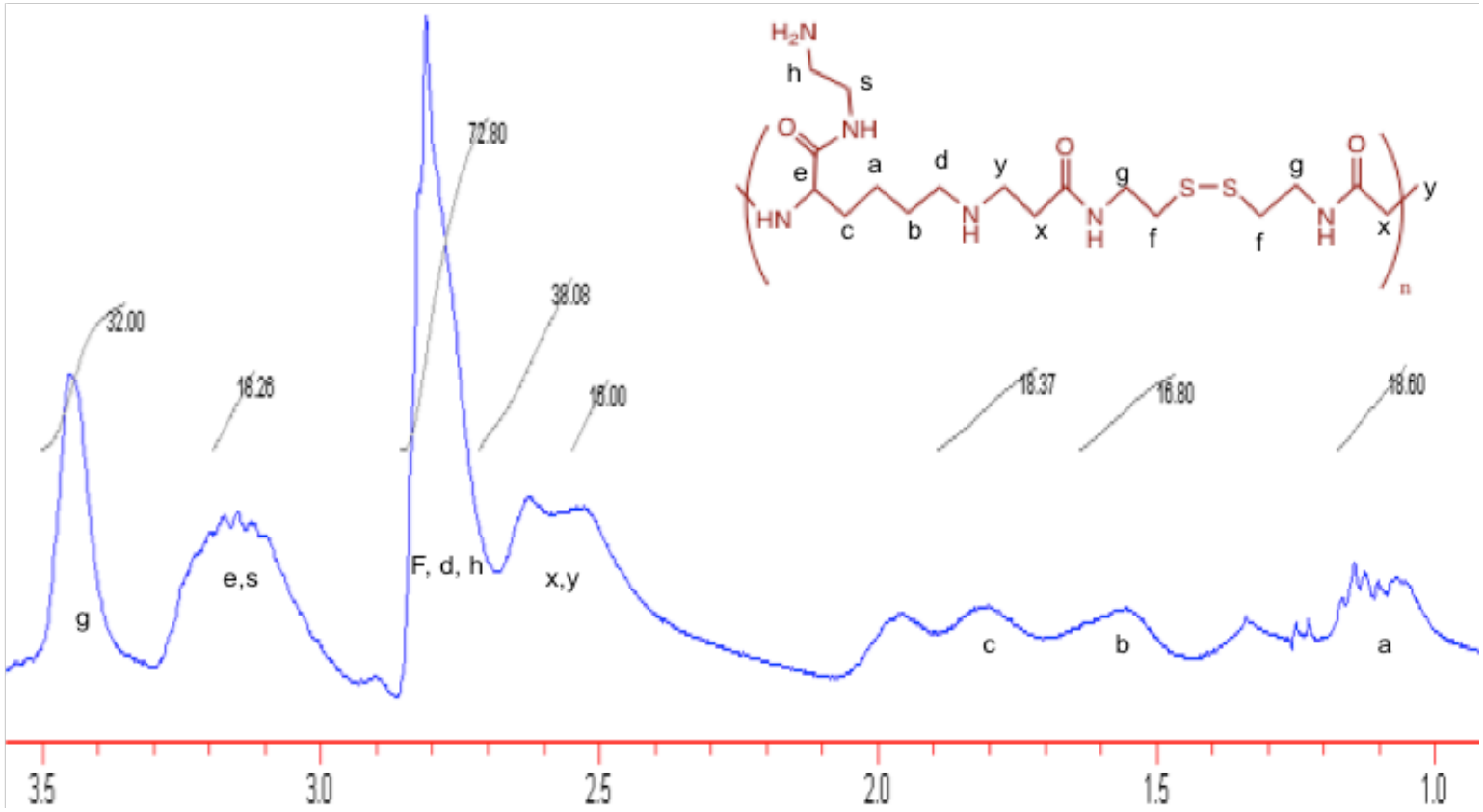

Figure 3.9: ^{1}H-NMR spectra of Linear L-lysine Modified Copolymers (LLCs).

Final copolymers synthesized with excess molar ratios of EDC and N-boc-ethylenediamine	Actual % conjugation of ethylenediamine per repeating block	Number of conjugated branches per polymer chain	Mn (KD_a)	Mw (KD_a)	PDI
5	24.4%	1.95	3.565	3.851	1.08
10	41.6%	3.33	3.600	4.054	1.12
15	48%	3.84	3.540	3.698	1.04
20	93.9%	7.51	3.601	3.831	1.06
25	28.8%	2.3	3.423	3.701	1.08

Table 3.1: Conjugation percentage of ethylenediamine per repeating block and number of conjugated branches per polymer chain for intermediate (2).

Moreover, Ninhydrin assay showed that the final polymer has more primary amino groups ($1.44x10^{-4} \pm 3.5x10^{-5}$) than the primary polymer ($1.27x10^{-4} \pm 3.5x10^{-5}$) and the intermediate polymer ($1.03x10^{-4} \pm 3.2x10^{-5}$). The ninhydrin assay data confirm the ^{1}H-NMR data.

The molecular weight of polymers was measured by size exclusion chromatography (SEC) and calibrated by polyethylene glycol standards (Table 3.2).

The average molecular weight (Mn) of the synthesized LLCs was found to be 3601 D_a with a polydispersity index (PDI) of 1.06, which corresponded to 6-8 repeating units (MW = 436.64 D_a for each repeating unit) as determined with SEC and MALDI-TOF (Table 3.2, Figures 3.10-3.12). The range of the weighted average molecular weight (Mw) of these polymers was from 3.1 to 3.9 kD_a, while the range of the average molecular weight (Mn) was from 3.0 to 3.7 kD_a. The polydispersity index (PDI), ranging from 1.11 to 1.19, indicates that these LLCs have a narrow molecular weight distribution.

In addition, the molecular weights of the various polymers were confirmed through MALDI-TOF analysis (Table 3.2, Figure 3.13) and the results were comparable and consistent.

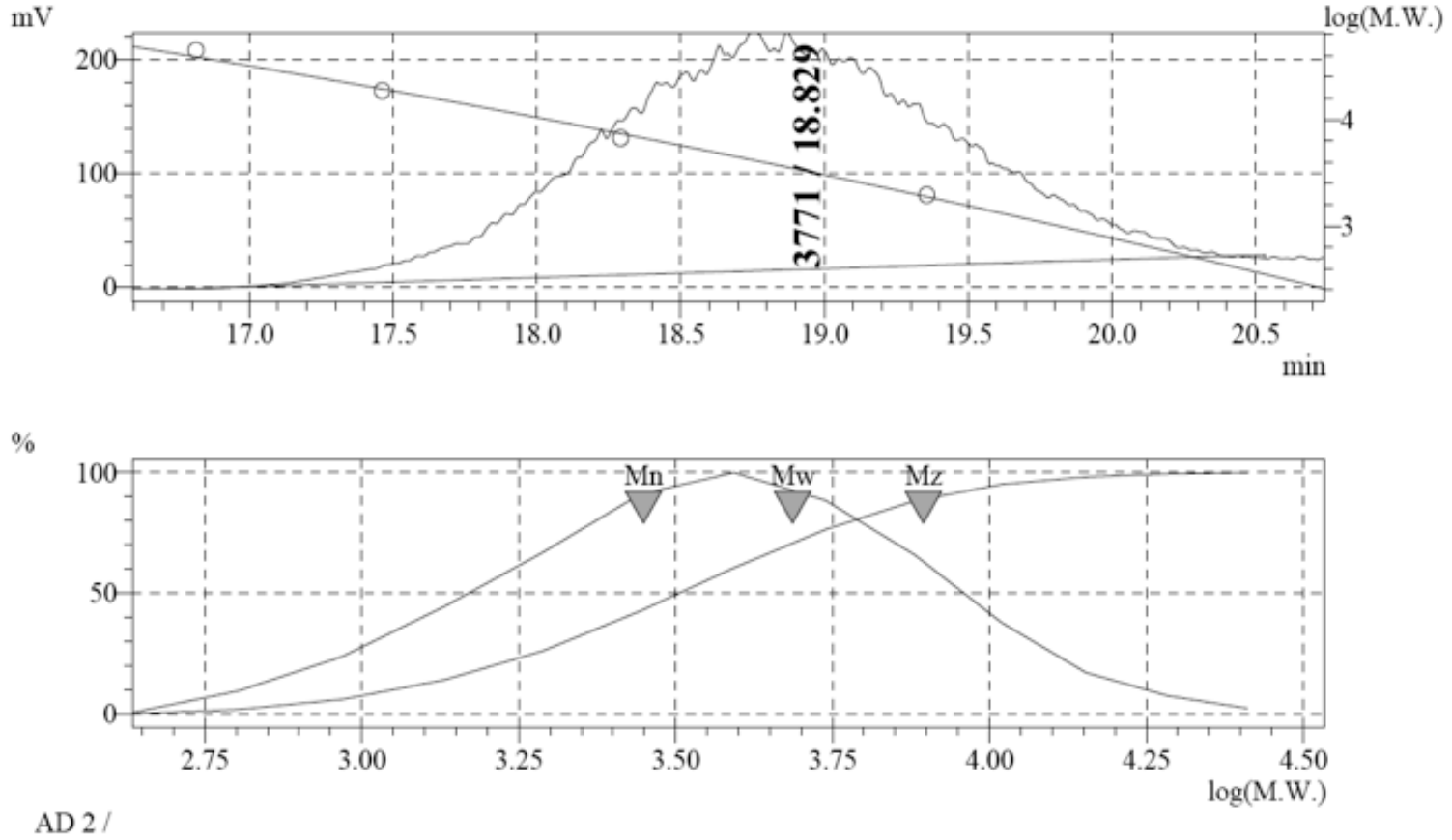

Figure 3.10: SEC HPLC chromatogram of Intermediate (1).

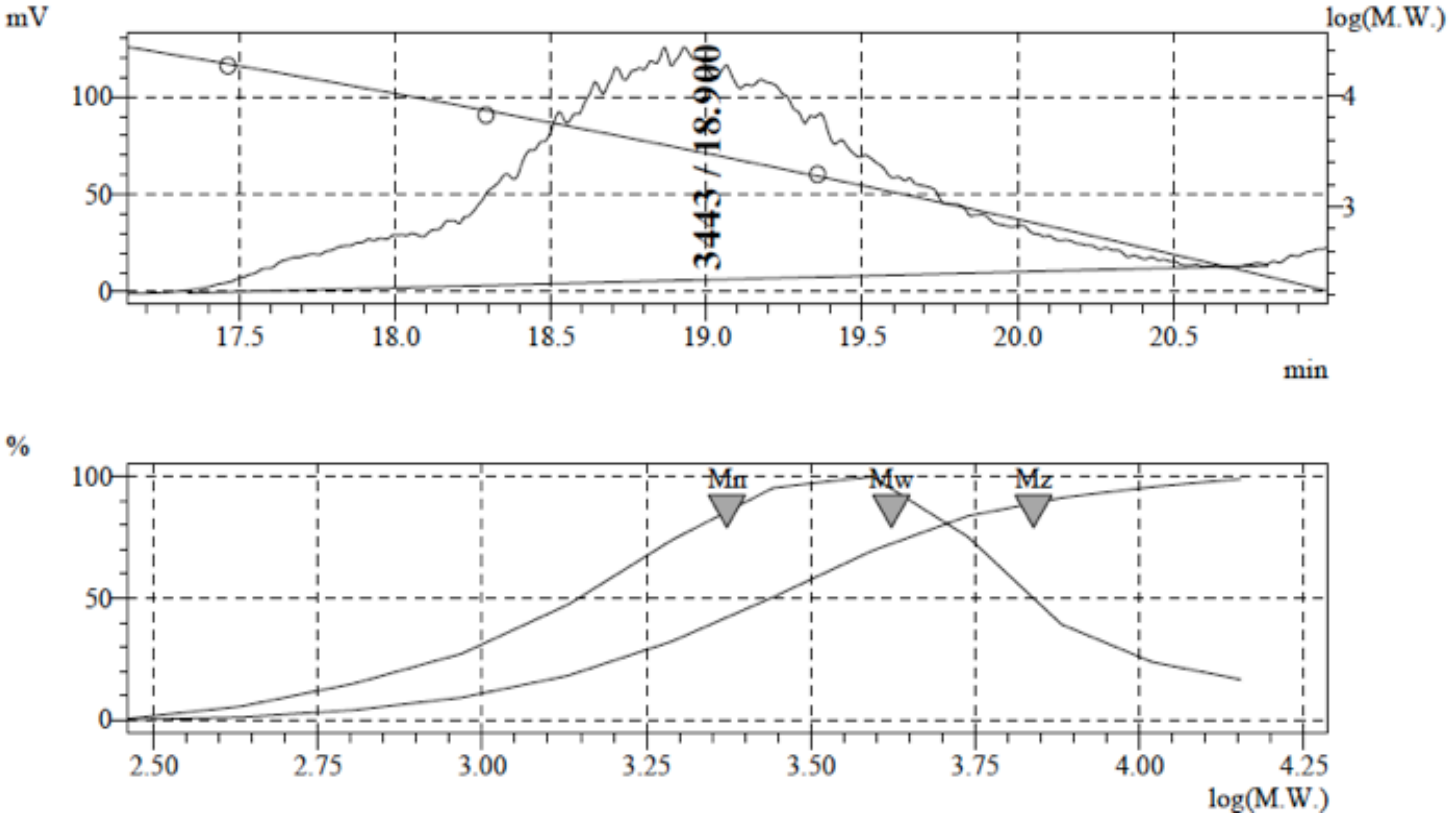

Figure 3.11: SEC HPLC chromatogram of Intermediate (2).

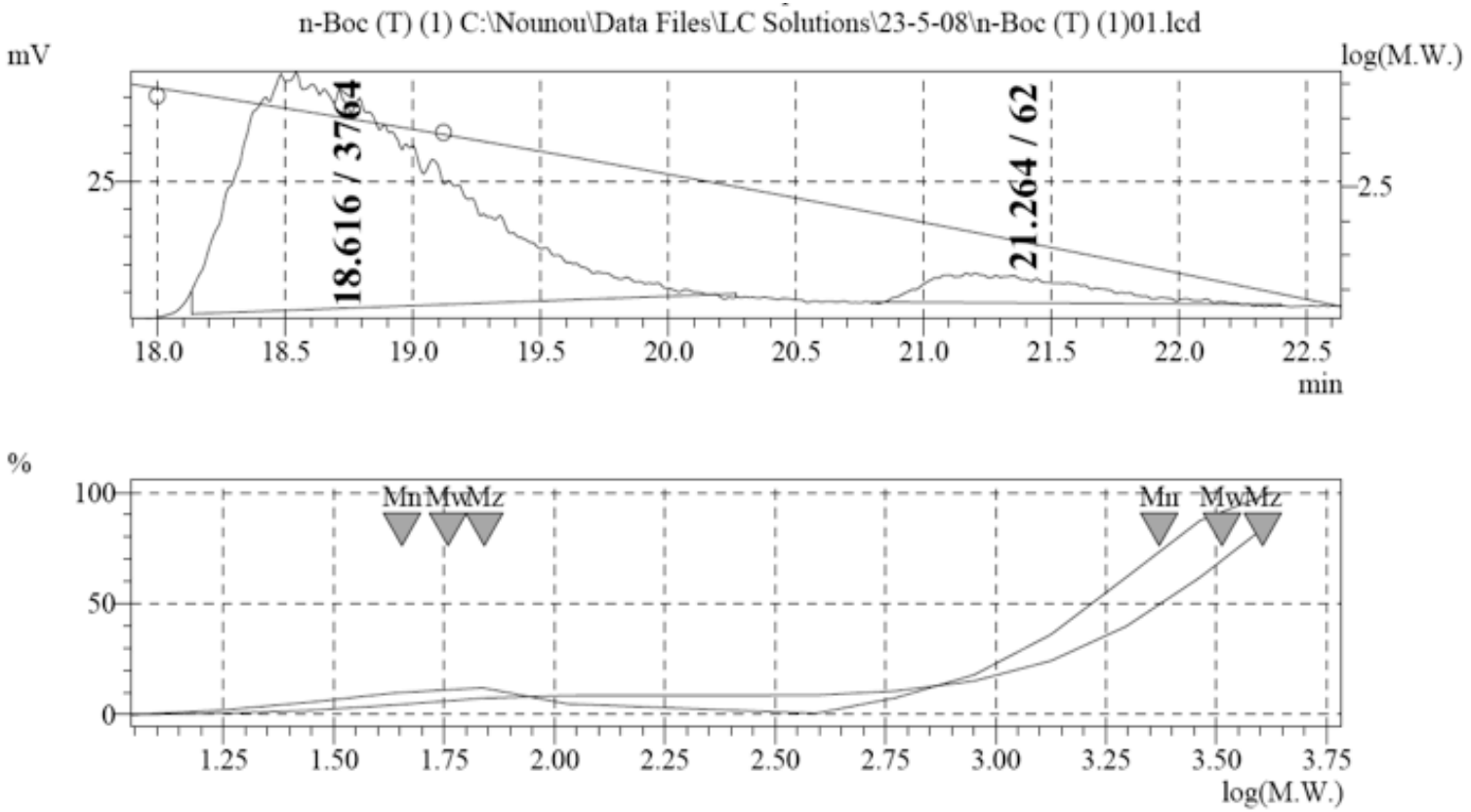

Figure 3.12: SEC HPLC chromatogram of Linear L-lysine Modified Copolymers (LLCs).

Polymer	Mn (KD_a)		Mw (KD_a)		PDI		Number of repeating units
	SEC	MALDI-TOF	SEC	MALDI-TOF	SEC	MALDI-TOF	
Intermediate (1)	3.489	3.538	3.771	3.881	1.08	1.09	~ 6 - 8
Intermediate (2)	3.118	3.216	3.443	3.429	1.10	1.06	
Final Polymer (LLCs)	3.468	3.601	3.764	3.831	1.09	1.06	

Table 3.2: SEC and MALDI-TOF molecular weight data of the various synthesized intermediates and the Linear L-lysine Modified Copolymers (LLCs).

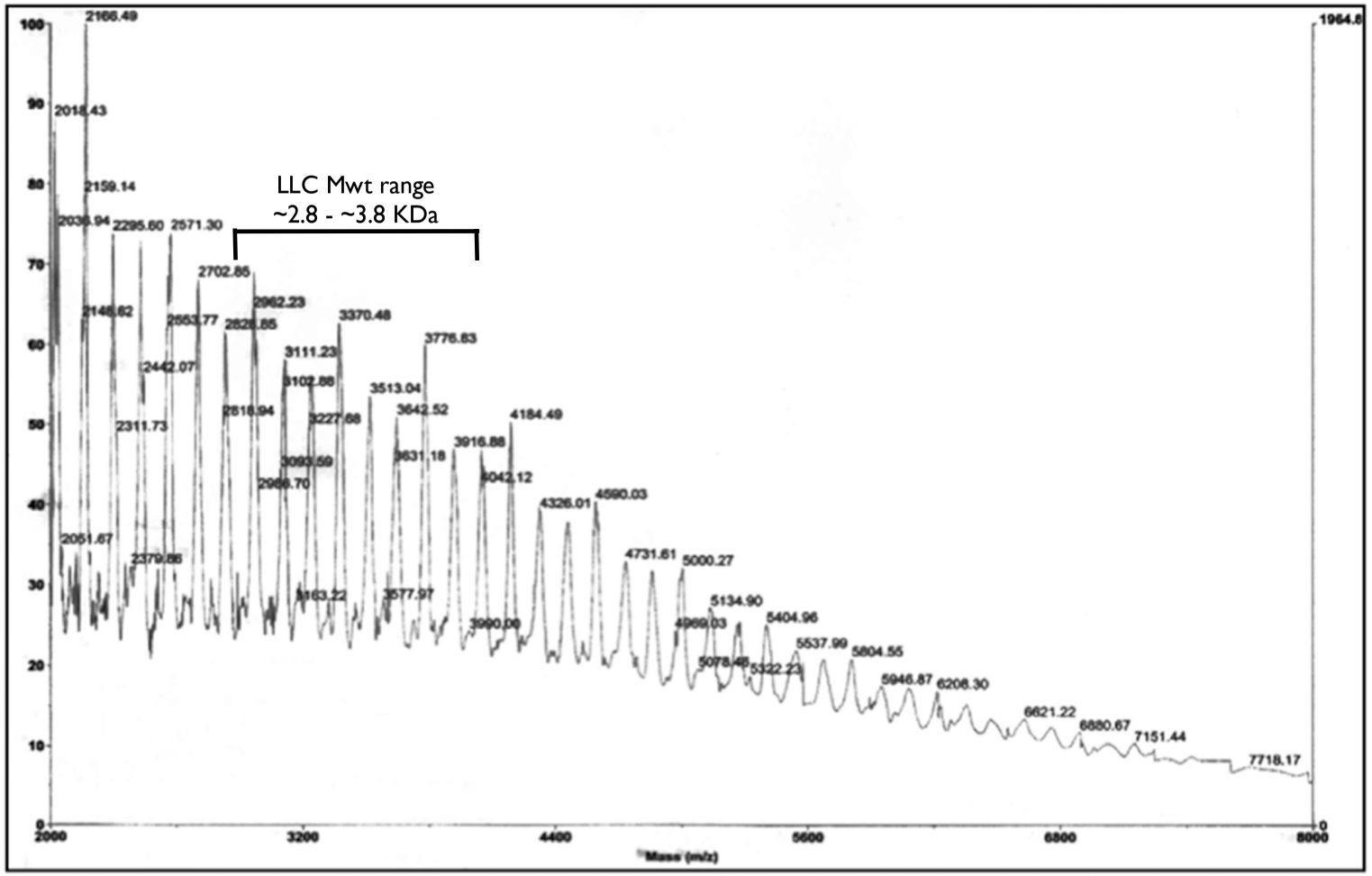

Figure 3.13: MALDI-TOF chromatogram of Linear L-lysine Modified Copolymers (LLCs).

4. Characterization of the physicochemical properties of DNA/LLC polyplexes in vitro

4.1. Introduction

Advancing biotechnology and bioconjugate chemistry spurs the development of new pharmaceutically engineered gene carrier systems with the capability to efficiently to condense and protect the gene load during its transportation to the cell nucleus (Benns and Kim 2000; Howard, Li et al. 2004; Kim, Jeong et al. 2009). The ability to condense and protect the genetic load is a rate-limiting step in the extent of the transfection efficiency (Benns and Kim 2000; Bos, Crommelin et al. 2001; Lim, Kim et al. 2002). To determine the capability of LLC copolymers in respect to condensing and protecting its DNA, transfection efficiency and its cytotoxicity, extensive *in-vitro* characterization techniques were used. The particle size and zeta potential of the LLC/pDNA polyplexes were determined with dynamic light scattering, while the ability of the LLCs to condense and protect pDNA was investigated with a gel retardation assay and a DNase I protection assay, respectively. The transfection efficiencies of LLC/pDNA polyplexes were evaluated in several cell lines including human dermal fibroblasts (HDFs), human breast adenocarcinoma cells (MCF-7), and mouse adipose stromal cells (MA) with luciferase and VEGF expression assays

as well as fluorescence and confocal microscopy. The cytotoxicities of the LLC/pDNA polyplexes were determined with MTT and LDH cell viability assays.

4.2. Materials and methods

4.2.1. Materials

Hyperbranched polyethylenimine (bPEI, MW 25 kD_a), poly-L-Lysine (PLL, MW 20900 D_a), dithiothreitol (DTT), ethidium bromide (EtBr), 3-(4,5-dimethyl-2-thiazolyl)-2,5-diphenyl-2H-tetrazolium bromide (MTT), and sodium dodecyl sulfate (SDS) were purchased from Sigma-Aldrich (St. Louis, MO). Dulbecco's Modified Eagle's Medium (DMEM), DMEM-F12 medium, penicillin-streptomycin, fetal bovine serum (FBS), Newborn Calf Serum (NCS), trypsin-like enzyme (TrypLE Express), Maxiprep kit, and Dulbecco's phosphate buffered saline (PBS) were purchased from Invitrogen-Gibco (Carlsbad, CA). A luciferase assay system with reporter lysis buffer and RQ1 RNase-free DNase I enzymes were purchased from Promega (Madison, WI). A bicinchoninic acid protein assay reagent (BCA) kit was purchased from Pierce (Rockford, IL). VEGF ELISA kit was purchased from R&D Systems (Minneapolis, MN). Chemiluminescence was assayed using a BioTek Instrument Synergy 2 luminometer system equipped with BioTek's Gen5™ reader control and data analysis software (Winooski, VT). 1H NMR data were obtained with a General Electric (GE) QE-300 300 MHz instrument (Boston, MA). Matrix-assisted laser desorption ionization-time-of-flight (MALDI-TOF) data were obtained with a Voyager-DE STR Biospectrometry Workstation from Applied Biosystems (Foster City, CA). Particle size and zeta potential (ζ) of the

nanoplexes were determined with a BI-200SM dynamic light scattering instrument (DLS, Brookhaven Instrument Corporation, Holtsville, NY). Fluorescence microscopy data were obtained using an Olympus BX 51 Series fluorescence microscope.

4.2.2. Cell Lines

Human dermal fibroblasts (HDFs) and human breast adenocarcinoma cells (MCF-7s) were purchased from American Type Culture Collection (ATCC) (Manassas, VA) and cultured in DMEM medium supplemented with 10% FBS and maintained at 37° C in a humidified atmosphere of 5% CO_2. Mouse adipose stromal cells (MA) were a generous gift from Professor Ke-He Ruan (University of Houston) and cultured in DMEM-F12 medium supplemented with 10% Newborn Calf Serum (NCF) and maintained at 37° C in a humidified atmosphere of 5% CO_2.

4.2.3. Controls used in *in-vitro* experiments

Poly-L-lysine (PLL) was used as the main positive control throughout all *in-vitro* experiments. The similarity between the backbone of PLL and LLC and the fact that LLC is a bioreducible derivative of PLL were the main reasons for

choosing PLL as the main positive control. Polyethylenimine (PEI) and Lipofectamine™ were also used as positive controls in some experiments. Naked DNA was used in all in vitro experiments as a negative control.

4.2.4. Preparation of reducible LLC/pDNA polyplexes

All polymer/plasmid DNA (pDNA) polyplexes were freshly prepared prior to use. LLC/pDNA polyplexes were prepared with a 1.74 mg/ml stock solution of a luciferase plasmid (pCMV-Luc), 0.196 mg/ml stock solution of a fluorescently labeled luciferase plasmid (pCMV-Luc) with Ethidium Monoazide (EMA), 0.63 mg/ml stock solution of an enhanced green fluorescent protein plasmid (pCMV-EGFP) or 0.8 mg/ml stock solution of a VEGF protein plasmid (pSV_{40}-VEGF). The solubility of LLC copolymers in deionized water was high (14 mg/ml). A 10 mg/ml Stock solution LLC copolymers in 5% glucose was used. Both polymer and plasmid were separately diluted to the appropriate concentration depending on the required N/P ratio (nitrogens of polymer/phosphates of pDNA) to a volume of 100 μl containing 5% glucose. The pDNA solutions then were added to the polymer solutions and complexation was allowed for 30 minutes prior to use.

4.2.5. Gel retardation assay

To evaluate the ability of the optimized reducible LLCs to complex pDNA, a

gel retardation assay was performed with the pCMV-Luc. The polymer/pDNA polyplexes were prepared by mixing 1 μg of the pCMV-Luc plasmid with increasing amounts of synthesized reducible LLCs in 5% glucose to form polyplexes at 1/1, 5/1, 10/1, 15/1, 20/1, 25/1, 30/1, 40/1 and 50/1 N/P ratios. The polyplexes then were subjected to electrophoresis on a 1% (w/v) agarose gel containing 0.5 μg/ml ethidium bromide for 30 minutes at 120 V in 1X tris-acetate-EDTA (TAE) buffer. The gel was run for 30 minutes at 120 V and the locations of the DNA bands were visualized with a UV transilluminator at a wavelength of 254 nm.

4.2.6. Particle size and zeta potential (ζ)

Polyplexes were formed as described above and incubated for 30 minutes prior to measurement. The average particle size and zeta potential of polyplexes were measured using a BI-200SM dynamic light scattering instrument (DLS, Brookhaven Instrument Corporation, Holtsville, NY). Measurements were made at 25° C using an ion-argon laser (λ = 677 nm) as the instrument beam at a scattering angle of 90°. For data analysis, the viscosity (0.8905 mPa s) and refractive index (1.333) of pure water at 25° C were used and measurements for particle size were reported as the effective mean diameters. Smoluchowski's equation was used to calculate the ζ potential values from the electrophoretic

mobility. Each sample was prepared in triplicate and the data were reported as mean ± standard deviations.

4.2.7. DTT reduction of LLCs

4.2.7.1. Gel retardation assay using DTT

To demonstrate the mechanism of pDNA release from polymer/pDNA polyplexes, a solution of LLC/pDNA polyplexes at an optimized N/P ratio of 25/1 was prepared as described above and the DTT reagent was added at different concentrations from 0.1 to 4 mM. Polyplexes were incubated in Eppendorf tubes at room temperature for 30 minutes. After incubation, the polyplexes were electrophoresed on a 1% agarose gel containing ethidium bromide with 1X TAE running buffer at 120 V for 30 minutes. The locations of the DNA bands were visualized with a UV illuminator at a wavelength of 254 nm.

The final DTT concentration was maintained at 4 mM in the liquid cell. This concentration is well below that (20 mM) which simulates physiological reducing environment of the cell (Ates, Ercal et al. 2009; Oupicky, Bisht et al. 2005; Wan, You et al. 2009). DTT is mainly used for its stability in various solution conditions (Getz, Xiao et al. 1999).

4.2.7.2. Fluorescence spectroscopy using DTT

To determine whether all of the pDNA was released from the LLC/pDNA

polyplexes, the reduction of the disulfide bonds with DTT was monitored with fluorescence spectroscopy. LLCs were complexed with EMA-labeled pCMV-Luc for 60 minutes at an optimized N/P ratio of 25/1. Afterward, 4 mM of DTT was added and the fluorescence was monitored for 120 minutes. The excitation and emission wavelengths were 480 ± 20 nm and 600 ± 35 nm respectively. All of the fluorescence spectroscopy data were normalized against the free pDNA and pDNA with 4 mM DTT fluorescence. Each sample was prepared in triplicate and the data were reported as mean ± standard deviations.

4.2.8. Heparin competition

The stabilities of the LLC/pCMV-Luc polyplexes were evaluated through a heparin competition assay. The LLCs copolymers and pCMV-Luc polyplexes were formed at N/P ratio of 40/1 and were mixed with increasing amounts of heparin (1-20 μg). The mixtures were analyzed on a 1% agarose gel via electrophoresis at 100 V for 60 minutes at various time points (1 hour to 24 hours). The pDNA were visualized using a UV transilluminator. Since Heparin is a highly negatively charged polysaccharide, it can interact competitively with the LLC/pDNA polyplexes.

4.2.9. Serum stability

The stabilities of the LLC/pCMV-Luc polyplexes were evaluated through a

serum stability assay. The LLCs copolymers and pCMV-Luc polyplexes were formed at N/P ratio of 40/1 and were mixed with increasing amounts of serum (0% to 80%). The mixtures were analyzed on a 1% agarose gel via electrophoresis at 100 V for 60 minutes at various time points (zero to 24 hours). The pDNA were visualized using a UV transilluminator.

4.2.10. DNase I protection assay

To investigate the ability of the LLCs to protect pDNA from endonucleases, a DNase I protection assay was performed. LLC/pCMV-Luc polyplexes were prepared at an optimized N/P ratio of 25/1 to a final pDNA concentration of 0.01 mg/ml. RQ1 RNase-free DNase I (6U) then was added either to naked or complexed pDNA and the samples were incubated at 37 °C. Then, 100 μl aliquots were removed at 0, 20, 40, 60, and 120 minutes post-incubation and added to labeled tubes containing 100 μl of stop solution (200 mM NaCl, 20 mM EDTA, 1% SDS). The tubes then were incubated at 60° C overnight to dissociate the pDNA from the polyplexes. The samples were electrophoresed and analyzed on a 1% agarose gel that was stained with ethidium bromide (0.5 μg/ml). Incubation of the polyplexes with the stop solution was not adequate to release the pDNA from the copolymers. Therefore, DTT was added to the polyplex solution after incubation with DNase. The tubes then were incubated at 25 °C for

an additional 60 minutes. The samples then were electrophoresed and analyzed on a 1% agarose gel that was stained with ethidium bromide (0.5 μg/ml).

4.2.11. Transfection efficiencies of LLC/pDNA polyplexes with luciferase assay

4.2.11.1. In serum-free media

LLC-mediated transfections were evaluated in HDFs, MCF-7s, MA stromal cells, HEK-293s, and hMSCs cells by using the reporter plasmid pCMV-Luc. HDFs, MCF-7s, and hMSCs were maintained in DMEM containing 10% FBS, streptomycin (100 μg/ml) and penicillin (100 units/ml) at 37° C in a humidified atmosphere with 5% CO_2 and DMEM-F12 media containing 10% NCS, streptomycin (100 μg/ml) and penicillin (100 units/ml) was used for the MA and stromal cell line. HEK-293s were maintained in EMEM containing 10% FBS, streptomycin (100 μg/ml) and penicillin (100 units/ml) at 37° C in a humidified atmosphere with 5% CO_2. 4T1s were maintained in RPMI containing 10% FBS, streptomycin (100 μg/ml) and penicillin (100 units/ml) at 37° C in a humidified atmosphere with 5% CO_2. Cells were seeded in 6-well plates at a density of 5 x 10^5 cells/well for at least 24 hours prior to transfection. DNA was complexed with the LLCs or PLL control at predetermined N/P ratios (1, 5, 10, 15, 20, 25, 30, 40, and 50) in 1X PBS buffer and incubated for 30 minutes before use. The cells

were washed with 1X PBS followed by the addition of serum-free media. Polyplexes (2 μg DNA/well) then were added to the cells, which were incubated for 4 hours at 37° C. Afterward, the media then was replaced with 2 ml of fresh complete media and the cells were incubated for an additional 44 hours. The cells then were washed with 1X PBS, treated with 200 μl cell lysis buffer, and incubated for 15 minutes. Cellular debris was removed by centrifugation at 8,000 rpm for 2-3 minutes. The luciferase activity in 25 μl of cell lysate was measured on a chemiluminometer. The relative luminescent unit (RLU) of luciferase expression was normalized against the protein concentration in the cell extracts as measured with a BCA protein assay kit. The LLC/pDNA polyplexes that produced the highest transfection efficiency with the least cytotoxicity in the cell lines tested was designated as the optimized N/P ratio and utilized in subsequent studies. Each sample was prepared in triplicate and the data were reported as mean ± standard deviations.

4.2.11.2. In serum

LLC-mediated transfections were evaluated in HDFs cells as described in the previous section with the exception of using complete DMEM media containing 10% fetal bovine serum (FBS) instead of serum-free media. DNA was complexed with the LLCs or PLL control at the N/P ratio that gave the highest

transfection efficiency in this cell line for both polymers based on the serum-free transfection study (N/P ratio of 50/1 for PLL and N/P ratio of 40/1 for LLC in HDF cells). Each sample was prepared in triplicate and the data were reported as mean ± standard deviations.

4.2.12. Transfection efficiencies of LLC/pDNA polyplexes with VEGF ELISA assay

LLC-mediated transfections were evaluated in hMSCs cells using the reporter plasmid pSV_{40}-VEGF as described in the previous section. DNA was complexed with the LLCs or PLL control at the N/P ratio that gave the highest transfection efficiency in this cell line for both polymers based on the luciferase transfection study (N/P ratio of 40/1 for PLL and LLC in hMSC cells). A VEGF ELISA kit was used in the quantitation of the VEGF (Pierce, Thermo Fisher Scientific Inc.). Each sample was prepared in triplicate and the data were reported as mean ± standard deviations.

4.2.13. Fluorescence microscopy of HDF cells transfected with commercial vectors

To evaluate the transfection efficiency of LLCs compared to other standard commercial nonviral gene delivery vectors, HDF cells were transfected with bPEI and Lipofectamine™ complexed with the pCMV-EGFP plasmids at an optimized

N/P ratio of 25/1 (least cytotoxicity as described above) and 10/1 for LLCs and bPEI respectively. The optimized N/P of 10/1 for bPEI was chosen as it yielded the highest transfection efficiency with the least cytotoxicity in HDF cells. In addition, Lipofectamine™/pDNA conjugates were prepared as per the manufacturer's instructions. Briefly, HDF cells were cultured on 2 X 2 glass slides placed into the wells of a 6-well plate. Following a PBS wash, polyplexes prepared with pCMV-EGFP were added to the cells, which were incubated for an additional 4 hours. The cells were washed in 1X PBS, pH 7.4 and fixed in 2% freshly prepared formaldehyde for 15 minutes. The HDF cells expressing EGFP were imaged and counted using an Olympus BX 51 Series fluorescence microscope per total amount of cells. The maximum excitation and emission wavelengths for EGFP detection were 488 ± 20 nm and 509 ± 20 nm respectively.

4.2.14. Confocal microscopy of HDF cells transfected with EMA-labeled pDNA

To determine whether pDNA is released from LLC/pDNA polyplexes as hypothesized upon exposure to the reducing environment of the cytosol and subsequent disulfide bond reduction, we viewed cells treated with LLC/EMA-labeled pDNA polyplexes with confocal microscopy. Briefly, HDFs were cultured

on 2 X 2 glass slides placed into the wells of a 6-well plate. The cells then were washed with 1X PBS buffer and transfected with polyplexes prepared with EMA-labeled pCMV-Luc for 4 hours as described previously. The cells were washed and fixed with 2% freshly prepared formaldehyde in 1X PBS buffer for 15 minutes at predetermined time intervals of 0, 4, 8, and 12 hours. The cells then were counterstained with a 10 μg/ml 4,6-diamidino-2-phenylindole (DAPI) solution to visualize the cells' nuclei. The labeled cells then were imaged using an Olympus BX 51 confocal laser scanning microscope. The EMA-labeled pDNA was excited using 488 to 541 nm illumination (TRITC range), while the DAPI stain was imaged at 358 nm.

4.2.15. MTT cytotoxicity assay

HDF, MCF-7s, and MA cells were transfected with LLC/pDNA polyplexes as described previously. The amount of DNA (2 μg/well) and volume of pDNA/polymer polyplexes solution (200 μl/well) were held constant throughout all of N/P ratios. 6-well plates were used in all transfection and cell viability studies. The high aqueous solubility of LLC copolymers (14 mg/ml) allowed the tight control over the amount of polymer solution used, which helped in the DNA and polyplexes volume control in all of the transfection and cell viability studies. After this, 120 μl (2mg/ml) MTT in 1X PBS was added to the transfected cells, which

were incubated for an additional 4 hours at 37° C. Afterward, the media was removed and 750 μl DMSO then was added to each well to dissolve the formazan crystals. The absorption was measured at 570 nm using a BioTek Instrument ELx800™ microplate reader. Each sample was prepared in triplicate and the data were reported as mean ± standard deviations. The percentage cell viability of each sample was determined relative to the control (untreated) cells as shown in equation 1.

$$\text{Cell Viability } (\%) = \frac{\text{Sample OD}_{570}}{\text{Control OD}_{570}} \text{ X } 100 \qquad (1)$$

Where:

Sample OD_{570} : Absorbance of the transfected cells.
Control OD_{570} : Absorbance of the untransfected cells.

4.2.16. LDH cytotoxicity assay

HDF, MCF-7s, and MA cells were transfected with LLC/pDNA polyplexes as described previously. After this, 100 μL of cell culture supernatant was mixed with the same volume of reaction mixture from the Cytotoxicity Detection Kit (LDH, Roche, Inc.) and incubated for 30 minutes. Then the absorbance of the samples in the wells was measured at 490 nm against medium. This kit allows monitoring of the rate of cell lysis by determination of the lactate dehydrogenase (LDH) amount released into culture medium.

4.2.17. Statistical analysis

The data were represented as the mean and standard deviations; differences were analyzed using the two-tailed student's t-test. A p-value of less than or equal to 0.05 was taken as significant (*). GraphPad Prism® version 5 was used to conduct the statistical analysis.

4.3. Results and discussion

PLL was able effectively to condense pDNA from an N/P ratio of 1/1 as evident by the absence of free pDNA from wells of the gel (Figure 4.1, lanes 2 – 11) compared to LLCs where effective condensation occurred from an N/P ratio of 5/1 (Figure 4.1, lanes 3 – 11). This could be because of the high MW PLL (~20900 D_a) chains that would be more effective at condensing pDNA at this N/P ratio compared to low the MW LLC (~ 3200 D_a) chains. However, both reducible LLCs and PLL were able to condense pDNA completely from an N/P ratio of 25/1 as apparent from the total absence of fluorescence in the wells (Figure 4.1, lanes 7 – 11).

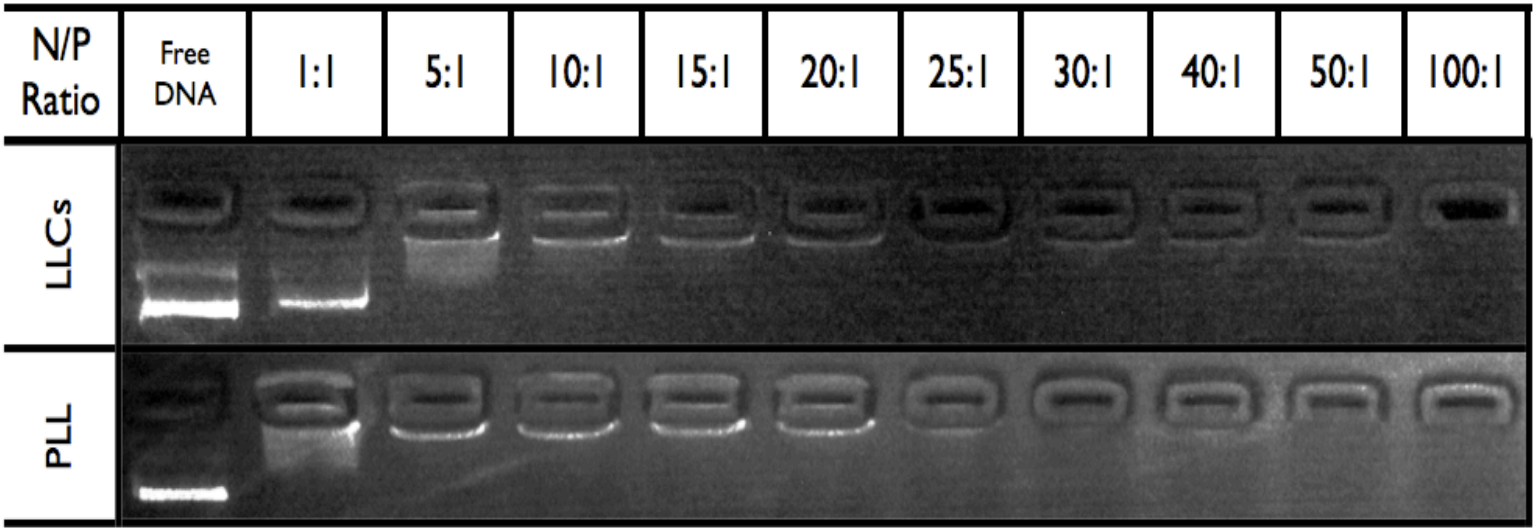

Figure 4.1: Agarose gel electrophoresis of LLCs and PLL with plasmid DNA polyplexes as a function of N/P ratio (Lane 1, naked pDNA; lanes 2–11, LLC/pDNA and PLL/pDNA at N/P ratios of 1:1, 5:1, 10:1, 15:1, 20:1, 25:1, 30:1, 40:1. 50:1 and 100:1).

The particle size distribution of the LLC/pDNA polyplexes showed that N/P ratios greater than 5/1 can condense pDNA efficiently into nanoparticles with effective diameters of less than 150 nm (Figure 4.2). In addition, the LLC copolymers produced slightly larger polyplexes than PLL, which could be attributed to the lower molecular weight chains as compared to the high molecular weight PLL chains. Overall, the majority of the polyplexes remained constant at ~150 nm at various N/P ratios in comparison to PLL, which showed an average particle size of ~125 nm from an N/P ratio of 20/1. Moreover, the particle size distribution of the LLC/pDNA polyplexes was found to be homogenous (Figure 4.2, inset), which could reflect the narrow PDI of the synthesized polymer chains. The zeta potential of the LLC/pDNA polyplexes ranged from ~ -4 ± 4.4 mV for N/P ratio of 1/1 to a maximum surface charge of ~ 17 ± 2.85 mV for N/P ratio of 50/1 (Figure 4.3) and the zeta potential of the PLL/pDNA polyplexes ranged from ~ -3 ± 2.21 for N/P ratio of 1/1 to a maximum surface charge of ~ 14 ± 4.3 mV for N/P ratio of 50/1 (Figure 4.3). There were no significant differences in zeta potential values between PLL and LLCs, which indicated the accuracy of the formulation of the polyplexes based on N/P ratios (p-value > 0.05). Moreover, the zeta potential values and particle size distribution of PEI and LLCs were comparable throughout the range of N/P ratios of 1/1 to 50/1 (Figures A4.1 and A4.2 respectively, Appendix). Furthermore, the calculated

zeta potential values of the LLC polyplexes were found to fit the extrapolated polynomial equation (Figure 4.3, inset), which reflected the accuracy of the zeta potential measurements for both LLCs and PLL polyplexes using Smoluchowski's equation.

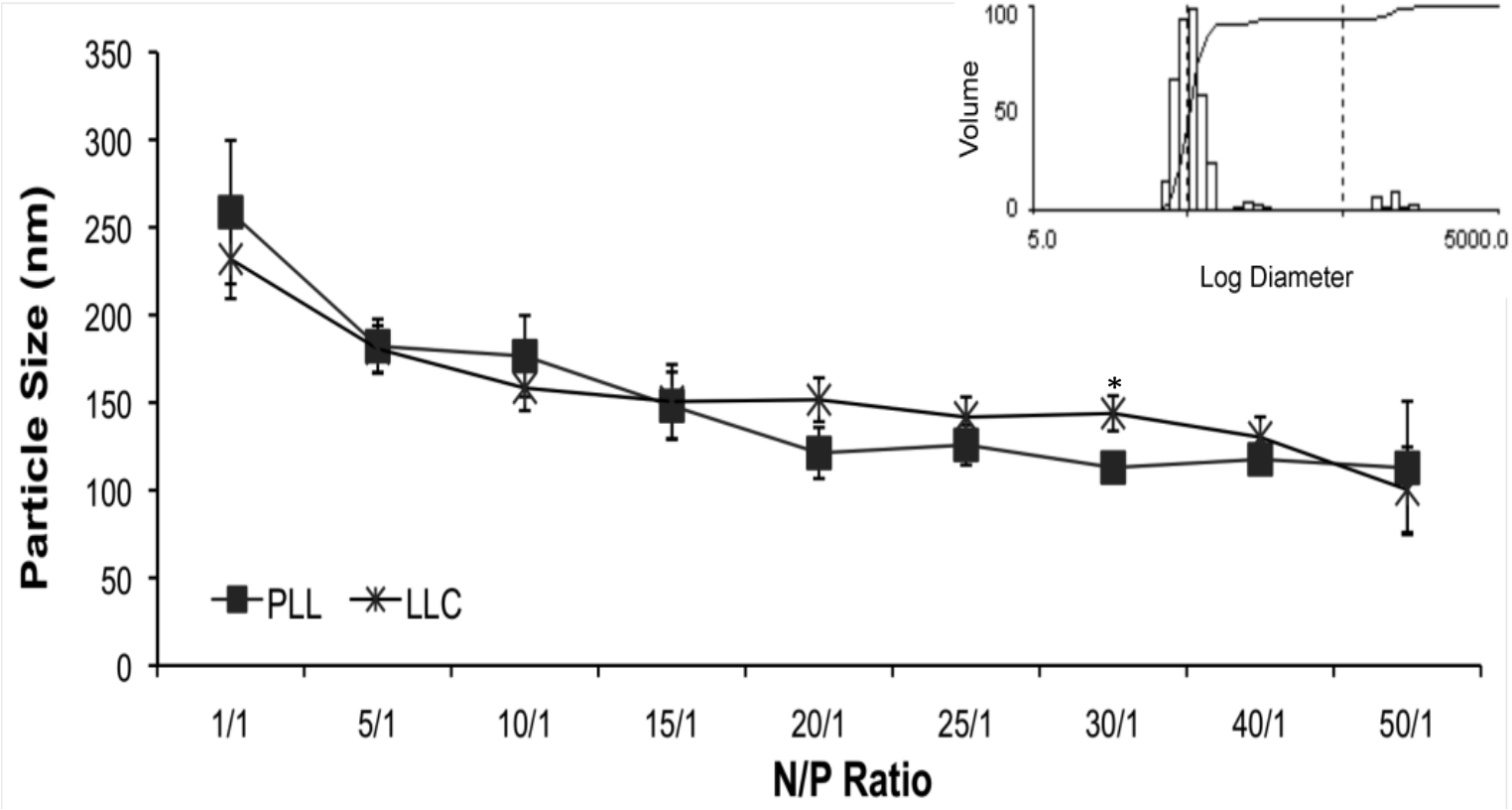

Figure 4.2: Particle size analysis of various LLC/pDNA polyplexes using dynamic light scattering as a function of N/P ratio. Average particle sizes of LLC/pDNA and PLL/pDNA polyplexes were measured at different N/P ratios from 1:1 to 50:1. A representative particle size distribution of the polyplexes prepared from the LLCs with pCMV-luc plasmids at N/P ratio of 25/1 is shown as the inset in the figure. Data represent mean ± SD, N=3. (* indicate p-values of < 0.05)

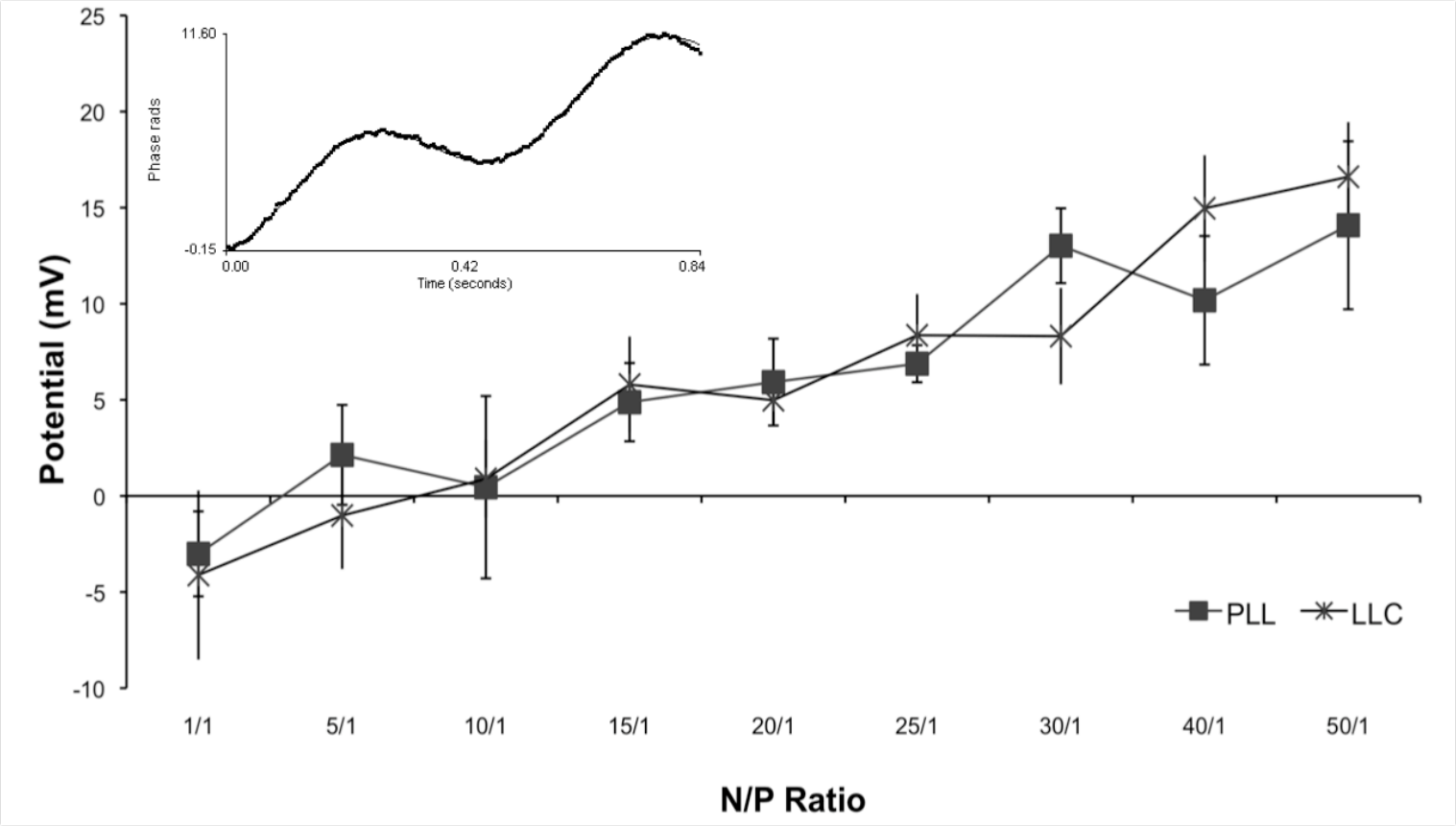

Figure 4.3: Zeta potential (ζ) of LLC/pCMV-Luc polyplexes as a function of N/P ratio. Average zeta potential of LLC/pDNA and PLL/pDNA polyplexes were measured at different N/P ratios from 1:1 to 50:1. A representative zeta potential profile of the polyplexes prepared from the LLCs with pCMV-luc plasmids at N/P ratio of 25/1 is shown as inset in the figure. Data represented as mean ± SD, N=3.

The mechanism of pDNA release from the LLC/pDNA polyplexes was investigated in two reduction assays with the optimized 25/1 N/P ratio polyplexes. In the first study, a gel retardation assay was used to verify pDNA release from the polyplexes as a function of DTT concentration. This data showed that the reduction of the disulfide bonds occurred from a low concentration of ~0.5 mM, which was apparent from the increase in fluorescence in the wells but that higher concentrations of ≥ 3 mM DTT were required to reduce the disulfide bonds completely to release the pDNA from the polyplexes (Figure 4.4, lanes 10-12). Since the intracellular concentration of the reducing agent glutathione (GSH) has been found to be 1-11 mM depending on the cell type, the reduction of LLC/pDNA polyplexes at 3 mM DTT showed that there would be an adequate concentration of GSH in cells to reduce the synthetic disulfide bonds of the LLCs completely. However, even though ≥90% of the pDNA was released from the polyplexes upon reduction, we observed residual pDNA in the wells of the gel retardation assay (Figure 4.4, lane 12) despite treatment with ≥40 mM DTT (data not shown).

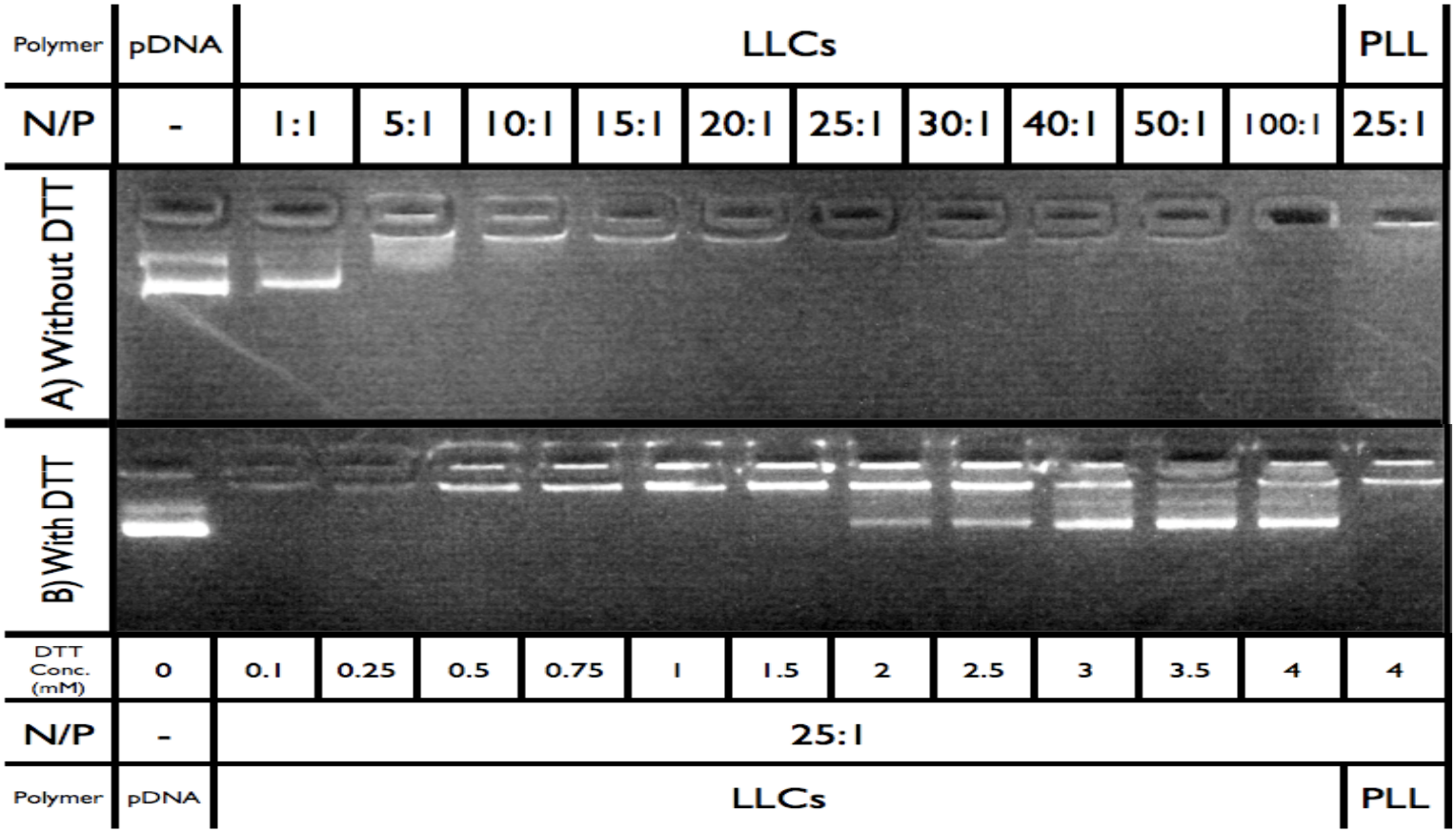

Figure 4.4: Agarose gel electrophoresis of final LLCs with plasmid DNA polyplexes as a function of N/P ratio with increasing concentrations of DTT incubation at 37 ˚C for 30 min (Lane 1, naked pDNA; lanes 2–12, LLC/pDNA at N/P ratio of 25:1 with increasing concentrations of DTT (0.1, 0.25, 0.5, 0.75, 1, 1.5, 2, 2.5, 3, 3.5 and 4 mM of DTT) and lane 13, PLL with 4 mM DTT).

In the second study, fluorescence spectroscopy was used to verify fluorescently labeled pDNA release from the polyplexes as a function of DTT concentration. As shown in Figure 4.5, the fluorescence of the labeled pDNA diminished rapidly after the addition of the LLCs, which corresponded to pDNA complexation (Figure 4.5, inset, lanes 3 and 4). The subsequent addition of DTT resulted in an increase in fluorescence as opposed to the non-reducible PLL control but only to ~90% of the original fluorescence. These data indicated that some of the pDNA remained associated with the LLCs despite complete reduction of the disulfide bonds, which could be because of the residual electrostatic interactions between the positively charged polymer fragments and the negatively charged pDNA. These findings thus were consistent with the gel retardation assay.

The stabilities of the LLC/pCMV-Luc polyplexes were evaluated through a heparin competition and serum stability assays. In heparin competition assay, The PLL/pDNA polyplexes released its DNA load at high concentration of heparin (10-20 μg) at one- and two-hour time points. While on longer time points, pDNA was released at lower heparin concentrations. Whereas the LLC/pDNA polyplexes retained its DNA load at all heparin concentrations over a time frame from one to 24 hours. These results suggest the LLCs copolymers can form strong complexes with pDNA compared to a PLL/pDNA polyplexes (Figure 4.6).

While in serum stability test, the PLL/pDNA polyplexes released its DNA load at high serum concentration (40% to 80%) at 1, 2, 4, 6 and 8-hour time points. While on longer time points, pDNA was released at low serum concentrations (less than 20%), whereas the LLC/pDNA polyplexes released its DNA load in 1 hour at high serum concentrations ranging from 60% to 80%. Furthermore, LLC/pDNA polyplexes never released its DNA load at serum concentrations ranging from 0% to 20% over all time points. These results suggest that the LLCs copolymers can form strong complexes with pDNA compared to a PLL/pDNA polyplexes (Figure 4.7).

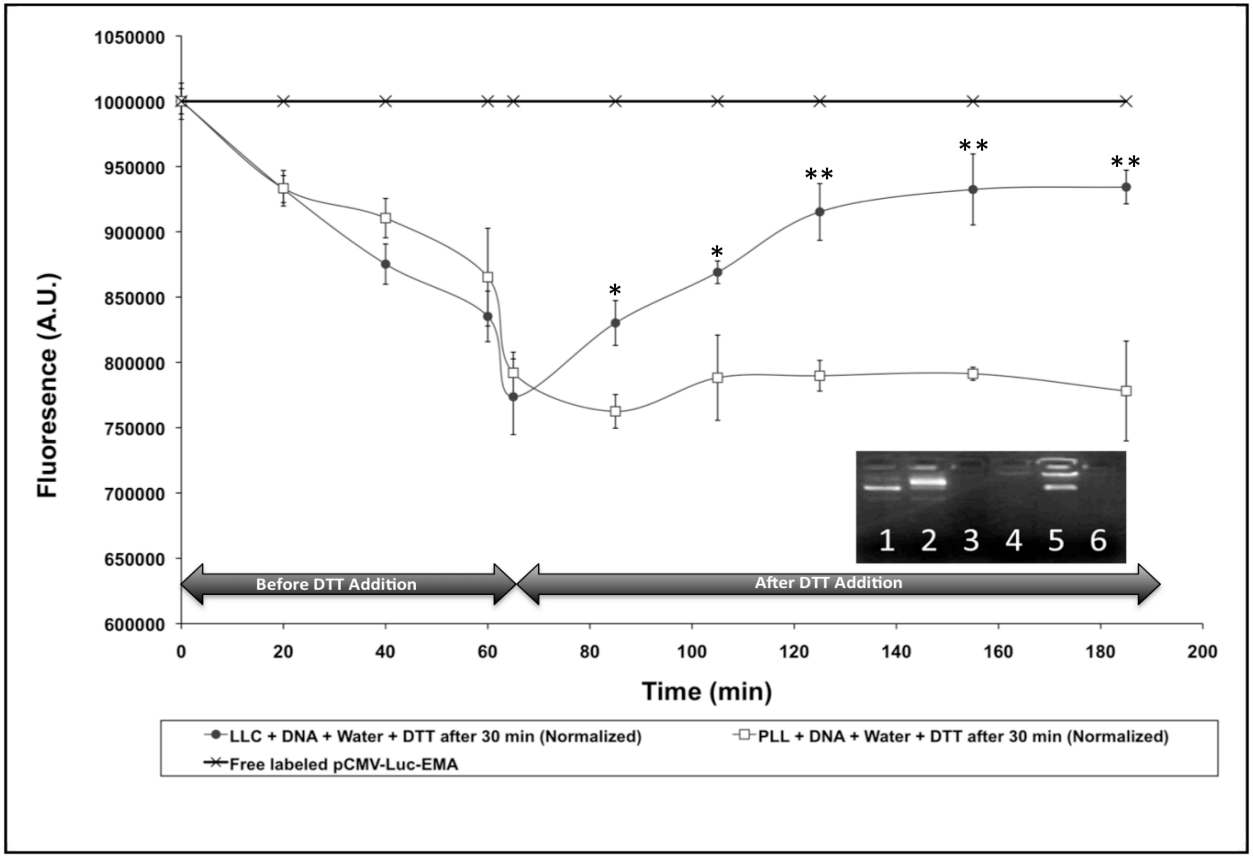

Figure 4.5: Effect of DTT on the release of EMA-labeled pCMV-Luc from LLC/pDNA polyplexes using fluorescence spectroscopy and gel electrophoresis. Lanes 1-6 represented free DNA, DNA with DTT (4 mM), LLCs with DNA, PLL with DNA, LLCs with DNA and DTT (4 mM) and PLL with DNA and DTT (4 mM) respectively. Data represented as mean ± SD, N=3. (* and ** indicates p-value < 0.05 and < 0.01 respectively)

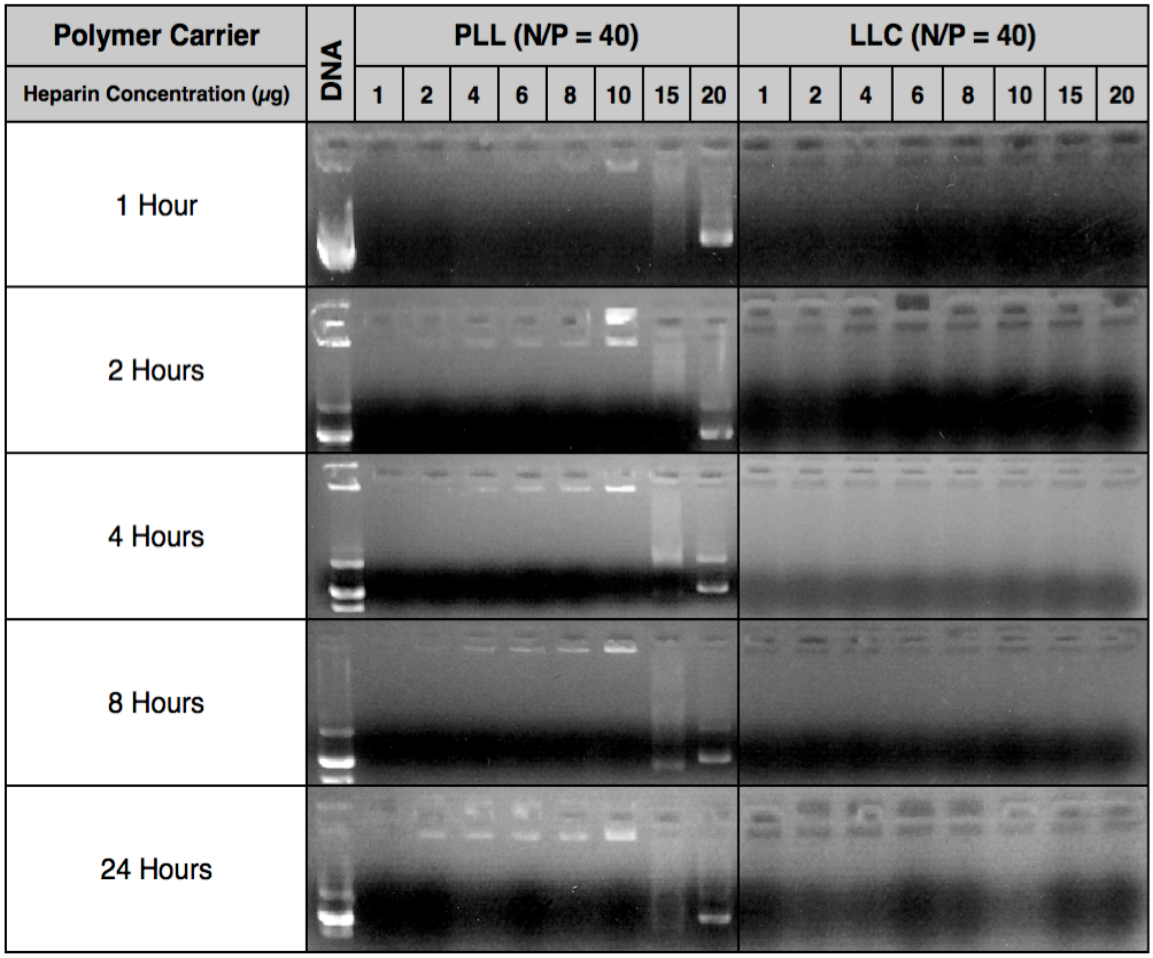

Figure 4.6: Agarose gel electrophoresis of LLC/pDNA and PLL/pDNA polyplexes (N/P=40) with increasing concentrations of heparin (1-20 μg) at various time points (1, 2, 4, 8 and 24 hours).

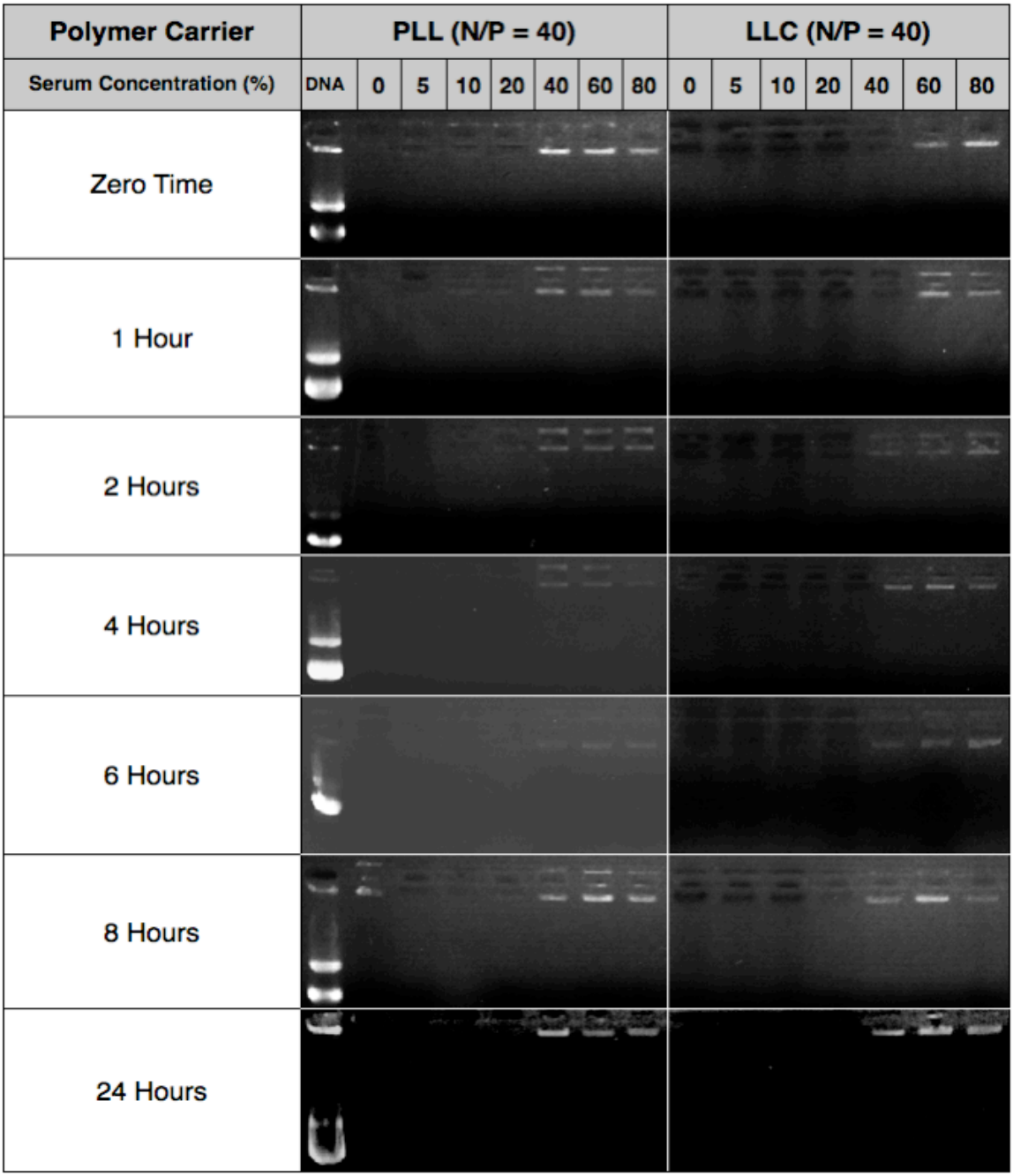

Figure 4.7: Agarose gel electrophoresis of LLC/pDNA and PLL/pDNA polyplexes (N/P=40) with increasing concentrations of serum (0% to 80%) at various time points (0, 1, 2, 4, 6, 8 and 24 hours).

We conjectured that the DNA/LLC polyplexes would protect the conjugated DNA from metabolic degradation by serum endonucleases. The metabolic stability was evaluated by subjecting pDNA(pCMV-Luc)/LLC polyplexes to DNase I for up to 2 hours followed by gel electrophoresis. The DNase I protection assay showed that the LLCs were able to form tight polyplexes, which completely protected the pDNA from degradation by the endonucleases at 37 °C for up to 2 hours as shown by the intact pDNA bands on the stained agarose gel (Figure 4.8, lane 10). In contrast, the naked pDNA was fully degraded by DNase I in 20 minutes (Figure 4.8, lane 2).

Despite the presence of the negatively charged SDS molecules that typically exchange with the polycationic carriers to release the DNA cargo in the assay, LLC copolymer protected the pDNA and prevented its release from the pDNA/LLC polyplexes (Figure 4.8, lanes 6-10, without DTT). pDNA was only released from the polyplexes only in a reducing environment generated by the addition of DTT (reducing agent) for 60 minutes followed by immediate gel electrophoresis (Figure 4.8, lanes 6-10, with 4 mM DTT).

The stability of these polyplexes in the non-reducing environment is very important to ensure safe delivery of the therapeutic plasmid to its target. Moreover, the data showed that pDNA release only occurred in a reductive

environment, despite the presence of other negatively charged SDS molecules that typically exchange with the polycationic carriers to release the DNA cargo in this assay. The unusual stability of these reducible complexes could be because of the low molecular weight polymers that effectively coat the DNA macromolecules to produce very stable complexes.

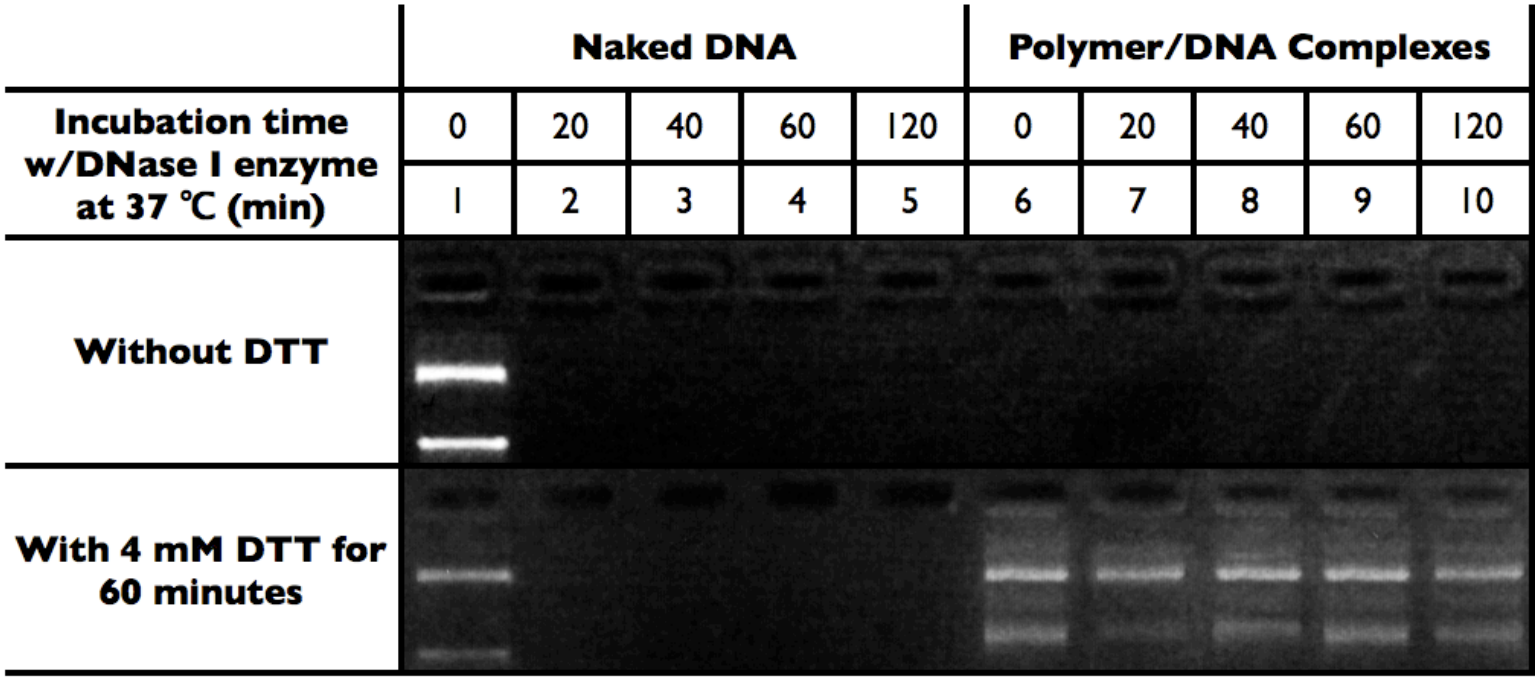

Figure 4.8: DNase I protection assay for LLC/pDNA polyplexes at 25/1 N/P ratio. Lanes 1-5 and 6-10 represent dissociated and reisolated plasmids from naked pDNA and polymer/pDNA polyplexes respectively after exposure to DNase I (1) without DTT and (2) with 4 mM DTT for 120 minutes followed by electrophoresis on a 1% agarose gel at 80 V for 60 minutes.

Genetic reporters are used commonly in cell biology to study gene expression and other cellular events coupled to gene expression, such as receptor activity, intracellular signal transduction, mRNA processing, protein folding and protein:protein interactions. Firefly luciferase is used widely as a reporter for the following reasons:

- Reporter activity is available immediately upon translation since the protein does not require post-translational processing.

- The assay is very sensitive because its light production has the highest quantum efficiency known for any chemiluminescent reaction, and no background luminescence is found in the host cells or the assay chemistry.

The assay is rapid, requiring only a few seconds per sample. The Luciferase Assay System is improved substantially over conventional assay methods in both sensitivity and simplicity. Light is produced by converting the chemical energy of luciferin oxidation through an electron transition, forming the product molecule oxyluciferin. Firefly luciferase, a monomeric 61kD$_a$ protein, catalyzes luciferin oxidation using ATP•Mg^{2+} as a cosubstrate. In the conventional assay for luciferase, a flash of light is generated that decays rapidly after the enzyme and substrates are combined. The Luciferase Assay System incorporates coenzyme A (CoA) for improved kinetics, allowing greater enzymatic

turnover and resulting in increased light intensity that is nearly constant for at least 1 minute. The Luciferase Assay System yields linear results over at least 8 orders of magnitude. Less than 10^{-20} moles of luciferase have been detected under optimal conditions.

When comparing the transfection efficiency of LLC compared to PLL, the luciferase assay showed that LLC/pDNA polyplexes of N/P ratio 40/1 resulted in a 5.5-fold higher transfection efficiency in comparison to the optimal PLL control at an N/P ratio of 50/1 in HDF cells ($p < 0.05$) (Figure 4.9). The LLC/pDNA polyplexes of N/P ratio 20/1 showed a 3-fold higher gene transfection efficiency than the optimal PLL control at an N/P ratio of 20/1 in MCF-7 cells ($p < 0.05$) (Figure 4.10). In MA cells, the LLC/pDNA polyplexes at an N/P ratio of 50/1 resulted in a 4.4-fold higher gene transfection efficiency than the optimal PLL control at an N/P ratio of 50/1 ($p < 0.05$) (Figure 4.11). In HEK-293 cells, the optimal N/P ratio of LLC/pDNA polyplexes (N/P=40) showed over 6 times higher transfection efficiency than the optimal N/P ratio of PLL/pDNA polyplexes (N/P=30) (Figure 4.12). The LLC/pDNA polyplexes of N/P ratio 40/1 showed at least a 5-fold higher gene transfection efficiency than the optimal PLL control at an N/P ratio of 25/1 in MEF cells ($p < 0.05$) (Figure 4.13). In hMSC cells, the LLC/pDNA polyplexes at an N/P ratio of 40/1 resulted in over 10-fold higher gene transfection efficiency than the optimal PLL control at an N/P ratio of 40/1 ($p <$

0.05) (Figure 4.14). These higher transfection efficiencies of the LLCs as compared to the PLL control could be attributed to the more efficient release of the pDNA from the LLC polyplexes into the cytosol of the cells because of reduction of the disulfide bonds along the polymer backbone. In addition, the higher transfection efficiencies of the LLCs could also be because of the higher viabilities of the cells treated with the LLC polyplexes, as compared with the PLL control (Figures 4.24-4.41, discussed in detail later). The LLC/pDNA polyplexes at an N/P ratio of 25/1 were selected as the optimum complexes for use in subsequent studies since these produced high transfection efficiencies in both HDF and MCF-7 cells with the least cytotoxicity in all cell lines. While, in case of hMSC cells, the N/P ratio of 40/1 was selected.

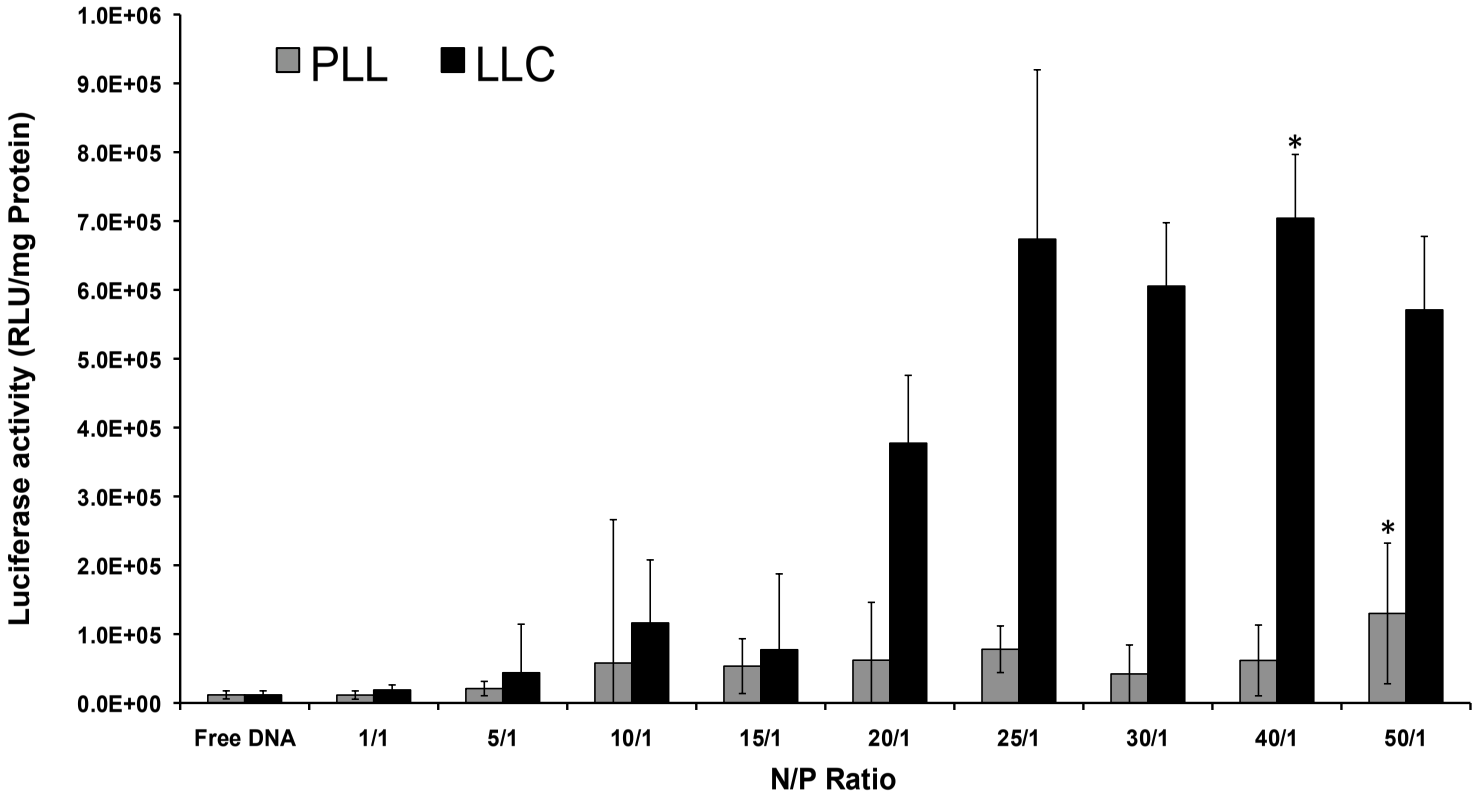

Figure 4.9: In vitro transfection efficiency of the LLC/pCMV-Luc and PLL/pCMV-Luc polyplexes as a function of N/P ratio in HDF cells. Data represented as mean ± SD, N=3. (* indicates p-value < 0.05 between the transfection efficiency generated by optimal PLL and optimal LLCs in each cell line)

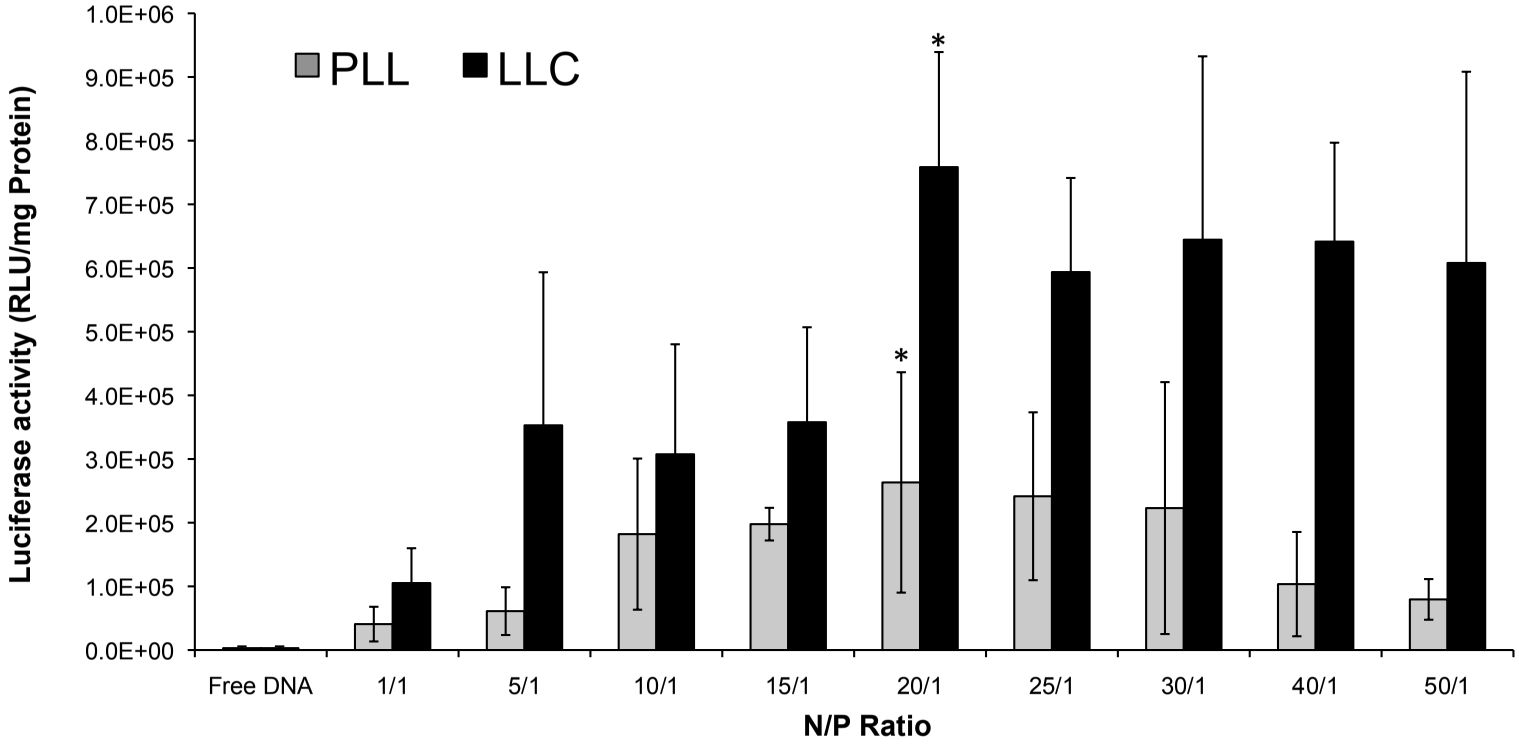

Figure 4.10: In vitro transfection efficiency of the LLC/pCMV-Luc and PLL/pCMV-Luc polyplexes as a function of N/P ratio in MCF-7 cells. Data represented as mean ± SD, N=3. (* indicates p-value < 0.05 between the transfection efficiency generated by optimal PLL and optimal LLCs in each cell line)

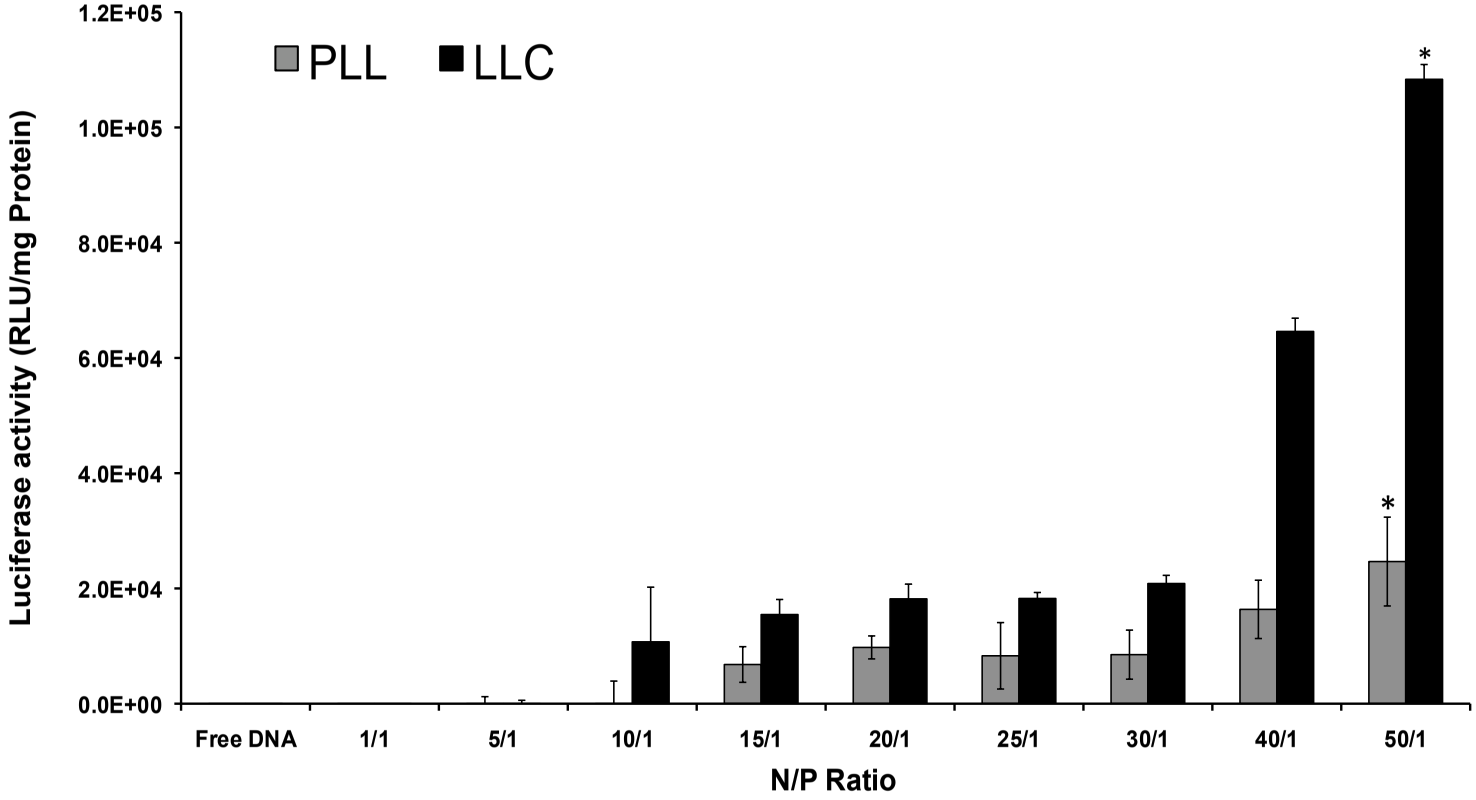

Figure 4.11: In vitro transfection efficiency of the LLC/pCMV-Luc and PLL/pCMV-Luc polyplexes as a function of N/P ratio in MA cells. Data represented as mean ± SD, N=3. (* indicates p-value < 0.05 between the transfection efficiency generated by optimal PLL and optimal LLCs in each cell line)

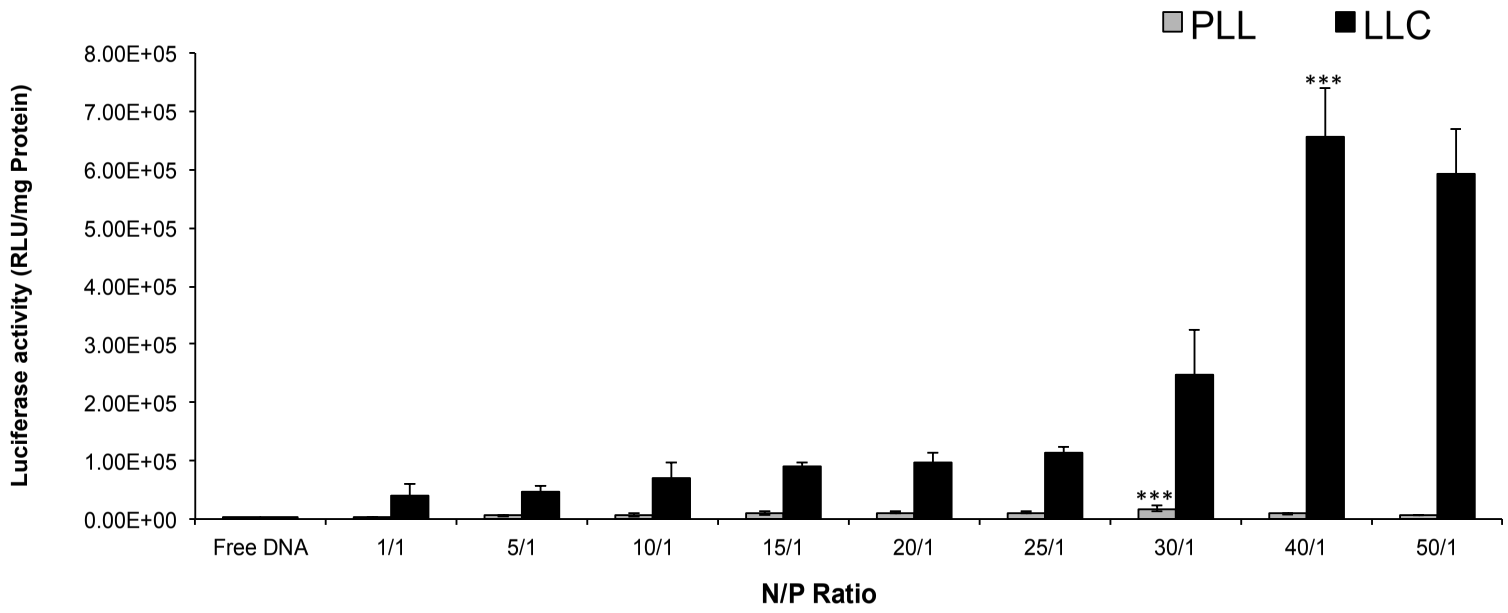

Figure 4.12: In vitro transfection efficiency of the LLC/pCMV-Luc and PLL/pCMV-Luc polyplexes as a function of N/P ratio in HEK293 cells. Data represented as mean ± SD, N=3. Data represented as mean ± SD, N=3. (*** indicates p-value < 0.001 between the transfection efficiency generated by optimal PLL and optimal LLCs in each cell line)

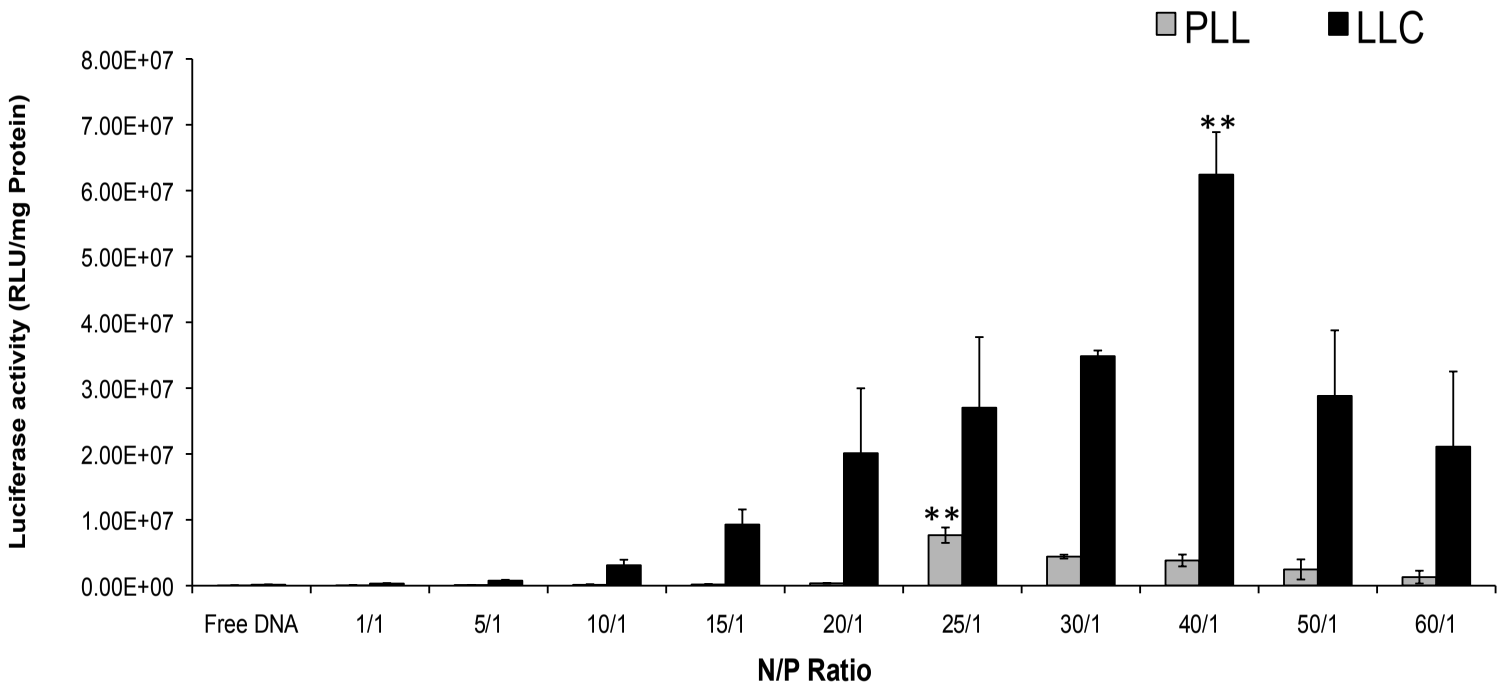

Figure 4.13: In vitro transfection efficiency of the LLC/pCMV-Luc and PLL/pCMV-Luc polyplexes as a function of N/P ratio in MEF cells. Data represented as mean ± SD, N=3. Data represented as mean ± SD, N=3. (** indicates p-value < 0.01 between the transfection efficiency generated by optimal PLL and optimal LLCs in each cell line)

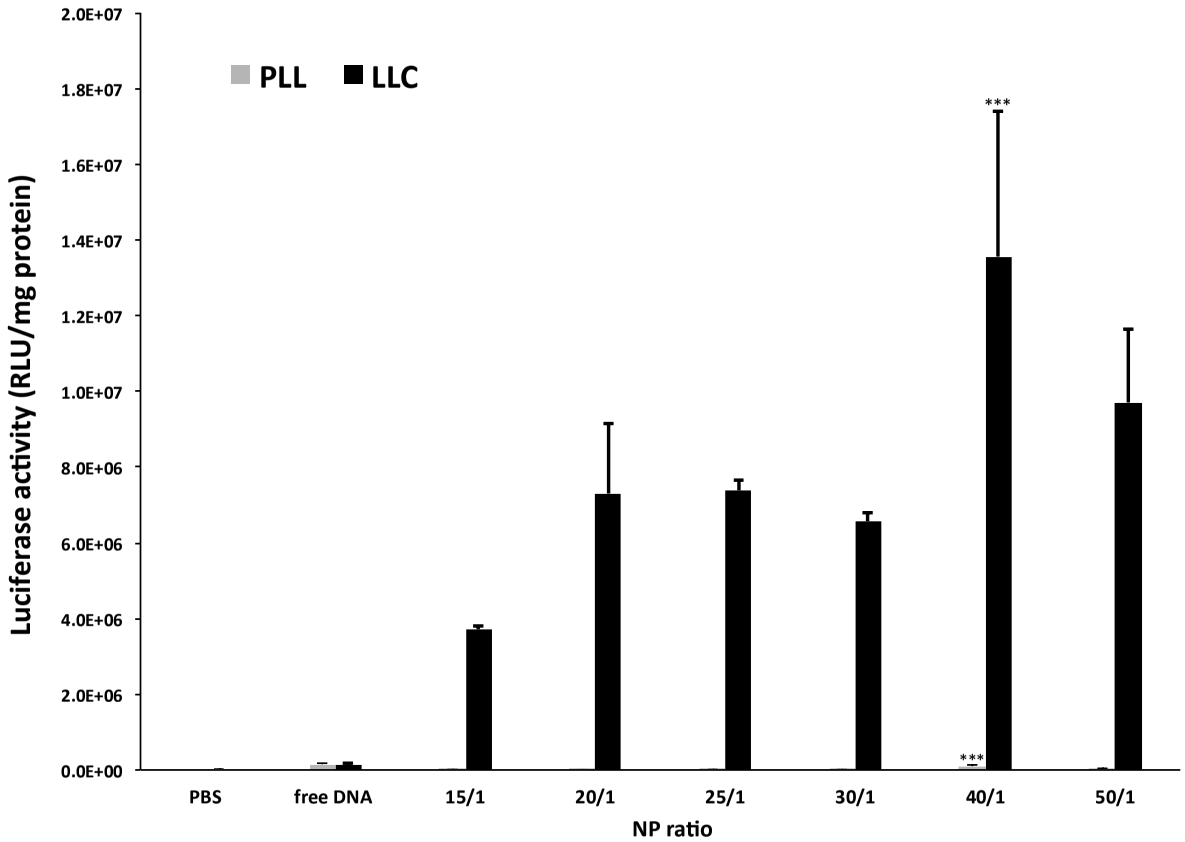

Figure 4.14: In vitro transfection efficiency of the LLC/pCMV-Luc and PLL/pCMV-Luc polyplexes as a function of N/P ratio in human mesenchymal stem cells (hMSC) cells. Data represented as mean ± SD, N=3. Data represented as mean ± SD, N=3. (*** indicates p-value < 0.001 between the transfection efficiency generated by optimal PLL and optimal LLCs in each cell line)

In all of the previous transfection efficiency studies, PLL was used as the main positive control because of the similarities between the backbone structure of PLL and LLC and because both of PLL and LLC are lysine-based polymers.

Other positive controls such as Lipofectamine™ and PEI were also used for the estimation of the efficacy of LLC transfection. Since its commercial launch in 1993, Lipofectamine™ reagents have become one of the most widely used transfection reagents with over 42,000 citations to date. Lipofectamine™ is a liposomal vesicular carrier system formulated using cationic lipids. The positively charged Lipofectamine™ complexes to the negatively charged genetic material through the electrostatic attraction (Clements, Incani et al. 2007; Dalby, Cates et al. 2004; Margineanu, De Feyter et al. 2007). It is worth mentioning that Lipofectamine™ does not encapsulate the genetic materials within the vesicular liposomal structure, as most researchers outside the field of gene delivery believe. Moreover, there is a huge debate over whether encapsulation is beneficial over complexion or not (Dodds, Dunckley et al. 1998; Egilmez, Cuenca et al. 1996; Margineanu, De Feyter et al. 2007; Zhu, Zhang et al. 1996).

The luciferase assay showed that LLC/pDNA polyplexes and Lipofectamine™ lipolexes have comparable transfection efficiency in human mesenchymal stem cells (hMSC), cells with no statistical significance difference

(Figure 4.15).

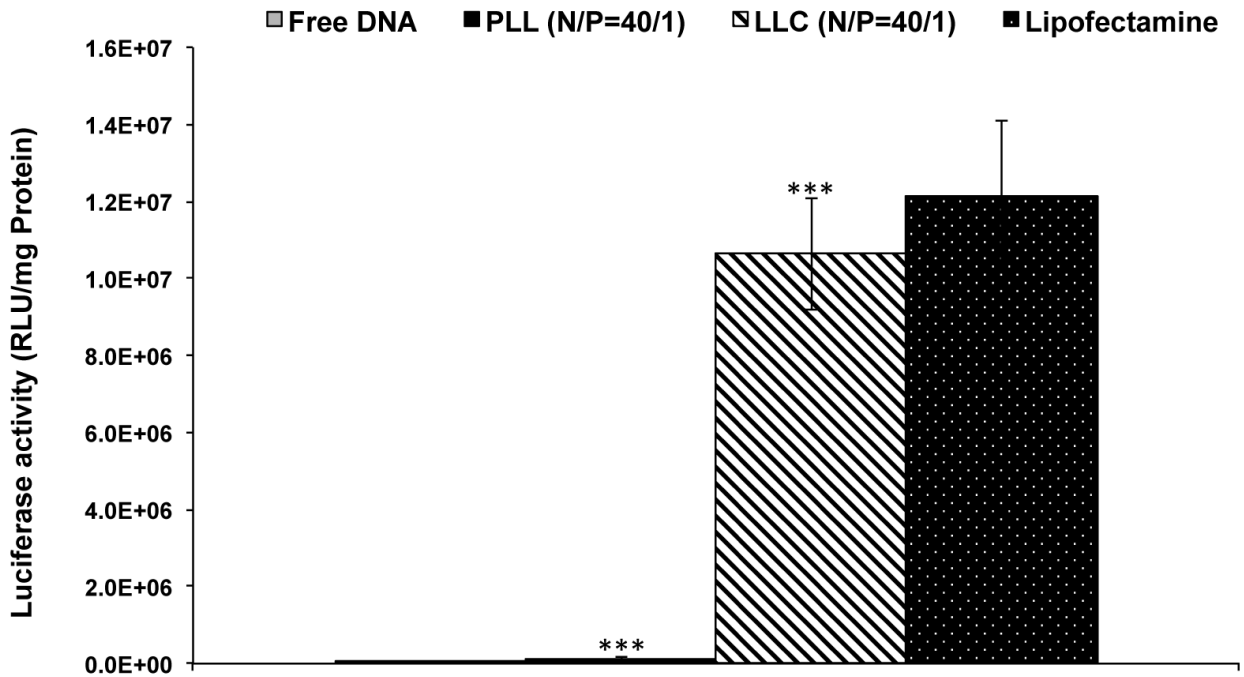

Figure 4.15: *In-vitro* transfection efficiency of the LLC/pCMV-Luc, PLL/pCMV-Luc polyplexes at N/P ratio of 40/1 and Lipofectamine™ (10 μl/1μg pDNA) in human mesenchymal stem cells (hMSC) cells. Data represented as mean ± SD, N=3. No significant difference was observed between LLC and Lipofectamine™. (*** indicates p-value < 0.001 between the transfection efficiency generated by optimal PLL and optimal LLCs in each cell line)

The second positive control used in the transfection efficiency study is polyethylenimine (PEI). PEI is one of the most widely studied polymers in nonviral gene delivery because of its very high efficacy. PEI has the highest cationic density of any synthetic polymer currently available (Arote, Kim et al. 2007; Kim, Cook et al. 2007; Kim, Park et al. 2005).

The PEI/pDNA polyplexes of N/P ratio 40/1 showed two-fold higher gene transfection efficiency than the optimal LLC control at the same N/P ratio HDF cells ($p < 0.05$) (Figure 4.16).

Moreover, PEI showed higher transfection efficiency than LLC in MCF-7 and MA cells. In MCF-7 and MA cells, PEI/pDNA polyplexes showed at least 6-fold and 8-fold higher thransfection efficiency than LLC/pDNA polyplexes at the optimal N/P ratio of 50/1.

The main reason for the effectiveness of PEI as a gene delivery carrier is because of its tremendous buffering capacity commonly referred to as the 'proton sponge effect' ranging between pH 7.2 and 5.0. The average pKa's of bPEI are reported to be 9.5, 6.9, and 3.9 for the protonable 1°, 2°, and 3° amines in a 1:2:1 ratio respectively. In the proton sponge effect, there is a lowering of pH because of the ATPase pumps activated by the maturation of the endosomes to lysosomes, which actively move protons into the vesicles accompanied by

passive influx of chloride and water ions (Boussif, Lezoualc'h et al. 1995; De Smedt, Demeester et al. 2000; Kircheis, Wightman et al. 2001; Kircheis, Wightman et al. 2001; Zanta, Boussif et al. 1997). As a consequence, the endosomal vesicles swell and rupture and their contents are delivered into the cytosol. For this reason, PEI overcomes the limitations of the endosomal degradative pathway and provides high transfection efficiency (Eliyahu, Barenholz et al. 2005; Lungwitz, Breunig et al. 2005; Vasir and Labhasetwar 2006). Moreover, the high cationic charge on PEI facilitates more stable complex formation with the genetic material (De Smedt, Demeester et al. 2000; Luo and Saltzman 2000). The properties that make PEI the most powerful polymeric gene carrier system also contributes to its high cytotoxicity. Such high toxicity limits its in-vivo application (De Smedt, Demeester et al. 2000; Luo and Saltzman 2000).

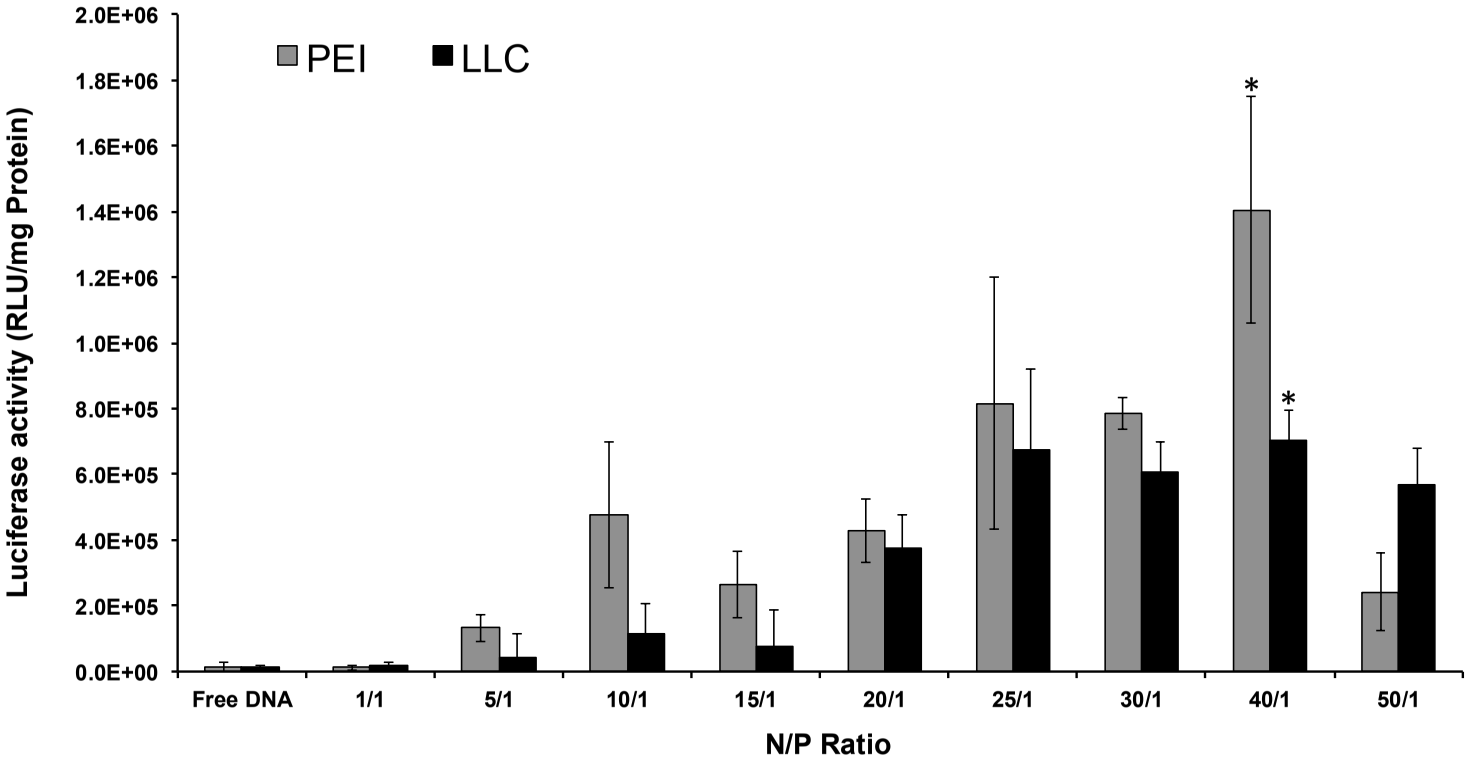

Figure 4.16: In vitro transfection efficiency of the LLC/pCMV-Luc and PEI/pCMV-Luc polyplexes as a function of N/P ratio in HDF cells. Data represented as mean ± SD, N=3. (* indicates p-value < 0.05 between the transfection efficiency generated by optimal PEI and optimal LLCs in each cell line)

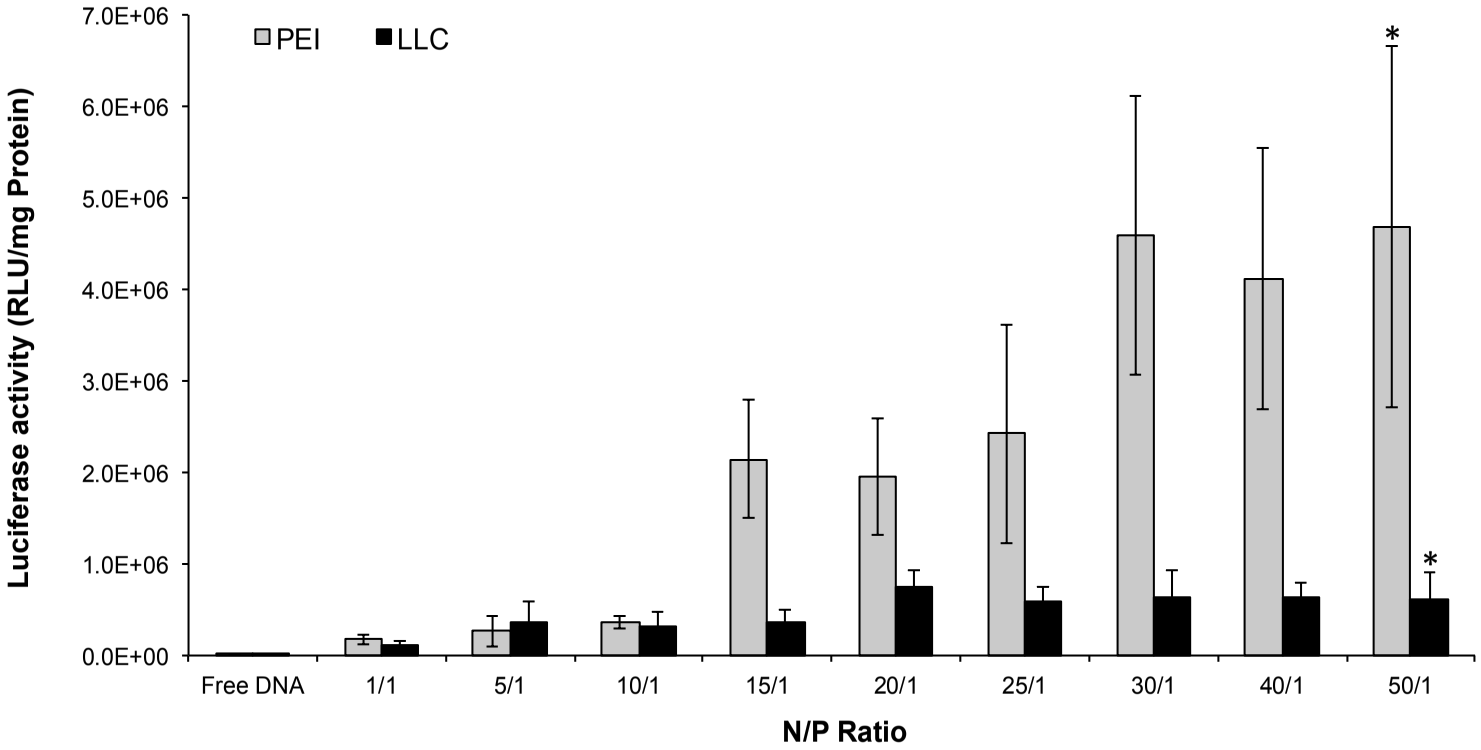

Figure 4.17: In vitro transfection efficiency of the LLC/pCMV-Luc and PEI/pCMV-Luc polyplexes as a function of N/P ratio in MCF-7 cells. Data represented as mean ± SD, N=3. (* indicates p-value < 0.05 between the transfection efficiency generated by optimal PEI and optimal LLCs in each cell line)

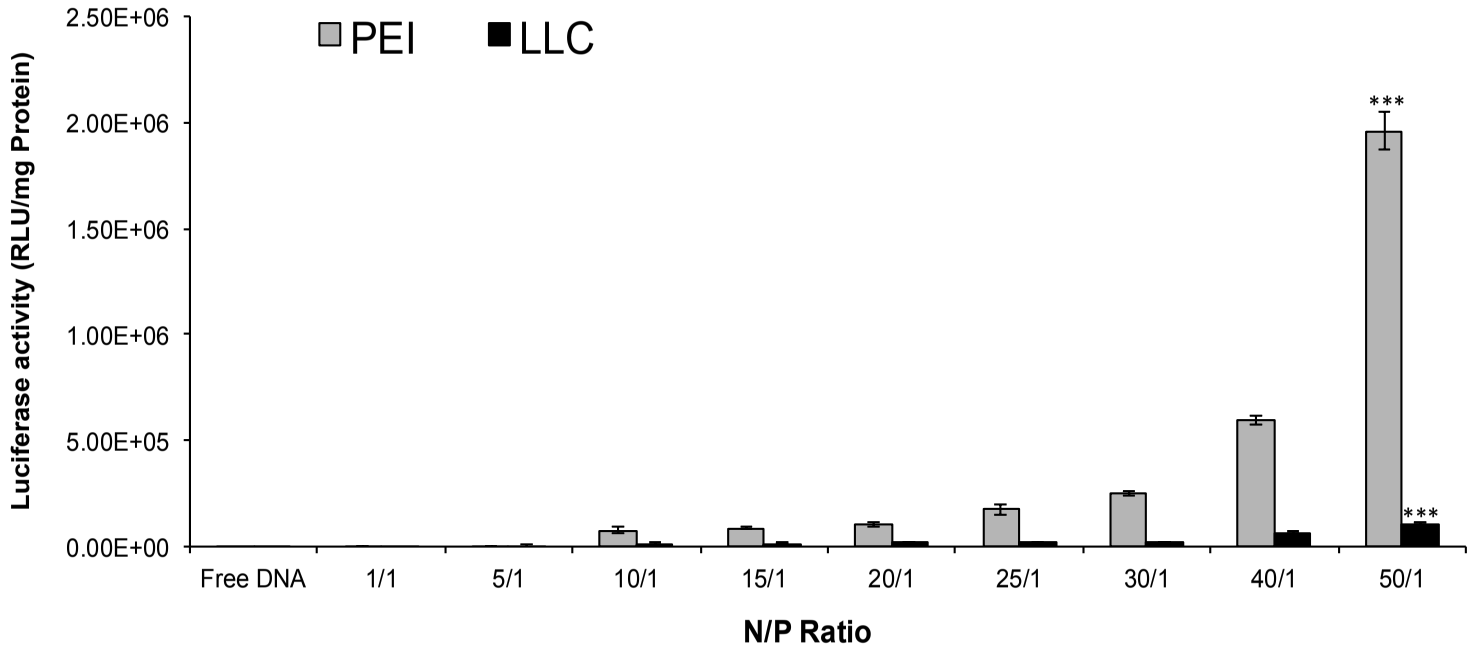

Figure 4.18: In vitro transfection efficiency of the LLC/pCMV-Luc and PEI/pCMV-Luc polyplexes as a function of N/P ratio in MA cells. Data represented as mean ± SD, N=3. (*** indicates p-value < 0.001 between the transfection efficiency generated by optimal PEI and optimal LLCs in each cell line)

The effect of serum on the transfection efficiency of LLC polyplexes was investigated at the N/P ratios for LLC and PLL polyplexes that produced the highest transfection efficiencies (50/1 and 40/1 respectively) in HDF cells. The results showed that LLCs and PLL polyplexes in serum produced a 5-fold and 4-fold reduction in luciferase activity respectively. This could be because of the binding of the positively charged polyplexes with the negatively charged serum proteins that typically reduce the cellular uptake of polymer/pDNA polyplexes (Figure 4.19). However, the relative difference in transfection efficiency between LLCs and PLL polyplexes was found to be serum independent, since the statistical significance was maintained despite the presence of serum (p-value < 0.05).

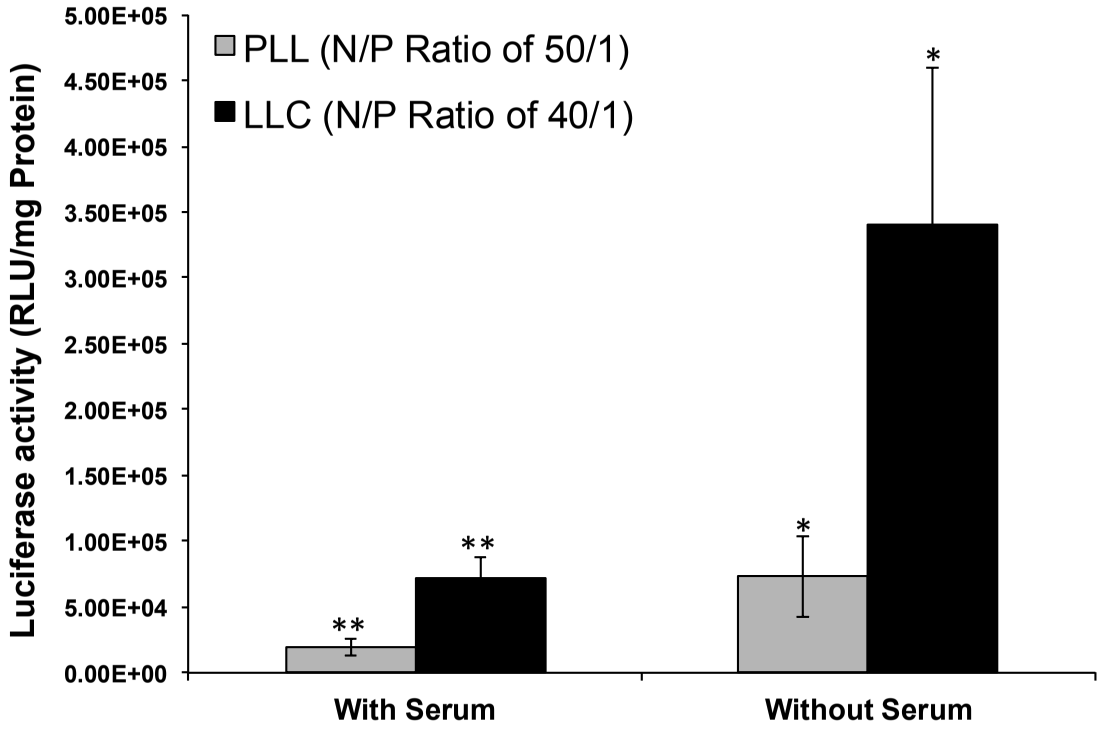

Figure 4.19: In vitro transfection efficiency of the LLC/pCMV-Luc and PLL/pCMV-Luc polyplexes in serum at optimal N/P ratio for PLL (N/P of 50/1) and LLCs (N/P of 40/1) in HDF cells. Data represented as mean ± SD, N=3. No significant difference was observed between LLC and Lipofectamine™. (* and ** indicates p-value < 0.05 and < 0.01 respectively between the transfection efficiency generated by optimal PLL and optimal LLCs in each cell line)

Furthermore, LLC-mediated transfections were evaluated in hMSCs stem cells using the reporter plasmid pSV_{40}-VEGF. pSV_{40}-VEGF is the main therapeutic gene used in the investigation of the ex-vivo efficacy of DNA/LLC polyplexes through treatment of myocardial infarction using ex-vivo gene therapy to generate genetically modified stem cells (discussed in detail in chapter 5). The Human Vascular Endothelial Growth Factor (Hu VEGF) ELISA was used for the in vitro quantitative determination of Hu VEGF in human serum, plasma, buffered solution, or cell culture medium.

Vascular Endothelial Growth Factor (VEGF), originally named vascular permeability factor (VPF), is an important regulator of angiogenesis and vasculogenesis. Angiogenesis occurs in normal processes related to the female reproductive cycle and in pathological processes such as tumor growth and metastasis, diabetic retinopathy, rheumatoid arthritis, or after tissue ischemia. Vasculogenesis involves the formation of blood vessels through the differentiation of endothelial cells from mesodermal precursors. Whereas vasculogenesis is restricted to embryonic development, angiogenesis operates throughout life when new vascularization is required (Ribatti 2005).

Alternative splicing of VEGF mRNA accounts for 5 isoforms of 121, 145, 165, 189, and 206 amino acids, of which the 165 amino acid form is the most abundant and biologically active. The active forms of these isoforms are disulfide-

linked homodimers. VEGF-121 differs from the larger VEGF isoforms in that it is the only one that does not bind to heparin. The 165 amino acid protein is a 46 kD_a homodimer that is produced by numerous cell types that include a variety of tumors, macrophages, and folliculostellate cells.

There are two known high affinity receptors for VEGF, fms-like tyrosine kinase (Flt-1) and fetal liver kinase (Flk-1). Both are tyrosine kinases and appear to be exclusively expressed on endothelial cells. The binding of VEGF to its receptors activates a signaling cascade that results in the activation of the mitogen-activated kinase (MAPK) and the tyrosine phosphorylation of phospholipase Cγ1 (PLCγ 1), which in turn leads to increases in the intracellular levels of inositol 1,4,5-triphosphate and calcium. The increase in calcium triggers nitric oxide synthase (NOS) to produce NO. This NOS activity is necessary for VEGF to stimulate angiogenesis and increase vascular permeability. Expression of VEGF and its receptor occurs during angiogenesis and vasculogenesis.

The human VEGF kit is a solid phase sandwich Enzyme Linked-Immuno-Sorbent Assay (ELISA). A polyclonal antibody specific for human VEGF has been coated onto the wells of the microtiter strips provided. Samples, including standards of known human VEGF content, control specimens, and unknowns, are pipetted into these wells. During the first incubation, the Hu VEGF antigen binds to the immobilized (capture) antibody on one site. After washing, a

biotinylated monoclonal antibody specific for Hu VEGF is added. During the second incubation, this antibody binds to the immobilized Hu VEGF captured during the first incubation.

After removal of the excess second antibody, Streptavidin-Peroxidase (enzyme) is added. This binds to the biotinylated antibody to complete the four-member sandwich. After a third incubation and washing to remove all the unbound enzyme, a substrate solution is added, which is acted upon by the bound enzyme to produce color. The intensity of this colored product is directly proportional to the concentration of Hu VEGF present in the original specimen.

The LLC/pDNA polyplexes at an N/P ratio of 40/1 resulted in over 10-fold higher gene transfection efficiency than the optimal PLL control at an N/P ratio of 40/1 ($p < 0.05$) (Figure 4.20). Such results are very consistent with the results from the reporter plasmid pCMV-Luc.

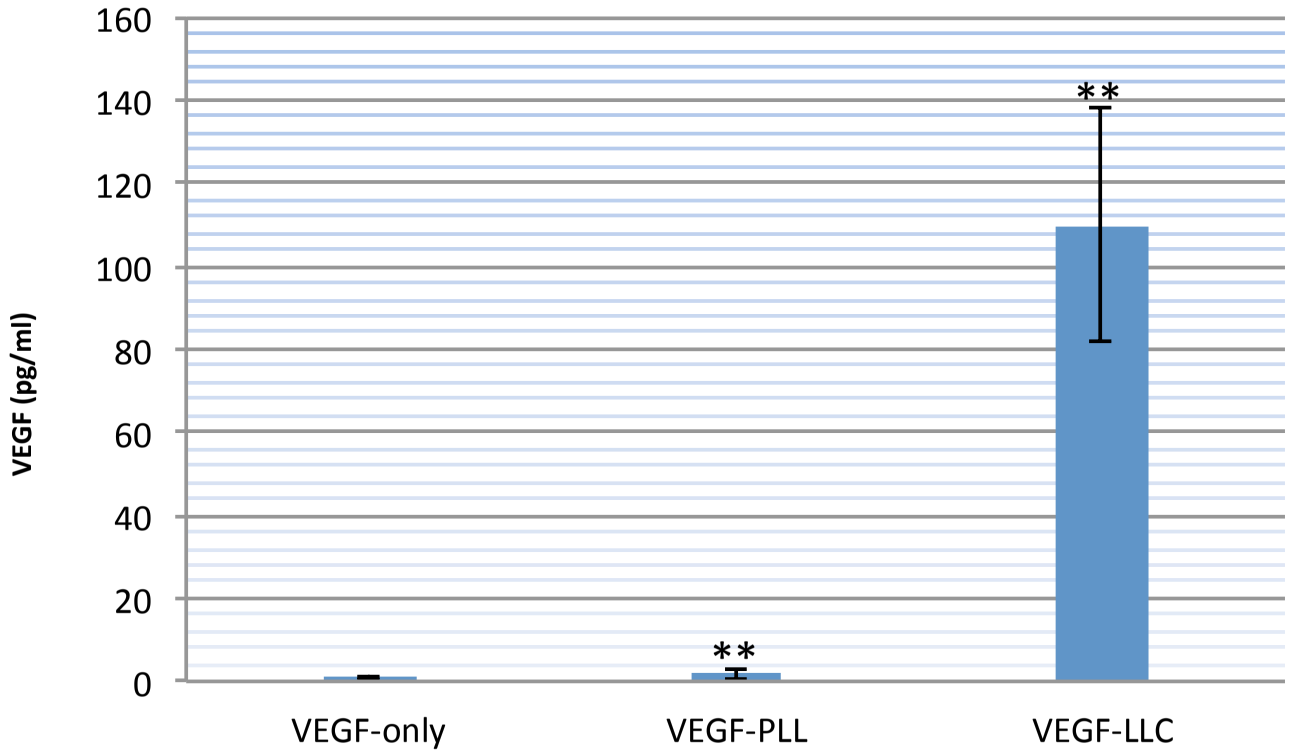

Figure 4.20: hVEGF$_{165}$ expression in hMSCs transfected with pSV$_{40}$-VEGF$_{165}$ gene using PLL and LLC as the transfecting agent at N/P ratio of 40/1 using VEGF ELISA Kit. (n=3). Data represented as mean ± SD, N=3. Data represented as mean ± SD, N=3. (** indicates p-value < 0.01 between the transfection efficiency generated by optimal PLL and optimal LLCs in each cell line)

HDF cells were transfected with LLC, bPEI and Lipofectamine™ complexed with the pCMV-EGFP plasmids to evaluate the transfection efficiency of LLCs compared to other standard commercial nonviral gene delivery vectors using fluorescence microscopy to detect the generated green fluorescent protein. The fluorescence microscopy data (Figure 4.21) showed that the transfection efficiency of the bioreducible LLC polyplexes was comparable to the commercial vectors. Specifically, quantitative analysis of the data showed that the percentage of cells expressing EGFP from the LLC/pDNA polyplexes was not significantly different from the gene expression obtained from the PEI and Lipofectamine™ commercial vectors ($p > 0.05$) (Figure 4.22). These data confirmed that LLCs are efficient gene transfection agents compared to the commercially used nonviral transfection agents such as PEI and Lipofectamine™.

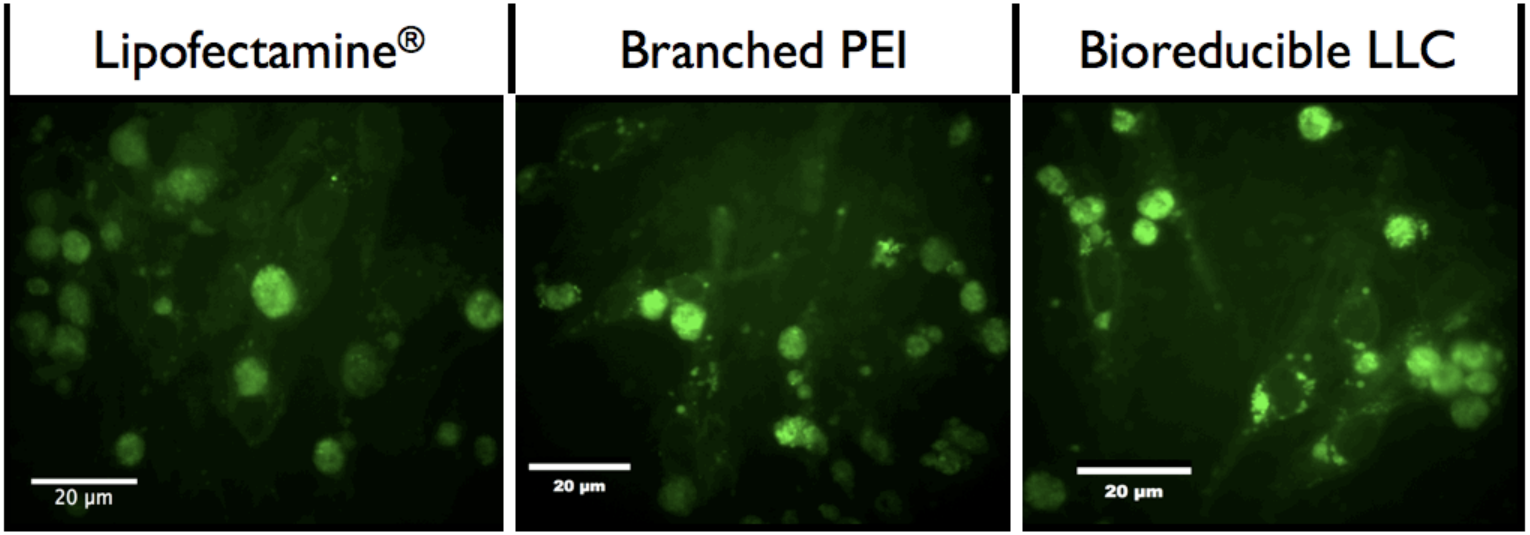

Figure 4.21: Fluorescence microscopy images of transfected HDF cells with pCMV-EGFP complexed with either branched PEI, or Lipofectamine™, and reducible LLCs at N/P ratio of 25/1 after 48 hours of transfection.

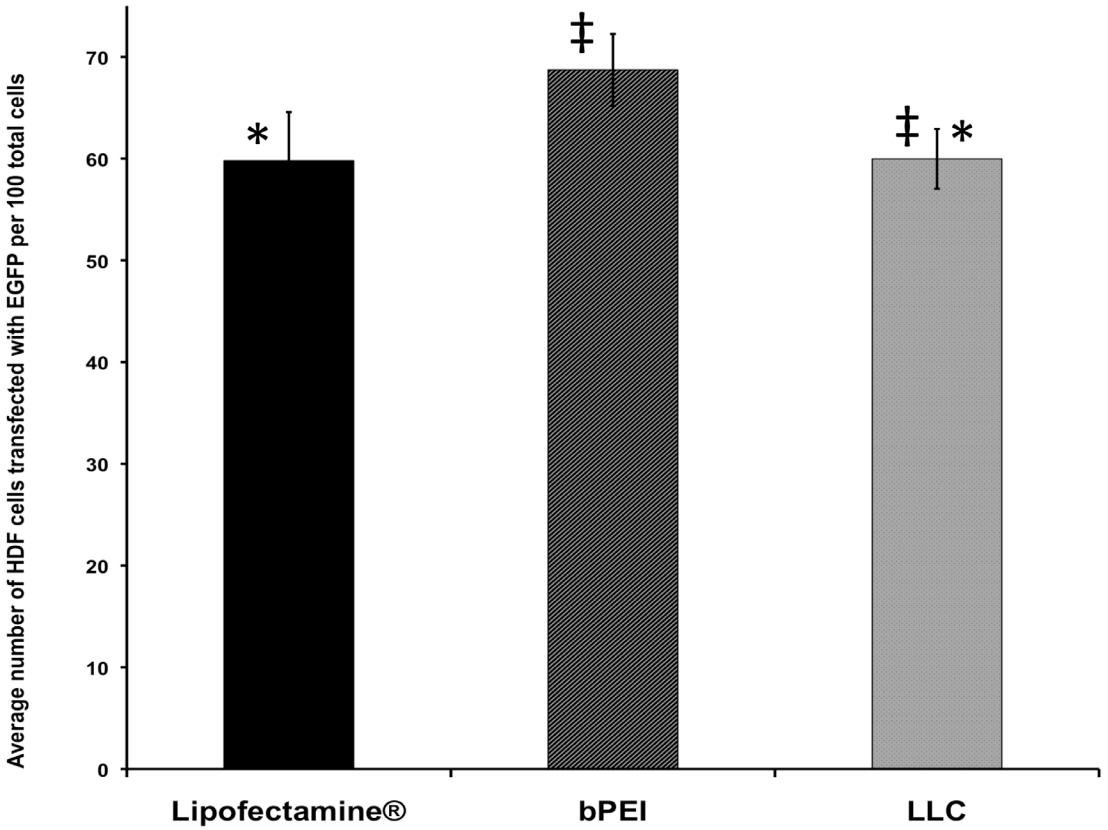

Figure 4.22: Transfection efficiency of reducible LLCs, Lipofectamine™ and branched PEI as a percentage of EGFP positive cells per total amount of HDF cells. Data represented as mean ± SD, N=3 (*, ‡ indicate p-value > 0.05).

HDF cells transfected with fluorescently labeled pCMV-Luc plasmid with ethidium monoazide (EMA) and polyplexed with LLC copolymers were viewed with confocal microscopy to determine whether pDNA released from LLC/pDNA polyplexes would be observed in the cytosol of treated cells. The confocal microscopy data showed red punctate staining indicative of the presence of EMA-labeled pDNA in the cytosol, aggregated around the nucleus, and possibly within the nucleus of DAPI-stained cells transfected with LLC/pDNA polyplexes after 4, 8, and 12 hours (Figure 4.23). The delivery of the pDNA around and possibly in the nucleus could reflect the efficient reduction of the disulfide bonds of the copolymer chains and hence efficient release of pDNA that was trafficked to the nucleus. Nevertheless, these data doesn't discriminate perinuclear from nuclear delivery. A more detailed future confocal microscopy study, using Z-stacks, can help in identifying the exact location of the pDNA. Moreover, since the polymers were not labeled, the observed fluorescence could have represented either free pDNA or pDNA still associated with the copolymers after disulfide reduction, which was actually shown in the DTT fluorescence assay (discussed earlier in Figure 4.5). These data together with the fluorescence microscopy studies (Figures 4.21 and 4.22) suggested that low MW reducible LLCs were capable of delivering its DNA cargo into the cytosol and possibly into the nucleus of transfected cells, which resulted in transfection efficiencies

comparable to higher MW non-degradable systems without compromising cell viabilities (discussed later), which is a known limiting factor for commercial delivery systems such as PEI. Further studies are underway to determine specific subcellular localization of both polymer and plasmids following transfection of cells with LLC/pDNA polyplexes.

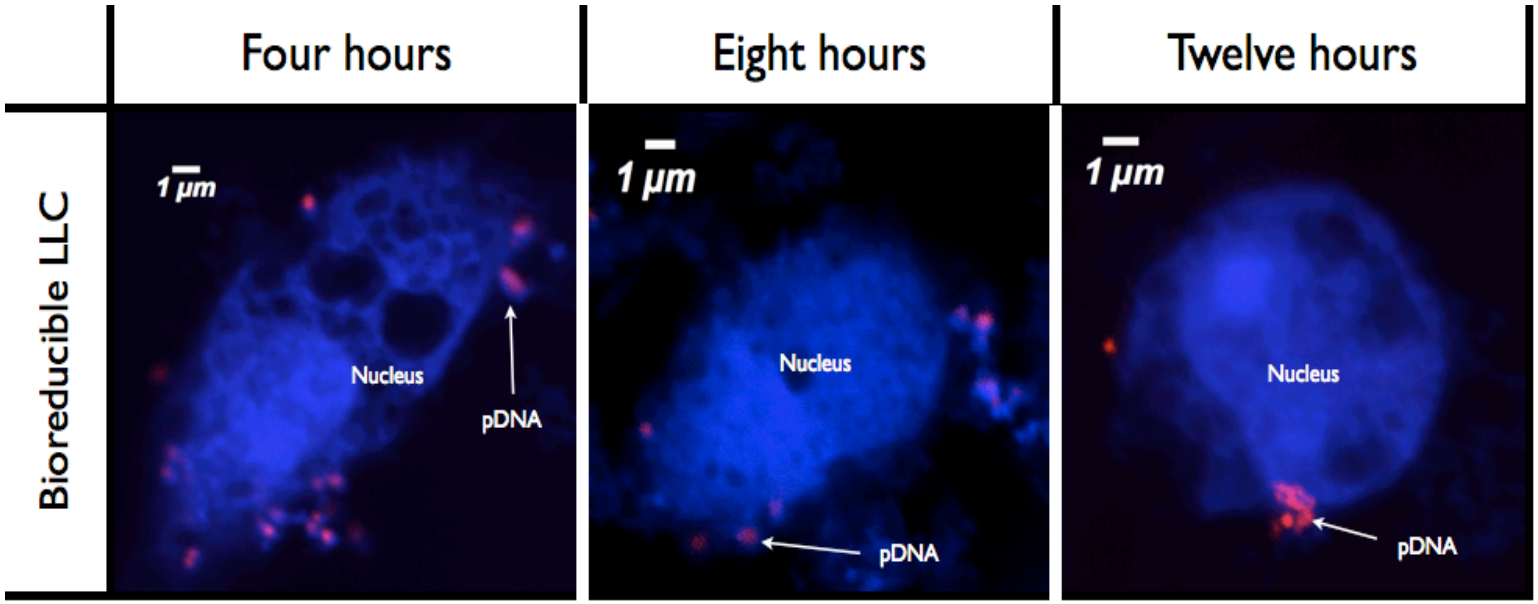

Figure 4.23: Confocal microscopy images of transfected HDF cells with EMA-labeled pCMV-Luc using reducible LLCs at N/P ratio of 25/1 after 4, 8 and 12 hours post transfection.

Cell death can occur either by apoptosis, a highly regulated pathway involving signal transduction cascades, or by necrosis. There are a number of screening techniques available that detect cytotoxicity and cell death, independent of mechanism. The need for profound, quantitative and reliable for the precise detection of cell death led to the development of several standard assays for the quantification of cellular viability (Bonfoco, Krainc et al. 1995).

MTT and LDH assay were used to evaluate the effect of LLC polyplexes on the cell viability. PLL, PEI and lipofectamine™ were used as positive control. MTT assay is a standard colorimetric assay for measuring the activity of enzymes that reduce MTT to formazan, giving a purple color. This mostly happens in mitochondria, and as such it is in large a measure of mitochondrial activity. It is used to determine cytotoxicity of potential medicinal agents and other toxic materials.

Yellow MTT (3-(4,5-Dimethylthiazol-2-yl)-2,5-diphenyltetrazolium bromide, a tetrazole) is reduced to purple formazan in the mitochondria of living cells. Dimethyl sulfoxide (DMSO) is added to dissolve the insoluble purple formazan product and form a colored solution. The absorbance of this solution can be quantified by UV spectrophotometer at a wavelength usually around 570 nm.

The MTT assay showed that LLC polyplexes produced lower cytotoxicity compared to PLL at N/P ratios up to 50/1. LLC polyplexes at 20/1 N/P ratio

maintained the highest cell viability in all cell lines in comparison to PLL at the same N/P ratio. PLL at 20/1 N/P ratio showed a decrease in cell viability to 82%, 77%, 81%, 92%, 93%, 83% and 82% for HDF, MCF-7, MA, 4T1, MEF, HEK-293 and hMSC cells respectively with ~100% cell viability for LLC/pDNA polyplexes in all cell lines (Figures 4.24-4.30). PLL at 25/1 N/P ratio resulted in a decrease in cell viability to 80%, 81%, 65%, 91%, 91%, 77% and 76% for HDF, MCF-7, MA, 4T1, MEF, HEK-293 and hMSC cells respectively as compared to ~100% cell viability for LLC/pDNA polyplexes in all cell lines at this N/P ratio (Figures 4.24-4.30). In addition, LLC polyplexes produced almost no cytotoxicity in HDF cells at N/P ratios from 1/1 to 40/1 compared to PLL ($p < 0.05$) (Figure 4.24). For an N/P ratio of 30/1, LLC polyplexes showed ~100% cell viability for all cell lines as compared to PLL at the same N/P ratio, which produced an 81%, 75%, 60%, 90%, 88%, 75% and 74% reduction in cell viability in for HDF, MCF-7, MA, 4T1, MEF, HEK-293 and hMSC cells respectively (Figures 4.24-4.30). Moreover, a cell viability of ~100% was maintained for LLC/pDNA polyplexes as compared to a reduced 75%, 75% and 74% cell viability for PLL from an N/P ratio of 1/1 to 30/1 for MCF-7, HEK-293 and hMSC cells respectively ($p < 0.05$) (Figures 4.25, 4.29 and 4.30). LLC/pDNA polyplexes showed negligible cytotoxicity in MA cells at N/P ratios from 1/1 to 25/1 compared to PLL ($p < 0.05$) (Figure 4.26). However, the cytotoxicity of LLC/pDNA polyplexes in MA and MCF-7 cells was higher than

that of HDF cells at N/P ratios of 40/1 and 50/1. This observation influenced our choice of the HDF cell line for use in subsequent studies.

It was observed that the cytotoxicity in case of PLL and LLC polyplexes in HDF cells were mainly correlated to the polymers not the pDNA. A separated MTT experiment was done on HDF cells using LLC and PLL polymers without the inclusion of the pDNA yielded comparable results to the polyplexes with no significant differences (Data not shown).

It was also observed that using different plasmids did not affect the cytotoxicity profile of the gene carrier system. This was observed in the cell viability profile of LLC and PLL polyplexes with two different plasmids, pCMV-Luc and pSV_{40}-VEGF, in hMSC cells (Figures 4.30 and 4.31). The cell viability of LLC/pCMV-Luc and LLC/pSV_{40}-VEGF polyplexes in hMSC cells was 82% and 83% at the optimal N/P ratio of 40/1. Moreover, the cell viability of PLL/pCMV-Luc and PLL/pSV_{40}-VEGF polyplexes in hMSC cells was 72% and 75% at the optimal N/P ratio of 40/1 (Figures 4.30 and 4.31).

The cytotoxicity profile of LLC also was compared to the nonviral gene carrier polymer, PEI. Although, PEI showed better transfection efficiency than LLC, it was much more toxic than LLC. The MTT assay showed that LLC polyplexes produced lower cytotoxicity compared to PEI at N/P ratios up to 50/1. LLC polyplexes at 20/1 N/P ratio maintained the highest cell viability in all cell

lines in comparison to PLL at the same N/P ratio. PEI at 20/1 N/P ratio showed a decrease in cell viability to 62%, 74% and 50% for HDF, MCF-7 and 4T1 cells respectively with ~100% cell viability for LLC/pDNA polyplexes in all cell lines (Figures 4.32-4.34). PEI at 25/1 N/P ratio resulted in a decrease in cell viability to 58%, 61% and 54% for HDF, MCF-7 and 4T1 cells respectively as compared to ~100% cell viability for LLC/pDNA polyplexes in all cell lines at this N/P ratio (Figures 4.32-4.34). In addition, LLC polyplexes produced almost no cytotoxicity in HDF cells at N/P ratios from 1/1 to 40/1 compared to PEI ($p < 0.05$) (Figure 4.31). For an N/P ratio of 30/1, LLC polyplexes showed ~100% cell viability for all cell lines as compared to PEI at the same N/P ratio, which produced an 52%, 57%, 54% and 52% reduction in cell viability in for HDF, MCF-7 and 4T1 cells respectively (Figures 4.32-4.34).

Furthermore, the cytotoxicity profile was also compared to Lipofectamine™. There was no statistical significance difference in cell viability of Lipofectamine™/pDNA lipoplexes and LLC/pDNA polyplexes in hMSC cells using two different plasmids pSV_{40}-VEGF and pCMV-Luc (Figures 4.35 and 4.36 respectively).

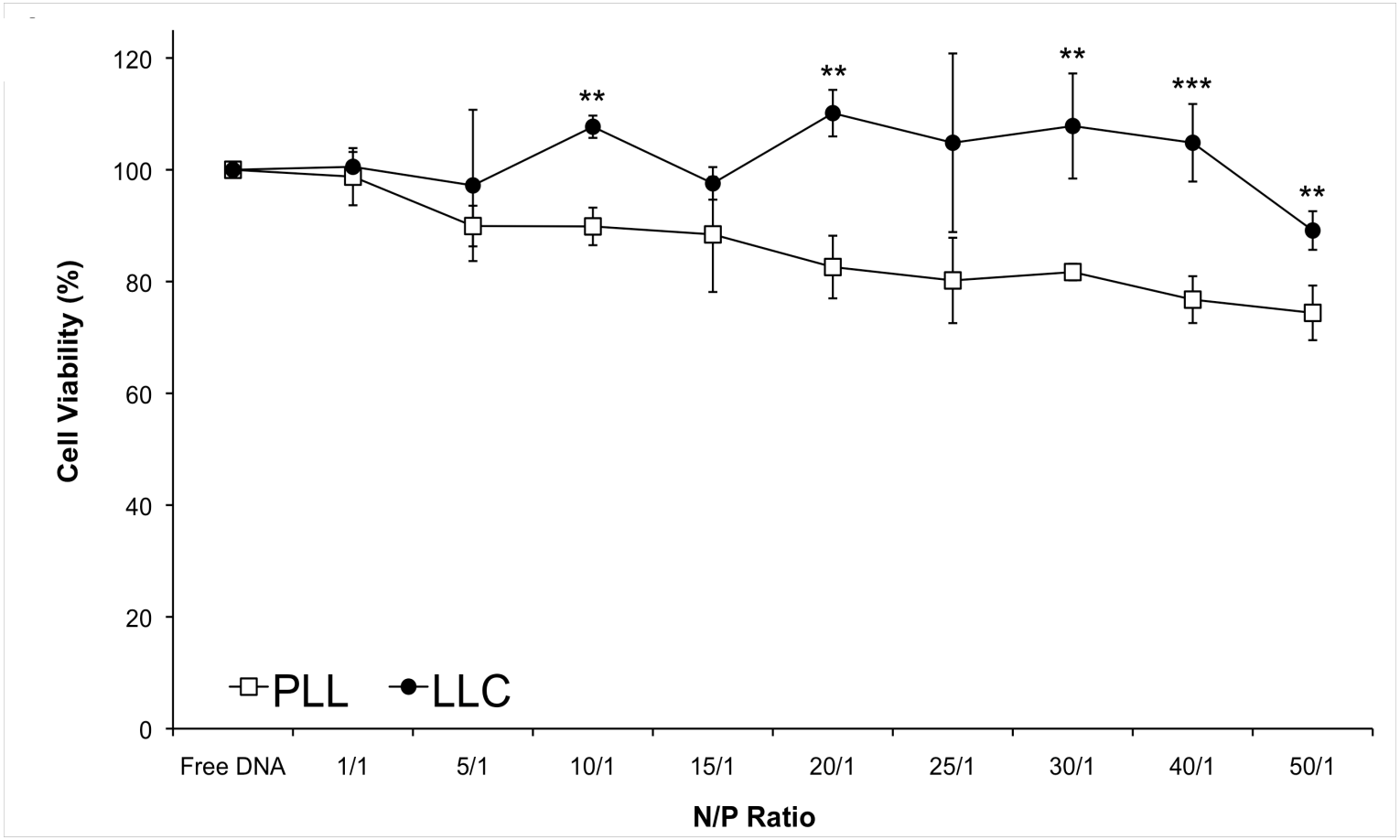

Figure 4.24: Cell viability of LLC/pCMV-Luc and PLL/pCMV-Luc polyplexes as a function of N/P ratios with an MTT assay for HDF cells. Data represent mean ± SD, N=3. (*, **, *** indicate p-values of < 0.05, < 0.01 and < 0.001 respectively)

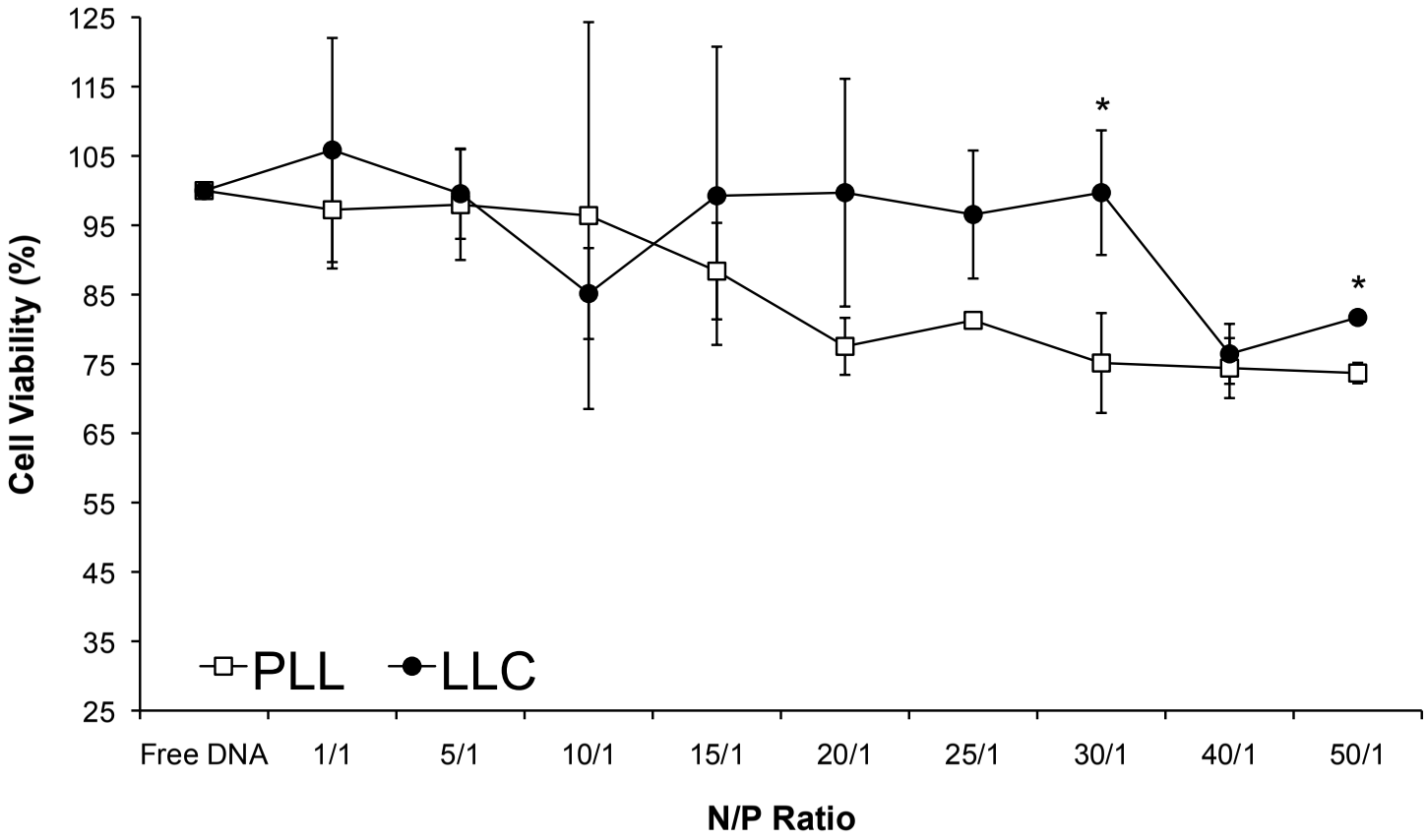

Figure 4.25: Cell viability of LLC/pCMV-Luc and PLL/pCMV-Luc polyplexes as a function of N/P ratios with an MTT assay for MCF-7 cells. Data represent mean ± SD, N=3. (*, **, *** indicate p-values of < 0.05, < 0.01 and < 0.001 respectively)

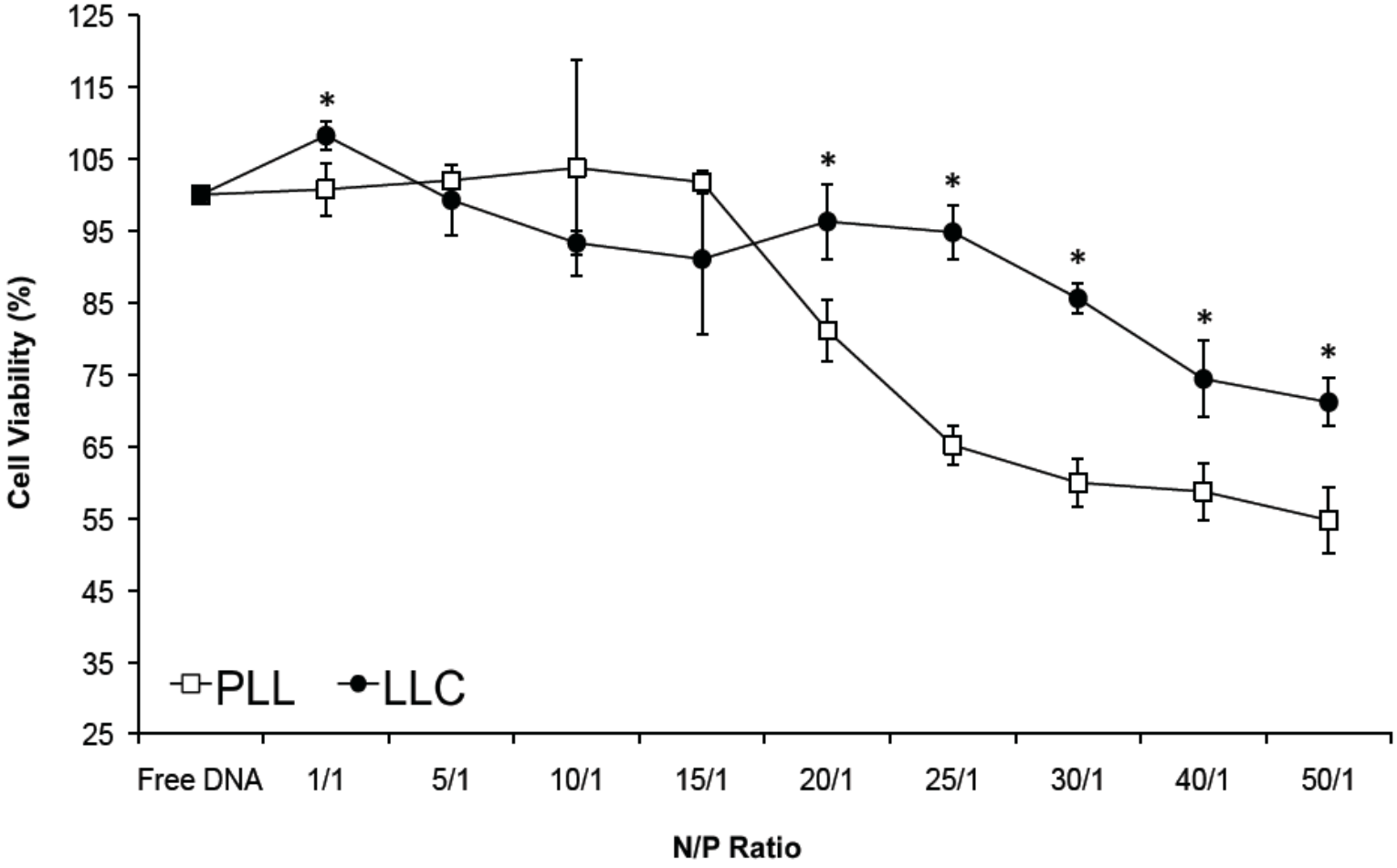

Figure 4.26: Cell viability of LLC/pCMV-Luc and PLL/pCMV-Luc polyplexes as a function of N/P ratios with an MTT assay for MA cells. Data represent mean ± SD, N=3. (* indicates p-value < 0.05).

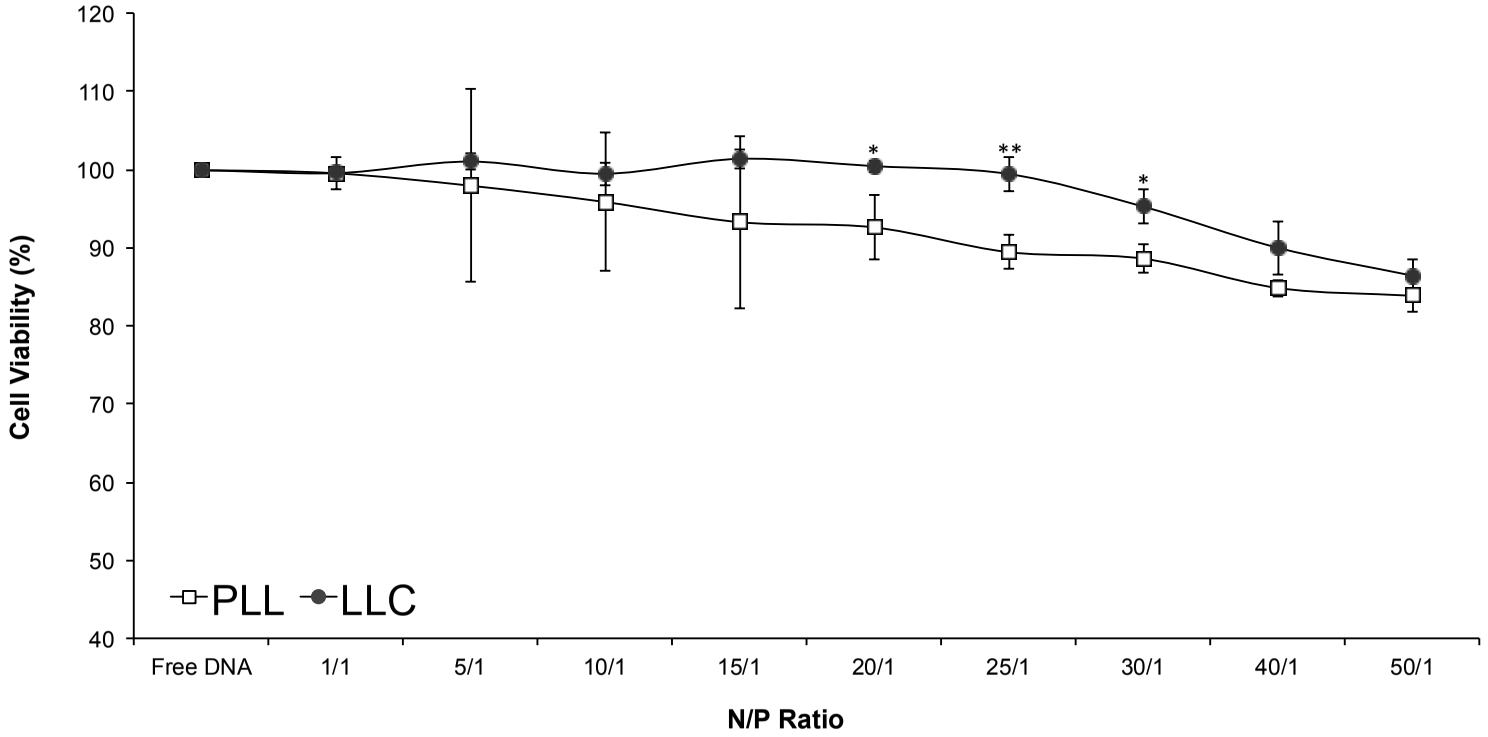

Figure 4.27: Cell viability of LLC/pCMV-Luc and PLL/pCMV-Luc polyplexes as a function of N/P ratios with an MTT assay for 4T1s cells. Data represent mean ± SD, N=3. (*, **, *** indicate p-values of < 0.05, < 0.01 and < 0.001 respectively)

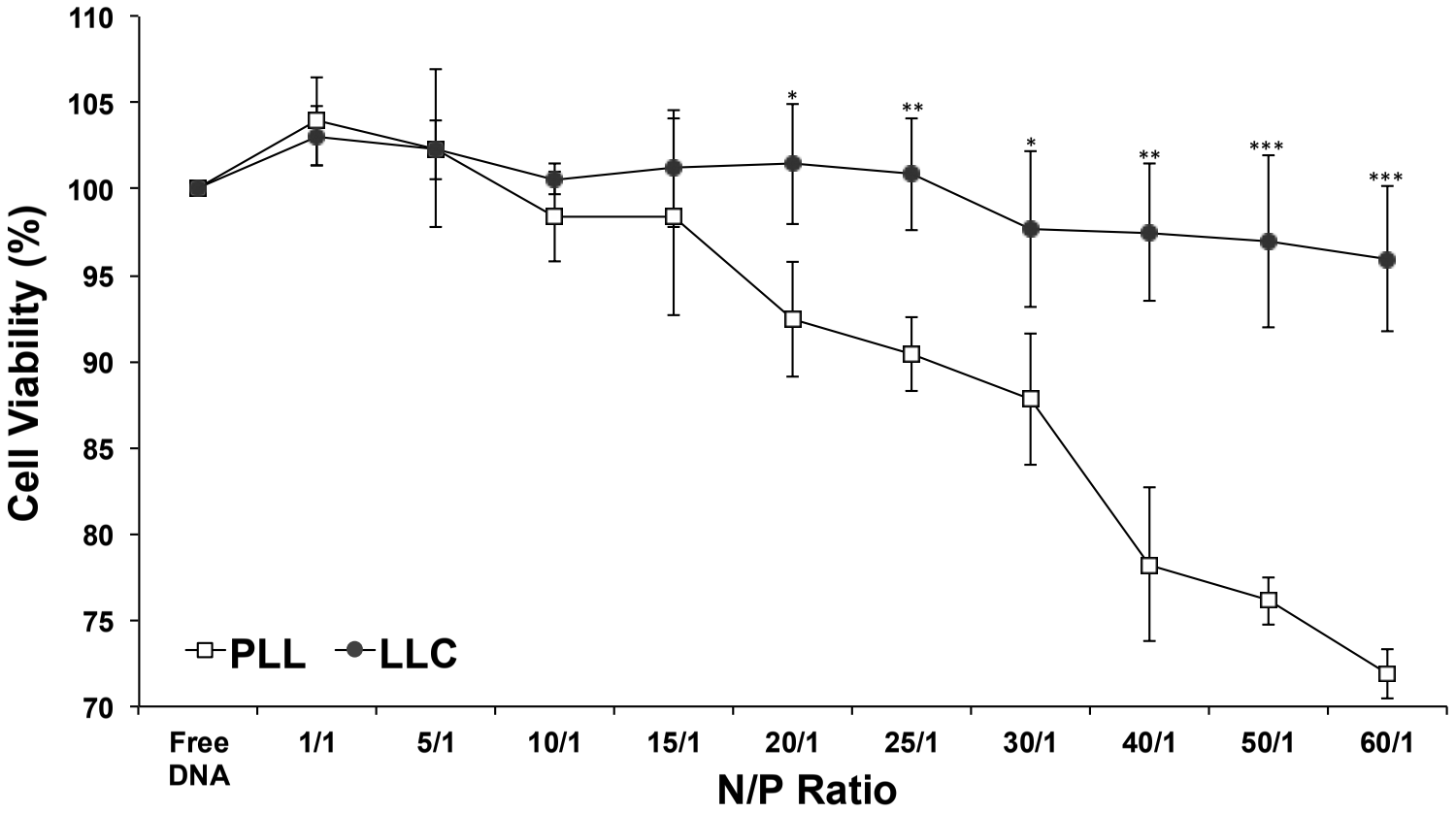

Figure 4.28: Cell viability of LLC/pCMV-Luc and PLL/pCMV-Luc polyplexes as a function of N/P ratios with an MTT assay for MEF cells. Data represent mean ± SD, N=3. (*, **, *** indicate p-values of < 0.05, < 0.01 and < 0.001 respectively)

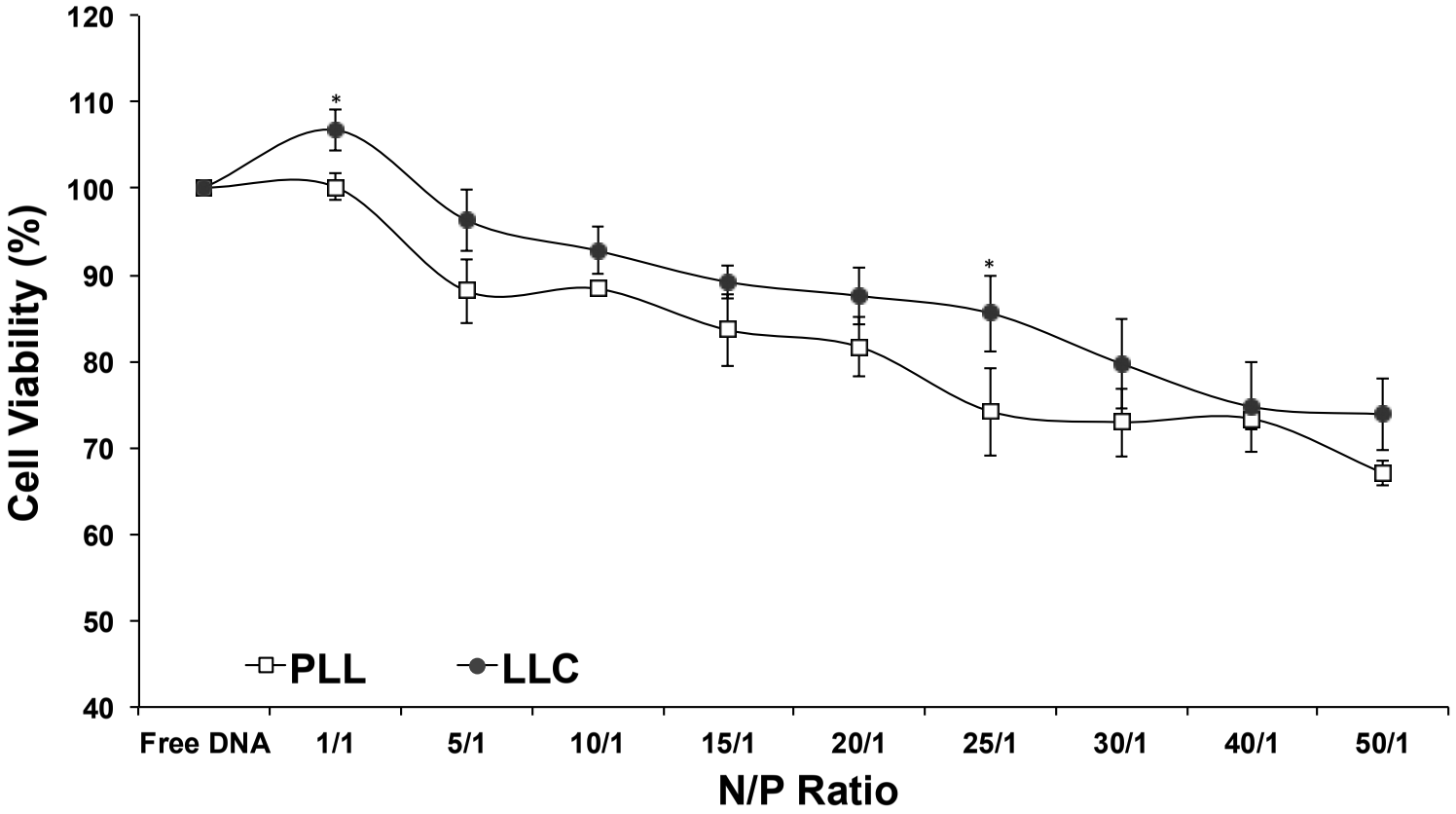

Figure 4.29: Cell viability of LLC/pCMV-Luc and PLL/pCMV-Luc polyplexes as a function of N/P ratios with an MTT assay for HEK-293 cells. Data represent mean ± SD, N=3. (*, **, *** indicate p-values of < 0.05, < 0.01 and < 0.001 respectively)

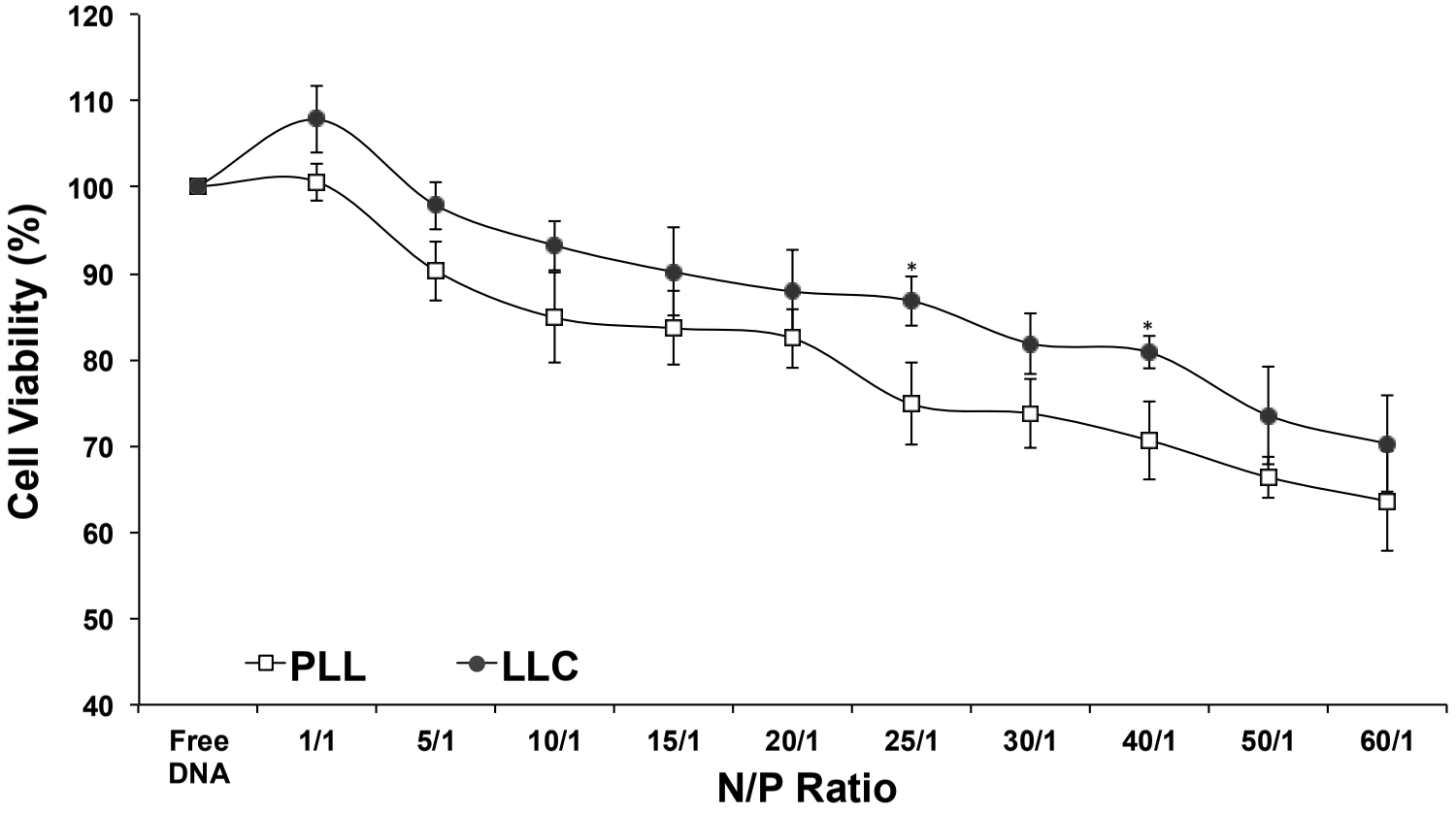

Figure 4.30: Cell viability of LLC/pCMV-Luc and PLL/pCMV-Luc polyplexes as a function of N/P ratios with an MTT assay for hMSC cells. Data represent mean ± SD, N=3. (*, **, *** indicate p-values of < 0.05, < 0.01 and < 0.001 respectively)

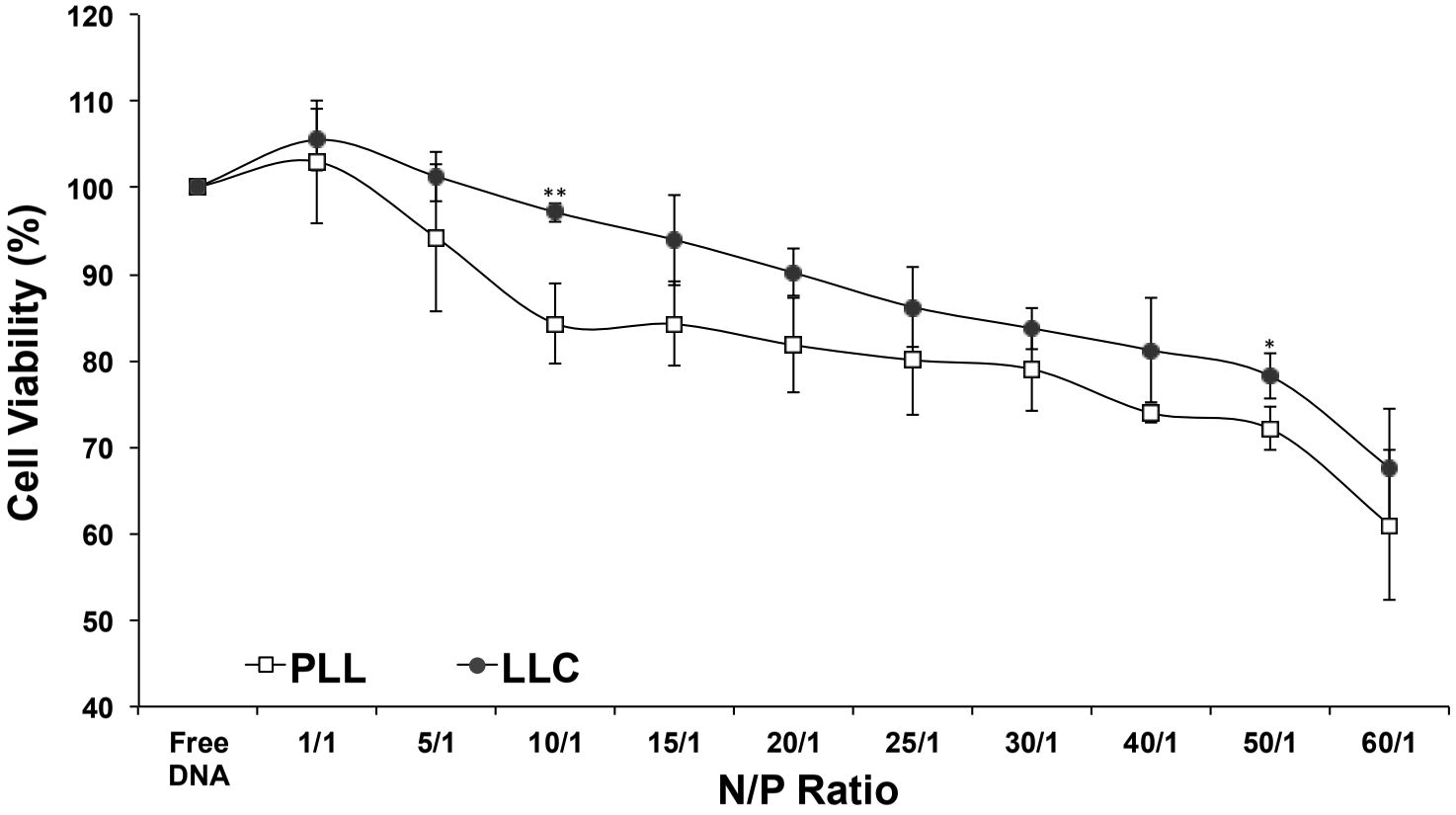

Figure 4.31: Cell viability of LLC/ pSV_{40}-VEGF and PLL/ pSV_{40}-VEGF polyplexes as a function of N/P ratios with an MTT assay for hMSC cells. Data represent mean ± SD, N=3. (*, **, *** indicate p-values of < 0.05, < 0.01 and < 0.001 respectively)

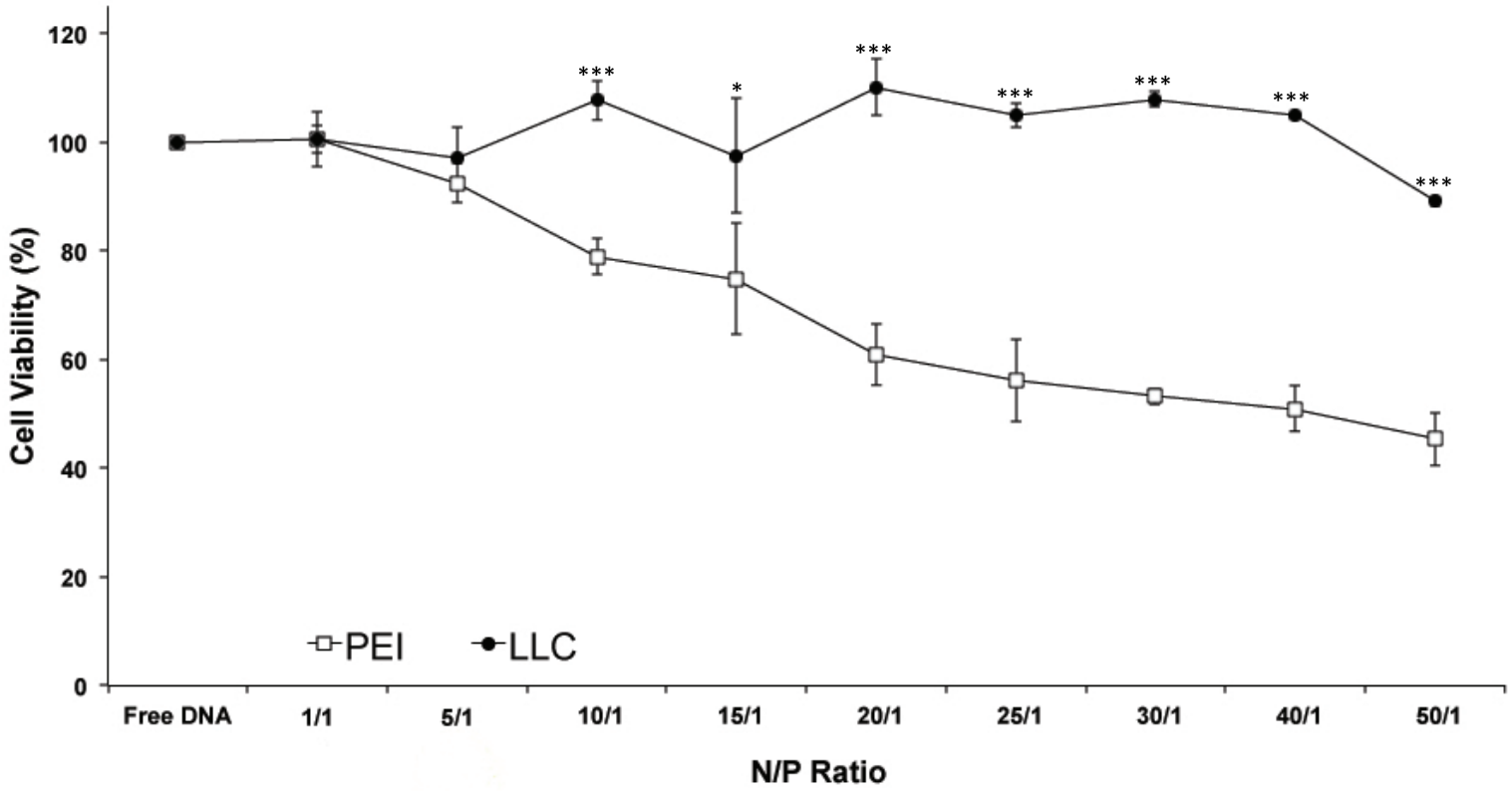

Figure 4.32: Cell viability of LLC/pCMV-Luc and PEI/pCMV-Luc polyplexes as a function of N/P ratios with an MTT assay for HDF cells. Data represent mean ± SD, N=3. (*, **, *** indicate p-values of < 0.05, < 0.01 and < 0.001 respectively)

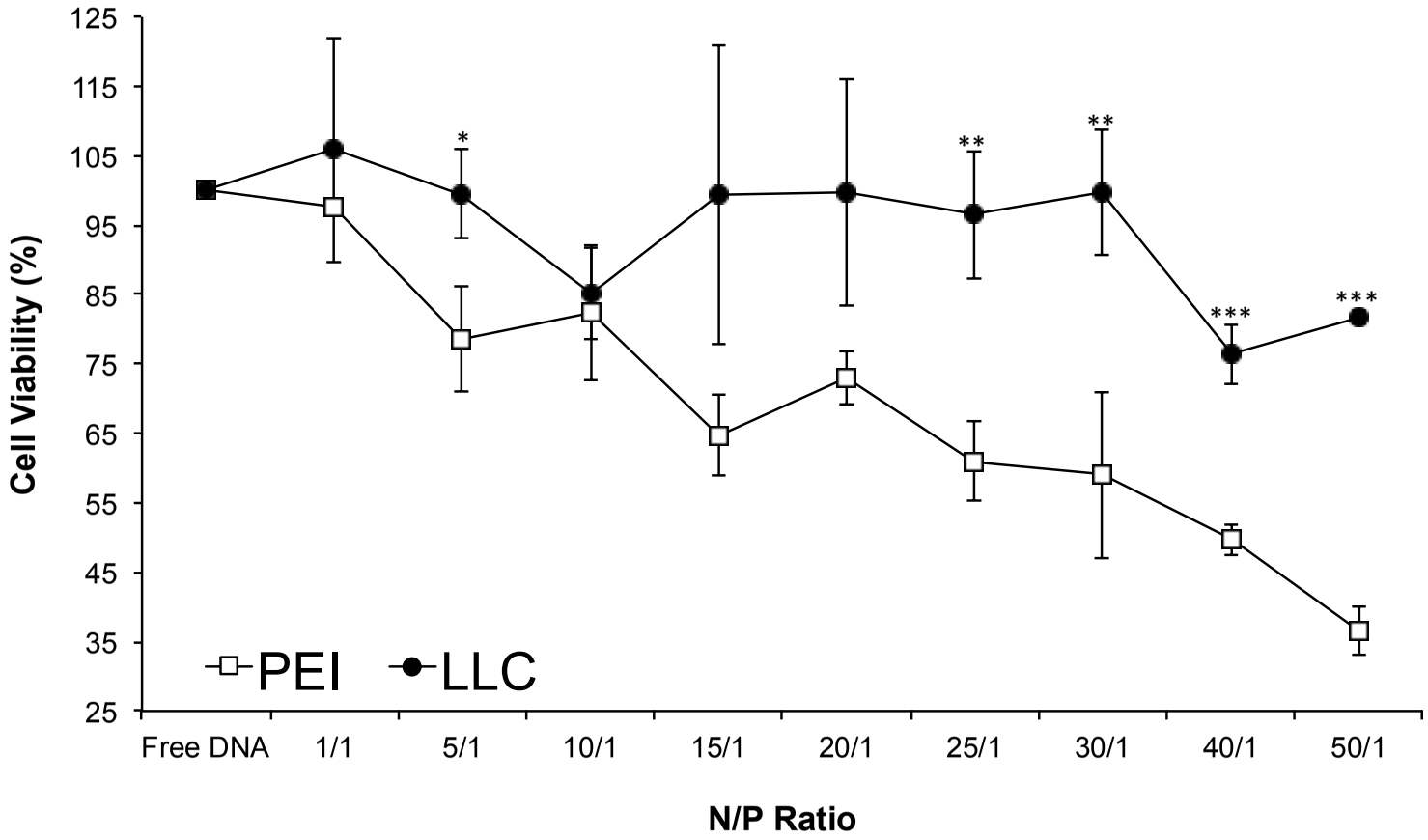

Figure 4.33: Cell viability of LLC/pCMV-Luc and PEI/pCMV-Luc polyplexes as a function of N/P ratios with an MTT assay for MCF-7 cells. Data represent mean ± SD, N=3. (*, **, *** indicate p-values of < 0.05, < 0.01 and < 0.001 respectively)

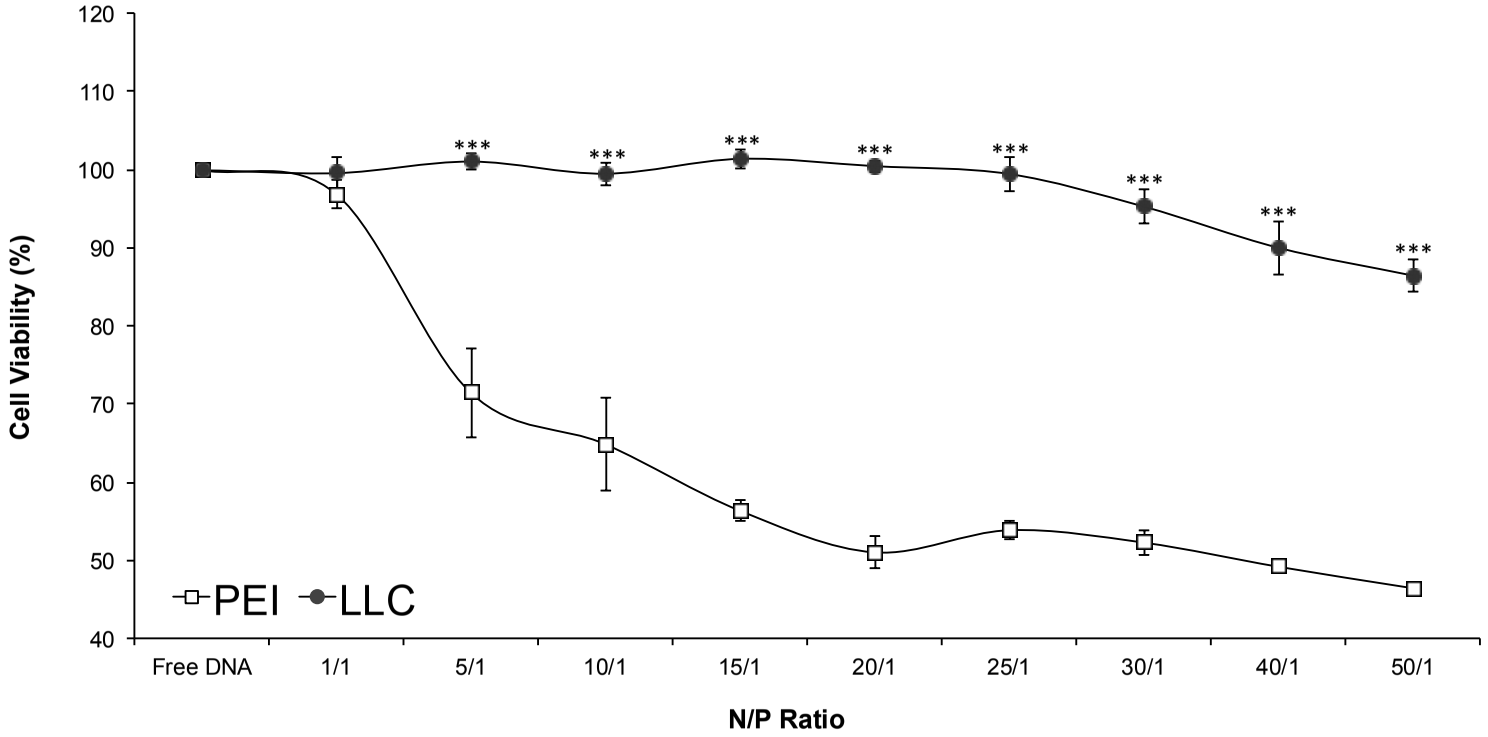

Figure 4.34: Cell viability of LLC/pCMV-Luc and PEI/pCMV-Luc polyplexes as a function of N/P ratios with an MTT assay for 4T1s cells. Data represent mean ± SD, N=3. (*, **, *** indicate p-values of < 0.05, < 0.01 and < 0.001 respectively)

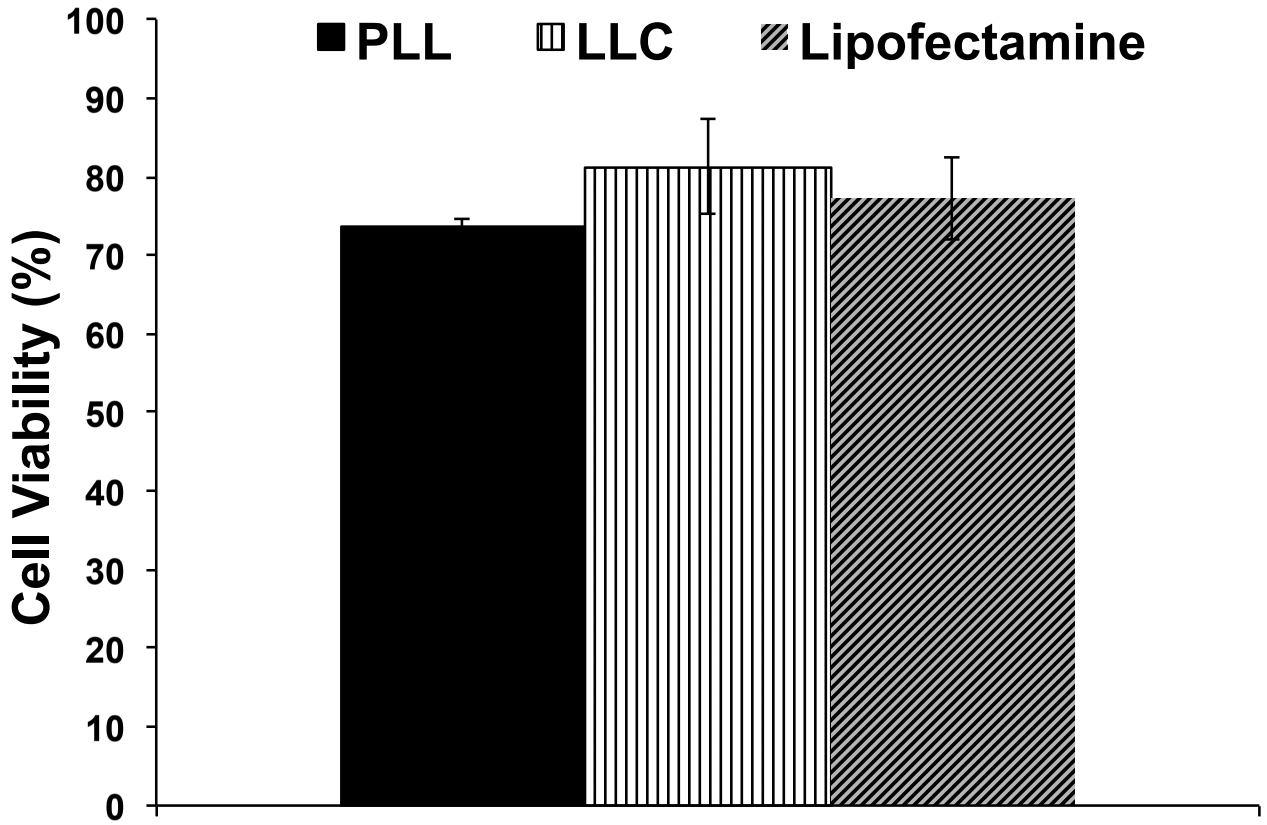

Figure 4.35: Cell viability of LLC and PLL pSV_{40}-VEGF polyplexes at N/P ratio of 40 and Lipofectamine™ lipoplexes (10 μl for 1 μg DNA) with an MTT assay for hMSc cells. Data represent mean ± SD, N=3.

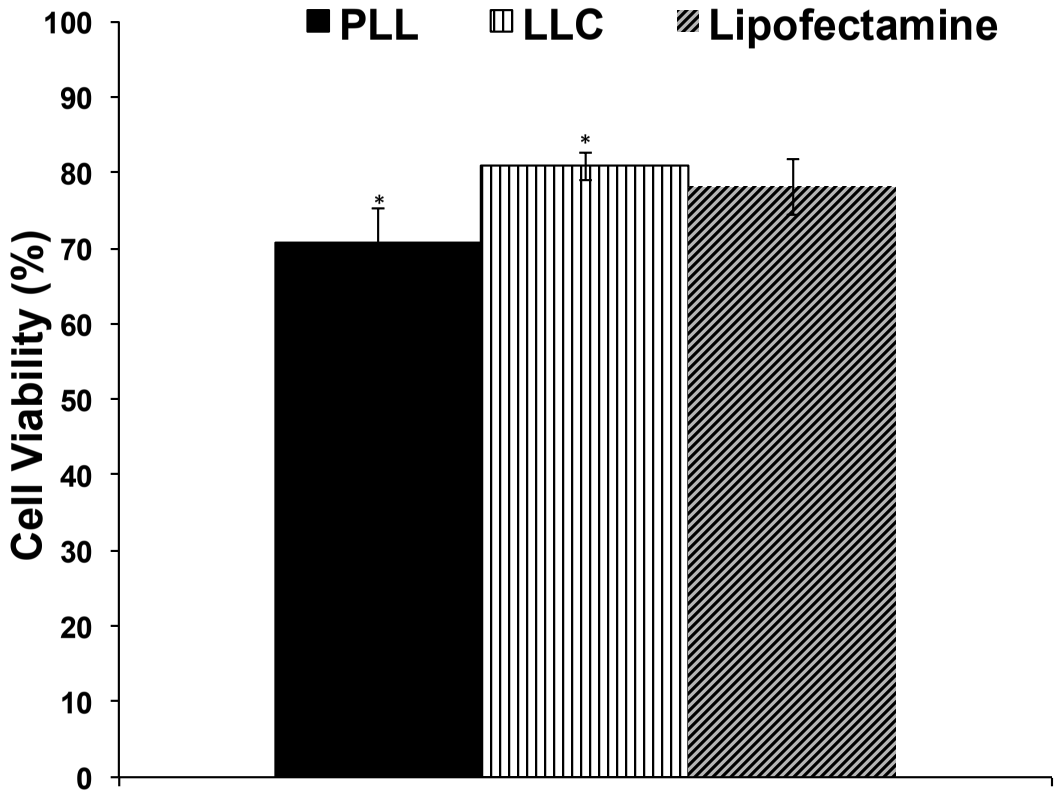

Figure 4.36: Cell viability of LLC and PLL pCMV-Luc polyplexes at N/P ratio of 40 and Lipofectamine™ lipoplexes (10 μl for 1 μg DNA) with an MTT assay for hMSc cells. Data represent mean ± SD, N=3. (* indicate p-values of < 0.05)

The effect of LLC polyplexes on the cell viability also was evaluated through the Lactate dehydrogenase (LDH) Cytotoxicity assay. LDH is a stable cytoplasmic enzyme present in all cells. It is rapidly released into the cell culture supernatant upon damage of the plasma membrane. With the use of the Cytotoxicity Detection Kit, LDH activity can be measured easily in culture supernatants by a single measurement at one time point. The use of a spectrophotometric microplate reader allows the simultaneous measurement of multiple probes and thereby guarantees the easy processing of a large number of samples.

Lactate dehydrogenase (LDH) is a soluble enzyme located in the cytosol. The enzyme is released into the surrounding culture medium upon cell damage or lysis, processes that occur during both apoptosis and necrosis (Bonfoco, Krainc et al. 1995). LDH activity in the culture medium can, therefore, be used as an indicator of cell membrane integrity, and thus a measurement of cytotoxicity. Since the activity of intracellular LDH corresponds to the number of cells in the culture, quantification of LDH in cell lysates can be used as a measurement of cell growth.

Lactate dehydrogenase (LDH or LD) is an enzyme present in a wide variety of organisms, including plants and animals. Lactate dehydrogenases exist in four distinct enzyme classes. Two of them are cytochrome c-dependent

enzymes with each acting on D-lactate or L-lactate. The other two are NAD(P)-dependent enzymes with each acting on D-lactate or L-lactate. This dissertation is about the NAD(P)-dependent L-lactate dehydrogenase.

Cell death can be assayed by quantifying plasma membrane damage or rupture. The LDH Cytotoxicity assay offers a simple way to measure plasma membrane damage, based on the release of lactate dehydrogenase (LDH), a stable cytoplasmic enzyme present in most cells.

The LDH Cytotoxicity assay is a simple and accurate colorimetric assay for dead and plasma membrane-damaged cells. LDH present in the culture supernatant (because of plasma membrane damage) participates in a coupled reaction, which converts a yellow tetrazolium salt into a red, formazan-class dye, which is measured by absorbance at 490 nm. The amount of formazan is directly proportional to the amount of LDH in the culture, which is in turn directly proportional to the number of dead or damaged cells. The assay is extremely sensitive: as few as 2,000 dead or damaged cells per well can be detected (Haslam, Wyatt et al. 2000; Wolterbeek and van der Meer 2005).

The culture supernatant is collected cell-free and incubated with the reaction mixture from the kit. The LDH activity is determined in an enzymatic test: In the first step NAD+ is reduced to NADH/ H+ by the LDH-catalyzed conversion of lactate to pyruvate. In the second step the catalyst (diaphorase) transfers H/H^+

from NADH/H+ to the tetrazolium salt INT, which is reduced to formazan (Wolterbeek and van der Meer 2005).

The LDH assay showed that LLC polyplexes produced lower cytotoxicity compared to PLL at N/P ratios up to 50/1. LLC polyplexes at 20/1, 25/1 and 30/1 N/P ratios maintained the highest cell viability in the hMSC cell line in comparison to PLL at the same N/P ratio using pCMV-Luc and pSV_{40}-VEGF plasmids. PLL at 20/1, 25/1 and 30/1 N/P ratios showed a decrease in cell viability to 83%, 80%, and 77% for hMSC cells respectively with approximately 92-100% cell viability for LLC/pDNA polyplexes using pCMV-Luc plasmid (Figure 4.37). Moreover, PLL at 20/1, 25/1 and 30/1 N/P ratios showed a decrease in cell viability to 83%, 81%, and 80% for hMSC cells respectively with approximately 94-100% cell viability for LLC/pDNA polyplexes using pSV_{40}-VEGF plasmid (Figure 4.38).

It also was observed that using different plasmids of comparable sizes did not affect the cytotoxicity profile of the gene carrier system. This was observed in the cell viability profile of LLC and PLL polyplexes with the two different plasmids, pCMV-Luc and pSV_{40}-VEGF, in hMSC cells (Figures 4.37 and 4.38). This observation is consistent with the MTT cytotoxicity assay results (Figures 4.30 and 4.31). Further investigation of the effect of larger plasmids on cell viability and transfection efficiency off the polyplexes is beneficial to test for the effect of plasmid size on the cell viability and transfection efficiency.

Finally, the cytotoxicity profile also was compared to Lipofectamine™ using LDH assay. There was no statistical significance difference in cell viability of Lipofectamine™/pDNA lipoplexes and LLC/pDNA polyplexes in hMSC cells using two different plasmids pSV_{40}-VEGF and pCMV-Luc (Figures 4.39 and 4.40 respectively). Although there is no improvement in cell viability or transfection efficiency using LLC copolymers as transfection agent compared to Lipofectamine™, LLC copolymers is superior to Lipofectamine™ in terms of stability and cost. Lipofectamine™ suffers from physical and chemical instability problems hindering taking it from bench-to-bedside. Lipofectamine™ is a colloidal system, which is stabilized electrostatically, sterically or electrosterically. Lipofectamine™ suffers, as any other colloidal dosage form, from aggregation overtime, followed by fusion or phase change after aggregation. These factors adversely affect the Lipofectamine™ shelf and half lives. Moreover, Lipofectamine™ suffers from other chemical stability problems such as hydrolysis and oxidation of the phospholipids used in the Lipofectamine™ formulation. On the contrary, LLC copolymers showed improved chemical and physical stability compared to Lipofectamine™. All of the LLC copolymers batches were synthesized in 2008 on large scale and all of these batches were stable till May 2011. The stability of the various batches were tested constantly

between 2008 and 2011 using gel electrophoresis and particle size analysis to ensure its stability and the reproducibility of the data.

The improvements in cell viability for LLCs as compared to PLL and PEI could be because of the low molecular weight LLC copolymers and their byproducts, which produce lower charge densities and hence lower cytotoxicities as compared to high molecular weight PLL and high cationic charged PEI. The cytotoxicities of high molecular weight PLL has been studied extensively in various cells lines, which have shown that high charge densities can result in an increase in cellular toxicities (Choi, Liu et al. 1999; Choi, Liu et al. 1998; Choi, Liu et al. 1998; Gonzalez, Hwang et al. 1999; Hong, Leroueil et al. 2006; Toncheva, Wolfert et al. 1998). In addition, the results of previous biophysical studies, which showed that polycationic polymers could disrupt liposomal lipid bilayer vesicles because of their high charge densities, support our current observations that these high molecular weight PLL polymers can produce significant cytotoxicities that adversely affect cell viability as opposed to low molecular weight LLCs (Hong, Leroueil et al. 2006). In case of cationic PEI, since its introduction in 1995, it is considered one of the most efficient and most toxic non-viral gene-transfection agents. PEI cationic groups (protonated nitrogens on primary amines) provide spots for unfavorable electrostatic interactions with negatively charged serum proteins such as albumin. Furthermore, the extensive cationic

charge is a leading reason for the destabilization of the cell membrane, thereby inducing local toxicity and cell death (Brunot, Ponsonnet et al. 2007; Choi, Kang et al. 2010; He, Guo et al. 2011; Park 2009).

A main drawback in the current characterization parameters discussed in this chapter is the use of only two plasmids (pCMV-Luc and pSV_{40}-$VEGF_{165}$) of comparable sizes (~5 kbp). More plasmids with larger sizes should be used in further investigations to test for the effect of plasmid size on the ability of the various carrier systems to complex the pDNA of variable sizes, cell viability and transfection efficiency.

Further investigation of the cell viability of pDNA/LLC polyplexes using MTT and LDH assays compared to PLL over multiple time points post-transfection (for example 2, 4, 6 and 8 hours post-transfection) will be beneficial to test cell viability pattern over time. This could help in the prediction of the percentage and the number of viable productive cells post-transfection as a function of time.

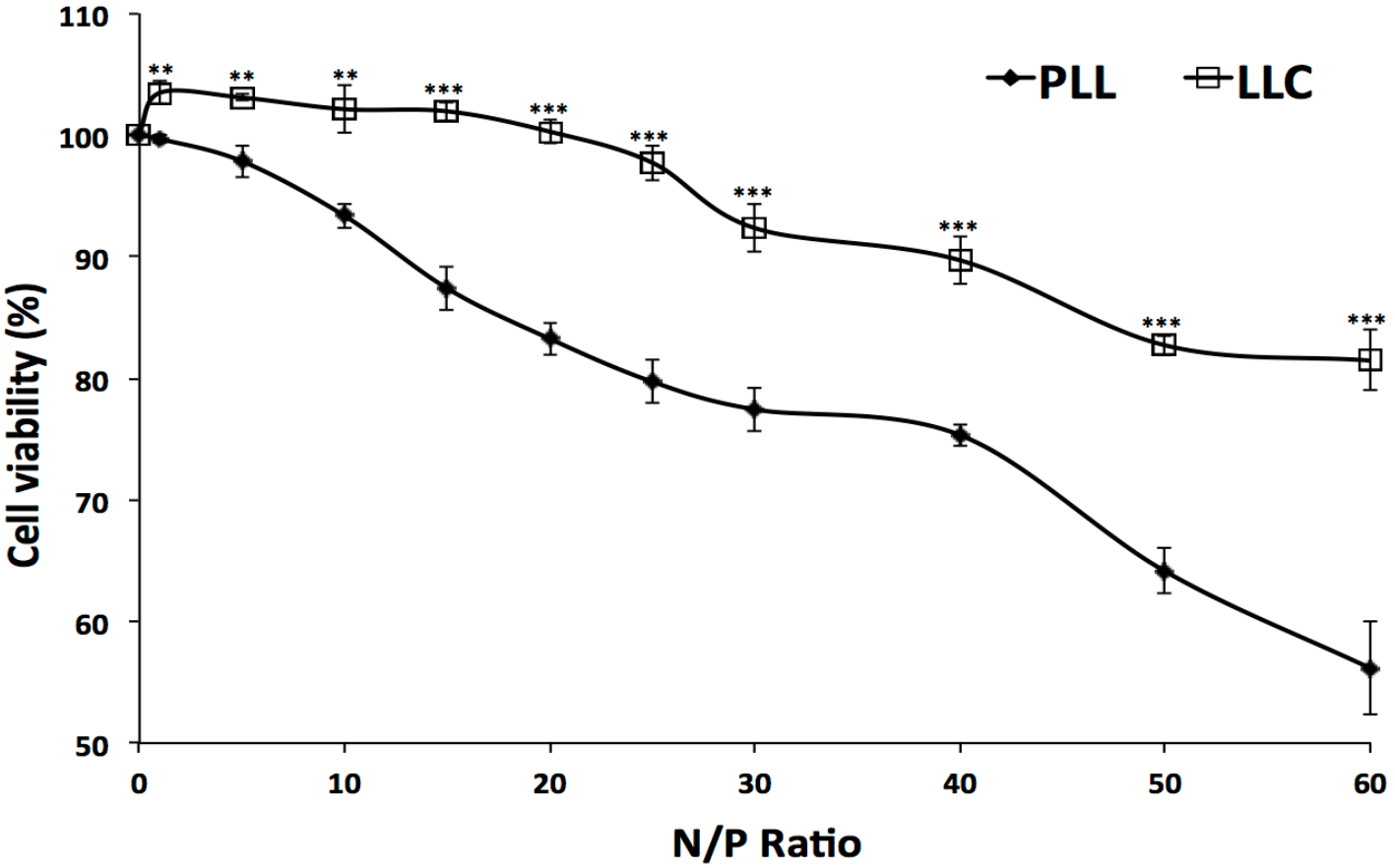

Figure 4.37: Cell viability of LLC/pCMV-Luc and PLL/pCMV-Luc polyplexes as a function of N/P ratios with an LDH assay for hMSC cells. Data represent mean ± SD, N=3. (*, **, *** indicate p-values of < 0.05, < 0.01 and < 0.001 respectively)

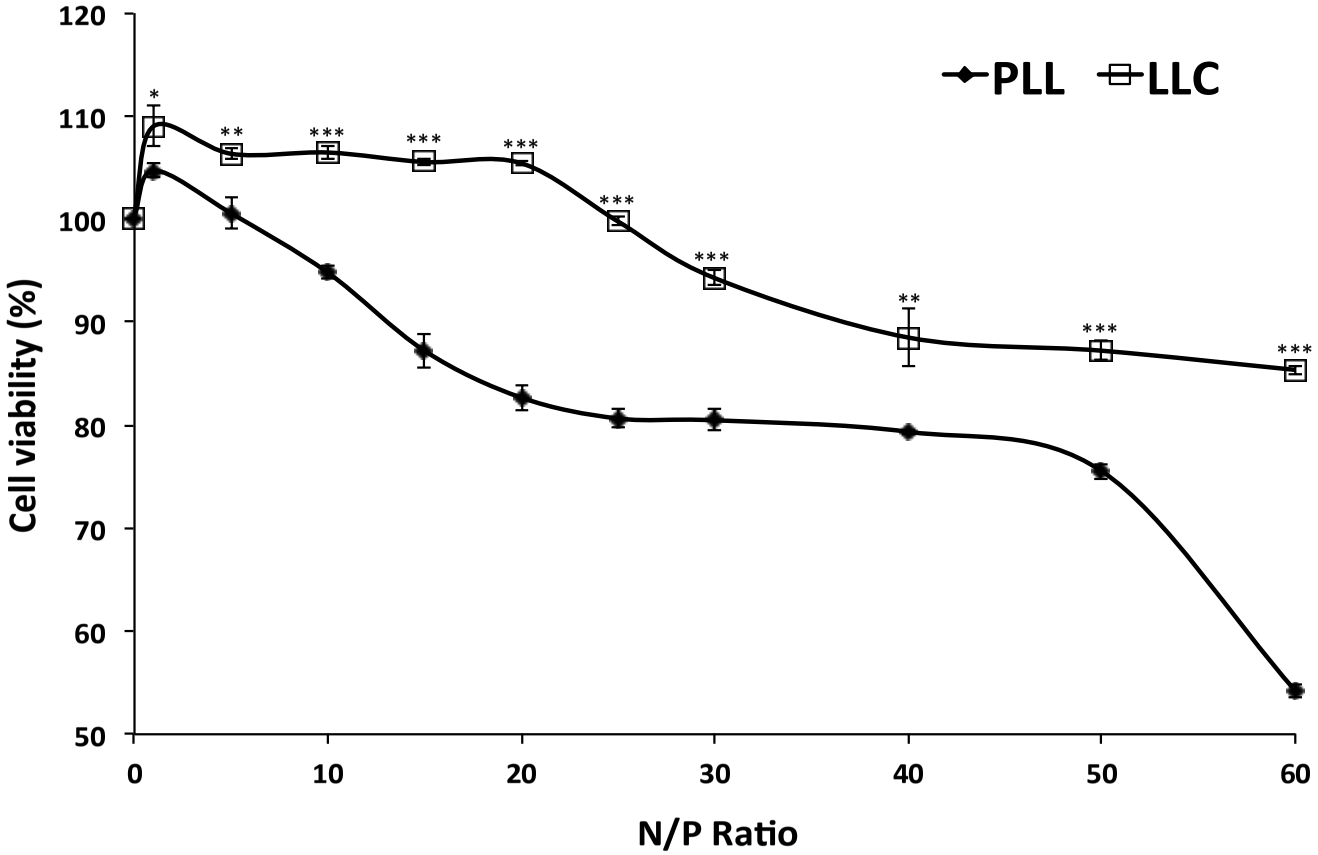

Figure 4.38: Cell viability of LLC/ pSV_{40}-VEGF and PLL/ pSV_{40}-VEGF polyplexes as a function of N/P ratios with an LDH assay for hMSC cells. Data represent mean ± SD, N=3. (*, **, *** indicate p-values of < 0.05, < 0.01 and < 0.001 respectively)

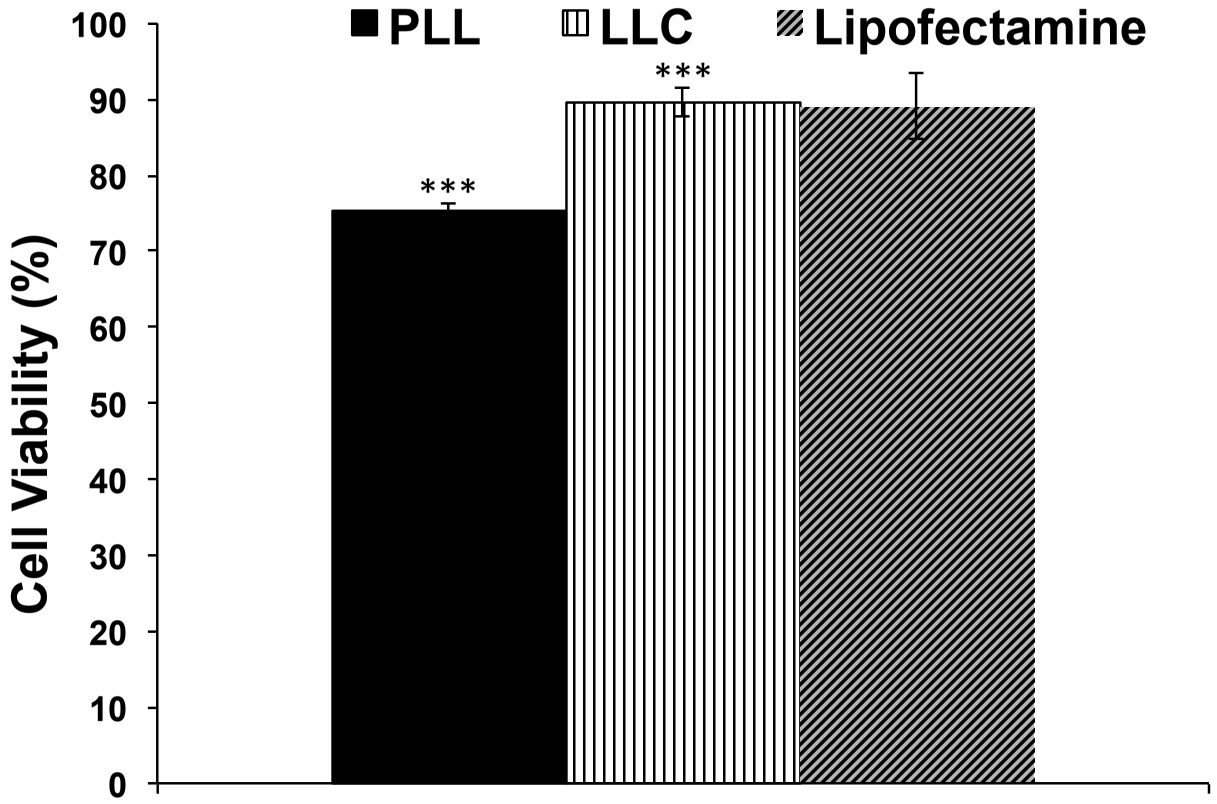

Figure 4.39: Cell viability of LLC and PLL pCMV-Luc polyplexes at N/P ratio of 40 and Lipofectamine™ lipoplexes (10 μl for 1 μg DNA) with an LDH assay for hMSc cells. Data represent mean ± SD, N=3. (*, **, *** indicate p-values of < 0.05, < 0.01 and < 0.001 respectively)

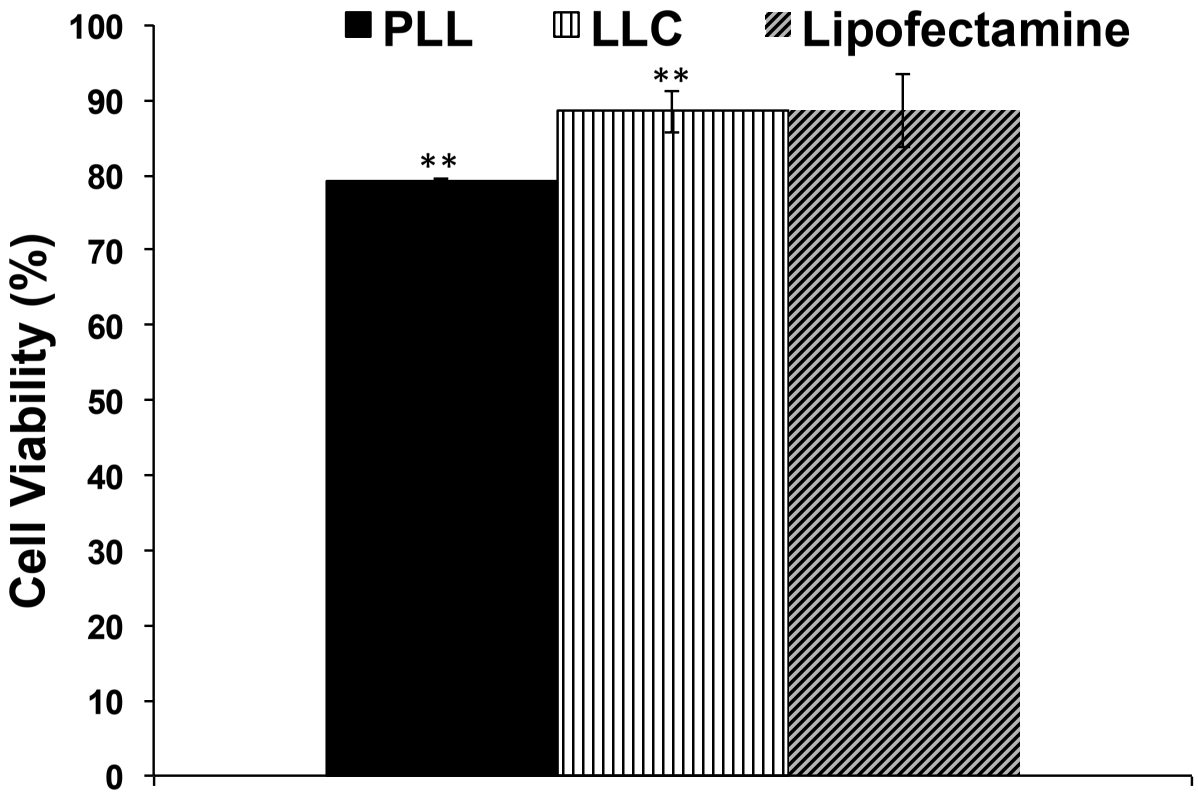

Figure 4.40: Cell viability of LLC and PLL pSV_{40}-VEGF polyplexes at N/P ratio of 40 and Lipofectamine™ lipoplexes (10 μl for 1 μg DNA) with an LDH assay for hMSc cells. Data represent mean ± SD, N=3. (*, **, *** indicate p-values of < 0.05, < 0.01 and < 0.001 respectively)

5. Investigation of the *ex vivo* efficacy of DNA/LLC polyplexes through treatment of myocardial infarction using *in vitro* gene delivery to generate genetically modified stem cells

5.1. Introduction

Despite the fast improvement in pharmacological therapies, organ transplantation, mechanical assist devices, and cardiovascular surgery, more than half of the patients with heart failure die within five years of the initial diagnosis. Moreover, ischemic heart disease (IHD) or coronary artery disease (CAD) remains a leading cause of death in the United States (Heidenreich, Trogdon et al. 2011). The poor prognosis of IHD is related directly to a build-up of atherosclerotic plaque that produces narrowing of the coronary artery lumen (Wellnhofer, Bocksch et al. 2002). The rupture of the artery and/or narrowing of the artery lumen results in myocardial ischemia, which can lead to myocardial infarction resulting in increased pressure and/or volume overload on the heart (Sharpe 2004). Such injuries may lead to ventricular (cardiac) remodeling. Cardiac remodeling is a process in which the injury in the ventricles of the heart resulting from acute myocardial infarction, chronic hypertension, congenital heart disease or valvular heart disease leads to changes in size, shape, and function of the heart, which leads to a significant decline in heart functions such as

diminished contractile function and reduced stroke volume (Cohn, Ferrari et al. 2000; Hong, Mintz et al. 2007; Sharpe 2004). The major cell types involved in ventricular remodeling are the cardiac myocyte, fibroblasts and collagen (Cohn, Ferrari et al. 2000). Following myocardial infarction, myocardial necrosis and disproportionate thinning of the ventricular wall of the heart takes place. These weakened thin spots are unable to withstand the pressure and volume load on the heart compared to other normal heart tissue, leading to a significant dilatation of the chamber originating from the infarcted region (Cohn, Ferrari et al. 2000; Hong, Mintz et al. 2007; Sharpe 2004). The ventricular remodeling takes place through two phases. The initial phase is a beneficial step and it involves repairing of the newly formed necrotic tissue and the myocardial scaring (Cohn, Ferrari et al. 2000; Sharpe 2004). On the other hand, over time, the heart becomes more spherical and less elliptical as a consequence of the subsequent continuous ventricular remodeling. This leads to a significant increase in the cardiac mass and volume leading to impaired heart diastolic functions (Cohn, Ferrari et al. 2000; Sharpe 2004). Unfortunately, many patients with IHD remain refractory to traditional pharmacological treatments (Bonaros, Bernecker et al. 2005; Perin and Silva 2011). In addition to pharmacotherapies, current treatments include bypass surgery, angioplasty, and stent implantation but unfortunately many patients are unsuitable candidates for surgical interventions (LaPar, Kron et al.

2009; Perin and Silva 2011; Povsic and Peterson 2005; Sunkomat and Gaballa 2003; Urbaszek, Modersohn et al. 1976). In addition, even if the diseased blood vessel is manipulated to increase blood flow, restenosis of the vessel lumen is a recurrent problem because of neointimal hyperplasia. Gene therapy is a promising alternative to conventional treatment strategies since the delivery of angiogenic cytokines such as vascular endothelial growth factor ($VEGF_{165}$) can stimulate angiogenesis in a process known as therapeutic angiogenesis or neovascularization (Bonaros, Bernecker et al. 2005). One of the new trends in the treatment of MI is the use of stem cells. Advances in stem cell biology have challenged the notion that the infarcted myocardium is irreparable (Bonaros, Bernecker et al. 2005; Heidenreich, Trogdon et al. 2011; Mushtaq, Oskouei et al. 2011; Perin and Silva 2011; Povsic and Peterson 2005). The pluripotent ability of stem cells to differentiate into specialized cell lines began to garner intense interest within cardiology for the regeneration of infarcted regions of the heart (Mushtaq, Oskouei et al. 2011).

In this study, we have used *ex vivo* nonviral gene delivery to generate genetically modified stem cells that are able to produce the angiogenic cytokine, vascular endothelial growth factor ($VEGF_{165}$).

There are a wide variety of stem cell types that have been investigated and used for cardiac regeneration in humans (Segers and Lee 2008). Embryonic

stem cells and human adult mesenchymal stem cells are the most predominantly used stem cells for cell-based therapeutic strategies for cardiac regeneration (Byun and Kim 2009; Flynn and O'Brien 2011; Honold, Assmus et al. 2004). The main source of human mesenchymal stem cells is bone marrow (Brignier and Gewirtz 2010). They are multipotent cells that can differentiate into osteoblasts, cardiomyocytes, chondrocytes and adipocytes (Leeper, Hunter et al. 2010). On the other hand, embryonic stem cells are derived from embryos that develop from eggs that have been fertilized in vitro and then donated for research purposes (Segers and Lee 2008). They are pluripotent cells that can differentiate into any cell present in the adult organism. They can potentially regenerate the myocardium (Leeper, Hunter et al. 2010). In this study human mesenchymal stem cells have been chosen for the regeneration of myocardium due to the limitations and obstacles that stand in the way of using embryonic stem cells in cell-based therapy. Embryonic stem cells suffer from immunological rejection (Flynn and O'Brien 2011). Moreover, they tend to form teratomas when injected *in vivo* due to their rapid mitosis (Leeper, Hunter et al. 2010). The main advantages of adult mesenchymal stem cells are being less immunogenic than other stem cells, potentially allowing allogenetic cell therapy (Segers and Lee 2008). Moreover, Mesenchymal stem cells can provide significant paracrine growth factor support for cardiac cells present in infarcted and non-infarcted

regions of the heart (Flynn and O'Brien 2011). This could be a major mechanism for the beneficial effects of these cells (Flynn and O'Brien 2011). Furthermore, hMSCs have been genetically customized to overexpress angiogenic factors, growth factors, prosurvival factors, or stem-cell homing factors such as VEGF to increase the therapeutic potency of mesenchymal stem cells and their ability to differentiate into myocardiocytes (Flynn and O'Brien 2011; Honold, Assmus et al. 2004; Leeper, Hunter et al. 2010; Naftilan and Schuening 2011; Segers and Lee 2008).

VEGF promotes revascularization of an infarcted region of the heart, which can reduce myocardial damage and scar formation. Moreover, VEGF induces angio-arteriogenesis, promotes proliferation of myocyte precursors and adult cardiomyocyte mitosis, reduces per-infarct fibrosis and decreases myofibroblast proliferation (Zisa, Shabbir et al. 2011). Furthermore, VEGF acts in remote zones, increasing mitotic index of adult cardiomyocytes in non-injected, non-ischemic territories and inducing arteriolar growth (Vera Janavel, De Lorenzi et al. 2011).

In this study, the novel linear L-lysine reducible modified copolymer (LLCs) was used as an alternative to high molecular weight non-degradable poly-L-lysine (PLL) for efficient, safe and bioresponsive nonviral gene delivery. The transfection efficiencies of the polyplexes, as determined with luciferase and

ELISA assay, showed that LLC polyplexes produced over 10 times higher transfection efficiencies and lower cytotoxicities in human mesenchymal stem cells (hMSCs) as compared to the optimal PLL control. The effect of hMSCs transfected with the LLC/$VEGF_{165}$ gene on infarcted regions of the heart in a MI animal model was investigated. The myocardial infarction (MI) was created by permanent ligation of the left anterior descending coronary artery (LAD). Immediately after the creation of MI, the transfected cells were injected into the infarcted area of the heart of severe combined immunodeficient (SCID) mice. The injection of the transfected cells immediately post-infarction could be beneficial to counterpart the ventricular remodeling, which takes place immediately after the cardiac injury. The mesenchymal stem cells can provide significant paracrine growth factor support for cardiac myocytes present in infarcted and non-infarcted regions of the heart (Honold, Assmus et al. 2004; Leeper, Hunter et al. 2010; Segers and Lee 2008). Moreover, hMSCs have been genetically altered to overexpress the VEGF growth factors to increase the therapeutic potency of mesenchymal stem cells and their ability to differentiate into myocardiocytes. Such genetically modified stem cells overexpressing VEGF could potentially initiate stem cells differentiation into cardiomyocytes and endothelial and smooth muscle cells. They would also provide a significant paracrine growth factor support for cardiac cells in infarcted and non-infarcted regions of the heart. These

ex vivo genetically modified stem cells overexpressing VEGF could have significant potential positive effects on the regeneration of the myocardial infarction tissues. At time points (1 week, 2 weeks and 4 weeks) following MI induction and cell injection, cardiac hemodynamic analysis was performed. Finally, 4 weeks after induction of MI, the mice were sacrificed for immunofluorescence analysis.

5.2. Materials and methods

5.2.1. Experimental Design and Animal Care

Animals received care in compliance with the Guide for the Care and Use of Laboratory Animals published by the National Institutes of Health (NIH Publication No. 85-23, 8th Edition)[*] . Surgical and animal care protocols were reviewed and approved by the Institutional Animal Care and Use Committee (IACUC) (the University of Houston, Animal Protocol Number: 08013). SCID mice (CB17 SCID strain, males, 6-8 weeks old, 23-25 g, Tacomic Farms Inc.) were randomly assigned to different groups based on the experimental design (Figure 1). The number of mice per group per week ranged from 2 to 3. Mice were injected with 5mg/kg Carpofen (Rimadyl Injection, Pfizer Inc.) post-operative every 24 hours for 3 days.

The experimental design is shown in Figure 1. Two preliminary studies were performed. The first preliminary study was a 1 week, 2 weeks and 4 weeks study. Mice were assigned randomly to four groups: (1) sham group, (2) MI followed by PBS injection (control group), (3) MI followed by hMSC stem cells injection, and (4) MI followed by hMSC stem cells transfected with pSV_{40}-VEGF gene using LLC as carrier system injection. Ventricular pressure measurements

[*] Webpage: http://grants.nih.gov/grants/olaw/Guide-for-the-care-and-use-of-Laboratory-animals.pdf

enabling the determination of maximum and minimum first derivatives of the LV pressure (+dP/dtmax and –dP/dtmax, respectively), end-diastolic pressure (EDP) and end-systolic pressure (ESP) were performed at 1, 2, and 4 weeks after MI for all mice in all groups. Additionally, ejection fraction, stroke work (SW), heart rate, end-diastolic volume (EDV), end-systolic volume (ESV), diastolic chamber stiffness (normalized β), time constant of relaxation (τ) and the pressure-volume loop analysis of all mice in all groups was performed at 1, 2, and 4 weeks after MI. The hearts were harvested after the 1, 2, or 4 weeks hemodynamic measurements for histopathological analysis and VEGF gene quantitation. The total number of SCID mice used in this preliminary study was 26. The survival rate was 95%. The surgeon in this study was Dr. Yi Zheng, MD (Texas heart institute, St. Lukes hospital). Ms. Dongling Li, Ms. Cori Wijaya (Dr. Bradley McConnell Laboratory, University of Houston) and Mohamed Ismail Nounou performed the PV loops measurements along with the ELISA quantitation of VEGF.

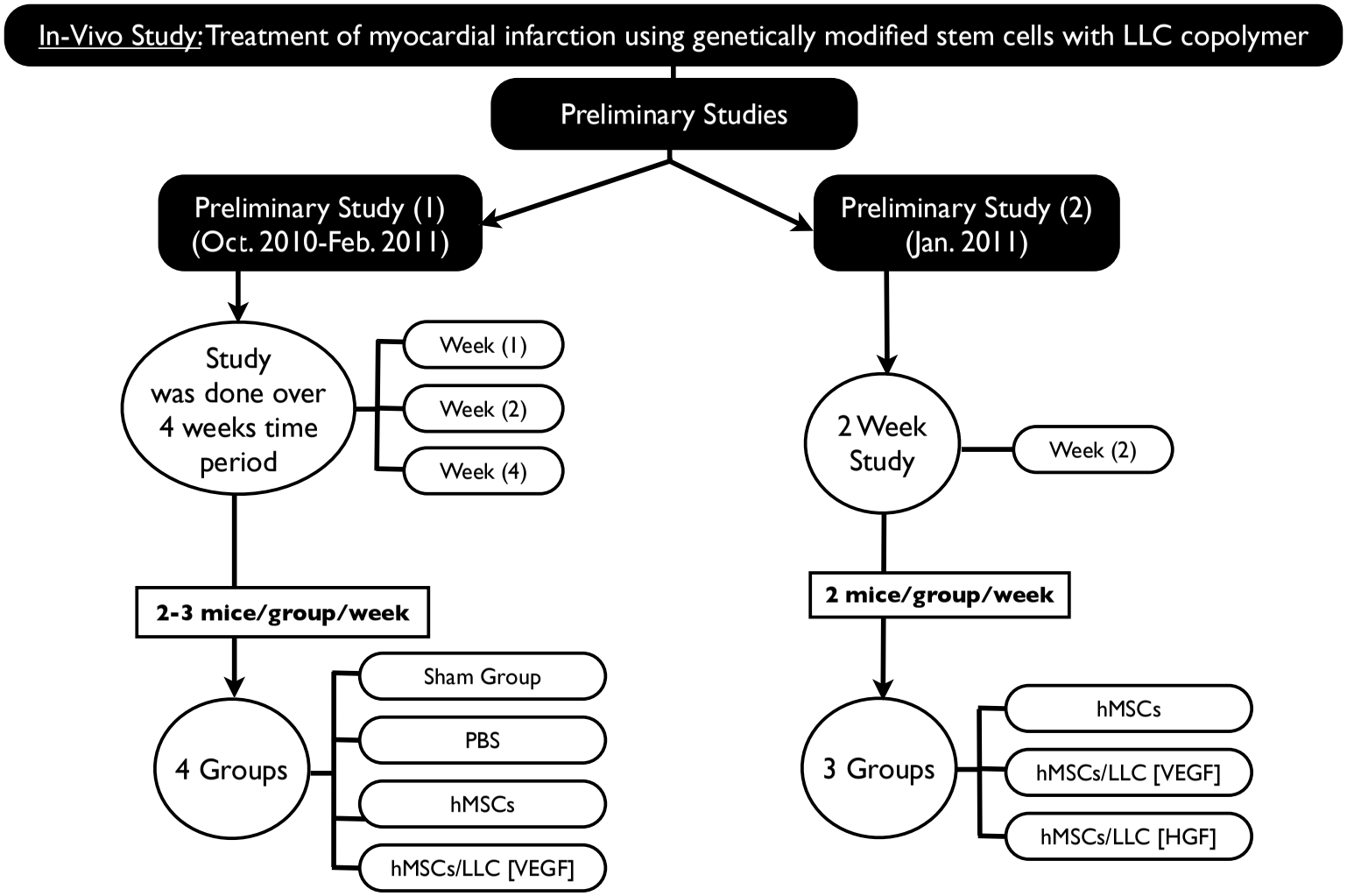

Figure 5.1: Flowchart of *ex vivo* study experimental design.

The second preliminary study was a two-week study. The number of mice per group was two. Mice were assigned randomly to three groups: MI followed by hMSC stem cells injection, MI followed by hMSC stem cells transfected with pSV_{40}-HGF gene using LLC for carrier system injection and MI followed by hMSC stem cells transfected with pSV_{40}-VEGF gene using LLC for carrier system injection. The second preliminary study was abandoned because of the low survival rate (~33%, 2 mice survived out of the total six SCID mice used). The surgeon in this study was Dr. Xing Yin, MD (Dr. Bradley McConnell Laboratory, University of Houston). Ms. Cori Wijaya (Dr. Bradley McConnell Laboratory, University of Houston) and Mohamed Ismail Nounou performed the PV loops measurements.

All mice from all groups after the week 1, week 2 and week 4 studies were subjected to pressure volume (PV) loops and hemodynamic measurements, hearts collection, H&E staining and immunohistostaining. One heart of each group for all preliminary studies was preserved intact in liquid nitrogen for quantitation of VEGF expression using VEGF ELISA kit.

5.2.2. hMSCs transfection with pSV_{40}-VEGF plasmid using LLCs

Human mesencymal stem cells (hMSCs) were transfected with the VEGF protein expressing plasmid pSV_{40}-VEGF using LLC as the cationic nonviral gene carrier. hMSCs were maintained in DMEM containing 10% FBS, streptomycin (100 μg/mL) and penicillin (100 units/mL) at 37° C in a humidified atmosphere with 5% CO_2. Cells were seeded in 6-well plates at a density of 5 x 10^5 cells/well for at least 24 hours prior to transfection. DNA was complexed with the LLCs at N/P ratio 40 in 1X PBS buffer and incubated for 30 minutes before use. The cells were washed with 1X PBS followed by the addition of serum-free media. Polyplexes (2 μg DNA/well) then were added to the cells, which were incubated for 4 hours at 37° C. Afterward, the media was replaced with 2 mL of fresh complete media and the cells were incubated for an additional 44 hours. Forty-eight hours after transfection, cells were collected using 1X Trypsin solution. Cells were washed twice using 1X PBS and pelleted by centrifugation at 8,000 rpm for 2-3 minutes. Cells were finally reconstituted in 1X PBS at a concentration of 0.2 million-cells/10 μl.

5.2.3. Left anterior descending (LAD) coronary artery ligation and Local Injections

Isoflurane inhalation anesthesia was used. The animals were placed individually in an induction chamber, and anesthesia was induced with 5% isoflurane (USP, Piramal Healthcare) in 100% oxygen using a Surgivet® series 100 vaporizer for 5 minutes with a delivery rate of 0.5 liter/minute until loss of righting reflex. After induction, the animals were moved onto a size 5 heated fixed temperature surgical table (Harvard Apparatus Inc.) and placed in dorsal recumbence. Mice were intubated with PE90 tubing through tracheal exposure and then connected to a respirator (Inspira Advanced safety single animal volume controlled ventilator, Harvard Apparatus Inc.). Anesthesia then was maintained at 1.5-3% isoflurane in 100% oxygen with a flow of 0.5 liter/min. Deep surgical anesthesia was confirmed by ensuring that muscle reflexes no longer are responsive to needle poking stimuli.

The heart was exposed via thoracotomy. Anterior myocardial infarction was created by permanent ligation of the left anterior descending coronary (LAD) artery using 8-0 silk sutures. Successful infarction was determined by observing a pale discoloration of the left ventricular muscle. The consistency of the infarction site was validated through placing a suture in the apex of the heart to facilitate the ligation of the left anterior descending artery.

Immediately after LAD ligation, PBS, untransfected hMSCs or LLCs transfected hMSCs were injected in a total volume of 10 µl (0.2×10^6 total hMSCs diluted in PBS, Lonza Walkersville Inc.), 2 μl each, at five injection sites into anterior and lateral aspects of the viable myocardium bordering on the infarction with a 32- gauge needle (Hamilton Bonaduz, AG, 701RN). Sham operated mice underwent identical surgical procedures without permanent LAD ligation or any injections. The number of mice per group (4 groups) per week (1, 2 and 4 week post-surgery) ranged from 2 to 3. The total number of SCID mice used in the first preliminary study was 26 (2 mice died out of the total 26 mice). Injection of cells or PBS was performed in a randomized fashion by a single investigator. After injection, the thorax was closed and all animals were allowed to recover.

5.2.4. Pressure volume (PV) loops and Hemodynamic measurements

Left ventricular pressure-volume (PV) loops are derived from pressure and volume information in the cardiac cycle. To generate a PV loop for the left ventricle, the left ventricular pressure (LVP) is plotted against left ventricular volume (LV) at multiple time points during a complete cardiac cycle.

Animals were placed in a chamber with 5% isoflurane supplemented with 100% oxygen for approximately 3-5 minutes until the mouse became recumbent. A nose cone with 1.5-3% isoflurane supplemented with 100% oxygen was

attached to the nose of the animal. Isoflurane was dispensed from a calibrated, precision vaporizer that allows for isoflurane to be delivered at 1 to 5%. Exhaust was directed to a carbon filter that scavenges isoflurane.

LV systolic and diastolic properties were measured using a miniaturized impedance / micro-manometer catheter to derive real-time LV pressure-volume relationships. A 1.4-French (F) micromanometer-tipped catheter (Millar) was inserted via the left carotid artery and then into the LV to measure LV pressures, followed by slight retraction of the catheter into the aorta to measure aortic pressures. The maximum and minimum first derivatives of the LV pressure (+dP/dtmax and –dP/dtmax, respectively), ejection fraction, stroke work (SW), heart rate and R-R interval, end-diastolic volume (EDV), end-diastolic pressure (EDP), end-systolic volume (ESV), and end-systolic pressure (ESP), diastolic chamber stiffness (normalized β), and time constant of relaxation (τ) were measured or derived. LV pressure and its first derivative were monitored continuously using a multiple channel recording system (Biopac System Amplifier; data acquisition and analysis using AcqKnowledge software). All volume measurements were done through relative volume unit (RVU) calibration and cuvette calibration using the mouse PV catheter that is equipped with a pressure sensor located in the center of the catheter, between six platinum electrodes. Relative Volume Unit calibration is where voltage signal output is

used to calibrate the signal into arbitrary relative volume units (RVUs). On the other hand, cuvette calibration is used to transform the RVUs to absolute volume units. The volume calibration cuvette used along with the mouse PV catheter is the 910-1049 Volume Calibration Cuvette (1.5-4.0 mm) (ADInsturments, Inc.). After these hemodynamic measurements, the animals were euthanized with either pentobarbital or isoflurane.

5.2.5. Hearts collection and sectioning

After study of cardiac function as discussed in the previous section, the hearts were arrested at diastole by infusing 4% buffered paraformaldehyde.

One heart of each group in case of the first preliminary study was cut in half horizontally above the infarction site and the lower part of the hearts were transferred to fixation 10% neutral buffered formalin solution (Sigma, Inc.) for 24 hours at room temperature.

Afterwards, tissue dehydration was accomplished by passing the heart tissue through a series of increasing alcohol concentrations. The blocks of tissue are transferred sequentially to aqueous solutions of 30%, 50%, 70%, 80%, 90%, 95%, and 100% ethyl alcohol for approximately two hours each. The blocks then were placed in a second 100% ethanol solution to ensure that all water is removed.

After dehydration, tissue blocks were cleared by moving the tissues into a 50:50 mixture of absolute ethanol:toluene for two hours. The tissue blocks then were transferred to pure liquid paraffin in an oven (56-58° C) for 1 hour and then into a second pot of melted paraffin for an additional 2-3 hours (56-58° C). During this time, the tissue block is completely infiltrated with melted paraffin.

Subsequent to infiltration, the tissues were placed into an embedding mold and melted paraffin is poured into the mold to form a block. The blocks were allowed to cool and then were ready for sectioning. Five μm sections were prepared from the paraffin embedded blocks.

5.2.6. H & E Staining

The sections then were stained with hematoxylin and eosin, or H&E stain. The staining method involves application of hemalum, which is a complex formed from aluminum ions and oxidized haematoxylin. This colors nuclei of cells blue (and a few other objects, such as keratohyalin granules). The nuclear staining is followed by counterstaining with an aqueous or alcoholic solution of eosin Y, which colors other eosinophilic structures in various shades of red, pink and orange (Jorundsson, Lumsden et al. 1999).

4-6 sections of each heart were stained. All slides were stained using an automatic rotary slide-staining machine (Shandon Varistain 24-4 Slide Stainer,

Thermo Scientific, Inc.) Hematoxylin positive areas stained in blue or violet (infarction zone) and the infarct wall thickness of left ventricular (LWT) were analyzed using the computerized planimetry (Macnification software Ver. 2, Orbicule, Inc.). The infarcted wall thickness was determined as the ratio of the thickness of the infarcted wall to that of the non-infarcted septal wall. The computerized planimetry software was used to obtain the length of the entire endocardial circumference and that segment of the endocardial circumference made up by the infarcted portion in the section. The infarct size, expressed as a percentage of the left ventricle, was calculated by dividing the circumference of the infarct by the total circumference of the left ventricle including the septum. The person who measured the infarct size was unaware of the treatment group.

The infarct size (%) was calculated using the following equation:

$$\left(\frac{\text{Total infarction size surface area}}{\text{Total cross sectional area}}\right) * 100$$

5.2.7. Immunofluorescence

Angiogenesis was evaluated by determining the presence of human angiogenic marker proteins, originating from the human mesenchymal stem cells, by immunofluorescence. The markers used and the corresponding antibodies used to detect the markers listed in table 5.1. (Abcam, Inc.). The appropriate

corresponding secondary antibodies used were tagged with AlexaFlour 594 (stained red) and AlexaFlour 488 (stained green).

Two negative controls were used to ensure the specificity of the immunofluorescence signal. The first negative control was sample stained with only primary antibody without secondary antibody. The second negative control was sample stained with only secondary antibody without primary antibody.

For immunofluorescence detection of stem cells, heart tissue sections (5 μm) (n=3 for each time point and group) were incubated with α-Smooth muscle actin (α-SMA), Cardiac Troponin-T (TnT), CD-31, Myosin heavy chain, Connexin 43 or Von Willebrand Factor (Factor VIII) polyclonal antibodies. All these antibodies were raised against human proteins. Subsequently, the sections were incubated with either anti rabbit Alexa-Fluor 488 conjugated or anti mouse Alexa-Fluor 594 conjugated secondary antibodies (Abcam®). Labeled sections were observed using an Olympus BX 51 confocal laser-scanning microscope (Olympus inc., USA). All morphometric studies were independently performed by at least 2 examiners per study (Mohamed Ismail Nounou, Sameer Saifuddin, Saher Ahmed and/or Kirk Braggs) and who were blinded to the treatment.

Antibody	AbCam® Code	Efficiency & Working Status	Specific to Human
α-Smooth muscle actin (α-SMA)	ab49481	Not working	Not Specific (Reacts with Human & Mice)
Cardiac Troponin-T (TnT)	ab91605	Working	Specific to Human (No mice interaction)
CD-31	ab9498	Not working	Not Specific (Reacts with Human & Mice)
	ab76533	To Be Tested	Specific to Human (No mice interaction)
Myosin heavy chain	ab50967	Not Working	Not Specific (Reacts with Human & Mice)
Connexin 43	ab62689	To Be Tested	Specific to Human (No mice interaction)
Von Willebrand Factor (Factor VIII)	ab93708	To Be Tested	Specific to Human (Unknown mice interaction)

Table 5.1: Antibodies corresponding to the aniogenic markers antigens used for detecting and visualizing angiogenesis from human origin.

5.2.8. Statistical Analysis

All the data are reported as mean ± standard deviation (SD). GraphPad Prism® version 5 was used to conduct the statistical analysis. The comparisons between the two groups were carried out using a Student t-test. A $p < 0.05$ was considered significant.

5.3. Results and Discussion

The results described in this section are limited to the first preliminary study.

Heart function post MI, and the effect of injection of transfected and non-transfected hMSCs were evaluated by measuring the pressure and volume of the heart using a P-V catheter (Figures 5.2-5.4). The LV dp/dt and PV loop, which represent heart contractility, appeared to suggest considerable recovery in hearts injected with VEGF transfected hMSCs compared to untreated cells. While encouraging, the small sample size prevents any conclusions to be made.

Hemodynamic studies suggested that hearts injected with LLC/$VEGF_{165}$ transfected hMSCs following the MI had ~ 1.2 to 1.4 times cardiac contractility and systolic and diastolic functions, as defined by the maximum and minimum rate of pressure change in the left ventricle (LV dP/dt max and LV dP/dt min, respectively), as compared to untreated cell controls (Figures 5.5 and 5.6).

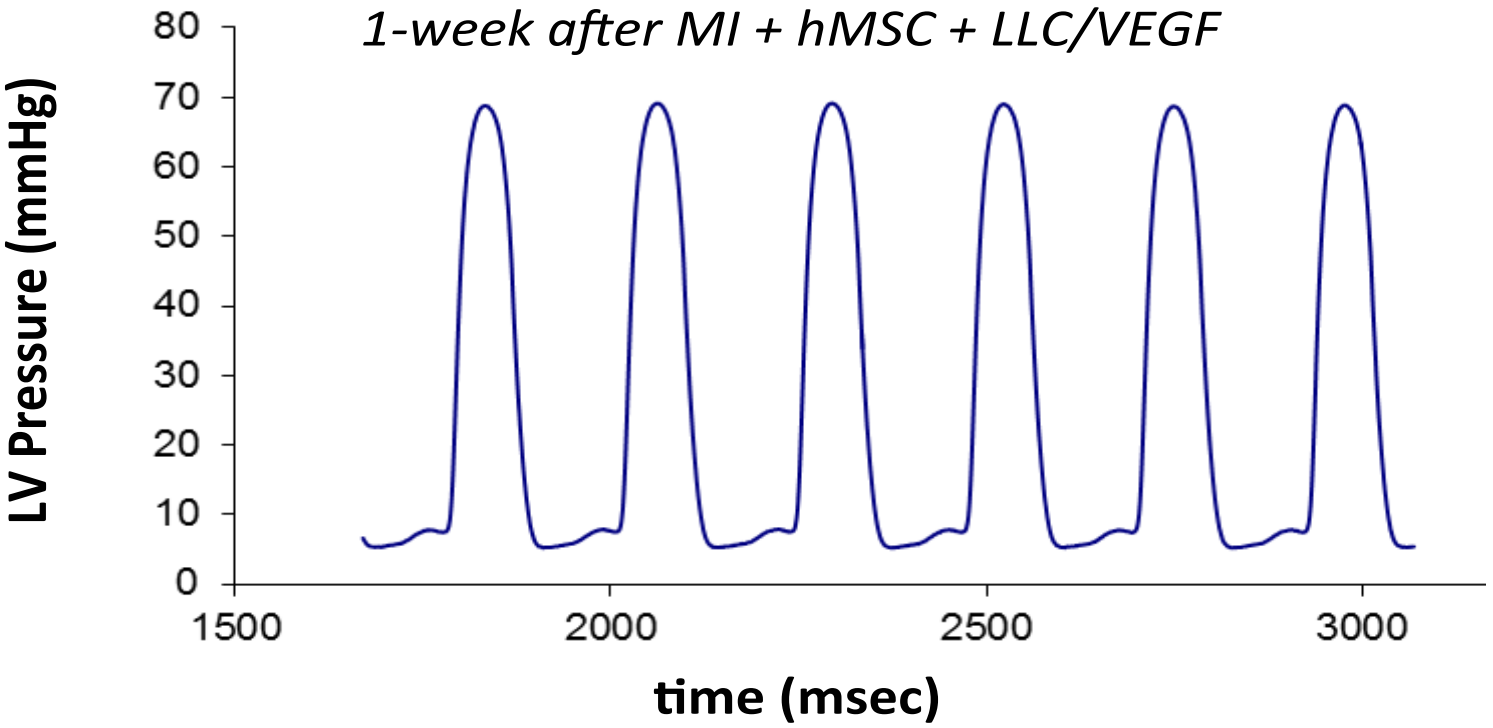

Figure 5.2: An example of LV pressure 1 week following MI induction plus immediate injection of VEGF-transfected hMSC in the region surrounding the site of infarction.

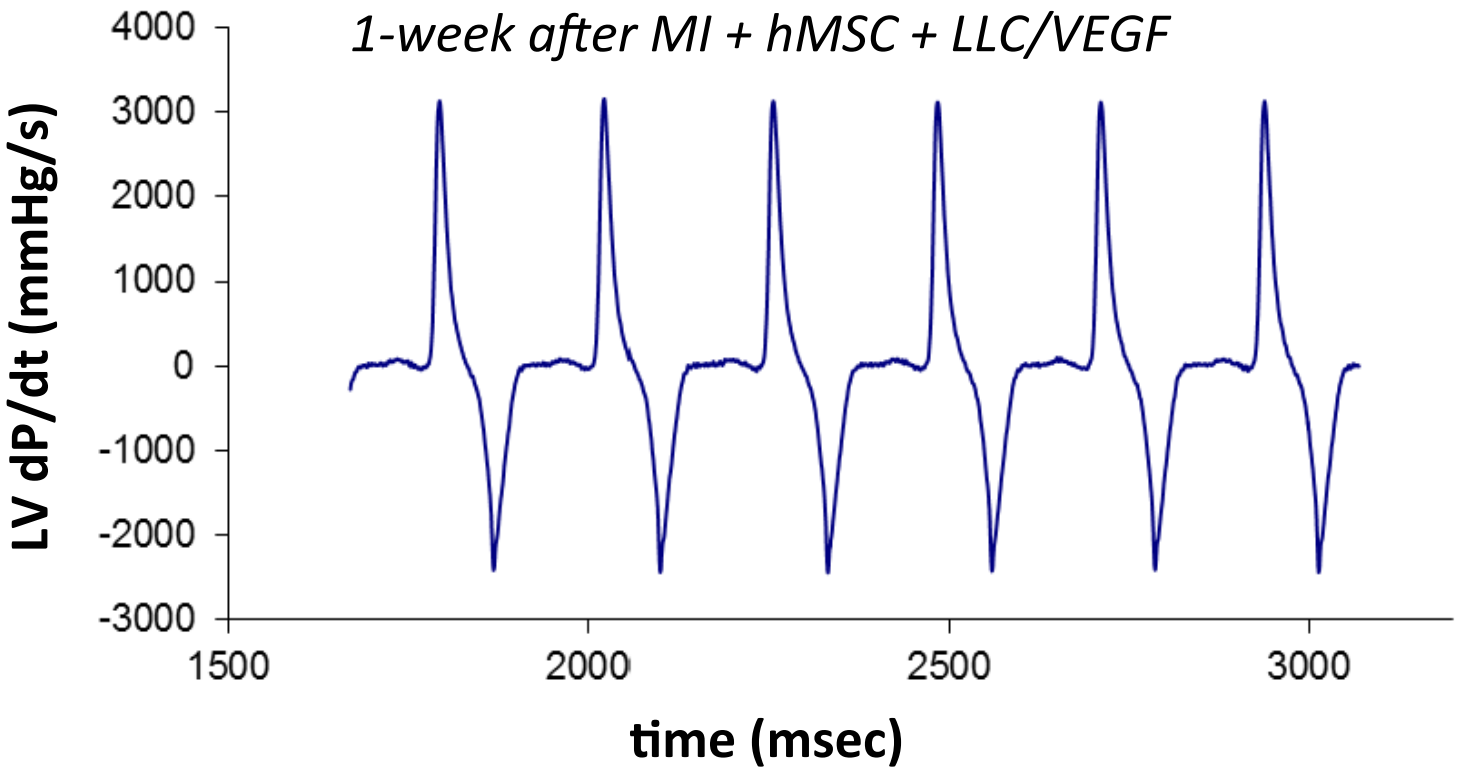

Figure 5.3: An example of LV dP/dt 1 week following MI induction plus immediate injection of VEGF-transfected hMSC in the region surrounding the site of infarction.

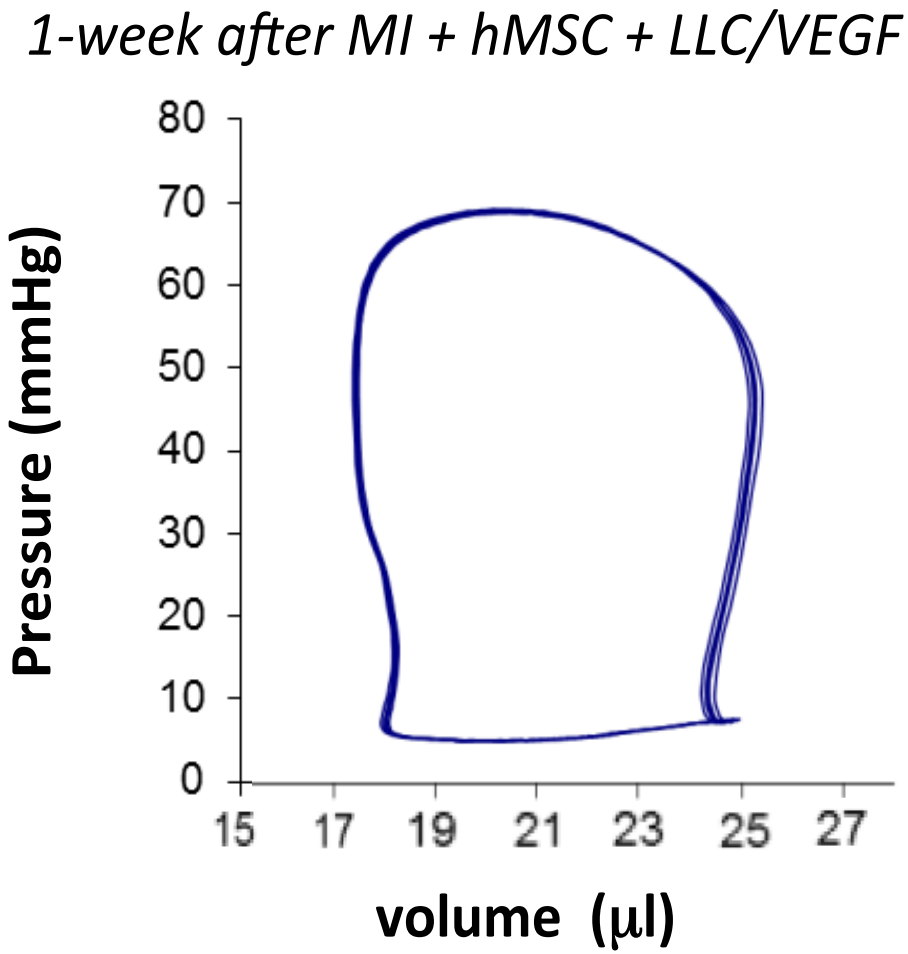

Figure 5.4: An example of Pressure-volume loop 1 week following MI induction plus immediate injection of VEGF-transfected hMSC in the region surrounding the site of infarction.

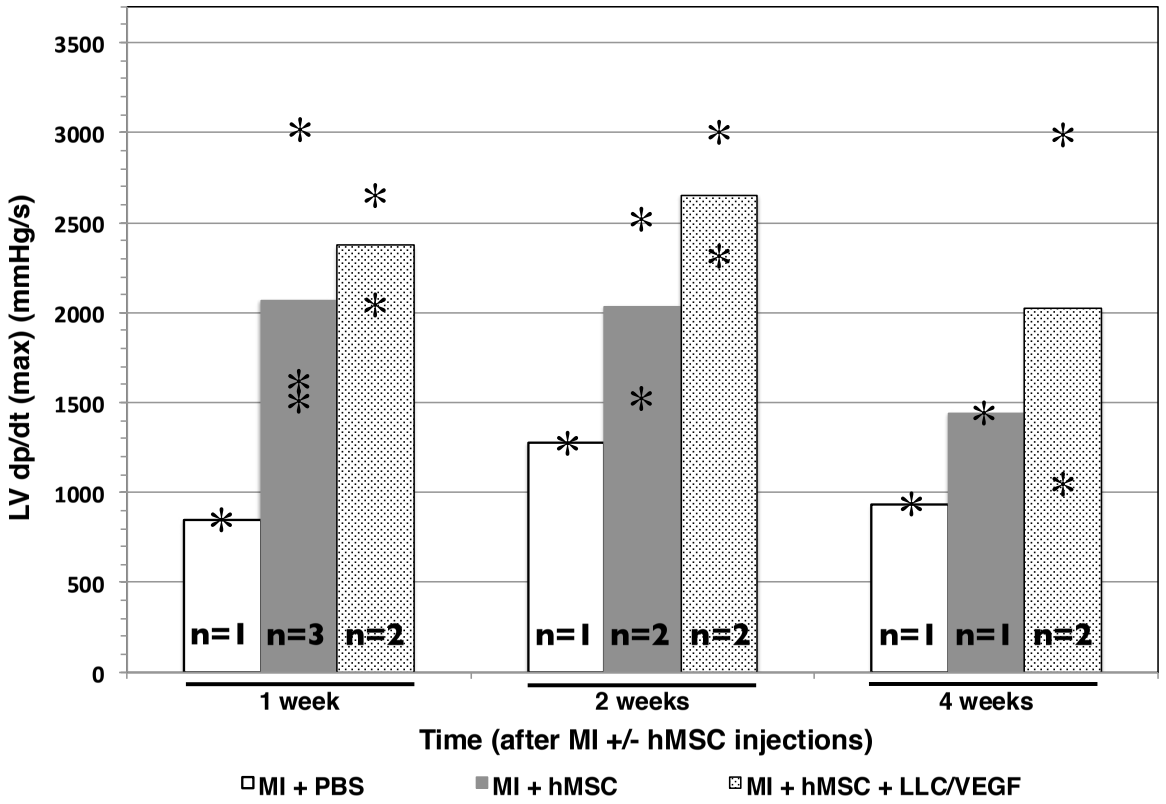

Figure 5.5: LV dP/dt (max) 1-week, 2-weeks and 4-weeks following MI induction and immediate injection of PBS buffer, hMSC cells or VEGF-transfected hMSC in the region surrounding the site of infarction. Each bar represents an average of different mice. (n is the number of animals ,* represents each data point)

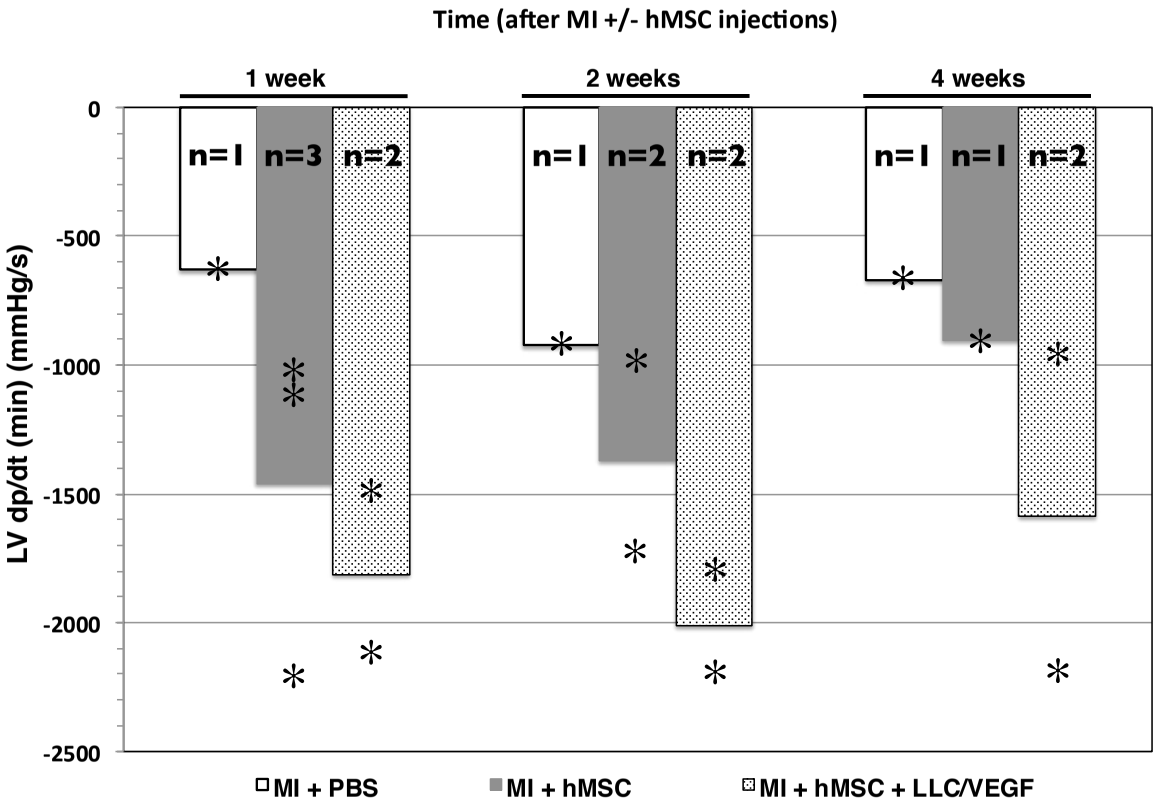

Figure 5.6: LV dP/dt (min) 1-week, 2-weeks and 4-weeks following MI induction and immediate injection of PBS buffer, hMSC cells or VEGF-transfected hMSC in the region surrounding the site of infarction. Each bar represents an average of different mice. (n is the number of animals ,* represents each data point)

Histological analysis appeared to provide preliminary evidence suggesting that the LLC/pSV_{40}-$VEGF_{165}$ transfected human mesenchymal stem cells could regenerate heart muscle in the infarcted area. H&E staining of the histology sections indicates minimal fibrous tissue at the infarcted area in the animals treated with genetically modified stem cells (Figure 5.7). In the PBS and stem cells only treated groups, the wall of the infarcted area was thinner, and this area was stained blue, indicating the formation of fibrous tissue (Figure 5.7). In the animal group treated with LLC/pSV_{40}-$VEGF_{165}$ tranfected human mesenchymal stem cells, there appeared to be evidence suggesting that myocardial regeneration occurred in the infarcted area after 4 weeks of treatment compared to untreated cell control. Figures 5.8 and 5.9 show quantitative analysis of the infarct size and the wall thickness of each group, respectively. The percentage of infarcted region of the mice hearts treated with transfected stem cells were less than 5% throughout the 4-week period. The percentage of infarcted region in the untreated cells group increased to approximately 10%, 30% and 50% after one, two and four weeks of treatment respectively (Figure 5.8). The wall thicknesses

of the infarcted areas of the hearts were approximately 200%, 300-400% and over 500% higher in animals treated with transfected stem cells compared to the animals injected with untreated cells at 1, 2 and 4 weeks post MI respectively (Figure 5.9). These preliminary and limited results appear to suggest that the LLC/pSV_{40}-$VEGF_{165}$ transfected human mesenchymal stem cells may be able to protect the infarcted heart tissues from muscle loss.

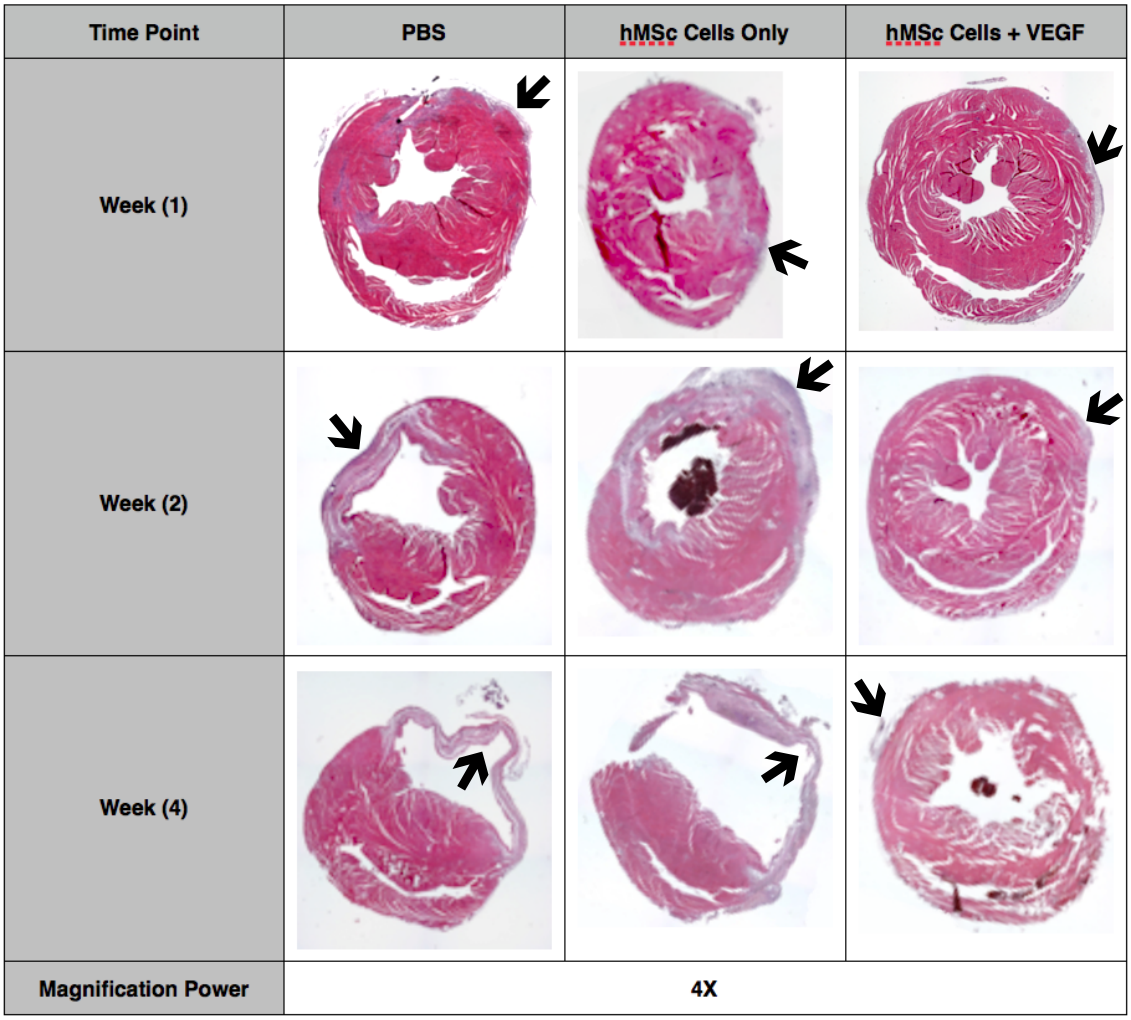

Figure 5.7: Hematoxylin and eosin (H & E) staining of myocardial tissue sections 1, 2 and 4 weeks post-MI plus immediate injection of PBS, hMSCs only, or hMSCs transfected with the pSV_{40}-$hVEGF_{165}$ gene using LLCs. The images suggest reduced infarct size in the animals injected with pSV_{40}-$hVEGF_{165}$ transfected cells compared to animals injected with PBS or non-transfected hMSCs. Black arrows indicate the infarction site.

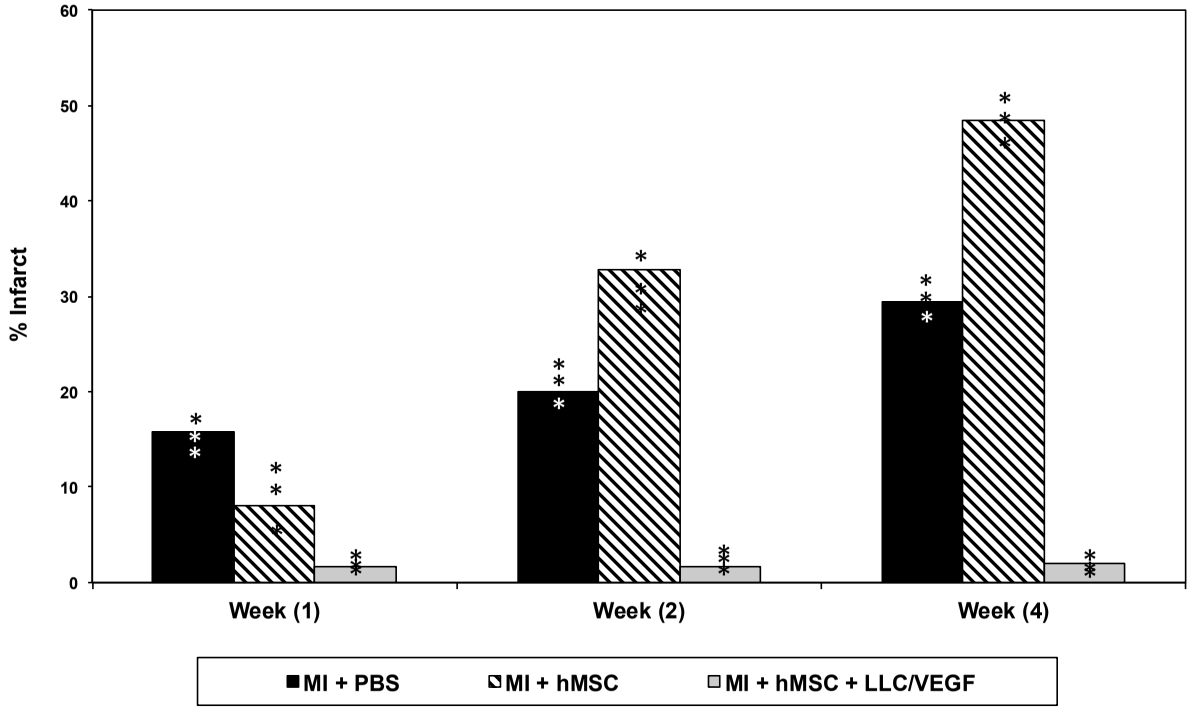

Figure 5.8: Average extent of fibrosis (expressed as percentage of infarct that is fibrotic) in the H & E stained heart tissues of animals 1, 2 and 4 weeks post-MI plus immediate injection of PBS, hMSCs only or LLC transfected hMSCs expressing $hVEGF_{165}$. (Each bar represents an average of three different sections around infarction site of one heart, * represents each data point and one heart only contributed to each bar)

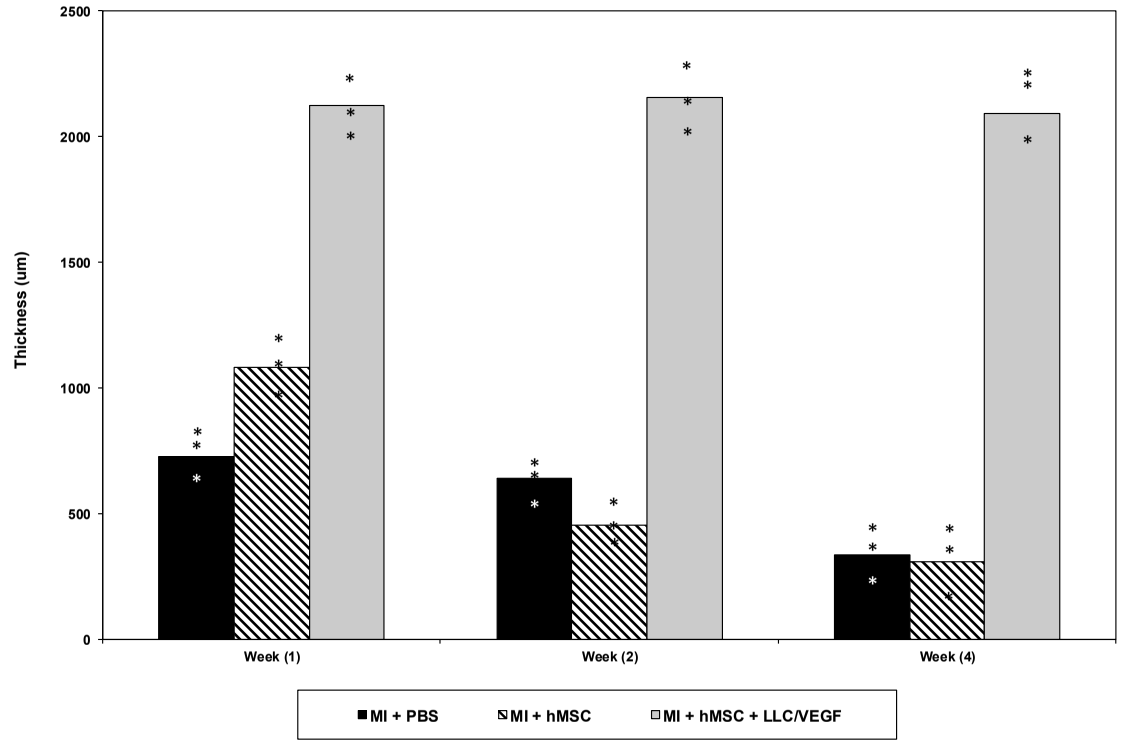

Figure 5.9: The infarct wall thickness of left ventricular wall (LWT) of H & E stained heart tissues of infarcted animals injected with phosphate buffered saline (PBS), hMSCs only and LLC transfected hMSCs expressing $hVEGF_{165}$ after 1, 2 and 4 weeks. (Each bar represents an average of three different sections around infarction site of one heart, * represents each data point and one heart only contributed to each bar)

Immunofluorescence also suggested the possible formation of new human cardiac muscle tissue and blood vessels in the LLC/pSV$_{40}$-VEGF$_{165}$ treated stem cells group. Immunofluorescence staining of tissue sections was done for the detection of differentiation of hMSCs into cardiomyocytes. As shown in figure 5.16, well-defined tubular structures that were stained positive for human cardiac troponin T (TnT) which are key markers of human cardiac muscle tissue were detected. All heart tissue sections from the LLC/pSV$_{40}$-hVEGF$_{165}$ transfected hMSCs group (three heart sections from one mouse) showed strong expression of TnT as opposed to non-transfected hMSCs (Figure 5.10). These data indicated potential differentiation of hMSCs into myocardial-like cells as well as neovascular transformation of the modified injected cells. This suggests that the use of genetically modified hMSCs to produce more VEGF$_{165}$ may have facilitate myocardial differentiation and vascular formation compared to unmodified cells.

Human alpha smooth muscle actin (α-SMA, Abcam® part number: ab49481) primary antibody failed to provide any reproducible or significant data. This is mainly attributed to the antibody non-specificity as it interacted with mice heart tissues as illustrated in the immunohistostaining sections for the mice hearts injected with buffer only (Figure 5.11). Moreover, proteins like alpha smooth muscle actin are very highly conserved in evolution and their antibodies will likely cross-react among other mammalian species.

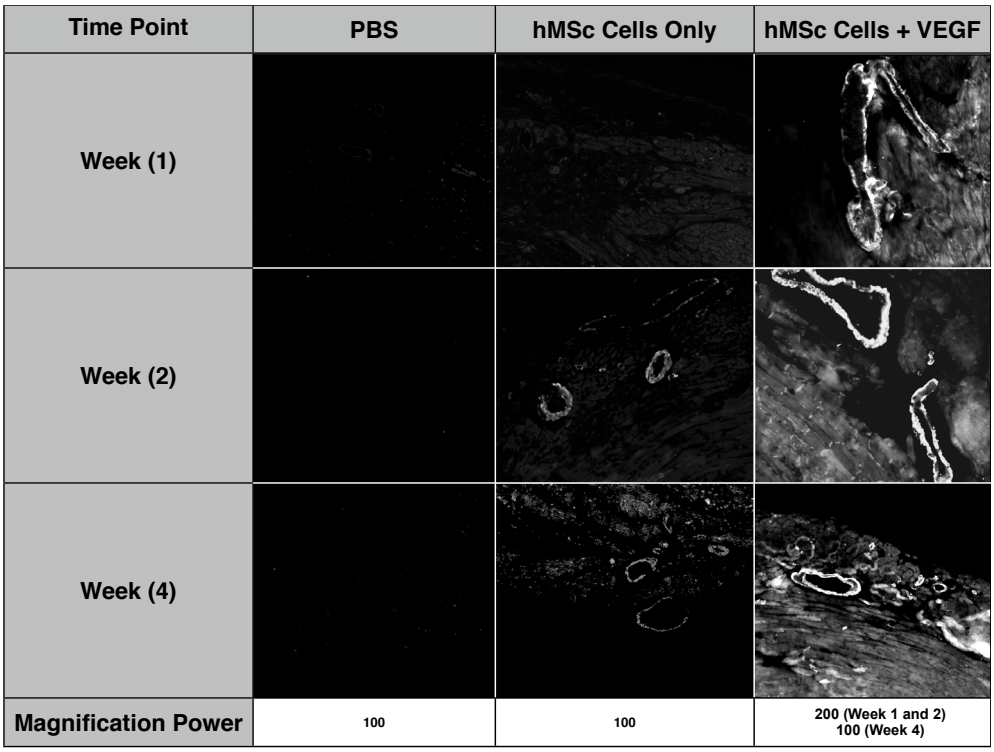

Figure 5.10: Immunofluorescent confocal images of representative heart sections after MI. Hearts were injected with PBS, hMSC, or hMSC transfected to express $hVEGF_{165}$ immediately following MI. Sections were treated with primary antibody raised against hTnT, followed by a fluorescently tagged secondary antibody. Sections were obtained 1, 2 and 4 weeks post MI plus injection. All images were grey-scales using Adobe Photoshop CS5. Human troponin T-associated fluorescence appears as white in the grey-scaled images. Lack of overall tissue fluorescence in PBS injected hearts and focal fluorescence in hMSC injected heart suggests that the antibody may be preferentially detecting human, hMSC-derived TnT and that this may be increased in transfected vs. non-transfected hMSC. These images were obtained from 3 sections from one heart in each group. Similar images were obtained in approximately 100% of all sections examined for each group.

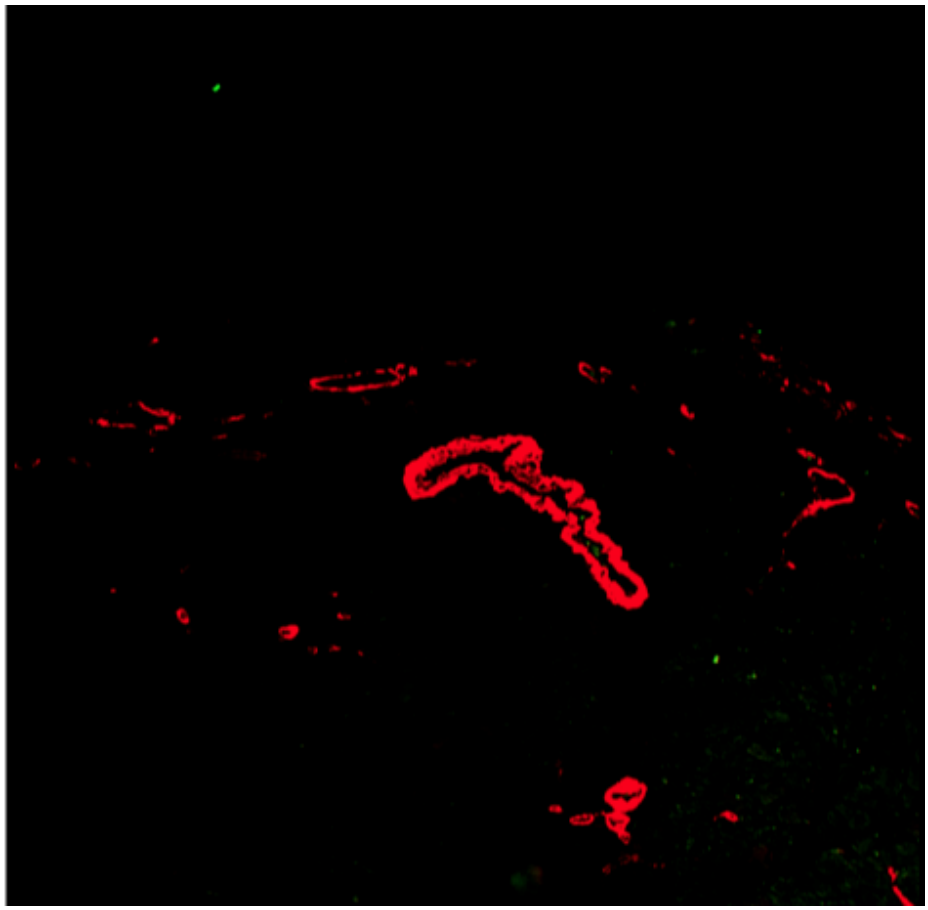

Figure 5.11: Immunofluorescence confocal image (magnification power of 100) of a heart section from a mouse after MI plus PBS injection. Sections were treated with antibody raised against human alpha smooth muscle actin (hα-SMA) and a fluorescently tagged secondary antibody. Red fluorescence, indicative of reactivity with hα-SMA antibody is clearly visible in this image from a PBS injected heart, suggesting significant cross-reactivity of the antibody with murine α-SMA.

Moreover, CD-31 (Abcam® part number: ab9498) and myosin heavy chain (Abcam® part number: ab50967) primary antibody did not provide any reproducible or significant data as shown in figure 5.12. This indicated that these two antibodies were non-specific to human tissues and interacted heavily with mouse tissues. Furthermore, the CD-31 primary antibodies generated a significant green fluorescence background despite being introduced to the tissue without its counterpart secondary antibody.

For this reason, a new CD-31 primary antibody (Abcam® part number: ab76533) will be tested for tissue specificity. Moreover, two other primary antibodies raised aganist endothelial and angiogenic markers, Von Willebrand Factor (Factor VIII) (Abcam® part number: ab93708) and connexin 43 (Abcam® part number: ab62689), respectively, will be tested for human tissue specificity (Table 5.1).

These preliminary studies have many significant limitations. First and foremost amongst these limitations is the fact that data from only one or two animals are provided in each group. A much larger study is required before any conclusions can be drawn regarding the potential benefit of VEGF-transfected hMSC. Having said this, other limitations of design of the study exist. First, the stem-ness of the transfected hMSC was not tested prior to injection. The stem-ness of the cells should be investigated via detection of the human mesenchymal

stem cell markers such CD105, CD166, CD29, and CD44. hMSCs test negative for CD14, CD34 and CD45 after transfection and before cell injection into the heart. Furthermore, due to the inherently transient nature of transgene expression, future studies should attempt to assess VEGF expression at various intervals after cell injection to verify expression after injection as well as determine the persistence of transgene expression. These *ex vivo* studies are still very preliminary due to the different variables involved that should be completely optimized and fully controlled. Surgical manipulation is another main limitation. The surgical skills of the surgeon are rate-limiting step in the success of this experiment through creating a consistent infarction with respect to size and location. Moreover, the uniformity of gene expression with respect to transfection efficiency and cell viability is important in yielding reproducible results. Finally, the uniformity of the site of injection and the amount of cell injections are important. Any variations within the amount of cell injections or their locations could yield highly scattered results.

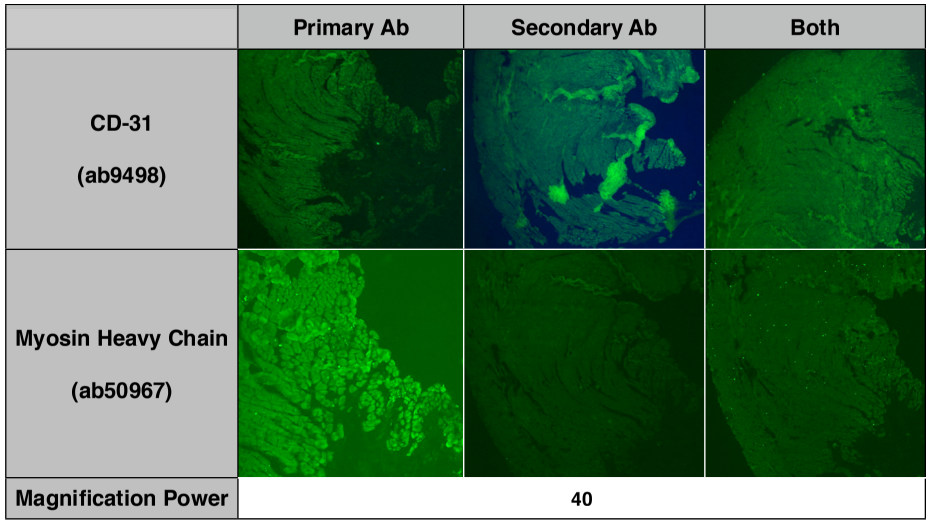

Figure 5.12: Representative immunofluorescent images from section of mouse heart obtained after MI plus VEGF165-transfected hMSC. Images shown were obtained from hearts harvested 4 weeks after MI. Sections were treated with primary antibodies raised again human CD-31 or myosin heavy chain followed by appropriate fluorescently tagged secondary antibodies. The images indicate fluorescence after treatment with only the secondary antibody in the case of CD-31, indicative of non-specific fluorescence. For myosin heavy chain, significant fluorescence was observed with the primary antibody only, also suggestive of non-specific fluorescence. These images were obtained from 3 sections from one heart and are representative of ~ 100% of the sections examined.

6. Second Generation Lysine-based Carrier Systems Synthesis Trials

6.1. Introduction

Lately, the amino acid histidine has been used in the design of nonviral gene delivery carriers because of histidine's fusogenic activity. Histidine-containing polymers disrupt the endosomes and lysosomes acidic subcellular compartments membranes. Histidines are uncharged at physiological pH and positively charged in acidic environment, which imparts selective membrane disruption in the acidic endosome. The imidazole group of histidine has a pKa of ~6.0, allowing it to become protonated in the acidic environment of the endosome. This induces a strong buffering capacity within the cells (Figure 6.1) (Kichler, Leborgne et al. 2003; Midoux, Kichler et al. 1998; Midoux, LeCam et al. 2002; Midoux and Monsigny 1999; Pichon, Goncalves et al. 2001). In addition, histidine has the ability to fuse with lipid bilayers when the imidazole groups of histidine are protonated as a result of its interaction with negatively charged membrane phospholipids (Wang and Huang 1984). Many research groups have studied the improvement in transfection upon conjugation of various polymeric carrier systems with histidine (Benns, Choi et al. 2000; Benns and Kim 2000; Lee, Choi et al. 2007).

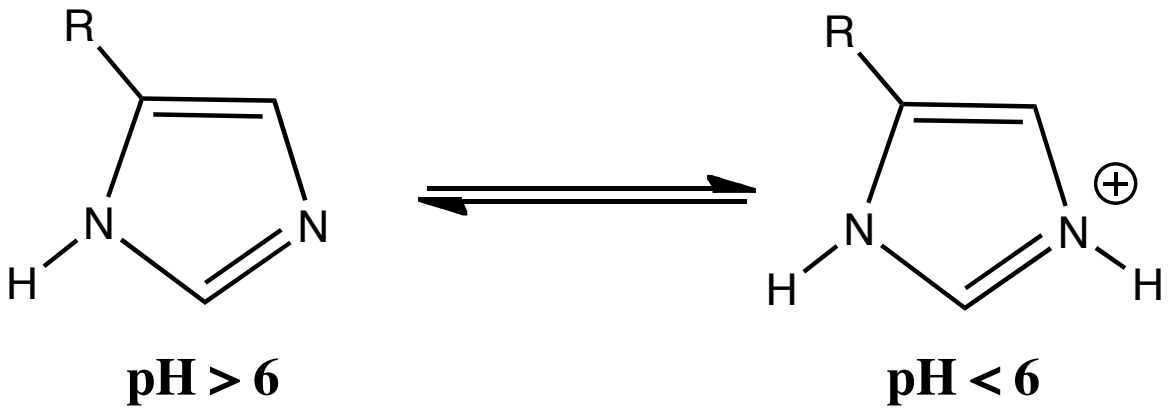

Figure 6.1: pH dependence of the imidazolium protonation state.

Histidylated polylysine (HpK) isone of the profound examples of a nonviral histidine-based gene carrier system. HpK was prepared by substitution of poly-L-lysine with histidine residues in the polymerization process. These HpK systems were found to be 3-4.5 times more efficient for the transfection of HepG2 cells than poly-L-lysine polymers (Midoux and Monsigny 1999). Depending on the cell type, optimal transfection was achieved with HpK containing 63-100 (33-50%) histidyl residues. The transfection efficiency was reduced dramatically when cells were transfected in the presence of bafilomycin A1, a specific inhibitor of the ATPase responsible for the accumulation of protons inside the endosome lumen. In this case, the endosomal compartment is rendered neutral and protonation of the imidazole ring of HpK is totally hindered, preventing membrane destabilization. (Wang and Huang 1984, Midoux, Kichler et al. 1998).

Furthermore, Lee et al. (Lee, Shin et al. 2003) studied the amphoteric property of the imidazole group of histidine and used this property to create pH-sensitive micelles for the treatment of solid tumor. In this study, poly-L-histidine poly(ethylene glycol) diblock copolymers (polyHis-b-PEG) were synthesized for the formulation of a pH sensitive polymeric micelles. Protonation of the amine group at lower pH will render the hydrophobic imidazole group in the histidine-repeating units hydrophilic. This feature can be extremely beneficial in the

treatment of solid tumors through a switching mechanism based on the local pH environment for the release of drugs or genes. The extracellular pH (pH_e) in many tumors is lower than in the corresponding normal tissue (Gerweck and Seetharaman 1996). According to Lee et al. (Lee, Shin et al. 2003), polyHis5K–b–PEG2K micelles can selectively trigger anticancer drugs release at tumor extracellular low pH levels at tumor sites through physical destabilization of long-circulating polymeric micelles (targeted high-dose cancer therapy).

Thus, to develop biocompatible PLL derivatives capable of efficient endocytic release and subcellular trafficking, we propose the development of second-generation peptidomimetic biocompatible reducible copolymers (BRCs) as efficient and safe nonviral gene delivery systems (Figure 6.2). BRCs consist of repeating peptidomimetic blocks of lysine (K) and histidine (H) of either (KKHKKHKK) or (KHK) backbone arrangement (Figure 6.2A and 6.2B respectively). In addition, some lysines are functionalized with dimethylaminoethanoic acid as 3° amines, joined together by reducible disulfide bonds. This polymer design is projected to overcome the endo-lysosomal degradative pathway, which is a critical barrier against efficient gene transfection (Figure 6.3). This will be achieved by integrating two unique endosomolytic moieties, namely histidines and 3° amines. The imidazole functionality will buffer the endosome and potentially induce its rupture (proton sponge effect) facilitating

enhanced efficacy and competent DNA release into the cytoplasm. In addition, histidine has the ability to destabilize lipid bilayers in a slightly acidic medium promoting endosomal membranes disruption and thus, favoring the delivery of DNA into the cytosol. Moreover, the assimilation of 3° amines within the polymer backbone structure will augment the buffering capacity of the carrier system further. The 3° amines, along with 1° and 2° amines present on the polymer backbone will generate a wide range of pKa values, which will enhance and contribute to the proton sponge effect. Therefore, the use of histidines and 1°, 2° and 3° amines will overcome the endo-lysosomal degradative pathway, and subsequently enhance the transfection efficacy of the polymeric carrier system. Moreover, the reducible disulfide bond will enhance the intracellular delivery of the carrier system, as it is stable in the oxidative extracellular space and unstable in the reducing intracellular environment. The disulfide backbone breaks down to free thiol groups in the reducing cytoplasmic environment resulting in the efficient release of the DNA load from the carrier system within the cytoplasm. The combination of a reducible disulfide backbone structure and dual endosomal release mechanisms will facilitate efficient delivery of nucleic acid cargo into the cytoplasm and significantly increase the transfection efficiency with negligible cytotoxicity.

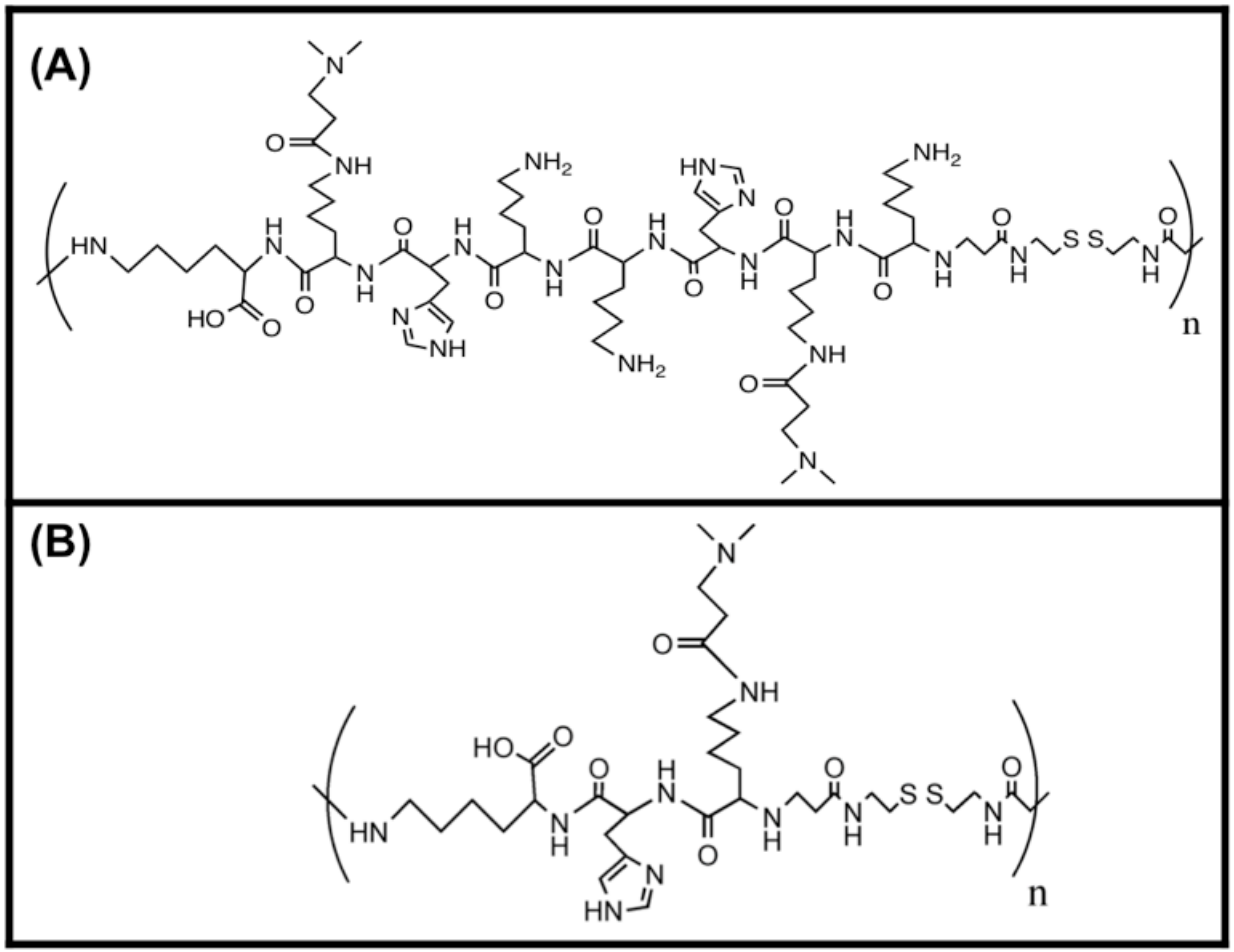

Figure 6.2: Chemical structure of proposed lysine-based final Biocompatible Reducible Copolymer (BRC) with (A) KKKKHKK and (B) KHK peptide backbone structures respectively.

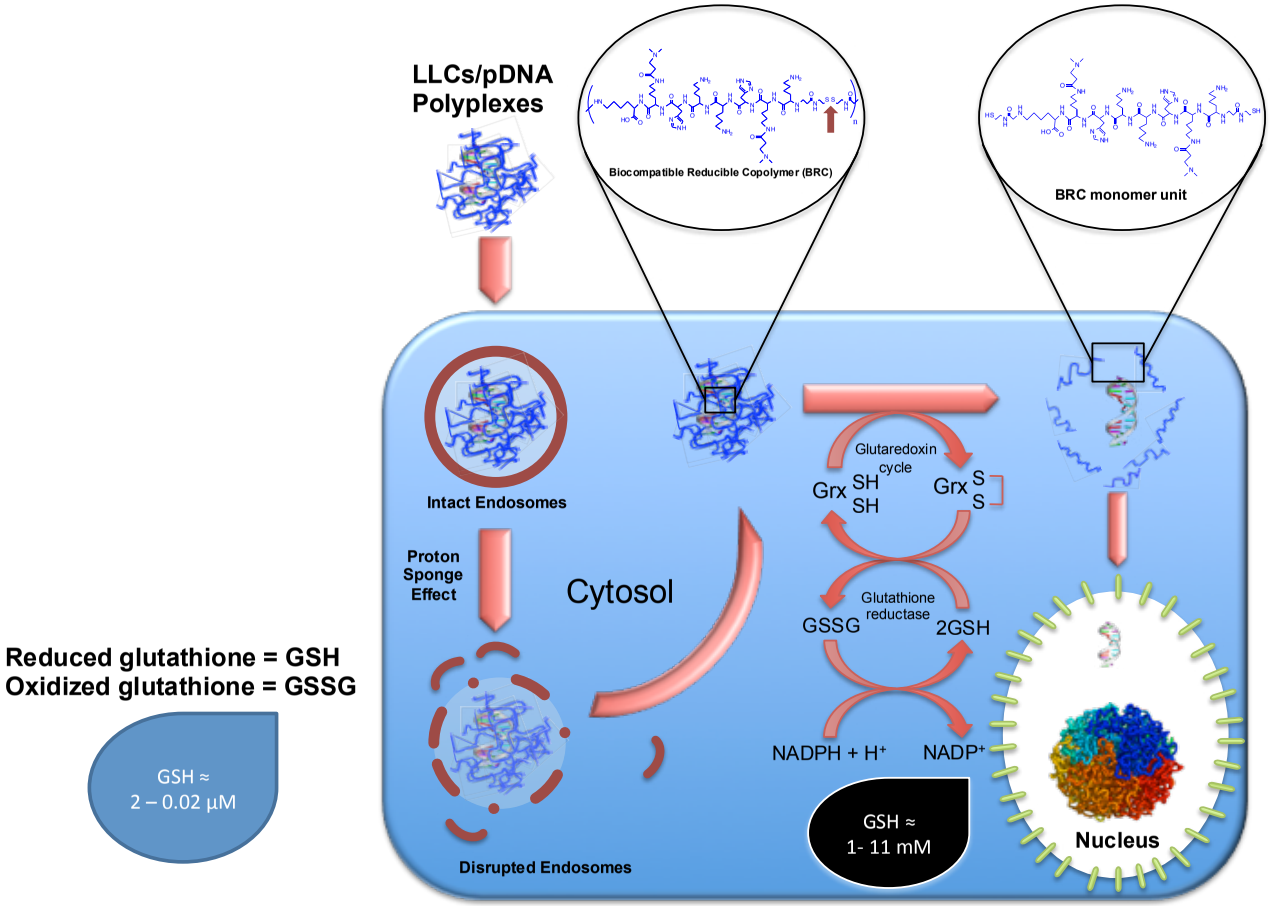

Figure 6.3: Schematic diagram of the endosomal escape of the BRC/pDNA polyplexes and DNA release inside the cytosol from the BRC/pDNA polyplexes upon the reduction of the disulfide bonds within the polymer backbone.

6.2. Materials and methods

6.2.1. Materials

N-butyloxycarbonyl ethylenediamine, trifluoroacetic acid (TFA), 1-ethyl-3-(3-dimethylaminopropyl) carbodiimide) (EDC coupling agent) and sodium dodecyl sulfate (SDS) were purchased from Sigma-Aldrich (St. Louis, MO). N,N´-cystaminebisacrylamide (CBA) was purchased from PolySciences, Inc. (Warrington, PA). (2-(7-Aza-1H-benzotriazole-1-yl)-1,1,3,3-tetramethyluronium hexafluorophosphate) (HATU peptide coupling agent), N-methyl-2-pyrrolidinone (NMP), N,N-Diisopropylethylamine, piperidine solution, dichloromethane (DCM), dimethyl formamide (DMF), Fmoc-Lys-Boc amino acid, Fmoc-His-Trt amino acid, Fmoc-Lys-(Mtt)-OH amino acid and 2-chloro trityl chloride resin were purchased from Novabiochem, Inc. (Merck KGaA, Darmstadt, Germany). ^{1}H NMR data were obtained with a General Electric (GE) QE-300 300 MHz instrument (Boston, MA). Matrix-assisted laser desorption ionization-time-of-flight (MALDI-TOF) data were obtained with a Voyager-DE STR Biospectrometry Workstation from Applied Biosystems (Foster City, CA). The molecular weights of the various polymers were determined by size exclusion chromatography (SEC) on a Shimatzu Prominence HPLC system (Shimadzu Scientific Instruments, MD) equipped with a Shodex SB-803-HQ (Particle size = 6 nm) and Shodex SB-806-HQ (particle

size = 13 nm) columns in series and detected with photodiode array (PDA) and ELSD-LTII (low temperature evaporative light scattering detector) detectors (Columbia, MD).

6.2.2. Synthesis of BRCs

6.2.2.1. Synthesis of peptide sequence(s) building blocks for BRCs

The general process for synthesizing peptides on a resin begins by attaching the first amino acid, the C-terminal residue, to the resin. To prevent the polymerization of the amino acid, the alpha amino group is protected with a temporary protecting group. Once the amino acid is attached to the resin, the resin is filtered and washed to remove byproducts and excess reagents. Next, the N-alpha protecting group is removed in a deprotection process and the resin is again washed to remove byproducts and excess reagents. Then the next amino acid is coupled to the resin-peptide. This is followed by another washing procedure, which leaves the resin-peptide ready for the next coupling cycle. The cycle is repeated until the peptide sequence is complete. Then typically, the final N-alpha protecting group is removed, the peptide resin is washed, and the peptide is cleaved from the resin (Figure 6.4).

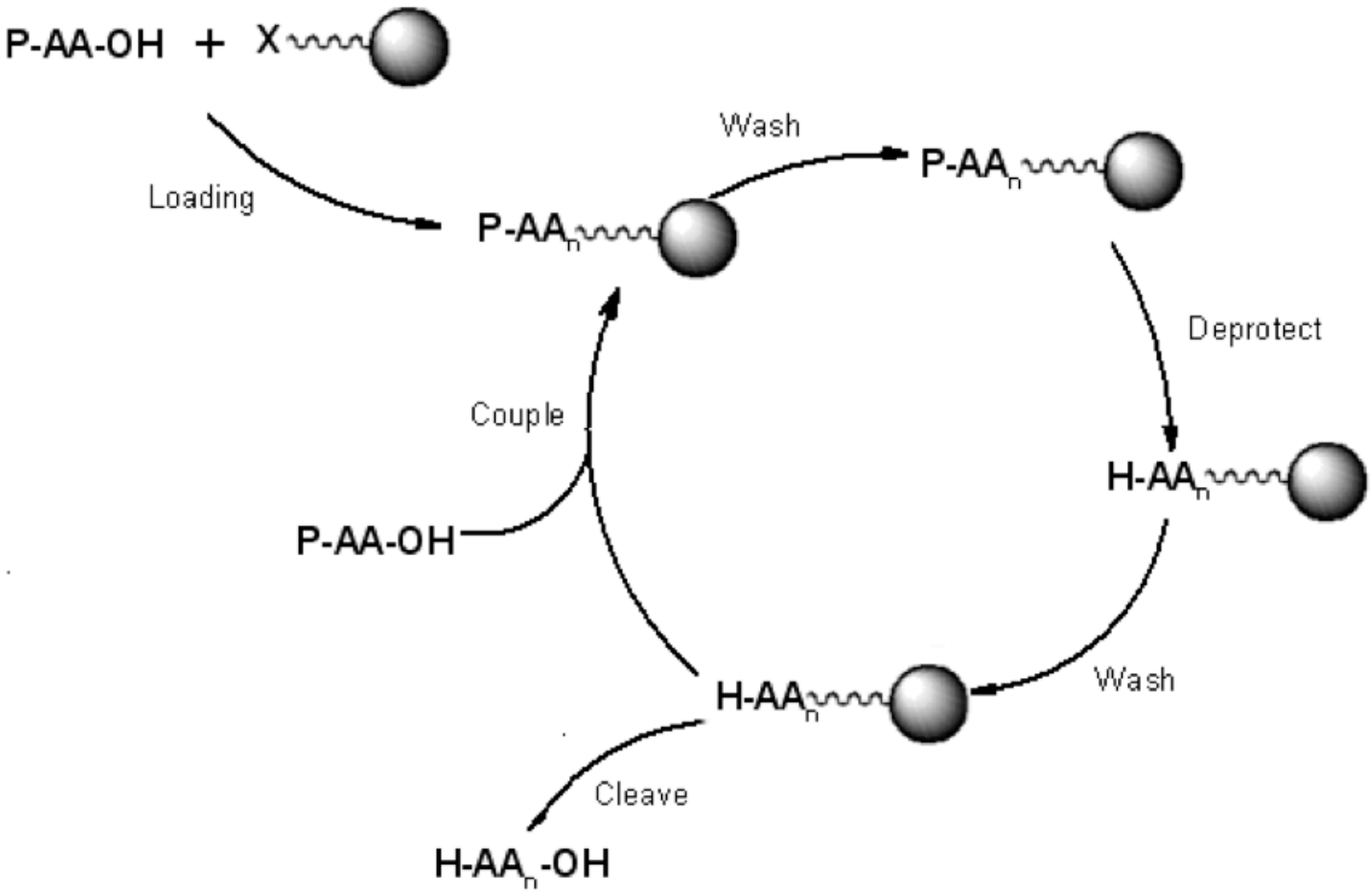

Figure 6.4: General Solid Phase Peptide Synthesis Cycle (Copyrighted image from AAPPTEC®, Inc).

The side chains of many amino acids are reactive and may form side products if left unprotected. For successful peptide synthesis, these side chains must remain protected despite repeated exposure to N alpha deprotection conditions. Ideally, the N alpha protecting group and the side chain protecting groups should be removable under completely different conditions, such as basic conditions to remove the N alpha protection and acidic conditions to remove the side chain protection. Such a protection scheme is called 'orthogonal' protection.

The novel lysine-based BRCs were constructed using lysine and histidine-based peptide sequences (KKHKKHKK) and (KHK) as shown in Figure 6.2. The synthesis of the various building blocks was done automatically through an AAPPTEC Apex 396® peptide synthesizer or manually with manual solid-state peptide synthesis. Initially, the 2-chloro trytyl chloride resin was loaded with the first lysine amino acid (Fmoc-lys-(mtt)-OH). The initial amino acid substitution was calculated by UV spectroscopy to determine the resin loading capacity. The resin loading capacity determines the molar concentration of amino acids that can attach to this resin. The main reason for using Fmoc-lys-(mtt)-OH as the first lysine amino acid in the peptide sequence, is because of the mtt protective group. The mtt protective group would be cleaved easily with only 5% to 10% TFA (compared to the Boc (Di-tert-butyl dicarbonate) protecting group, which requires 50% TFA to be cleaved). In this way, selective deprotection of mtt group

would be possible leaving the Boc group intact on the rest of the amino acids. This allows selectivity in the polymerization reaction to yield a linear final polymer and prevents any crosslinking. The peptide sequences initially were synthesized through multiple couplings steps with (fmoc)-Hist-(TRT), (fmoc)-Lys-(Boc) and cystamine bisacrylamide (CBA). The triphenylmethyl (TRT) and tert-Butyl carbamates (Boc) protecting groups were removed with 1/1 TFA (Triflouroacetic acid)/methylene chloride while the fluorenylmethyloxycarbonyl (fmoc) groups were removed during the deprotection cycle. To the lysine core, activated amino acids that comprise the lysine-rich and histidine-rich domain were added sequentially according to the proposed design with the aid of the proposed synthesis protocol. To the amine groups of this lysine, activated amino acids of the terminal branches were added. The peptides were cleaved from the resin and precipitated per the protocol as previously described (Zhang, Ambulos et al. 2004). Afterward, the mtt protective group was cleaved from the peptide sequences KKHKKHKK and KHK using 5% TFA (Figure 6.5 and 6.6 respectively).

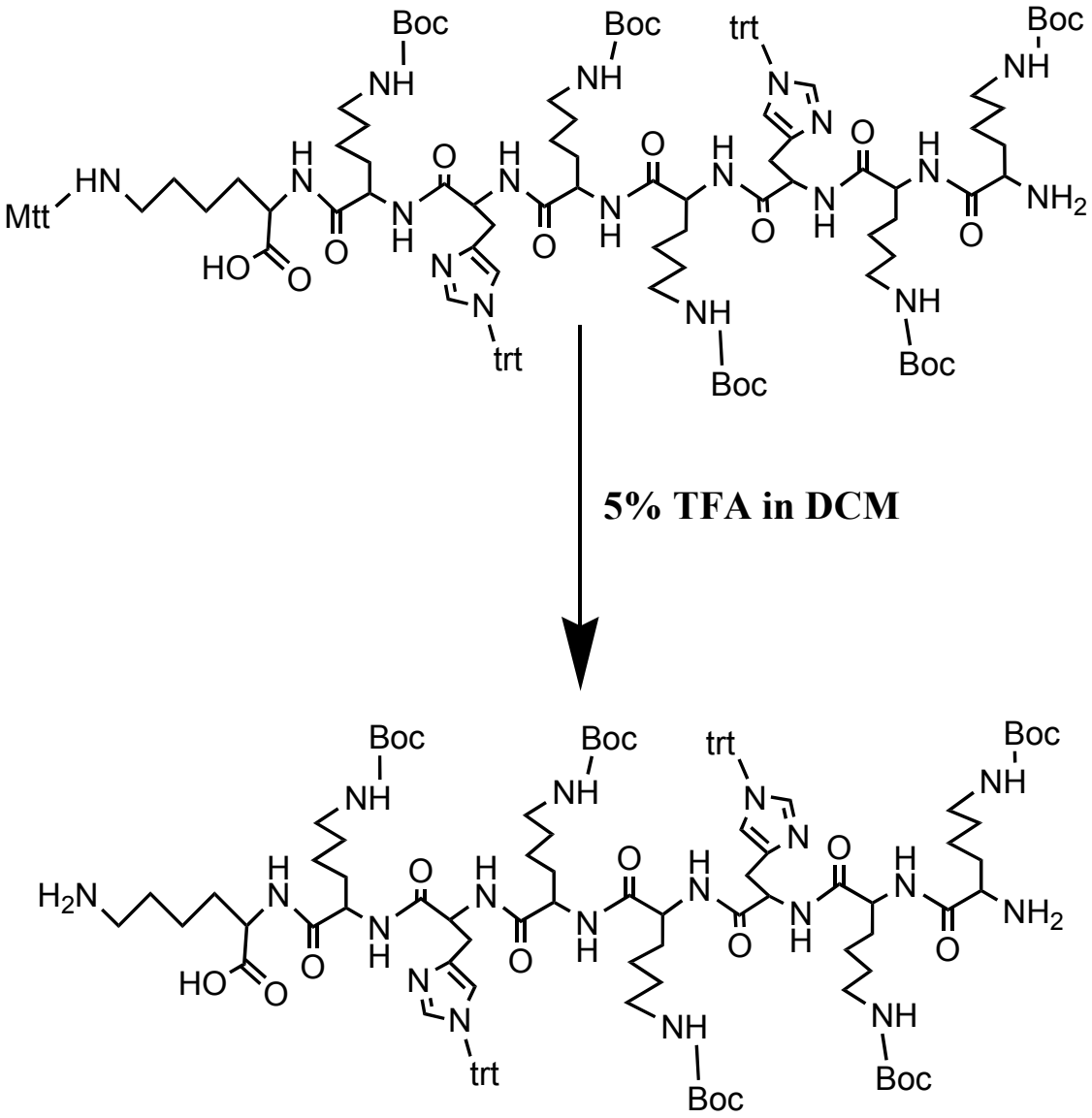

Figure 6.5: Mtt deprotection from KKHKKHKK peptide sequence.

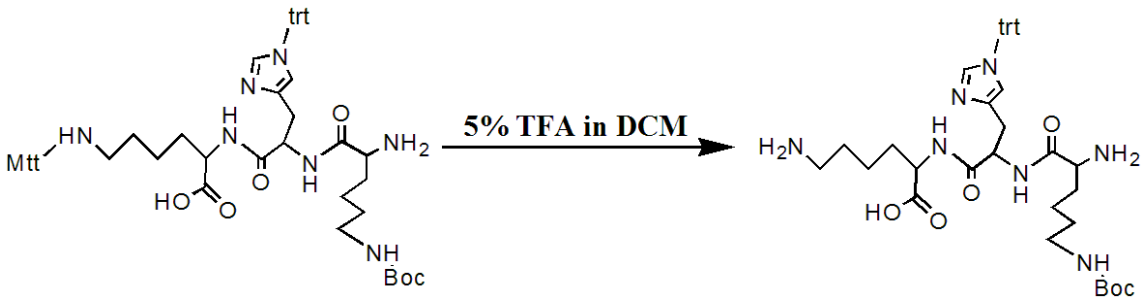

Figure 6.6: Mtt deprotection from KHK peptide sequence.

6.2.2.2. Polymerization of the synthesized peptide sequence

The synthesized monomeric peptide sequences KKHKKHKK and KHK were activated with a basic or acid catalyst and the activated monomer units will react with CBA in a Michael addition reaction (Figure 6.7 and 6.8 respectively). In some reactions, no catalyst was used. Table 6.1 lists all of the various reaction conditions and catalysts used in the various trials for the polymerization reaction. The reaction mixture was stirred in an oil bath at 45° C to dissolve the reagents. The reaction then was stirred in the dark under a nitrogen atmosphere for 4 days.

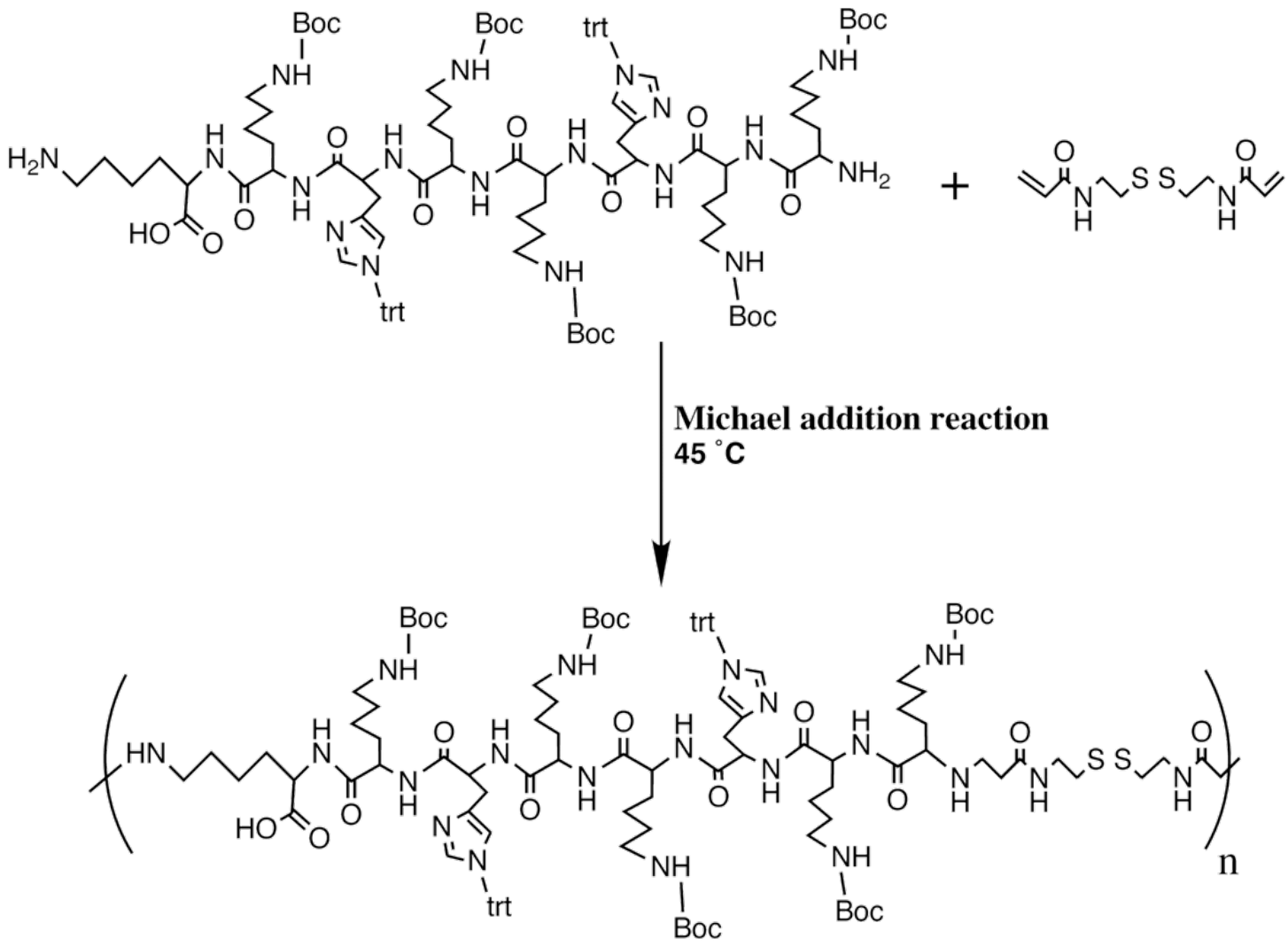

Figure 6.7: Polymerization of KKHKKHK peptide sequence to yield BRCs via Michael addition.

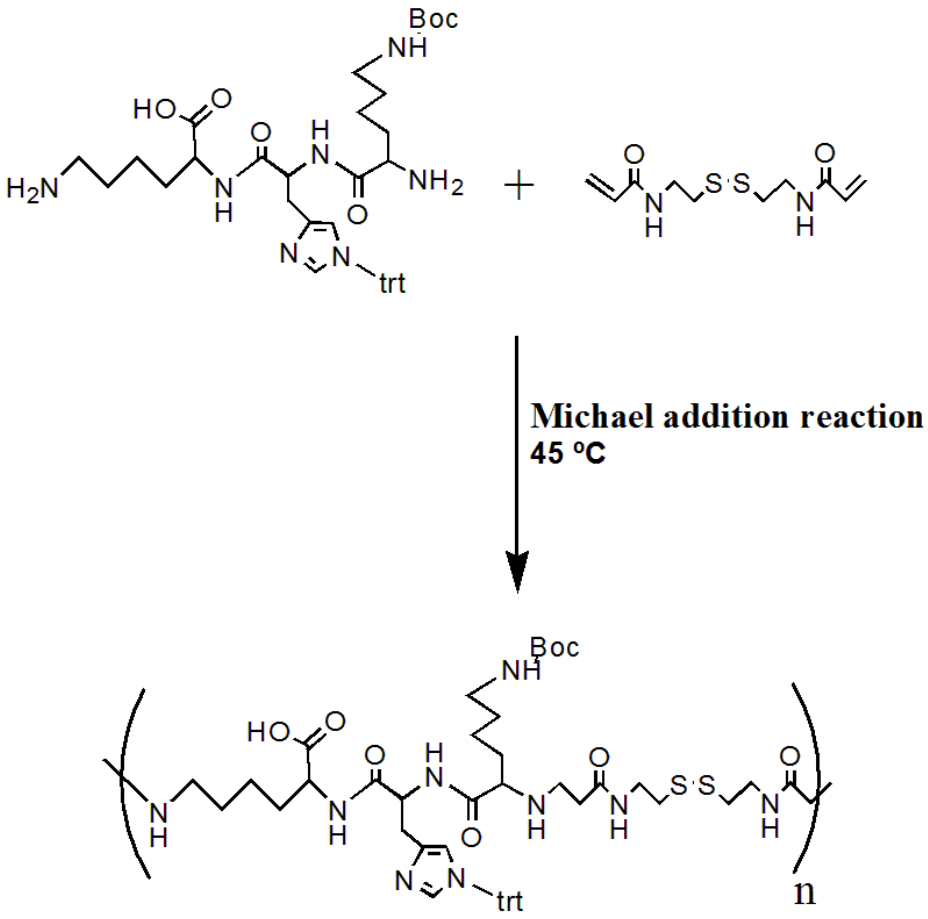

Figure 6.8: Polymerization of KHK peptide sequence to yield BRCs via Michael addition.

Reaction	Catalyst		Solvent	Reaction Volume (ml)	Excess Molar ratio of catalyst	Result
1	Base Catalysis	NaOH	Methanol	3	2X	No Product MALDI, 2266 D_a
2			90/10 MeOH/H_2O	5	2X	MALDI: 1461 D_a SEC: 926 D_a
3			90/10 MeOH/H_2O	5	2X	SEC: < 100 D_a
4		DIPEA	90/10 MeOH/H_2O	5	2X	SEC: < 100 D_a
5			DMSO	3	2X	1161 D_a
6			Methanol	3	2X	MALDI: 2566 D_a, 4770 D_a (10%)
7			Methanol	5	10X	No Product (SEC)
8		TEA	Methanol	5	10X	No Product (SEC)
9	Acid Catalysis	Acetic acid	Methanol	5	5X	No Product (SEC)
10	No Catalyst		Methanol	3	-	MALDI: 2649 D_a
11			90/10 MeOH/H_2O	3		SEC: 1040 D_a, 6 D_a
12			90/10 MeOH/H_2O	5		SEC: < 100 D_a
13			90/10 MeOH/H_2O	10		SEC: 257 D_a, 11 D_a
14			Methanol	5		No Product (SEC)

Table 6.1: List of all of the reactions conditions and catalysts used in the various trials for the polymerization reaction of BRCs. The table summarizes the results of the various Michael addition reactions. The results listed are the molecular weights of the various reactions products measured using either size exclusion chromatography (SEC) or matrix-assisted laser desorption/ionization-time of flight (MALDI-TOF).

6.2.2.3. Conjugation of dimethylaminoethanoic acid to polymerized peptide sequence

To introduce tertiary amines on the polymer backbone, dimethylaminoethanoic acid was conjugated selectively along the polymer backbone to produce the final BRCs. Initially, the Boc and trt protecting groups were removed from the polymer via 90 TFA in DCM for 45 minutes (Figure 6.9). Conjugation of dimethylaminoethanoic acid with the polymer backbone took place using the water-soluble coupling agent 1-Ethyl-3-(3-dimethylaminopropyl)-carbodiimide (EDC). To the dissolved polymer, 20 molar excess of EDC and dimethylaminoethanoic were added to the reaction mixture, which was stirred in an oil bath at 40° C in the dark under a nitrogen atmosphere for 4 hours (Figure 6.10). Afterward, the reaction solution was transferred to separate dialysis bags (MWCO 2000) and dialyzed against deionized water for 2 days to purify the copolymer from the starting materials. The dialyzed polymers then were transferred to sterile conical tubes and dried on a lyophilizer for 2 days.

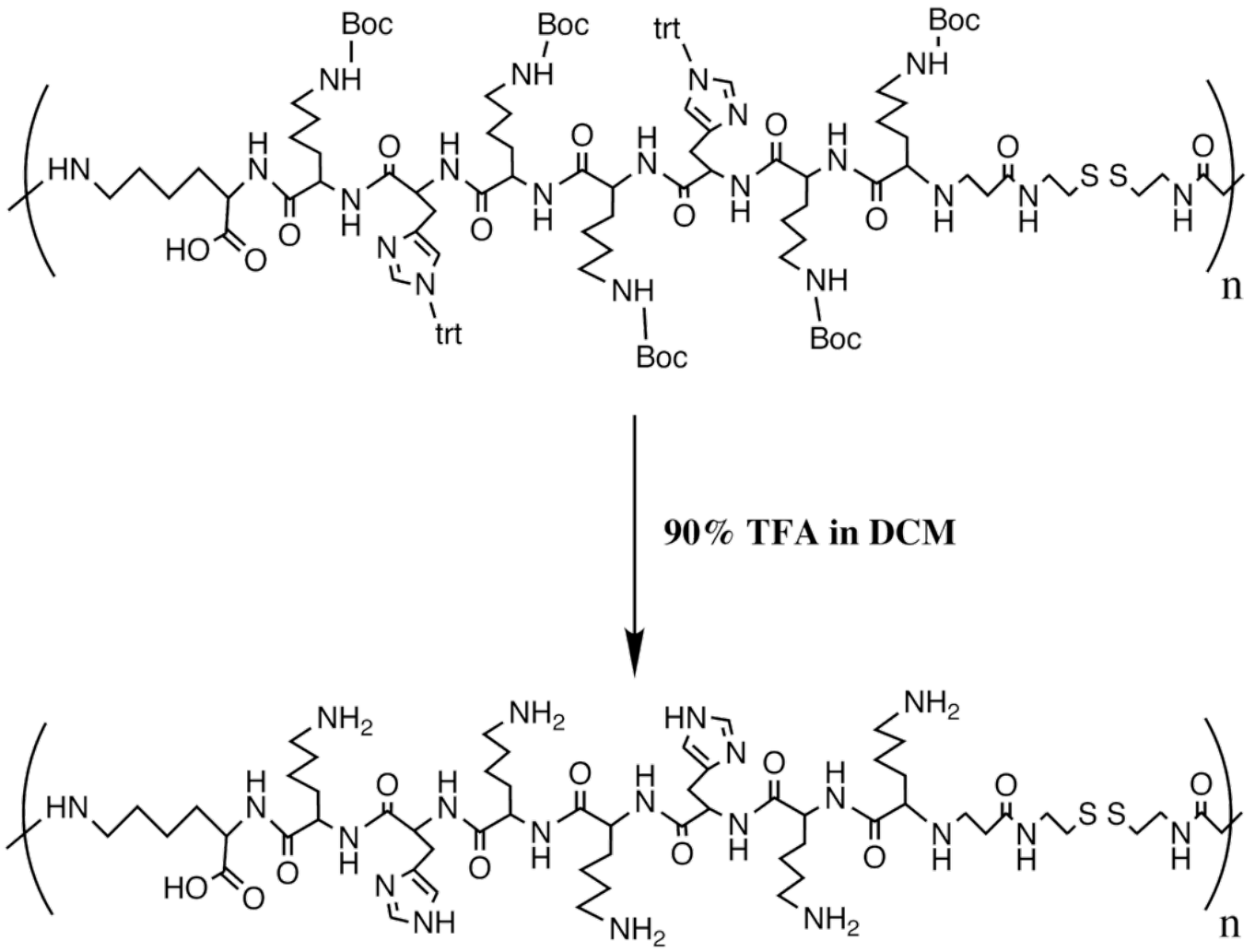

Figure 6.9: Boc and trt deprotection from the BRC backbone via 90 TFA in DCM for 45 minutes.

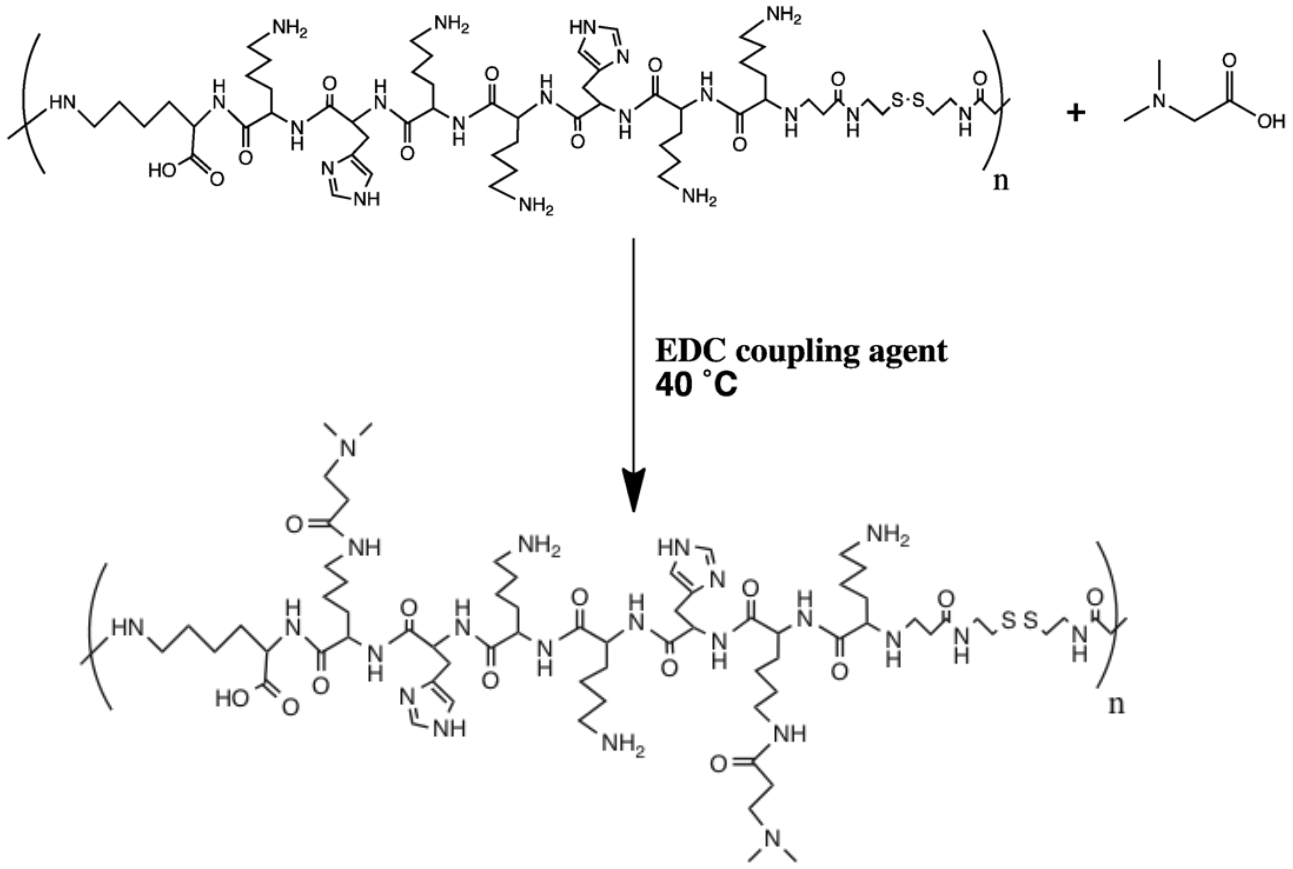

Figure 6.10: Conjugation of dimethylaminoethanoic acid with the BRC backbone.

6.2.3. Physicochemical characterization of the synthesized copolymers

6.2.3.1. Elucidation and confirmation of the copolymers chemical structures

6.2.3.1.1. Nuclear magnetic resonance (^{1}H-NMR):

The copolymers and all intermediates were analyzed by ^{1}H-NMR (300 MHz, D_2O).

6.2.3.1.2. Infra-red spectroscopy (IR):

Fourier Transform-Infrared (FT- IR) spectra were obtained using a Mattson Galaxy Series 3000 FT-IR from Mattson Instruments Inc. (Madison, WI). A KBr pellet was prepared by grinding the solid sample with solid potassium bromide (KBr) and applying great pressure to the dry mixture.

6.2.3.2. Determination of the molecular weight of the copolymers

6.2.3.2.1. Size exclusion chromatography (SEC):

The copolymers were purified on a Shimatzu Prominence HPLC system (Shimadzu Scientific Instruments, MD) equipped with a Shodex SB-803-HQ (Particle size = 6 nm) and Shodex SB-806-HQ (particle size = 13 nm) columns in

series and detected with photodiode array (PDA) and low temperature evaporative light scattering detectors (ELSD-LTII) (Columbia, MD).

6.2.3.2.2. Matrix-assisted laser desorption/ionization (MALDI-TOF):

Matrix-assisted laser desorption ionization-time-of-flight (MALDI-TOF) data were obtained using a Voyager-DE STR Biospectrometry Workstation from Applied Biosystems (Foster City, CA). Saturated alpha-cyano-4-hydroxycinnamic acid dissolved in 50/50 acetonitrile/water with 0.1% TFA was used to make the matrix.

6.3. Results and discussion

The flowchart illustrated in Figure 6.11 summarizes the different steps and trials adopted to synthesize the biocompatible reducible copolymers (BRCs) either using KKHKKHKK or KHK peptide sequences as a backbone structure.

As indicated in figure 6.12, the electron spray ionization MALDI-TOF showed that the main moiety in the sample has a molecular weight of 2046 D_a (Shown in figure as 1023.852 D_a, as the compound was found to have two free electrons).

Automated peptide synthesis failed to produce any intact peptide sequence. Various trials have been made to use the automated peptide synthesis, but none of them yielded the desired peptide sequence. Based on this, the manual peptide synthesis was the method of choice and the desired peptide sequence was synthesized successfully. Moreover, manual peptide sequence provided the flexibility to check amino acid substitution in every additional step via ninhydrin assay and chloranil test.

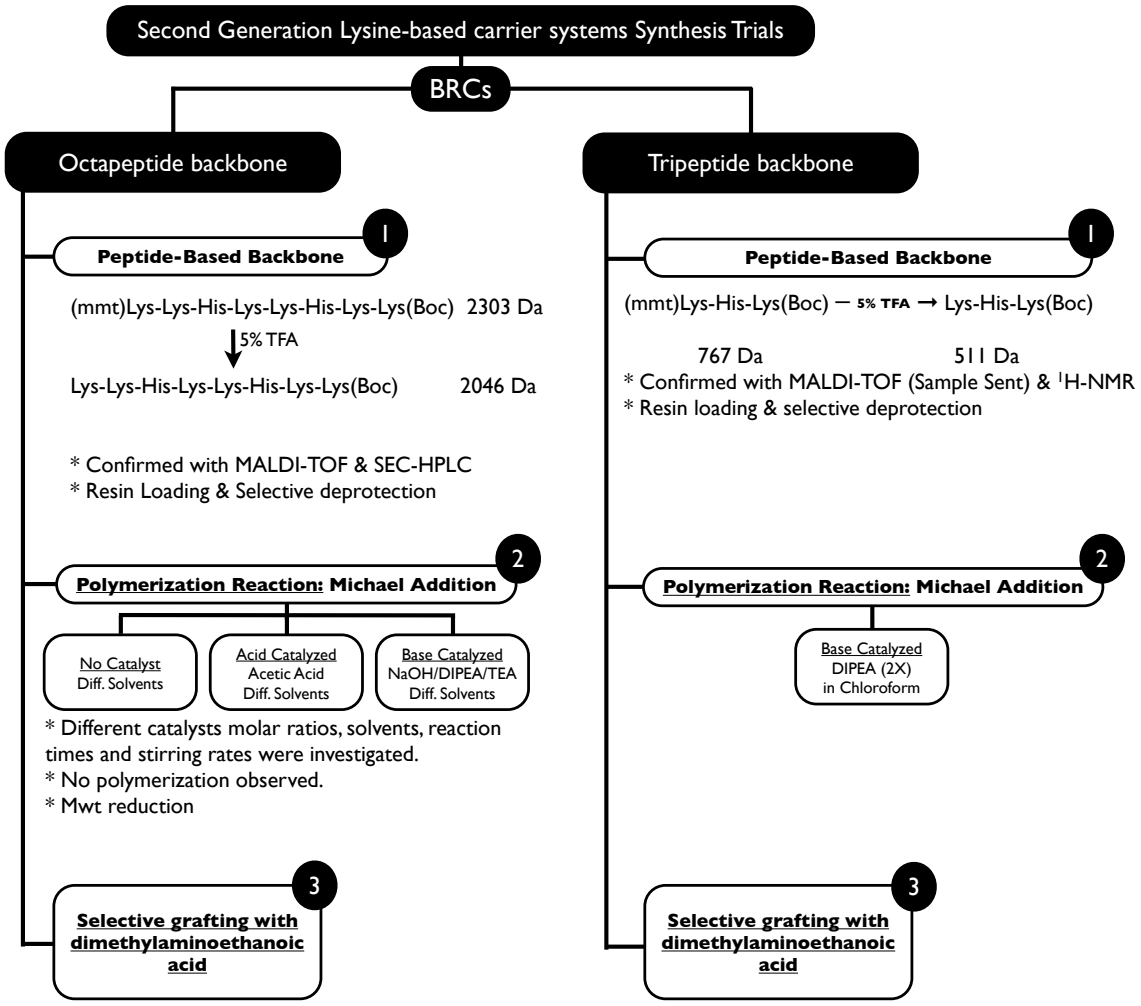

Figure 6.11: Flowchart summarizing the different steps and trials adopted to synthesize the biocompatible reducible copolymers (BRCs) either using KKHKKHKK or KHK peptide sequences as a backbone structure.

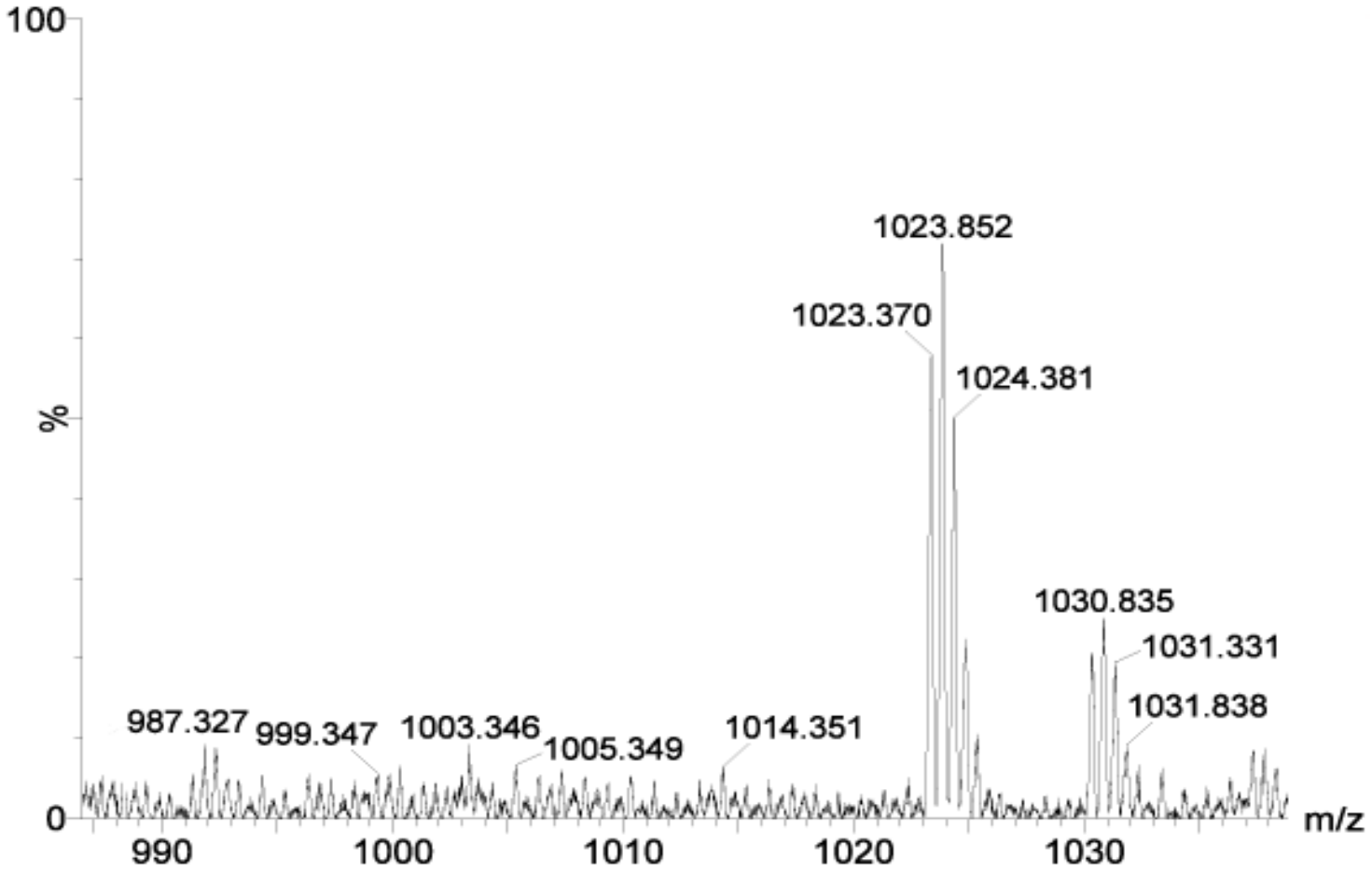

Figure 6.12: Electron spray ionization MALDI-TOF of KKHKKHKK peptide sequence.

After the successful synthesis of the KKHKKHKK peptide sequence, various Michael addition polymerization reactions and conditions were tried (Table 6.1). All of the reaction conditions failed to yield a polymerized product. Michael addition reactions were tried with acid and base catalysis. In other Michael addition reactions, no catalyst was used. Moreover, different solvents were used including methanol, water, DMSO and 90% methanol in water. Table 6.1 summarizes the results of the various Michael addition reactions. The results listed are the molecular weights of the various reactions products measured using either size exclusion chromatography (SEC) or matrix-assisted laser desorption/ionization-time of flight (MALDI-TOF). All of these reactions did not yield any reproducible increase in molecular weight as shown in table 6.1. It is worth mentioning that one of the Michael addition reactions using DIPEA as a catalyst and methanol as solvent yielded a significant increase in molecular weight. The MALDI-TOF molecular weight spectrum showed a 2566 D_a peak and a 4770 D_a peak. The 4770 D_a peak represented approximately 10% of the sample. These data could suggest a dimer formation. This reaction was repeated multiple times after the initial reaction and none of the subsequent reactions generated molecular a weight higher than 2000 D_a. Moreover, a pattern of decreased molecular weight was observed with most of the used reaction

conditions. This could indicate a stability problem in the synthesized peptide sequence (KKHKKHKK).

After the failed trials with the polymerization of the KKHKKHKK peptide sequence, KHK peptide sequence was synthesized successfully as confirmed with ^{1}H-NMR. A Michael addition reaction of KHK peptide synthesis was done using DIPEA as a basic catalyst in chloroform. The reaction product was precipitated in ether. The analysis of the addition reaction product is ongoing.

7. Conclusions and future directions

7.1. Summary of results and conclusions

In this thesis, we report the synthesis of novel reducible polymers based on the natural amino acid, L-lysine, as cationic polymers for non-viral gene delivery. We hypothesized that the use of natural amino acids can yield polymers that have very low cytotoxicity but high transfection efficiencies due to the presence of reducible disulfide bonds in the polymer backbone structure. To test our hypothesis, we have synthesized novel biodegradable polymers (reducible linear L-lysine-modified copolymers (LLC)) from lysine and cystamine bisacrylamide (CBA) via a Michael addition reaction. To sequester the hydroxyl functionality of the α-carboxylic groups of the lysine amino acids as well as to introduce primary amines for complete condensation of DNA, ethylenediamine was conjugated along the polymer backbone. The chemical structure of the polymers was characterized using ^{1}H-NMR, ninhydrin assay and IR spectroscopy. The molecular weight and the polydispersity of the synthesized copolymers were calculated using size exclusion chromatography (SEC) and matrix assisted laser desorption ionization time-of-flight (MALDI-TOF). The reducible LLC/pDNA nanoplexes were characterized through dynamic light scattering to measure the particle size and zetapotential and stability of the

polyplexes were determined with gel electrophoresis. The ability of the synthesize copolymers to protect pDNA was evaluated using a DNase I protection assay. The bioactivity of the copolymers was evaluated in HDFs cells (hamster dermal fibroblasts), MCF-7s cells (human breast adenocarcinoma cell line), 4T1s (metastatic mouse breast cancer cell line), hMSC (human mesenchymal stem cells) and other cell lines using a luciferase assay and fluorescence microscopy. The cytotoxicity of polymer/pDNA complexes was evaluated by a MTT and LDH cell viability assays in vitro in various cell lines. The transfection efficiencies of the polyplexes as determined with luciferase and ELISA assay showed that LLC polyplexes produced over 20 times higher transfection efficiencies and lower cytotoxicities in human mesenchymal stem cells (hMSCs) as compared to the optimal PLL control. Remarkably, release of DNA from the polyplexes was only possible after treatment with the reducing agent DTT, which simulated the intracellular reductive environment of the cell as illustrated in Figure 7.1. This would be highly desirable for *in vivo* administration since polyplex stability is greatly affected by blood components such as highly negatively charged albumin molecules. It was also demonstrated that these LLCs could deliver pDNA to the cytosol of cells and possibly to the nucleus. Thus, these PLL derivatives represent novel bioreducible copolymers with a unique backbone structure, in which we have demonstrated, as a proof of concept, that

these LLCs are efficient biodegradable and bioreducible copolymers. LLCs may be used as a promising reducible platform for nonviral gene therapy.

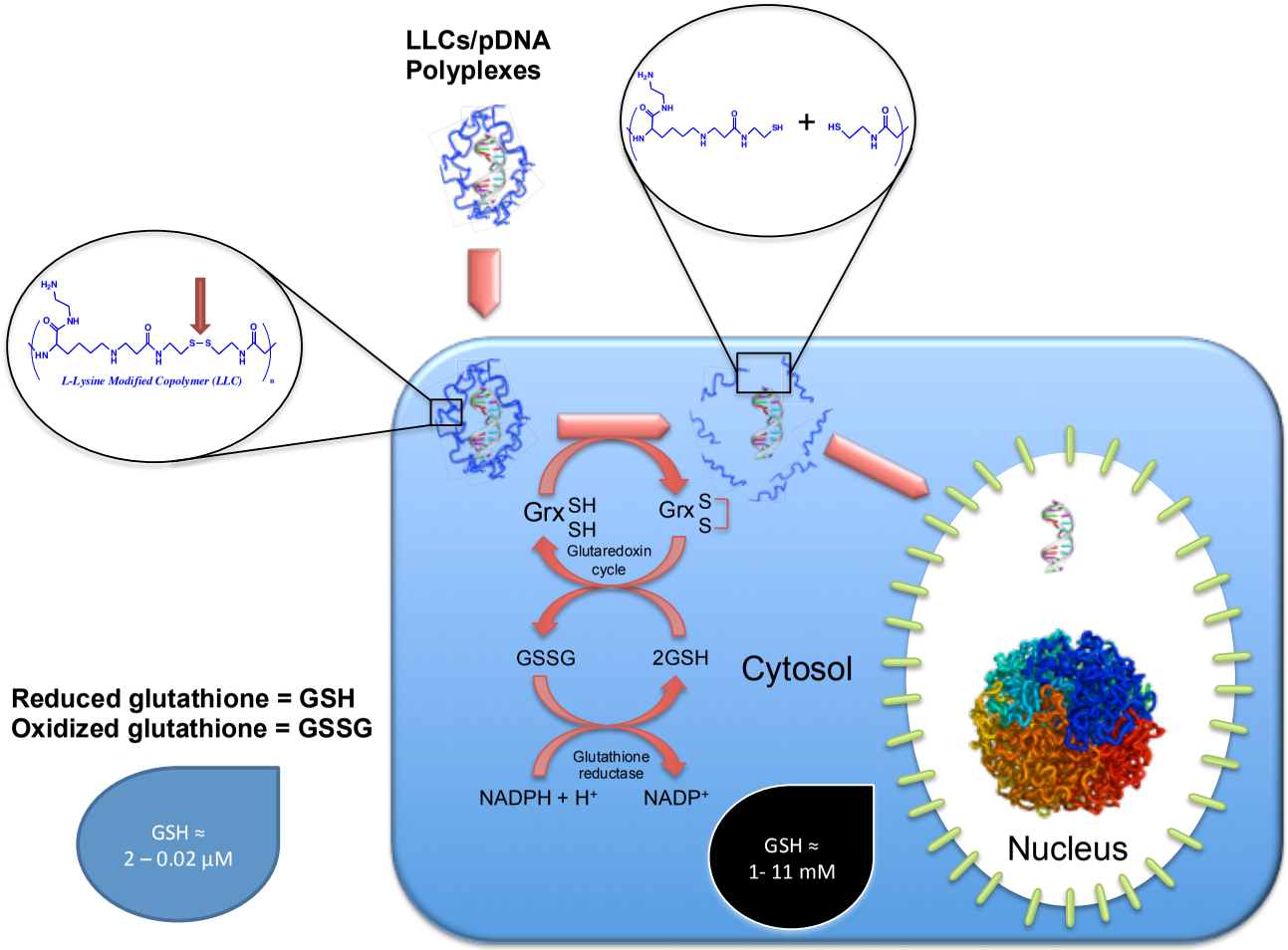

Figure 7.1: Schematic diagram of the DNA release inside the cytosol from the LLC (L-lysine modified copolymers)/pDNA polyplexes upon the reduction of the disulfide bonds within the polymer backbone.

After the in-vitro characterization of the linear lysine copolymers (LLCs) with respect to its stability, efficacy and safety, LLCs were tested for its *ex vivo* efficacy. In this *ex vivo* study, LLC was used to genetically modify human mesenchymal stem cells *in vitro* and these modified cells were injected into infarcted regions of the heart for the treatment of myocardial ischemia. Ischemic heart disease (IHD) or coronary artery disease (CAD) is a leading cause of death in the United States. Gene therapy is a promising alternative to conventional treatment strategies since the delivery of angiogenic cytokines such as vascular endothelial growth factor ($VEGF_{165}$) can stimulate angiogenesis in a process known as therapeutic angiogenesis as well as neovascularization. Moreover, advances in stem cell biology have challenged the belief that infarcted myocardium is un-repairable. Our preliminary data suggest that this novel therapeutic strategy might be effectively used to treat myocardial infarction. We have investigated the efficacy of our novel non-viral lysine based gene carrier system *ex vivo* to genetically modify human mysenchymal stem cells (hMSCs) for the treatment of myocardial infarction. The pluripotent ability of stem cells to differentiate into specialized cell lines began to garner intense interest within cardiology for the regeneration of infarcted regions of the heart. In this study, we have used gene therapy to generate genetically modified stem cells that are able to produce angiogenic cytokines to promote revascularization of an infarcted

region of the heart, which can reduce myocardial damage and scar formation. To transfect the cells, reducible novel linear L-lysine modified copolymers (LLCs) were used as an alternative to high molecular weight non-degradable poly(L-lysine) (PLL) for nonviral gene delivery. The hMSCs transfected with the LLC/$VEGF_{165}$ gene were then injected into the infarcted area of the heart of severe combined immunodeficient (SCID) mice. The myocardial infarction (MI) was created by permanent ligation of the left anterior descending artery (LAD). At time points (1, 2, or 4-weeks) following MI induction and cell injection, cardiac hemodynamic analysis was performed and then the mice were sacrificed for immunofluorescence analysis. Hemodynamic studies in a very limited number of animals provided some reason to suggest that hearts, injected with LLC/$VEGF_{165}$ transfected hMSCs, had positive effects on cardiac contractility that exceeded that produced by non-transfected stem cells. Moreover, immunofluorescence staining of tissue sections for differentiation of hMSCs into cardiomyocytes showed well defined tubular like structures that were stained positive for human cardiac troponin T (TnT). These data indicated potential differentiation of hMSCs into myocardial-like cells.

Incorporation of the VEGF gene within hMSC should be considered as one of the candidates for future molecular or genetic preconditioning in hMSC cell based therapy. In conclusion, the use of gene therapy to genetically modify stem

cells with $VEGF_{165}$ gene using the safe and efficient LLC copolymers is a promising and novel therapeutic strategy for the treatment of MI.

7.2. Future directions

Further work on the LLC copolymers includes optimization of the polymer backbone structure, incorporation of targeting moieties (e.g., folate, cholesterol, sulfonyl urea, and galactose), and transitioning of an effective and safe multifunction nonviral gene carrier formulation based on LLC copolymer from bench to bedside. Modifying the structure of the backbone of LLC copolymers to incorporate endosomal escaping moieties, cell-penetrating moieties (cationic arginines) as well as targeting moieties for further improvements in gene expression, which could potentially enhance gene expression of second generation LLC/pDNA polyplexes.

7.2.1. Active Targeting and formulation of a multifunctional LLC/pDNA Complexes

Active targeting and functionalizing of polymers and lipids both for gene delivery and drug delivery has long been studied. Recently, there is a growing interest in the nonviral gene delivery field to develop gene carrier systems that are 200 nm or less in size. Moreover, these systems should be modified with

multifunctional components, which enable the systems to facilitate targeting, cellular uptake, intracellular trafficking, endosomal escape and nuclear uptake. Our novel LLC-based gene carrier system can be modified to develop a multifunctional system with increased targeting ability, ability to evade the immune system, limited cytotoxicity and increased transfection efficiency. Such multifunctional carrier systems hold the promise of overcoming many traditional hurdles to successful nonviral gene delivery including sub-optimal targeting, lack of efficacy and unwanted side effects. Multifunctional components could include targeting ligands such as sugar moieties (such as galactose, lactose and mannitol) (Biessen, Beuting et al. 1995; Cook, Park et al. 2005; Midoux, Mendes et al. 1993; Sun, Hai et al. 2005) and asialofetuin (for targeting the asialoglycoprotein receptors) (Diez, Navarro et al. 2009; Kao, Change et al. 1996; Li, Wen et al. 1999; Martinez-Fong, Mullersman et al. 1994; Watanabe, Liu et al. 2000) for liver targeting. Moreover, cholesterol and low density lipoproteins could be used to target breast carcinoma (Antalis, Arnold et al. 2010). Folic acid is another important targeting ligand for cancer cells (Benns and Kim 2000; Cho, Kim et al. 2005; D'Angelica, Ammori et al. 2011; Morris and Sharma 2011; Turk, Reddy et al. 2002). Other functional components that can be used in designing multifunctional gene carrier systems include pH-sensitive fusogenic peptides, cell penetrating peptides and protein transduction domain peptides. Besides targeting

of the nonviral gene carrier itself, further optimization of the formulation and the genetic material should be taken into consideration. Typical routes for increased genetic material transfection using molecular biology tools and techniques include enhancer modifications (e.g., SV_{40} promoter), transcriptional regulators, tissue-specific promoters and nuclear localization signals (NLS).

7.2.2. LLC copolymers backbone modifications

One of the main future directions is the modification of the LLC copolymers backbone structure to develop biocompatible PLL derivatives capable of efficient endocytic release and subcellular trafficking. Maintaining the same linear low molecular weight bioreducible backbone structure while incorporating histidine and arginine amino acids to the polymer backbone could be beneficial in enhancing the transfection efficiency and limiting the cytotoxicity of the gene carrier system. Our rationale is that the combination of a reducible disulfide backbone structure, a cell penetrating moiety (arginine) and an endosomal release moiety (histidine) will facilitate efficient delivery of nucleic acid cargo into the cytoplasm and significantly increase the transfection efficiency with negligible cytotoxicity.

Arginine along with lysine are main components in Cell-penetrating peptides (CPP)s, which are known to enhance the delivery of various molecules

to the cell (Brooks, Lebleu et al. 2005; Zhao and Weissleder 2004). Moreover, arginine-rich peptides were reported to have great cell-penetrating ability (Tung and Weissleder 2003). Furthermore, arginine posses a combination of primary and secondary amines with different pKa values. Such combination of primary and secondary amines increases arginine positive charge density allowing it to better electrostatically bind the negatively charged DNA.

On the other hand, the amino acid histidine has been used in nonviral gene delivery carriers due to its fusogenic activity. Such fusogenic activity disrupts the envelope membrane of acidic subcellular compartments such as endosomes and lysosomes. Histidines are uncharged at physiological pH and positively charged in acidic environment, which imparts selective membrane disruption in the acidic endosome. The imidazole group of histidine has a pKa of ~6.0, therefore allowing it to become protonated in the acidic environment of the endosome, an induce of a strong buffering capacity within the cells (Kichler, Leborgne et al. 2003; Midoux, Kichler et al. 1998; Midoux, LeCam et al. 2002; Midoux and Monsigny 1999; Pichon, Goncalves et al. 2001). In addition, histidine has been shown to fuse with lipid bilayers upon protonation of imidazole groups as a result of interaction with negatively charged membrane phospholipids (Wang and Huang 1984).

Therefore, combining the unique properties of bioreducible polymers with the advantages of arginine and histidine residues, we expect that the arginine and histidine derivative of bioreducible LLC would show high transfection efficiency, while maintaining its low cytotoxicity.

7.2.3. Mechanistic study of the intra-cellular Trafficking of LLC/pDNA polyplexes

A comprehensive mechanistic study of complex formation and trafficking would be beneficial to understand mysterious areas of gene delivery. Moreover, improved understanding of the intracellular trafficking of synthetic delivery vehicles may help guide the rational design of nonviral vectors used for gene delivery. The trafficking of the gene carrier system across the cytoplasm to the nucleus has been shown to be a main hurdle in nonviral gene delivery. It would be significant to investigate the intracellular transport and pDNA release mechanisms of LLC/pDNA polyplexes within the cells. High-resolution fluorescence techniques (Kulkarni, Wu et al. 2005) and multiple particle tracking (Dawson, Krauland et al. 2004; Dawson, Wirtz et al. 2003; Lai and Hanes 2008; Suh, Dawson et al. 2005; Suh, Wirtz et al. 2003; Suh, Wirtz et al. 2004) could be used to investigate the intracellular trafficking of nonviral gene delivery carrier systems. The working hypothesis is that LLCs would facilitate the unpacking of

the LLC/pDNA polyplexes and increase DNA release into the cytoplasm to provide efficient intracellular delivery, and hence high transfection efficiency.

References

Abdallah, B., A. Hassan, C. Benoist, D. Goula, J. P. Behr and B. A. Demeneix (1996). "A powerful nonviral vector for in vivo gene transfer into the adult mammalian brain: polyethylenimine." Hum Gene Ther **7**(16): 1947-1954.

Abuchowski, A., J. R. McCoy, N. C. Palczuk, T. van Es and F. F. Davis (1977). "Effect of covalent attachment of polyethylene glycol on immunogenicity and circulating life of bovine liver catalase." J Biol Chem **252**(11): 3582-3586.

Ahn, C. H., S. Y. Chae, Y. H. Bae and S. W. Kim (2004). "Synthesis of biodegradable multi-block copolymers of poly(L-lysine) and poly(ethylene glycol) as a non-viral gene carrier." J Control Release **97**(3): 567-574.

Akinc, A., M. Thomas, A. M. Klibanov and R. Langer (2005). "Exploring polyethylenimine-mediated DNA transfection and the proton sponge hypothesis." J Gene Med **7**(5): 657-663.

Antalis, C. J., T. Arnold, T. Rasool, B. Lee, K. K. Buhman and R. A. Siddiqui (2010). "High ACAT1 expression in estrogen receptor negative basal-like breast cancer cells is associated with LDL-induced proliferation." Breast Cancer Res Treat **122**(3): 661-670.

Aronsohn, A. I. and J. A. Hughes (1998). "Nuclear localization signal peptides enhance cationic liposome-mediated gene therapy." J Drug Target **5**(3): 163-169.

Arote, R., T. H. Kim, Y. K. Kim, S. K. Hwang, H. L. Jiang, H. H. Song, J. W. Nah, M. H. Cho and C. S. Cho (2007). "A biodegradable poly(ester amine) based on polycaprolactone and polyethylenimine as a gene carrier." Biomaterials **28**(4): 735-744.

Arote, R. B., S. K. Hwang, M. K. Yoo, D. Jere, H. L. Jiang, Y. K. Kim, Y. J. Choi, J. W. Nah, M. H. Cho and C. S. Cho (2008). "Biodegradable poly(ester amine) based on glycerol dimethacrylate and polyethylenimine as a gene carrier." J Gene Med **10**(11): 1223-1235.

Ashcroft, R. E. (2004). "Gene therapy in the clinic: whose risks?" Trends Biotechnol **22**(11): 560-563.

Ates, B., B. C. Ercal, K. Manda, L. Abraham and N. Ercal (2009). "Determination of glutathione disulfide levels in biological samples using thiol–disulfide exchanging agent, dithiothreitol." Biomedical Chromatography **23**(2): 119-123.

Benns, J. M., J. S. Choi, R. I. Mahato, J. S. Park and S. W. Kim (2000). "pH-sensitive cationic polymer gene delivery vehicle: N-Ac-poly(L-histidine)-graft-poly(L-lysine) comb shaped polymer." Bioconjug Chem **11**(5): 637-645.

Benns, J. M. and S. W. Kim (2000). "Tailoring new gene delivery designs for specific targets." J Drug Target **8**(1): 1-12.

Bhadra, D., S. Bhadra, P. Jain and N. K. Jain (2002). "Pegnology: a review of PEG-ylated systems." Pharmazie **57**(1): 5-29.

Biessen, E. A., D. M. Beuting, H. C. Roelen, G. A. van de Marel, J. H. van Boom and T. J. van Berkel (1995). "Synthesis of cluster galactosides with high affinity for the hepatic asialoglycoprotein receptor." J Med Chem **38**(9): 1538-1546.

Bikram, M., M. Lee, C. W. Chang, M. M. Janat-Amsbury, S. E. Kern and S. W. Kim (2005). "Long-circulating DNA-complexed biodegradable multiblock copolymers for gene delivery: degradation profiles and evidence of dysopsonization." J Control Release **103**(1): 221-233.

Blacklock, J., Y. Z. You, Q. H. Zhou, G. Mao and D. Oupicky (2009). "Gene delivery in vitro and in vivo from bioreducible multilayered polyelectrolyte films of plasmid DNA." Biomaterials **30**(5): 939-950.

Boeckle, S., J. Fahrmeir, W. Roedl, M. Ogris and E. Wagner (2006). "Melittin analogs with high lytic activity at endosomal pH enhance transfection with purified targeted PEI polyplexes." J Control Release **112**(2): 240-248.

Bonaros, N., O. Bernecker, H. Ott, B. Schlechta and A. A. Kocher (2005). "Cell- and gene therapy for ischemic heart disease." Minerva Cardioangiol **53**(4): 265-273.

Bonfoco, E., D. Krainc, M. Ankarcrona, P. Nicotera and S. A. Lipton (1995). "Apoptosis and necrosis: two distinct events induced, respectively, by mild and intense insults with N-methyl-D-aspartate or nitric oxide/superoxide in cortical cell cultures." Proc Natl Acad Sci U S A **92**(16): 7162-7166.

Bos, G. W., D. J. Crommelin and W. E. Hennink (2001). "Water-soluble cationic methacrylate polymers for nonviral gene delivery." Methods Mol Med **65**: 35-60.

Boussif, O., F. Lezoualc'h, M. A. Zanta, M. D. Mergny, D. Scherman, B. Demeneix and J. P. Behr (1995). "A versatile vector for gene and oligonucleotide transfer into cells in culture and in vivo: polyethylenimine." Proc Natl Acad Sci U S A **92**(16): 7297-7301.

Breunig, M., C. Hozsa, U. Lungwitz, K. Watanabe, I. Umeda, H. Kato and A. Goepferich (2008). "Mechanistic investigation of poly(ethylene imine)-based siRNA delivery: Disulfide bonds boost intracellular release of the cargo." J Control Release.

Brignier, A. C. and A. M. Gewirtz (2010). "Embryonic and adult stem cell therapy." J Allergy Clin Immunol **125**(2 Suppl 2): S336-344.

Brooks, H., B. Lebleu and E. Vives (2005). "Tat peptide-mediated cellular delivery: back to basics." Adv Drug Deliv Rev **57**(4): 559-577.

Brunot, C., L. Ponsonnet, C. Lagneau, P. Farge, C. Picart and B. Grosgogeat (2007). "Cytotoxicity of polyethyleneimine (PEI), precursor base layer of polyelectrolyte multilayer films." Biomaterials **28**(4): 632-640.

Byk, G., C. Dubertret, V. Escriou, M. Frederic, G. Jaslin, R. Rangara, B. Pitard, J. Crouzet, P. Wils, B. Schwartz and D. Scherman (1998). "Synthesis, activity, and

structure--activity relationship studies of novel cationic lipids for DNA transfer." J Med Chem **41**(2): 229-235.

Byun, K. H. and S. W. Kim (2009). "Is stem cell-based therapy going on or out for cardiac disease?" Korean Circ J **39**(3): 87-92.

Caliceti, P. and F. M. Veronese (2003). "Pharmacokinetic and biodistribution properties of poly(ethylene glycol)-protein conjugates." Adv Drug Deliv Rev **55**(10): 1261-1277.

Carlisle, R. C., T. Etrych, S. S. Briggs, J. A. Preece, K. Ulbrich and L. W. Seymour (2004). "Polymer-coated polyethylenimine/DNA complexes designed for triggered activation by intracellular reduction." J Gene Med **6**(3): 337-344.

Chaudhari, K. R., M. Ukawala, A. S. Manjappa, A. Kumar, P. K. Mundada, A. K. Mishra, R. Mathur, J. Monkkonen and R. S. Murthy (2011). "Opsonization, Biodistribution, Cellular Uptake and Apoptosis Study of PEGylated PBCA Nanoparticle as Potential Drug Delivery Carrier." Pharm Res.

Cheng, M., Q. Li, T. Wan, X. Hong, H. Chen, B. He, Z. Cheng, H. Xu, T. Ye, B. Zha, J. Wu and R. Zhou (2011). "Synthesis and efficient hepatocyte targeting of galactosylated chitosan as a gene carrier in vitro and in vivo." J Biomed Mater Res B Appl Biomater **99**(1): 70-80.

Cho, K. C., S. H. Kim, J. H. Jeong and T. G. Park (2005). "Folate receptor-mediated gene delivery using folate-poly(ethylene glycol)-poly(L-lysine) conjugate." Macromol Biosci **5**(6): 512-519.

Choi, Y. H., F. Liu, J. S. Choi, S. W. Kim and J. S. Park (1999). "Characterization of a targeted gene carrier, lactose-polyethylene glycol-grafted poly-L-lysine and its complex with plasmid DNA." Hum Gene Ther **10**(16): 2657-2665.

Choi, Y. H., F. Liu, J. S. Kim, Y. K. Choi, J. S. Park and S. W. Kim (1998). "Polyethylene glycol-grafted poly-L-lysine as polymeric gene carrier." J Control Release **54**(1): 39-48.

Choi, Y. H., F. Liu, J. S. Park and S. W. Kim (1998). "Lactose-poly(ethylene glycol)-grafted poly-L-lysine as hepatoma cell-tapgeted gene carrier." Bioconjug Chem **9**(6): 708-718.

Choi, Y. J., S. J. Kang, Y. J. Kim, Y. B. Lim and H. W. Chung (2010). "Comparative studies on the genotoxicity and cytotoxicity of polymeric gene carriers polyethylenimine (PEI) and polyamidoamine (PAMAM) dendrimer in Jurkat T-cells." Drug Chem Toxicol **33**(4): 357-366.

Chollet, P., M. C. Favrot, A. Hurbin and J. L. Coll (2002). "Side-effects of a systemic injection of linear polyethylenimine-DNA complexes." J Gene Med **4**(1): 84-91.

Christensen, L. V., C. W. Chang, J. W. Yockman, R. Conners, H. Jackson, Z. Zhong, J. Feijen, D. A. Bull and S. W. Kim (2007). "Reducible poly(amido ethylenediamine) for hypoxia-inducible VEGF delivery." J Control Release **118**(2): 254-261.

Clements, B. A., V. Incani, C. Kucharski, A. Lavasanifar, B. Ritchie and H. Uludag (2007). "A comparative evaluation of poly-L-lysine-palmitic acid and Lipofectamine 2000 for plasmid delivery to bone marrow stromal cells." Biomaterials **28**(31): 4693-4704.

Cohn, J. N., R. Ferrari and N. Sharpe (2000). "Cardiac remodeling--concepts and clinical implications: a consensus paper from an international forum on cardiac remodeling. Behalf of an International Forum on Cardiac Remodeling." J Am Coll Cardiol **35**(3): 569-582.

Conese, M., F. Ascenzioni, A. C. Boyd, C. Coutelle, I. De Fino, S. De Smedt, J. Rejman, J. Rosenecker, D. Schindelhauer and B. J. Scholte (2011). "Gene and cell therapy for cystic fibrosis: from bench to bedside." J Cyst Fibros **10 Suppl 2**: S114-128.

Cook, S. E., I. K. Park, E. M. Kim, H. J. Jeong, T. G. Park, Y. J. Choi, T. Akaike and C. S. Cho (2005). "Galactosylated polyethylenimine-graft-poly(vinyl pyrrolidone) as a hepatocyte-targeting gene carrier." J Control Release **105**(1-2): 151-163.

Crane, L. M., H. J. Arts, M. van Oosten, P. S. Low, A. G. van der Zee, G. M. van Dam and J. Bart (2011). "The effect of chemotherapy on expression of folate receptor-alpha in ovarian cancer." Cell Oncol (Dordr).

D'Angelica, M., J. Ammori, M. Gonen, D. S. Klimstra, P. S. Low, L. Murphy, M. R. Weiser, P. B. Paty, Y. Fong, R. P. Dematteo, P. Allen, W. R. Jarnagin and J. Shia (2011). "Folate receptor-alpha expression in resectable hepatic colorectal cancer metastases: patterns and significance." Mod Pathol **24**(9): 1221-1228.

Dalby, B., S. Cates, A. Harris, E. C. Ohki, M. L. Tilkins, P. J. Price and V. C. Ciccarone (2004). "Advanced transfection with Lipofectamine 2000 reagent: primary neurons, siRNA, and high-throughput applications." Methods **33**(2): 95-103.

Dawson, M., E. Krauland, D. Wirtz and J. Hanes (2004). "Transport of polymeric nanoparticle gene carriers in gastric mucus." Biotechnol Prog **20**(3): 851-857.

Dawson, M., D. Wirtz and J. Hanes (2003). "Enhanced viscoelasticity of human cystic fibrotic sputum correlates with increasing microheterogeneity in particle transport." J Biol Chem **278**(50): 50393-50401.

De Smedt, S. C., J. Demeester and W. E. Hennink (2000). "Cationic polymer based gene delivery systems." Pharm Res **17**(2): 113-126.

Debyser, Z. (2003). "Biosafety of lentiviral vectors." Curr Gene Ther **3**(6): 517-525.

Dekie, L., V. Toncheva, P. Dubruel, E. H. Schacht, L. Barrett and L. W. Seymour (2000). "Poly-L-glutamic acid derivatives as vectors for gene therapy." J Control Release **65**(1-2): 187-202.

Demeneix, B., J. Behr, O. Boussif, M. A. Zanta, B. Abdallah and J. Remy (1998). "Gene transfer with lipospermines and polyethylenimines." Adv Drug Deliv Rev **30**(1-3): 85-95.

Diebold, S. S., M. Kursa, E. Wagner, M. Cotten and M. Zenke (1999). "Mannose polyethylenimine conjugates for targeted DNA delivery into dendritic cells." J Biol Chem **274**(27): 19087-19094.

Diebold, S. S., H. Lehrmann, M. Kursa, E. Wagner, M. Cotten and M. Zenke (1999). "Efficient gene delivery into human dendritic cells by adenovirus polyethylenimine and mannose polyethylenimine transfection." Hum Gene Ther **10**(5): 775-786.

Diez, S., G. Navarro and I. C. T. de (2009). "In vivo targeted gene delivery by cationic nanoparticles for treatment of hepatocellular carcinoma." J Gene Med **11**(1): 38-45.

Dixon, K. H., T. Mulligan, K. N. Chung, P. C. Elwood and K. H. Cowan (1992). "Effects of folate receptor expression following stable transfection into wild type and methotrexate transport-deficient ZR-75-1 human breast cancer cells." J Biol Chem **267**(33): 24140-24147.

Dodds, E., M. G. Dunckley, K. Naujoks, U. Michaelis and G. Dickson (1998). "Lipofection of cultured mouse muscle cells: a direct comparison of Lipofectamine and DOSPER." Gene Ther **5**(4): 542-551.

Dominska, M. and D. M. Dykxhoorn (2010). "Breaking down the barriers: siRNA delivery and endosome escape." J Cell Sci **123**(Pt 8): 1183-1189.

Duan, D. (2011). "Duchenne muscular dystrophy gene therapy: Lost in translation?" Res Rep Biol **2011**(2): 31-42.

Dubruel, P., L. Dekie, B. Christiaens, B. Vanloo, M. Rosseneu, J. Van De Kerckhove, M. Mannisto, A. Urtti and E. Schacht (2003). "Poly-l-glutamic acid derivatives as multifunctional vectors for gene delivery. Part B. Biological evaluation." Biomacromolecules **4**(5): 1177-1183.

Egilmez, N. K., R. Cuenca, S. J. Yokota, F. Sorgi and R. B. Bankert (1996). "In vivo cytokine gene therapy of human tumor xenografts in SCID mice by liposome-mediated DNA delivery." Gene Ther **3**(7): 607-614.

El-Aneed, A. (2004). "An overview of current delivery systems in cancer gene therapy." J Control Release **94**(1): 1-14.

Eliyahu, H., Y. Barenholz and A. J. Domb (2005). "Polymers for DNA delivery." Molecules **10**(1): 34-64.

Engel, B. C., D. B. Kohn and G. M. Podsakoff (2003). "Update on gene therapy of inherited immune deficiencies." Curr Opin Mol Ther **5**(5): 503-507.

Erbacher, P., S. Zou, T. Bettinger, A. M. Steffan and J. S. Remy (1998). "Chitosan-based vector/DNA complexes for gene delivery: biophysical characteristics and transfection ability." Pharm Res **15**(9): 1332-1339.

Felgner, P. L., T. R. Gadek, M. Holm, R. Roman, H. W. Chan, M. Wenz, J. P. Northrop, G. M. Ringold and M. Danielsen (1987). "Lipofection: a highly efficient, lipid-mediated DNA-transfection procedure." Proc Natl Acad Sci U S A **84**(21): 7413-7417.

Fisher, K. J. and J. M. Wilson (1994). "Biochemical and functional analysis of an adenovirus-based ligand complex for gene transfer." Biochem J **299 (Pt 1)**: 49-58.

Flynn, A. and T. O'Brien (2011). "Stem cell therapy for cardiac disease." Expert Opin Biol Ther **11**(2): 177-187.

Gao, S., J. Chen, X. Xu, Z. Ding, Y. H. Yang, Z. Hua and J. Zhang (2003). "Galactosylated low molecular weight chitosan as DNA carrier for hepatocyte-targeting." Int J Pharm **255**(1-2): 57-68.

Gao, X. and L. Huang (1991). "A novel cationic liposome reagent for efficient transfection of mammalian cells." Biochem Biophys Res Commun **179**(1): 280-285.

Gao, X., K.-S. Kim and D. Liu (2007). "Nonviral gene delivery: what we know and what is next." AAPS J **9**(1): E92-104.

Gerweck, L. E. and K. Seetharaman (1996). "Cellular pH gradient in tumor versus normal tissue: potential exploitation for the treatment of cancer." Cancer Res **56**(6): 1194-1198.

Getz, E. B., M. Xiao, T. Chakrabarty, R. Cooke and P. R. Selvin (1999). "A Comparison between the Sulfhydryl Reductants Tris(2-carboxyethyl)phosphine and Dithiothreitol for Use in Protein Biochemistry." Analytical Biochemistry **273**(1): 73-80.

Giordano, C., F. Causa and G. Candiani (2006). "Gene therapy: The state of the art and future directions." J Appl Biomater Biomech **4**(2): 73-79.

Godbey, W. T., K. K. Wu and A. G. Mikos (1999). "Tracking the intracellular path of poly(ethylenimine)/DNA complexes for gene delivery." Proc Natl Acad Sci U S A **96**(9): 5177-5181.

Gonzalez, H., S. J. Hwang and M. E. Davis (1999). "New class of polymers for the delivery of macromolecular therapeutics." Bioconjug Chem **10**(6): 1068-1074.

Gosselin, M. A., W. Guo and R. J. Lee (2001). "Efficient gene transfer using reversibly cross-linked low molecular weight polyethylenimine." Bioconjug Chem **12**(6): 989-994.

Green, J. J., B. Y. Zhou, M. M. Mitalipova, C. Beard, R. Langer, R. Jaenisch and D. G. Anderson (2008). "Nanoparticles for gene transfer to human embryonic stem cell colonies." Nano Lett **8**(10): 3126-3130.

Greenberg, F., V. Guzzetta, R. Montes de Oca-Luna, R. E. Magenis, A. C. Smith, S. F. Richter, I. Kondo, W. B. Dobyns, P. I. Patel and J. R. Lupski (1991). "Molecular analysis of the Smith-Magenis syndrome: a possible contiguous-gene syndrome associated with del(17)(p11.2)." Am J Hum Genet **49**(6): 1207-1218.

Griesenbach, U. and E. W. Alton (2011). "Current status and future directions of gene and cell therapy for cystic fibrosis." BioDrugs **25**(2): 77-88.

Guo, X. and L. Huang (2011). "Recent Advances in Nonviral Vectors for Gene Delivery." Acc Chem Res.

Guping, Y., T. Guping and Yanjie (2005). "A new biodegradable poly-amino acid: alpha,beta-poly[(N-hydroxypropyl/aminoethyl)-DL-aspartamide-co-L-lysine], a potential nonviral vector for gene delivery." Drug Deliv **12**(2): 89-96.

Hafez, I. M., N. Maurer and P. R. Cullis (2001). "On the mechanism whereby cationic lipids promote intracellular delivery of polynucleic acids." Gene Ther **8**(15): 1188-1196.

Han, J., M. Lim and Y. I. Yeom (1999). "Receptor-mediated gene transfer to cells of hepatic origin by galactosylated albumin-polylysine complexes." Biol Pharm Bull **22**(8): 836-840.

Hashida, M., S. Takemura, M. Nishikawa and Y. Takakura (1998). "Targeted delivery of plasmid DNA complexed with galactosylated poly(L-lysine)." J Control Release **53**(1-3): 301-310.

Haslam, G., D. Wyatt and P. A. Kitos (2000). "Estimating the number of viable animal cells in multi-well cultures based on their lactate dehydrogenase activities." Cytotechnology **32**(1): 63-75.

He, W., Z. Guo, Y. Wen, Q. Wang, B. Xie and S. Zhu (2011). "Alginate-Graft-PEI as a Gene Delivery Vector with High Efficiency and Low Cytotoxicity." J Biomater Sci Polym Ed.

Heidenreich, P. A., J. G. Trogdon, O. A. Khavjou, J. Butler, K. Dracup, M. D. Ezekowitz, E. A. Finkelstein, Y. Hong, S. C. Johnston, A. Khera, D. M. Lloyd-Jones, S. A. Nelson, G. Nichol, D. Orenstein, P. W. Wilson, Y. J. Woo, C. American Heart Association Advocacy Coordinating, C. Stroke, R. Council on Cardiovascular, Intervention, C. Council on Clinical, E. Council on, Prevention, A. Council on, Thrombosis, B. Vascular, C. Council on, C. Critical, Perioperative, Resuscitation, N. Council on Cardiovascular, D. Council on the Kidney in Cardiovascular, S. Council on Cardiovascular, Anesthesia, C. Interdisciplinary Council on Quality of and R. Outcomes (2011). "Forecasting the future of cardiovascular disease in the United States: a policy statement from the American Heart Association." Circulation **123**(8): 933-944.

Hida, K., S. K. Lai, J. S. Suk, S. Y. Won, M. P. Boyle and J. Hanes (2011). "Common gene therapy viral vectors do not efficiently penetrate sputum from cystic fibrosis patients." PLoS One **6**(5): e19919.

Hong, S., P. R. Leroueil, E. K. Janus, J. L. Peters, M. M. Kober, M. T. Islam, B. G. Orr, J. R. Baker, Jr. and M. M. Banaszak Holl (2006). "Interaction of polycationic polymers with supported lipid bilayers and cells: nanoscale hole formation and enhanced membrane permeability." Bioconjug Chem **17**(3): 728-734.

Hong, Y. J., G. S. Mintz, S. W. Kim, L. Lu, A. B. Bui, A. D. Pichard, L. F. Satler, R. Waksman, K. M. Kent, W. O. Suddath and N. J. Weissman (2007). "Impact of remodeling on cardiac events in patients with angiographically mild left main coronary artery disease." J Invasive Cardiol **19**(12): 500-505.

Honold, J., B. Assmus, R. Lehman, A. M. Zeiher and S. Dimmeler (2004). "Stem cell therapy of cardiac disease: an update." Nephrol Dial Transplant **19**(7): 1673-1677.

Hoon Jeong, J., L. V. Christensen, J. W. Yockman, Z. Zhong, J. F. Engbersen, W. Jong Kim, J. Feijen and S. Wan Kim (2007). "Reducible poly(amido ethylenimine) directed to enhance RNA interference." Biomaterials **28**(10): 1912-1917.

Howard, K. A., X. W. Li, S. Somavarapu, J. Singh, N. Green, K. N. Atuah, Y. Ozsoy, L. W. Seymour and H. O. Alpar (2004). "Formulation of a microparticle

carrier for oral polyplex-based DNA vaccines." Biochim Biophys Acta **1674**(2): 149-157.

Hsu, W. L., H. L. Chen, W. Liou, H. K. Lin and W. L. Liu (2005). "Mesomorphic complexes of DNA with the mixtures of a cationic surfactant and a neutral lipid." Langmuir **21**(21): 9426-9431.

Hung, W. C., M. D. Shau, H. C. Kao, M. F. Shih and J. Y. Cherng (2009). "The synthesis of cationic polyurethanes to study the effect of amines and structures on their DNA transfection potential." J Control Release **133**(1): 68-76.

Hunter, A. C. (2006). "Molecular hurdles in polyfectin design and mechanistic background to polycation induced cytotoxicity." Adv Drug Deliv Rev **58**(14): 1523-1531.

Jain, A. and S. K. Jain (2008). "PEGylation: an approach for drug delivery. A review." Crit Rev Ther Drug Carrier Syst **25**(5): 403-447.

Jain, S., G. Zon and M. Sundaralingam (1989). "Base only binding of spermine in the deep groove of the A-DNA octamer d(GTGTACAC)." Biochemistry **28**(6): 2360-2364.

Jans, D. A., C. K. Chan and S. Huebner (1998). "Signals mediating nuclear targeting and their regulation: application in drug delivery." Med Res Rev **18**(4): 189-223.

Jeon, E., H. D. Kim and J. S. Kim (2003). "Pluronic-grafted poly-(L)-lysine as a new synthetic gene carrier." J Biomed Mater Res A **66**(4): 854-859.

Jeong, J. H. and T. G. Park (2002). "Poly(L-lysine)-g-poly(D,L-lactic-co-glycolic acid) micelles for low cytotoxic biodegradable gene delivery carriers." J Control Release **82**(1): 159-166.

Jiang, H., H. Wu, Y. L. Xu, J. Z. Wang and Y. Zeng (2011). "Preparation of galactosylated chitosan/tripolyphosphate nanoparticles and application as a gene carrier for targeting SMMC7721 cells." J Biosci Bioeng **111**(6): 719-724.

Jiang, H.-L., T.-H. Kim, Y.-K. Kim, I.-Y. Park, M.-H. Cho and C.-S. Cho (2008). "Efficient gene delivery using chitosan-polyethylenimine hybrid systems." Biomed Mater **3**(2): 25013.

Jiang, H. L., Y. K. Kim, R. Arote, D. Jere, J. S. Quan, J. H. Yu, Y. J. Choi, J. W. Nah, M. H. Cho and C. S. Cho (2009). "Mannosylated chitosan-graft-polyethylenimine as a gene carrier for Raw 264.7 cell targeting." Int J Pharm **375**(1-2): 133-139.

Jiang, H. L., Y. K. Kim, S. M. Lee, M. R. Park, E. M. Kim, Y. M. Jin, R. Arote, H. J. Jeong, S. C. Song, M. H. Cho and C. S. Cho (2010). "Galactosylated chitosan-g-PEI/DNA complexes-loaded poly(organophosphazene) hydrogel as a hepatocyte targeting gene delivery system." Arch Pharm Res **33**(4): 551-556.

Jiang, H. L., J. T. Kwon, E. M. Kim, Y. K. Kim, R. Arote, D. Jere, H. J. Jeong, M. K. Jang, J. W. Nah, C. X. Xu, I. K. Park, M. H. Cho and C. S. Cho (2008). "Galactosylated poly(ethylene glycol)-chitosan-graft-polyethylenimine as a gene carrier for hepatocyte-targeting." J Control Release **131**(2): 150-157.

Jiang, H. L., J. T. Kwon, Y. K. Kim, E. M. Kim, R. Arote, H. J. Jeong, J. W. Nah, Y. J. Choi, T. Akaike, M. H. Cho and C. S. Cho (2007). "Galactosylated chitosan-graft-polyethylenimine as a gene carrier for hepatocyte targeting." Gene Ther **14**(19): 1389-1398.

Jorundsson, E., J. H. Lumsden and R. M. Jacobs (1999). "Rapid staining techniques in cytopathology: a review and comparison of modified protocols for hematoxylin and eosin, Papanicolaou and Romanowsky stains." Vet Clin Pathol **28**(3): 100-108.

Jun, Y. J., J. H. Kim, S. J. Choi, H. J. Lee, M. J. Jun and Y. S. Sohn (2007). "A tetra(L-lysine)-grafted poly(organophosphazene) for gene delivery." Bioorg Med Chem Lett **17**(11): 2975-2978.

Kaiser, J. (2003). "Gene therapy. Seeking the cause of induced leukemias in X-SCID trial." Science **299**(5606): 495.

Kaiser, J. (2005). "Gene therapy. Panel urges limits on X-SCID trials." Science **307**(5715): 1544-1545.

Kamiya, H., J. Yamazaki and H. Harashima (2002). "Size and topology of exogenous DNA as determinant factors of transgene transcription in mammalian cells." Gene Ther **9**(22): 1500-1507.

Kang, H. C., S. Kim, M. Lee and Y. H. Bae (2005). "Polymeric gene carrier for insulin secreting cells: poly(L-lysine)-g-sulfonylurea for receptor mediated transfection." J Control Release **105**(1-2): 164-176.

Kao, G. Y., L. J. Change and T. M. Allen (1996). "Use of targeted cationic liposomes in enhanced DNA delivery to cancer cells." Cancer Gene Ther **3**(4): 250-256.

Karmali, P. P. and A. Chaudhuri (2007). "Cationic liposomes as non-viral carriers of gene medicines: Resolved issues, open questions, and future promises." Medicinal Research Reviews **27**(5): 696-722.

Kasaai, M. R. (2009). "Various methods for determination of the degree of N-acetylation of chitin and chitosan: a review." J Agric Food Chem **57**(5): 1667-1676.

Kawakami, S., S. Fumoto, M. Nishikawa, F. Yamashita and M. Hashida (2000). "In vivo gene delivery to the liver using novel galactosylated cationic liposomes." Pharm Res **17**(3): 306-313.

Kawakami, S., Y. Higuchi and M. Hashida (2008). "Nonviral approaches for targeted delivery of plasmid DNA and oligonucleotide." J Pharm Sci **97**(2): 726-745.

Kay, M. A. (2011). "State-of-the-art gene-based therapies: the road ahead." Nat Rev Genet **12**(5): 316-328.

Kay, M. A., J. C. Glorioso and L. Naldini (2001). "Viral vectors for gene therapy: the art of turning infectious agents into vehicles of therapeutics." Nat Med **7**(1): 33-40.

Kichler, A., C. Leborgne, J. Marz, O. Danos and B. Bechinger (2003). "Histidine-rich amphipathic peptide antibiotics promote efficient delivery of DNA into mammalian cells." Proc Natl Acad Sci U S A **100**(4): 1564-1568.

Kim, S. H., J. H. Jeong, T. I. Kim, S. W. Kim and D. A. Bull (2009). "VEGF siRNA delivery system using arginine-grafted bioreducible poly(disulfide amine)." Mol Pharm **6**(3): 718-726.

Kim, S. H., J. H. Jeong, M. Ou, J. W. Yockman, S. W. Kim and D. A. Bull (2008). "Cardiomyocyte-targeted siRNA delivery by prostaglandin E(2)-Fas siRNA polyplexes formulated with reducible poly(amido amine) for preventing cardiomyocyte apoptosis." Biomaterials **29**(33): 4439-4446.

Kim, T. H., S. E. Cook, R. B. Arote, M. H. Cho, J. W. Nah, Y. J. Choi and C. S. Cho (2007). "A degradable hyperbranched poly(ester amine) based on

poloxamer diacrylate and polyethylenimine as a gene carrier." Macromol Biosci **7**(5): 611-619.

Kim, Y. H., J. H. Park, M. Lee, T. G. Park and S. W. Kim (2005). "Polyethylenimine with acid-labile linkages as a biodegradable gene carrier." J Control Release **103**(1): 209-219.

Kircheis, R., L. Wightman, A. Schreiber, B. Robitza, V. Rossler, M. Kursa and E. Wagner (2001). "Polyethylenimine/DNA complexes shielded by transferrin target gene expression to tumors after systemic application." Gene Ther **8**(1): 28-40.

Kircheis, R., L. Wightman and E. Wagner (2001). "Design and gene delivery activity of modified polyethylenimines." Adv Drug Deliv Rev **53**(3): 341-358.

Koltover, I., T. Salditt and C. R. Safinya (1999). "Phase diagram, stability, and overcharging of lamellar cationic lipid-DNA self-assembled complexes." Biophys J **77**(2): 915-924.

Kulkarni, R. P., D. D. Wu, M. E. Davis and S. E. Fraser (2005). "Quantitating intracellular transport of polyplexes by spatio-temporal image correlation spectroscopy." Proc Natl Acad Sci U S A **102**(21): 7523-7528.

Kwok, K. Y., D. L. McKenzie, D. L. Evers and K. G. Rice (1999). "Formulation of highly soluble poly(ethylene glycol)-peptide DNA condensates." J Pharm Sci **88**(10): 996-1003.

Lai, S. K. and J. Hanes (2008). "Real-time multiple particle tracking of gene nanocarriers in complex biological environments." Methods Mol Biol **434**: 81-97.

Lam, A. P. and D. A. Dean (2010). "Progress and prospects: nuclear import of nonviral vectors." Gene Ther **17**(4): 439-447.

LaPar, D. J., I. L. Kron and Z. Yang (2009). "Stem cell therapy for ischemic heart disease: where are we?" Curr Opin Organ Transplant **14**(1): 79-84.

Lee, E. S., H. J. Shin, K. Na and Y. H. Bae (2003). "Poly(L-histidine)-PEG block copolymer micelles and pH-induced destabilization." J Control Release **90**(3): 363-374.

Lee, K. Y., I. C. Kwon, Y. H. Kim, W. H. Jo and S. Y. Jeong (1998). "Preparation of chitosan self-aggregates as a gene delivery system." J Control Release **51**(2-3): 213-220.

Lee, M., J. S. Choi, M. J. Choi, Y. K. Pak, B. D. Rhee and K. S. Ko (2007). "DNA delivery to the mitochondria sites using mitochondrial leader peptide conjugated polyethylenimine." J Drug Target **15**(2): 115-122.

Lee, M., J. W. Nah, Y. Kwon, J. J. Koh, K. S. Ko and S. W. Kim (2001). "Water-soluble and low molecular weight chitosan-based plasmid DNA delivery." Pharm Res **18**(4): 427-431.

Lee, Y., H. Mo, H. Koo, J. Y. Park, M. Y. Cho, G. W. Jin and J. S. Park (2007). "Visualization of the degradation of a disulfide polymer, linear poly(ethylenimine sulfide), for gene delivery." Bioconjug Chem **18**(1): 13-18.

Leeper, N. J., A. L. Hunter and J. P. Cooke (2010). "Stem cell therapy for vascular regeneration: adult, embryonic, and induced pluripotent stem cells." Circulation **122**(5): 517-526.

Leonetti, J. P., G. Degols and B. Lebleu (1990). "Biological activity of oligonucleotide-poly(L-lysine) conjugates: mechanism of cell uptake." Bioconjug Chem **1**(2): 149-153.

Li, C., S. Wen, H. Zhai and M. Sun (1999). "Asialoglycoprotein receptor and liposome synergistically mediate the gene transfer into primary rat hepatocytes." Sci China C Life Sci **42**(4): 435-440.

Li, L., Y. Nie, R. Zhu, S. Shi, K. Luo, B. He, Y. Yang, J. Yang and Z. Gu (2008). "Preparation and gene delivery of alkaline amino acids-based cationic liposomes." Arch Pharm Res **31**(7): 924-931.

Li, W., F. Nicol and F. C. Szoka, Jr. (2004). "GALA: a designed synthetic pH-responsive amphipathic peptide with applications in drug and gene delivery." Adv Drug Deliv Rev **56**(7): 967-985.

Li, Y., L. Cui, Q. Li, L. Jia, Y. Xu, Q. Fang and A. Cao (2007). "Novel symmetric amphiphilic dendritic poly(L-lysine)-b-poly(L-lactide)-b-dendritic poly(L-lysine)

with high plasmid DNA binding affinity as a biodegradable gene carrier." Biomacromolecules **8**(5): 1409-1416.

Li, Y., L. C. Cui, Q. Li, L. Jia, Y. G. Xu, Q. Fang and A. Cao (2007). "Novel symmetric amphiphilic dendritic poly(L-lysine)-b-poly(L-lactide)-b-dendritic poly(L-lysine) with high plasmid DNA binding affinity as a biodegradable gene carrier." Biomacromolecules **8**(5): 1409-14216.

Li, Y., Y. Zhu, K. Xia, R. Sheng, L. Jia, X. Hou, Y. Xu and A. Cao (2009). "Dendritic poly(L-lysine)-b-Poly(L-lactide)-b-dendritic poly(L-lysine) amphiphilic gene delivery vectors: roles of PLL dendritic generation and enhanced transgene efficacies via termini modification." Biomacromolecules **10**(8): 2284-2293.

Lim, Y. B., S. M. Kim, H. Suh and J. S. Park (2002). "Biodegradable, endosome disruptive, and cationic network-type polymer as a highly efficient and nontoxic gene delivery carrier." Bioconjug Chem **13**(5): 952-957.

Lin, C., C.-J. Blaauboer, M. M. Timoneda, M. C. Lok, M. van Steenbergen, W. E. Hennink, Z. Zhong, J. Feijen and J. F. J. Engbersen (2008). "Bioreducible poly(amido amine)s with oligoamine side chains: synthesis, characterization, and structural effects on gene delivery." J Control Release **126**(2): 166-174.

Liu, F. and L. Huang (2002). "Development of non-viral vectors for systemic gene delivery." J Control Release **78**(1-3): 259-266.

Liu, Y., D. Liggitt, W. Zhong, G. Tu, K. Gaensler and R. Debs (1995). "Cationic liposome-mediated intravenous gene delivery." J Biol Chem **270**(42): 24864-24870.

Liu, Y., L. C. Mounkes, H. D. Liggitt, C. S. Brown, I. Solodin, T. D. Heath and R. J. Debs (1997). "Factors influencing the efficiency of cationic liposome-mediated intravenous gene delivery." Nat Biotechnol **15**(2): 167-173.

Louise, C. (2006). "Nonviral vectors." Methods Mol Biol **333**: 201-226.

Lu, B., D. Q. Wu, H. Zheng, C. Y. Quan, X. Z. Zhang and R. X. Zhuo (2010). "Galactosyl conjugated N-succinyl-chitosan-graft-polyethylenimine for targeting gene transfer." Mol Biosyst **6**(12): 2529-2538.

Lungwitz, U., M. Breunig, T. Blunk and A. Göpferich (2005). "Polyethylenimine-based non-viral gene delivery systems." Eur J Pharm Biopharm **60**(2): 247-266.

Luo, D. and W. M. Saltzman (2000). "Synthetic DNA delivery systems." Nat Biotechnol **18**(1): 33-37.

Luten, J., C. F. van Nostrum, S. C. De Smedt and W. E. Hennink (2008). "Biodegradable polymers as non-viral carriers for plasmid DNA delivery." J Control Release **126**(2): 97-110.

Luten, J., J. H. van Steenis, R. van Someren, J. Kemmink, N. M. Schuurmans-Nieuwenbroek, G. A. Koning, D. J. Crommelin, C. F. van Nostrum and W. E.

Hennink (2003). "Water-soluble biodegradable cationic polyphosphazenes for gene delivery." J Control Release **89**(3): 483-497.

Ma, H. and S. L. Diamond (2001). "Nonviral gene therapy and its delivery systems." Curr Pharm Biotechnol **2**(1): 1-17.

MacLaughlin, F. C., R. J. Mumper, J. Wang, J. M. Tagliaferri, I. Gill, M. Hinchcliffe and A. P. Rolland (1998). "Chitosan and depolymerized chitosan oligomers as condensing carriers for in vivo plasmid delivery." J Control Release **56**(1-3): 259-272.

Macosko, J. C., C. H. Kim and Y. K. Shin (1997). "The membrane topology of the fusion peptide region of influenza hemagglutinin determined by spin-labeling EPR." J Mol Biol **267**(5): 1139-1148.

Mannisto, M., M. Reinisalo, M. Ruponen, P. Honkakoski, M. Tammi and A. Urtti (2007). "Polyplex-mediated gene transfer and cell cycle: effect of carrier on cellular uptake and intracellular kinetics, and significance of glycosaminoglycans." J Gene Med **9**(6): 479-487.

Mansouri, S., P. Lavigne, K. Corsi, M. Benderdour, E. Beaumont and J. C. Fernandes (2004). "Chitosan-DNA nanoparticles as non-viral vectors in gene therapy: strategies to improve transfection efficacy." Eur J Pharm Biopharm **57**(1): 1-8.

Margineanu, A., S. De Feyter, S. Melnikov, D. Marchand, A. van Aerschot, P. Herdewijn, S. Habuchi, F. C. De Schryver and J. Hofkens (2007). "Complexation of lipofectamine and cholesterol-modified DNA sequences studied by single-molecule fluorescence techniques." Biomacromolecules **8**(11): 3382-3392.

Martin, M. E. and K. G. Rice (2007). "Peptide-guided gene delivery." AAPS J **9**(1): E18-29.

Martinez-Fong, D., J. E. Mullersman, A. F. Purchio, J. Armendariz-Borunda and A. Martinez-Hernandez (1994). "Nonenzymatic glycosylation of poly-L-lysine: a new tool for targeted gene delivery." Hepatology **20**(6): 1602-1608.

McKenzie, D. L., K. Y. Kwok and K. G. Rice (2000). "A potent new class of reductively activated peptide gene delivery agents." J Biol Chem **275**(14): 9970-9977.

McKenzie, D. L., E. Smiley, K. Y. Kwok and K. G. Rice (2000). "Low molecular weight disulfide cross-linking peptides as nonviral gene delivery carriers." Bioconjug Chem **11**(6): 901-909.

Merdan, T., K. Kunath, D. Fischer, J. Kopecek and T. Kissel (2002). "Intracellular processing of poly(ethylene imine)/ribozyme complexes can be observed in living cells by using confocal laser scanning microscopy and inhibitor experiments." Pharm Res **19**(2): 140-146.

Michael, A. (1887). "Ueber die Addition von Natriumacetessig- und Natriummalonsäureäthern zu den Aethern ungesättigter Säuren." Journal für Praktische Chemie **35**(1): 349-356.

Midoux, P., A. Kichler, V. Boutin, J. C. Maurizot and M. Monsigny (1998). "Membrane permeabilization and efficient gene transfer by a peptide containing several histidines." Bioconjug Chem **9**(2): 260-267.

Midoux, P., E. LeCam, D. Coulaud, E. Delain and C. Pichon (2002). "Histidine containing peptides and polypeptides as nucleic acid vectors." Somat Cell Mol Genet **27**(1-6): 27-47.

Midoux, P., C. Mendes, A. Legrand, J. Raimond, R. Mayer, M. Monsigny and A. C. Roche (1993). "Specific gene transfer mediated by lactosylated poly-L-lysine into hepatoma cells." Nucleic Acids Res **21**(4): 871-878.

Midoux, P. and M. Monsigny (1999). "Efficient gene transfer by histidylated polylysine/pDNA complexes." Bioconjug Chem **10**(3): 406-411.

Milla, P., F. Dosio and L. Cattel (2011). "PEGylation of Proteins and Liposomes: A Powerful and Flexible Strategy to Improve the Drug Delivery." Curr Drug Metab.

Minchin, R. F. and S. Yang (2010). "Endosomal disruptors in non-viral gene delivery." Expert Opin Drug Deliv **7**(3): 331-339.

Miyata, K., Y. Kakizawa, N. Nishiyama, A. Harada, Y. Yamasaki, H. Koyama and K. Kataoka (2004). "Block catiomer polyplexes with regulated densities of charge and disulfide cross-linking directed to enhance gene expression." J Am Chem Soc **126**(8): 2355-2361.

Moghimi, S. M., P. Symonds, J. C. Murray, A. C. Hunter, G. Debska and A. Szewczyk (2005). "A two-stage poly(ethylenimine)-mediated cytotoxicity: implications for gene transfer/therapy." Mol Ther **11**(6): 990-995.

Mok, H. and T. G. Park (2008). "Self-crosslinked and reducible fusogenic peptides for intracellular delivery of siRNA." Biopolymers **89**(10): 881-888.

Moncla, A., M. O. Livet, M. Auger, J. F. Mattei, M. G. Mattei and F. Giraud (1991). "Smith-Magenis syndrome: a new contiguous gene syndrome. Report of three new cases." J Med Genet **28**(9): 627-632.

Montier, T., T. Benvegnu, P. A. Jaffres, J. J. Yaouanc and P. Lehn (2008). "Progress in cationic lipid-mediated gene transfection: a series of bio-inspired lipids as an example." Curr Gene Ther **8**(5): 296-312.

Morris, V. B. and C. P. Sharma (2011). "Folate mediated l-arginine modified oligo (alkylaminosiloxane) graft poly (ethyleneimine) for tumor targeted gene delivery." Biomaterials **32**(11): 3030-3041.

Mushtaq, M., B. N. Oskouei and J. M. Hare (2011). "Cell therapy for heart disease: to genetically modify or not, that is the question." Circ Res **108**(4): 398-401.

Naftilan, A. J. and F. G. Schuening (2011). "Stem cell therapy for cardiac disease: what can be learned from oncology." Heart Fail Clin **7**(3): 345-355.

Nishikawa, M. (2005). "Development of cell-specific targeting systems for drugs and genes." Biol Pharm Bull **28**(2): 195-200.

Nounou, M. I., K. Emmanouil, S. Chung, T. Pham, Z. Lu and M. Bikram (2010). "Novel reducible linear L-lysine-modified copolymers as efficient nonviral vectors." J Control Release **143**(3): 326-334.

Ohlfest, J. R., A. B. Freese and D. A. Largaespada (2005). "Nonviral vectors for cancer gene therapy: prospects for integrating vectors and combination therapies." Curr Gene Ther **5**(6): 629-641.

Opanasopit, P., M. Nishikawa and M. Hashida (2002). "Factors affecting drug and gene delivery: effects of interaction with blood components." Crit Rev Ther Drug Carrier Syst **19**(3): 191-233.

Ou, M., X.-L. Wang, R. Xu, C.-W. Chang, D. A. Bull and S. W. Kim (2008). "Novel biodegradable poly(disulfide amine)s for gene delivery with high efficiency and low cytotoxicity." Bioconjug Chem **19**(3): 626-633.

Oupicky, D., H. S. Bisht, D. S. Manickam and Q. H. Zhou (2005). "Stimulus-controlled delivery of drugs and genes." Expert Opin Drug Deliv **2**(4): 653-665.

Oupický, D., K. A. Howard, C. Konák, P. R. Dash, K. Ulbrich and L. W. Seymour (2000). "Steric stabilization of poly-L-Lysine/DNA complexes by the covalent attachment of semitelechelic poly[N-(2-hydroxypropyl)methacrylamide]." Bioconjug Chem **11**(4): 492-501.

Park, I. Y., I. Y. Kim, M. K. Yoo, Y. J. Choi, M. H. Cho and C. S. Cho (2008). "Mannosylated polyethylenimine coupled mesoporous silica nanoparticles for receptor-mediated gene delivery." Int J Pharm **359**(1-2): 280-287.

Park, K. (2009). "PEI-DNA complexes with higher transfection efficiency and lower cytotoxicity." J Control Release **140**(1): 1.

Park, T. G., J. H. Jeong and S. W. Kim (2006). "Current status of polymeric gene delivery systems." Adv Drug Deliv Rev **58**(4): 467-486.

Patel, M. P., R. R. Patel and J. K. Patel (2010). "Chitosan mediated targeted drug delivery system: a review." J Pharm Pharm Sci **13**(4): 536-557.

Peng, H., Y. Xiao, X. Mao, L. Chen, R. Crawford and A. K. Whittaker (2009). "Amphiphilic triblock copolymers of methoxy-poly(ethylene glycol)-b-poly(L-lactide)-b-poly(L-lysine) for enhancement of osteoblast attachment and growth." Biomacromolecules **10**(1): 95-104.

Peng, Q., Z. Zhong and R. Zhuo (2008). "Disulfide cross-linked polyethylenimines (PEI) prepared via thiolation of low molecular weight PEI as highly efficient gene vectors." Bioconjug Chem **19**(2): 499-506.

Perin, E. C. and G. V. Silva (2011). "Cell-based therapy for chronic ischemic heart disease--a clinical perspective." Cardiovasc Ther **29**(3): 211-217.

Pichon, C., C. Goncalves and P. Midoux (2001). "Histidine-rich peptides and polymers for nucleic acids delivery." Adv Drug Deliv Rev **53**(1): 75-94.

Piest, M., C. Lin, M. A. Mateos-Timoneda, M. C. Lok, W. E. Hennink, J. Feijen and J. F. Engbersen (2008). "Novel poly(amido amine)s with bioreducible disulfide linkages in their diamino-units: structure effects and in vitro gene transfer properties." J Control Release **130**(1): 38-45.

Plank, C., B. Oberhauser, K. Mechtler, C. Koch and E. Wagner (1994). "The influence of endosome-disruptive peptides on gene transfer using synthetic virus-like gene transfer systems." J Biol Chem **269**(17): 12918-12924.

Pouton, C. W., P. Lucas, B. J. Thomas, A. N. Uduehi, D. A. Milroy and S. H. Moss (1998). "Polycation-DNA complexes for gene delivery: a comparison of the biopharmaceutical properties of cationic polypeptides and cationic lipids." J Control Release **53**(1-3): 289-299.

Povsic, T. J. and E. D. Peterson (2005). "Progenitor cell therapy of ischemic heart disease: the new frontier." Future Cardiol **1**(1): 87-98.

Prabaharan, M. (2008). "Review paper: chitosan derivatives as promising materials for controlled drug delivery." J Biomater Appl **23**(1): 5-36.

Rahbek, U. L., K. A. Howard, D. Oupicky, D. S. Manickam, M. Dong, A. F. Nielsen, T. B. Hansen, F. Besenbacher and J. Kjems (2008). "Intracellular siRNA and precursor miRNA trafficking using bioresponsive copolypeptides." J Gene Med **10**(1): 81-93.

Ribatti, D. (2005). "The crucial role of vascular permeability factor/vascular endothelial growth factor in angiogenesis: a historical review." Br J Haematol **128**(3): 303-309.

Ritter, W., C. Plank, J. Lausier, C. Rudolph, D. Zink, D. Reinhardt and J. Rosenecker (2003). "A novel transfecting peptide comprising a tetrameric nuclear localization sequence." J Mol Med (Berl) **81**(11): 708-717.

Roberts, M. J., M. D. Bentley and J. M. Harris (2002). "Chemistry for peptide and protein PEGylation." Adv Drug Deliv Rev **54**(4): 459-476.

Saito, G., J. A. Swanson and K. D. Lee (2003). "Drug delivery strategy utilizing conjugation via reversible disulfide linkages: role and site of cellular reducing activities." Adv Drug Deliv Rev **55**(2): 199-215.

Sano, A., M. Maeda, S. Nagahara, T. Ochiya, K. Honma, H. Itoh, T. Miyata and K. Fujioka (2003). "Atelocollagen for protein and gene delivery." Adv Drug Deliv Rev **55**(12): 1651-1677.

Satija, J., U. Gupta and N. K. Jain (2007). "Pharmaceutical and biomedical potential of surface engineered dendrimers." Crit Rev Ther Drug Carrier Syst **24**(3): 257-306.

Sato, A., S. Kawakami, M. Yamada, F. Yamashita and M. Hashida (2001). "Enhanced gene transfection in macrophages using mannosylated cationic liposome-polyethylenimine-plasmid DNA complexes." J Drug Target **9**(3): 201-207.

Sato, T., T. Ishii and Y. Okahata (2001). "In vitro gene delivery mediated by chitosan. effect of pH, serum, and molecular mass of chitosan on the transfection efficiency." Biomaterials **22**(15): 2075-2080.

Science, M. and AAAS (2000). "Controversy of the year. Biomedical ethics on the front burner." Science **290**(5500): 2225.

Segers, V. F. and R. T. Lee (2008). "Stem-cell therapy for cardiac disease." Nature **451**(7181): 937-942.

Sharpe, N. (2004). "Cardiac remodeling in coronary artery disease." Am J Cardiol **93**(9A): 17B-20B.

Shim, M. S. and Y. J. Kwon (2008). "Controlled delivery of plasmid DNA and siRNA to intracellular targets using ketalized polyethylenimine." Biomacromolecules **9**(2): 444-455.

Shim, M. S. and Y. J. Kwon (2009). "Acid-Responsive Linear Polyethylenimine for Efficient, Specific, and Biocompatible siRNA Delivery." Bioconjug Chem.

Shim, M. S. and Y. J. Kwon (2009). "Controlled cytoplasmic and nuclear localization of plasmid DNA and siRNA by differentially tailored polyethylenimine." J Control Release **133**(3): 206-213.

Smith, L. and J. F. Byers (2002). "Gene therapy in the post-Gelsinger era." JONAS Healthc Law Ethics Regul **4**(4): 104-110.

Somia, N. and I. M. Verma (2000). "Gene therapy: trials and tribulations." Nat Rev Genet **1**(2): 91-99.

Stevenson, M., V. Ramos-Perez, S. Singh, M. Soliman, J. A. Preece, S. S. Briggs, M. L. Read and L. W. Seymour (2008). "Delivery of siRNA mediated by histidine-containing reducible polycations." J Control Release **130**(1): 46-56.

Stolberg, S. G. (1999). "The biotech death of Jesse Gelsinger." N Y Times Mag: 136-140, 149-150.

Suh, J., M. Dawson and J. Hanes (2005). "Real-time multiple-particle tracking: applications to drug and gene delivery." Adv Drug Deliv Rev **57**(1): 63-78.

Suh, J., D. Wirtz and J. Hanes (2003). "Efficient active transport of gene nanocarriers to the cell nucleus." Proc Natl Acad Sci U S A **100**(7): 3878-3882.

Suh, J., D. Wirtz and J. Hanes (2004). "Real-time intracellular transport of gene nanocarriers studied by multiple particle tracking." Biotechnol Prog **20**(2): 598-602.

Suh, W., J. K. Chung, S. H. Park and S. W. Kim (2001). "Anti-JL1 antibody-conjugated poly (L-lysine) for targeted gene delivery to leukemia T cells." J Control Release **72**(1-3): 171-178.

Sun, X., L. Hai, Y. Wu, H. Y. Hu and Z. R. Zhang (2005). "Targeted gene delivery to hepatoma cells using galactosylated liposome-polycation-DNA complexes (LPD)." J Drug Target **13**(2): 121-128.

Sunkomat, J. N. and M. A. Gaballa (2003). "Stem cell therapy in ischemic heart disease." Cardiovasc Drug Rev **21**(4): 327-342.

Teichler Zallen, D. (2000). "US gene therapy in crisis." Trends Genet **16**(6): 272-275.

Thrasher, A. J., H. B. Gaspar, C. Baum, U. Modlich, A. Schambach, F. Candotti, M. Otsu, B. Sorrentino, L. Scobie, E. Cameron, K. Blyth, J. Neil, S. H. Abina, M. Cavazzana-Calvo and A. Fischer (2006). "Gene therapy: X-SCID transgene leukaemogenicity." Nature **443**(7109): E5-6; discussion E6-7.

Toncheva, V., M. A. Wolfert, P. R. Dash, D. Oupicky, K. Ulbrich, L. W. Seymour and E. H. Schacht (1998). "Novel vectors for gene delivery formed by self-

assembly of DNA with poly(L-lysine) grafted with hydrophilic polymers." Biochim Biophys Acta **1380**(3): 354-368.

Tros de Ilarduya, C., Y. Sun and N. Duzgunes (2010). "Gene delivery by lipoplexes and polyplexes." Eur J Pharm Sci **40**(3): 159-170.

Tung, C. H. and R. Weissleder (2003). "Arginine containing peptides as delivery vectors." Adv Drug Deliv Rev **55**(2): 281-294.

Turk, M. J., J. A. Reddy, J. A. Chmielewski and P. S. Low (2002). "Characterization of a novel pH-sensitive peptide that enhances drug release from folate-targeted liposomes at endosomal pHs." Biochim Biophys Acta **1559**(1): 56-68.

Urbaszek, W., D. Modersohn, J. Schauer and K. Gunther (1976). "[Current problems in the conservative long-term treatment of ischemic heart disease]." Z Arztl Fortbild (Jena) **70**(1): 2-13.

Vasir, J. K. and V. Labhasetwar (2006). "Polymeric nanoparticles for gene delivery." Expert Opin Drug Deliv **3**(3): 325-344.

Vera Janavel, G. L., A. De Lorenzi, C. Cortes, F. D. Olea, P. Cabeza Meckert, A. Bercovich, M. Criscuolo, R. Laguens and A. Crottogini (2011). "Effect of VEGF gene transfer on infarct size, left ventricular function and myocardial perfusion in sheep after two months of coronary artery occlusion." J Gene Med.

Veronese, F. M. and G. Pasut (2005). "PEGylation, successful approach to drug delivery." Drug Discov Today **10**(21): 1451-1458.

Wakebayashi, D., N. Nishiyama, Y. Yamasaki, K. Itaka, N. Kanayama, A. Harada, Y. Nagasaki and K. Kataoka (2004). "Lactose-conjugated polyion complex micelles incorporating plasmid DNA as a targetable gene vector system: their preparation and gene transfecting efficiency against cultured HepG2 cells." J Control Release **95**(3): 653-664.

Walsh, M., M. Tangney, M. J. O'Neill, J. O. Larkin, D. M. Soden, S. L. McKenna, R. Darcy, G. C. O'Sullivan and C. M. O'Driscoll (2006). "Evaluation of cellular uptake and gene transfer efficiency of pegylated poly-L-lysine compacted DNA: implications for cancer gene therapy." Mol Pharm **3**(6): 644-653.

Wan, L., Y. You, Y. Zou, D. Oupicky and G. Mao (2009). "DNA release dynamics from bioreducible poly(amido amine) polyplexes." J Phys Chem B **113**(42): 13735-13741.

Wang, C. Y. and L. Huang (1984). "Polyhistidine mediates an acid-dependent fusion of negatively charged liposomes." Biochemistry **23**(19): 4409-4416.

Wang, Y., P. Chen and J. Shen (2006). "The development and characterization of a glutathione-sensitive cross-linked polyethylenimine gene vector." Biomaterials **27**(30): 5292-5298.

Wasungu, L. and D. Hoekstra (2006). "Cationic lipids, lipoplexes and intracellular delivery of genes." J Control Release **116**(2): 255-264.

Watanabe, Y., X. Liu, I. Shibuya and T. Akaike (2000). "Functional evaluation of poly-(N-p-vinylbenzyl-O-beta-D-galactopyranosyl-[1-4]-D-gluconamide)(PVLA) as a liver specific carrier." J Biomater Sci Polym Ed **11**(8): 833-848.

Wellnhofer, E., W. Bocksch, N. Hiemann, M. Dandel, W. Klimek, R. Hetzer and E. Fleck (2002). "Shear stress and vascular remodeling: study of cardiac allograft coronary artery disease as a model of diffuse atherosclerosis." J Heart Lung Transplant **21**(4): 405-416.

Wilson, R. F. (2010). "The death of Jesse Gelsinger: new evidence of the influence of money and prestige in human research." Am J Law Med **36**(2-3): 295-325.

Wolfert, M. A., P. R. Dash, O. Nazarova, D. Oupicky, L. W. Seymour, S. Smart, J. Strohalm and K. Ulbrich (1999). "Polyelectrolyte vectors for gene delivery: influence of cationic polymer on biophysical properties of complexes formed with DNA." Bioconjug Chem **10**(6): 993-1004.

Wolterbeek, H. T. and A. J. van der Meer (2005). "Optimization, application, and interpretation of lactate dehydrogenase measurements in microwell determination of cell number and toxicity." Assay Drug Dev Technol **3**(6): 675-682.

Woods, N. B., V. Bottero, M. Schmidt, C. von Kalle and I. M. Verma (2006). "Gene therapy: therapeutic gene causing lymphoma." Nature **440**(7088): 1123.

Wu, G. Y. and C. H. Wu (1991). "Delivery systems for gene therapy." Biotherapy **3**(1): 87-95.

Xu, C. X., D. Jere, H. Jin, S. H. Chang, Y. S. Chung, J. Y. Shin, J. E. Kim, S. J. Park, Y. H. Lee, C. H. Chae, K. H. Lee, G. R. Beck, Jr., C. S. Cho and M. H. Cho (2008). "Poly(ester amine)-mediated, aerosol-delivered Akt1 small interfering RNA suppresses lung tumorigenesis." Am J Respir Crit Care Med **178**(1): 60-73.

Yamagata, M., T. Kawano, K. Shiba, T. Mori, Y. Katayama and T. Niidome (2007). "Structural advantage of dendritic poly(L-lysine) for gene delivery into cells." Bioorg Med Chem **15**(1): 526-532.

Yamanouchi, D., J. Wu, A. N. Lazar, K. Craig Kent, C. C. Chu and B. Liu (2008). "Biodegradable arginine-based poly(ester-amide)s as non-viral gene delivery reagents." Biomaterials **29**(22): 3269-3277.

Yang, H., S. T. Lopina, L. P. DiPersio and S. P. Schmidt (2008). "Stealth dendrimers for drug delivery: correlation between PEGylation, cytocompatibility, and drug payload." J Mater Sci Mater Med **19**(5): 1991-1997.

Yang, Y., Z. Xu, S. Chen, Y. Gao, W. Gu, L. Chen, Y. Pei and Y. Li (2008). "Histidylated cationic polyorganophosphazene/DNA self-assembled nanoparticles for gene delivery." Int J Pharm **353**(1-2): 277-282.

Yi, Y., M. J. Noh and K. H. Lee (2011). "Current advances in retroviral gene therapy." Curr Gene Ther **11**(3): 218-228.

You, Y. Z., D. S. Manickam, Q. H. Zhou and D. Oupicky (2007). "Reducible poly(2-dimethylaminoethyl methacrylate): synthesis, cytotoxicity, and gene delivery activity." J Control Release **122**(3): 217-225.

You, Y. Z., D. S. Manickam, Q. H. Zhou and D. Oupicky (2007). "A versatile approach to reducible vinyl polymers via oxidation of telechelic polymers prepared by reversible addition fragmentation chain transfer polymerization." Biomacromolecules **8**(6): 2038-2044.

You, Y. Z., Q. H. Zhou, D. S. Manickam, L. Wan, G. Z. Mao and D. Oupicky (2007). "Dually responsive multiblock copolymers via RAFT polymerization: Synthesis of temperature- and redox-responsive copolymers of PNIPAM and PDMAEMA." Macromolecules **40**(24): 8617-8624.

Zanta, M. A., P. Belguise-Valladier and J. P. Behr (1999). "Gene delivery: a single nuclear localization signal peptide is sufficient to carry DNA to the cell nucleus." Proc Natl Acad Sci U S A **96**(1): 91-96.

Zanta, M. A., O. Boussif, A. Adib and J. P. Behr (1997). "In vitro gene delivery to hepatocytes with galactosylated polyethylenimine." Bioconjug Chem **8**(6): 839-844.

Zelphati, O., L. S. Uyechi, L. G. Barron and F. C. Szoka, Jr. (1998). "Effect of serum components on the physico-chemical properties of cationic lipid/oligonucleotide complexes and on their interactions with cells." Biochim Biophys Acta **1390**(2): 119-133.

Zhang, L., N. Ambulos and A. J. Mixson (2004). "DNA delivery to cells in culture using peptides." Methods Mol Biol **245**: 33-52.

Zhang, S., Y. Xu, B. Wang, W. Qiao, D. Liu and Z. Li (2004). "Cationic compounds used in lipoplexes and polyplexes for gene delivery." J Control Release **100**(2): 165-180.

Zhang, S., B. Zhao, H. Jiang, B. Wang and B. Ma (2007). "Cationic lipids and polymers mediated vectors for delivery of siRNA." J Control Release **123**(1): 1-10.

Zhao, M. and R. Weissleder (2004). "Intracellular cargo delivery using tat peptide and derivatives." Med Res Rev **24**(1): 1-12.

Zhu, J., L. Zhang, U. K. Hanisch, P. L. Felgner and R. Reszka (1996). "A continuous intracerebral gene delivery system for in vivo liposome-mediated gene therapy." Gene Ther **3**(6): 472-476.

Zisa, D., A. Shabbir, M. Mastri, T. Taylor, I. Aleksic, M. McDaniel, G. Suzuki and T. Lee (2011). "Intramuscular VEGF activates an SDF1-dependent progenitor cell

cascade and an SDF1-independent muscle paracrine cascade for cardiac repair." Am J Physiol Heart Circ Physiol **301**(6): H2422-2432.

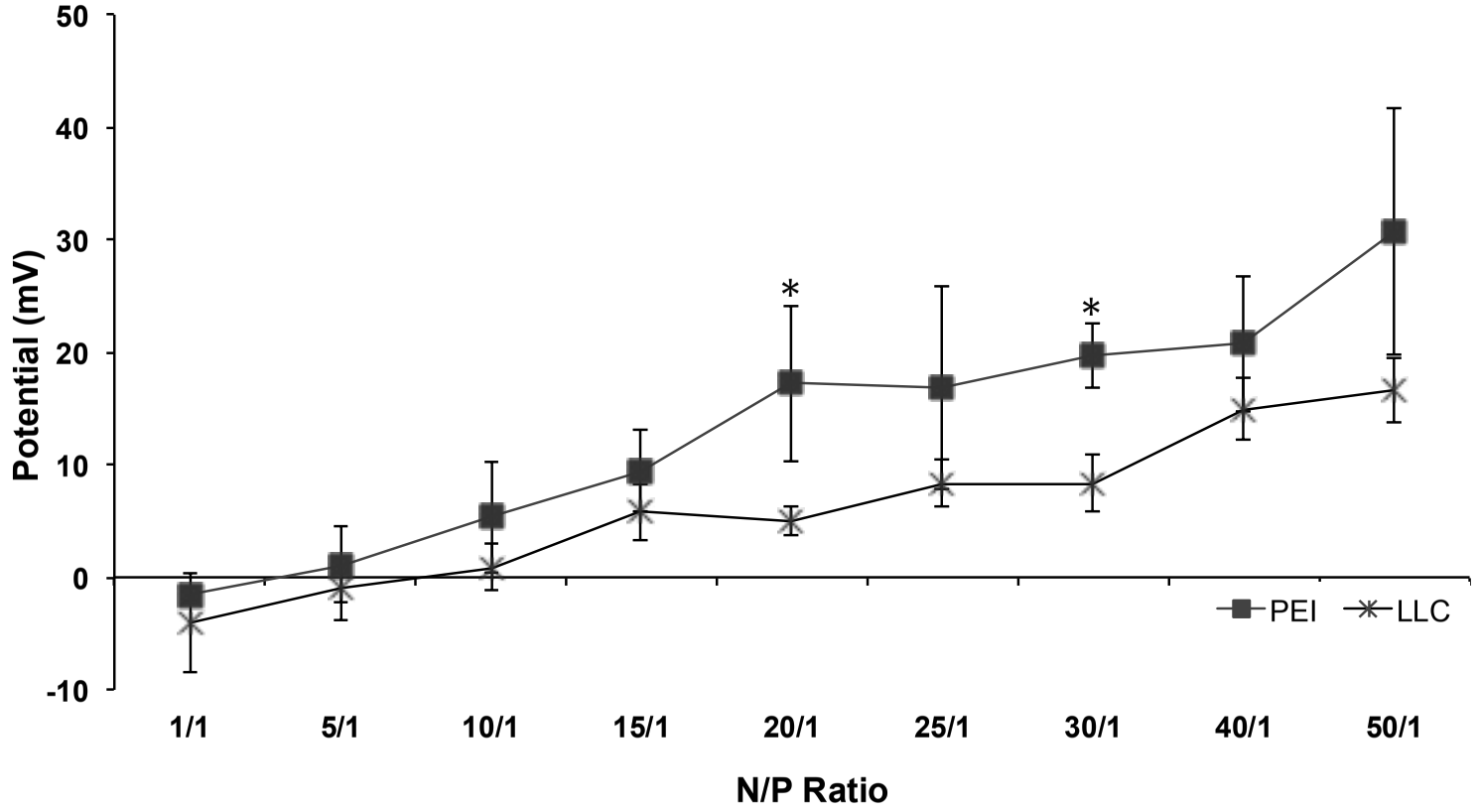

Figure A4.1: Zeta potential (ζ) of LLC/pCMV-Luc and PEI/pCMV-Luc polyplexes as a function of N/P ratio. Average zeta potential of LLC/pDNA and PEI/pDNA polyplexes were measured at different N/P ratios from 1:1 to 50:1. Data represented as mean ± SD, N=3. (* indicate p-values of < 0.05)

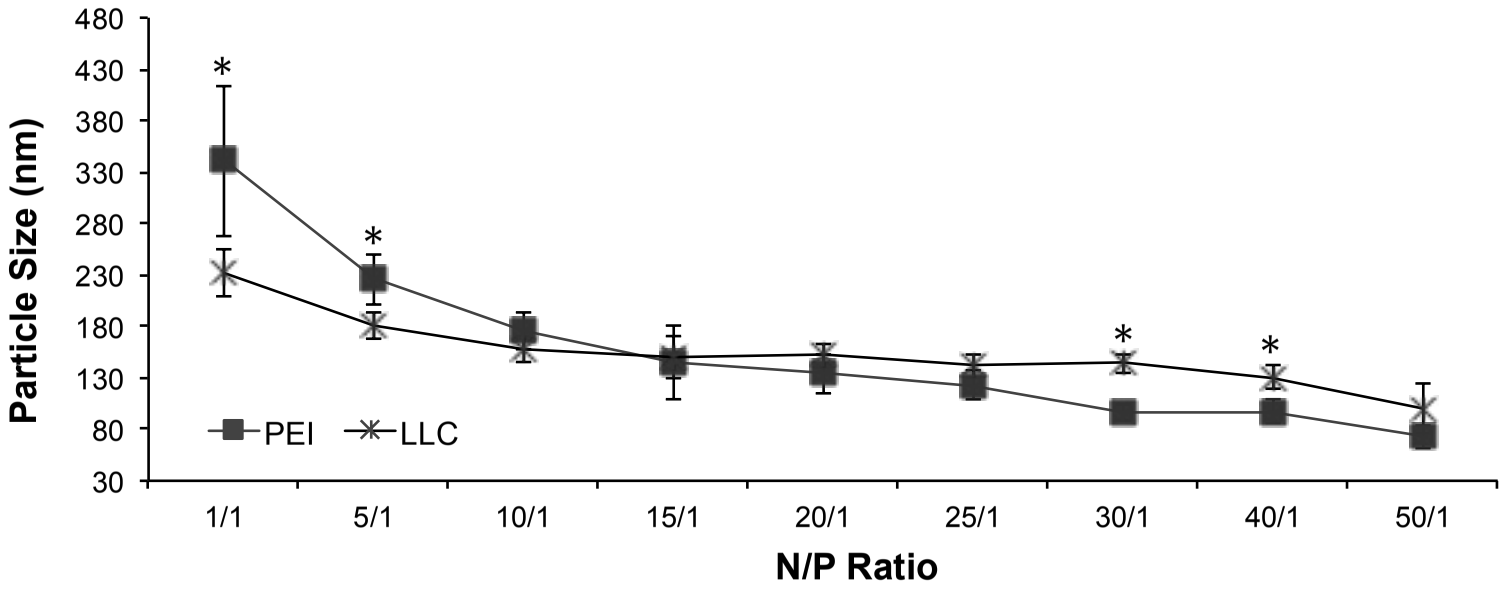

Figure A4.2: Particle size analysis of various LLC/pDNA and PEI/pDNA polyplexes using dynamic light scattering as a function of N/P ratio. Average particle sizes of LLC/pDNA and PEI/pDNA polyplexes were measured at different N/P ratios from 1:1 to 50:1. Data represent mean ± SD, N=3. (* indicate p-values of < 0.05)